Cranfield Institute
of Technology

SALIM Y. KASIM

Ride Analysis For Suspension System of Off-Road Tracked Vehicles

School of Mechanical Engineering
Turbomachinery & Engineering
Mechanics Department

Ph.D Thesis

Cranfield Institute of Technology
School of Mechanical
Engineering

Ph.D Thesis

Academic Year 1990-91

Salim Y. Kasim

Ride Analysis For Suspension System of Off-Road Tracked Vehicles

Supervisor: Dr A M El-Zafrany

This Thesis is Submitted in Candidature for
the Degree of Doctor of Philosophy.
August 1991

TO MY

FAMILY

ACKNOWLEDGEMENTS

The author is firstly, and mostly, indebted to the brave people of Iraq. There are not enough words to acknowledge their enormous sacrifice in order to send the author and many others like him to the U.K. and around the world for high education.

The author wishes to express his most sincere gratitude and his true feeling towards Professor Robin Leigh Elder, the Head of DTEM for his assistance and encouragement.

The author would like to express his sincere gratitude and thanks to Dr A M EL-Zafrany, for his stimulating supervision, invaluable guidance and human co-operation throughout this work, during meetings within and after working hours.

Last, but by no means least, I wish to express my appreciation to my wife Ahlam for here support and patience, and to my children Merwa, Ghadh, Arkan, and sifian who have been forced to sacrifice some of their fun because of a busy father.

SUMMARY

In this work, an attempt has been made to develop a programming package for ride analysis of off-road vehicles based upon a finite-element formulation of vehicle suspension systems. Mathematical modelling of generalised suspension systems has been carried out with several non-linear aspects being investigated and implemented in the programming package, such as large deflection, non-linear characteristics of springs and dampers, bump stops and wheel separation. Different types of soil have been considered together with an appropriate modelling of vehicle tracks. Several methods for time integration of dynamic equations have been investigated so as to deal with numerical instability problems expected for off-road suspension systems which often have "stiff" differential equations of motion. Three ride analysis criteria have also been considered in the programming package.

Several case studies have been analysed using the developed programming package. They consist of two simple case studies with known analytical solutions, an existing wheeled off-road vehicle with published analog computer results, and an off-road tracked vehicle with known experimental results. The package has been validated and proved to be an acceptable tool for the ride analysis of off-road vehicles, within the approximating assumptions considered. Several measures for future development have also been suggested.

CONTENTS

4. VEHICLE TERRAIN INTERACTION:

Page No.

7. RESULTS AND DISCUSSIONS:

8. CONCLUSIONS AND RECOMMENDATIONS:

LIST OF FIGURES

LIST OF TABLES

NOTATION

A	Amplitude of a harmonic wave.
B	Wave length of a harmonic wave.
C	Coefficient of the main damper.
C_T	Equivalent damping coefficient of a road wheel or tyre.
C_i	Distance between subsequent wheels i and i-1
$\underline{F}(t)$	General excitation force function of time.
g	Gravitational acceleration.
I_{xx}	Vehicle moment of inertia about the X-axis.
I_{yy}	Vehicle moment of inertia about the Y-axis.
K	Stiffness coefficient of the main spring.
K_s	Stiffness coefficient of soil.
K_ϕ	Frictional modulus of terrain deformation.
K_c	Cohesive modulus of terrain deformation.
K_{Bi}	Stiffness coefficient of i^{th} bump stop.
K_T	Equivalent stiffness coefficient of a road wheel or tyre.
L	Road wheel arm length.
L_2	Distance between torsion bar centre and point of attachment of the damper to the road wheel arm.

M_s Vehicle sprung mass.

m_i Unsprung mass of the i^{th} road wheel or tyre.

M_x External moment about the X-axis.

M_y External moment about the Y-axis.

N Number of wheels.

t_i Time node number i.

V Vehicle velocity.

X, Y, Z Vehicle fixed-ground parallel coordinates.

X_d, Y_d, Z_d Coordinates of the point of attachment of a damper to the vehicle hull.

X_1, Y_1, Z_1 Vehicle input data coordinates

X_2, Y_2, Z_2 Vehicle coordinates.

X_3, Y_3, Z_3 Ground-vehicle coordinates.

$\delta_o, \dot{\delta}_o, \ddot{\delta}_o$ Displacement, velocity, and acceleration of a point on the vehicle main frame.

$\delta_T, \dot{\delta}_T$ Displacement, velocity of point of contact of road wheel or tyre and the ground.

μ Coulomb friction coefficient.

θ_o Vehicle hull pitch angle.

ϕ_o	Vehicle hull roll angle.
λ	Transmission ratio of a four-bar linkage.
$\lceil \quad \rfloor$	Diagonal matrix.
$\lvert \underline{A} \rvert$	Determinant of matrix $\underline{A}$

Some other specific notations have been defined at the point in the text where they are used.

CHAPTER

ONE

INTRODUCTION

1.1 GENERAL INTRODUCTION:

There are two different types of ground vehicles; the guided vehicles and non-guided ground vehicles. The guided vehicles are constrained to move along a fixed path (guideway), such as railway vehicles. The second type represents the vehicles which can move, by choice, in various directions on the ground, such as road and off-road vehicles.

In general, the characteristics of a ground vehicle may be described in terms of its performance, handling and ride. Performance characteristics include the ability of the vehicle to accelerate, to overcome obstacles, and to decelerate. Handling can be defined as the vehicle mobility or its response to the driver commands and its ability to stabilise its motion against external agency. Ride characteristics are related to the vehicle comfort which is affected by its vibration excited by surface irregularities and its effects on passengers and cargo.

In the field of mobility and comfort the interaction between the vehicle and terrain is quite important. On the a smooth surface of rigid soil (prepared road), there is no significant problem for the mobility as well as the comfort of vehicles, but the behaviour of vehicles is different on unprepared terrain (off-road).

Tracked vehicles are, in general, unsuitable for road use, with the exception of a few specialised machines. They are either very low speed vehicles (<5 mile/h) designed to produce high tractive efforts or military vehicles capable of moving with higher speed (up to 40 mile/h)

An essential device for the reduction of the vibration of an off-road vehicle resulting from being driven on rough terrain, is the suspension system which usually consists of a number of springs and dampers laid on the road wheels.

The general requirements from an off-road vehicle suspension system are a low natural frequency and long wheel travel to maximise vibration isolation and maintain good ground/wheel contact, respectively. For the military applications the response to large individual (usually man-made) obstacles such as banks and ditches must be considered. Generally, military vehicles are required to operate on a wide variety of surfaces and it is not practical to "optimise" the suspension for any particular one.

1.2 OBJECTIVES OF THE WORK:

The basic objective of this work is to formulate a finite element model for off-road tracked suspension systems, the developed model will then be employed for the derivation of dynamic equations for generalised suspension systems, related to ride analysis.

Different measures for obtaining an acceptable simulation model for suspension systems will be considered. Ride analysis of off-road vehicles operating on different types of soil will be considered. The developed analysis should be capable of dealing with different sources of non-linearities such as:

(i) Non-linear characteristics and/or blow-off function of the main damper.

(ii) Non-linear characteristics of the main spring or torsion bar.

(iii) Non-linearity originating from the bump-stop action.

(iv) Non-linear characteristics of the tyre or the road wheel.

(v) Non-linearity resulting from large deflection consideration.

(vi) Non-linearity arising from wheel-ground separation.

A ride analysis programming package for off-road tracked vehicles will be designed based upon the previous derivations and with non-linear effects, track effects, and soil effects taken into considerations.

The package will be employed for the ride analysis of a number of case studies and the results obtained will be compared with the corresponding published experimental work so as to evaluate the validity and efficiency of the programming package.

1.3 THESIS LAYOUT:

In this chapter a general introduction about the subject and the objectives of the present work are laid out.

In chapter two the most relevant literature are reviewed to make a clear picture about the off-road vehicles modelling, interaction between the vehicle and the terrain, the ride tolerance criteria, and the numerical integration methods available, all these aspects are followed by some general conclusions.

The mathematical modelling of different suspension elements used in the off-road vehicles in addition to the track element simulation are demonstrated in chapter three.

Chapter four deals with the vehicle-terrain interaction. The tyre modelling, the types of soils used in this work, and the representation of the different expected excitation forces are reviewed.

Vehicle ride analysis is reviewed in chapter five. The ride tolerance criteria and the driver dynamics including the type of seat link together with the computer algorithm for each tolerance criterion are demonstrated.

In chapter six, the analysis of the general dynamic equations which simulate the vehicle suspension system is presented. The analysis includes a study of the system dynamic characteristics, such as the natural frequencies, the resonance frequencies, and the steady state response to periodic excitation. The numerical integration methods employed in this work are studied, and the non-linear effects are reviewed.

In chapter seven a verification of the package against analytical solutions, and published and experimental results of two case studies, wheeled and tracked vehicles is presented. Further analysis and general discussions are introduced.

In chapter eight conclusions and recommended future work are presented.

CHAPTER TWO

LITERATURE REVIEW

2.1 REVIEW OF THE MODELLING OF OFF-ROAD VEHICLES:

Over the years, particularly since World War II, a variety of mathematical models for off-road vehicle suspension systems has been developed. Most of the early models were based on the classical suspension elements (lumped mass-spring-damper), due to the lack of high-capacity computers as available nowadays.

In 1961 Clark [Ref. 1] developed a computational procedure that accounts for suspension deflections due to track tension. He concluded that the effect of the track mass on the dynamic response is negligible because the track flexural vibration frequencies are theoretically much higher than the resonant frequencies of the suspension, and the hull response and vibration amplitudes are correspondingly much lower. This conclusion was also supported by an experimental verification.

Lessem and Murphy [Ref. 2] conducted a study, in 1972, in which they used four different tracked vehicles over an assortment of obstacles, and they considered first the tracks been installed and then removed. They concluded that the track contribution to hull dynamics cannot be neglected for different ranges of vehicle characteristics, speeds, or obstacle sizes. Within the range of speeds studied, contributions of track were usually most pronounced at low speeds and of lesser importance at higher speeds. The type of the suspension system significantly affects the track contribution to dynamics.

A general, computerised module in simulating two-dimensional vehicle dynamic responses of rigid-frame vehicles configured with wheels, tracks, and half tracks, was developed by Murphy and Ahlvin [Ref. 3]. The module considers the effect of the track on the ride dynamics of a tracked vehicle in a simple way which affords suitable simulations of cross-country vibrations. The effects of the geometry of the road wheels are represented by radially projecting stiff springs, and the track tension is represented by interconnecting linear springs between adjacent road wheels. However, the authors anticipated that more study is needed to determine the sensitivity of absorbed power to acceleration and to compare simulations with representative field

test results.

Wheeler of Chrysler Corporation [Ref. 4], developed a two dimensional model for XM1 tank. The overall track tension was accounted for as forces acting on the wheels and sprocket. Local tension effects were neglected and excitation input was restricted to the vertical displacement profile imposed on wheels motion.

A finite element study of track tension for an M60 tank traversing square profile discrete obstacles was reported in 1979 by Doyle and Workman [Ref. 5]. They concluded that the track tension does not increase rapidly when traversing an obstacle at greater track pretensions, and parameters such as road wheel load, and torsion bar stiffness have only a small effect on track tension.

Giannopulos and Rao, in 1980 [Ref. 6], described a method for employing general purpose mechanisms programs to predict the loads induced in the suspension systems of ground vehicles traversing rough terrains. The mechanisms representation employed accounts for geometric non-linearities of the kinematics as well as the material non-linearities of the tyre, shock absorber, and rubber bushings. The compliance of the body structure is treated as a rigid link. They concluded that the dynamic loads obtained using this procedure can serve as input to detailed finite element models of vehicle components for stress analysis.

In 1981 Petrick, Janosi, and Haley [Ref. 7], reviewed the NATO Reference Mobility Model (NRMM), and they mentioned that the model is suited to calculate the maximum speed that a vehicle can attain in any terrain environment.The AMC-74 Vehicle dynamics module which was developed from the AMC-71 ride dynamics module represents the heart of the (NRMM) model. These modules are capable of predicting the dynamic response accurately only for relatively smooth terrain and fairly short distances.

In 1984 Kim, Shabana, and Haug [Ref. 8], introduced a method for non-linear, transient dynamic analysis of vehicle systems that are composed of interconnected rigid and flexible bodies. The

finite element method was used to characterize the deformation of each elastic body. The method is applied to a planar truck model with a flexible chassis and non-linear suspension components, giving simulation results for transient dynamic response as the vehicle traverses a bump, including the effect of bump-stops, and random terrains. One of the conclusions of this study was that the suspension link flexibility does not have noticeable effects on the vertical acceleration of the chassis. The same conclusion has been found by [Ref. 44].

The dynamics of several off-road vehicles have been investigated by Craighead, and Brown in 1984 [Ref. 9], using IBM's continuous systems modelling package, The considered models consisted of a number of rigid masses connected by non-linear springs and dampers, supported on linear springs and dampers representing the tyre characteristics. A library routine based on the QR algorithm was employed to provide the eigenvalues of the systems. Such codes may have limited accuracy and reliability since they are based on library routines which may have their own limitations.

A computer model to simulate the dynamic response of track laying vehicles traversing defined terrains was described by Bennent and Penny [Ref. 10]. Using a computer model, the analysis of two military vehicles was carried out. The authors concluded that numerical instabilities, may arise due to the "stiff" nature of the differential equations of motion which they solved using a fourth-order Runge-Kutta technique. These instabilities were observed in acceleration and velocity values and this problem may be overcome by decreasing the value of the integration time step but this can lead to a very long computer run time.

Horton and Crolla [Ref. 11], analysed the dynamic response of off-road wheeled vehicles using simple model. From the results of three different vehicles, they concluded that the simple Vehicle model contains many limiting assumptions, it is nevertheless useful in providing designers with some "feel" for ride vibration behaviour. Another justification from their point of view for considering only the simple model is that a more accurate

representation is limited due to the lack of an accurate tyre model.

A comparison between three known computer models; the highway-Vehicle Object Simulation Model (HVOSM), the Automatic Dynamic Analysis of Mechanical Systems (ADAMS), and the Automatic Generation of Equations of Motion (A'GEM) was carried out by Anderson and Hanna [Ref. 12]. Two military wheeled vehicles were used in this study, and it was concluded that the user of ADAMS spends a great deal of time preparing the input data file, and a similarly long time is required in preparing the vehicle data for HVOSM model, whilst, the A'GEM model requires less human effort than either of the other models and is more accurate than the HVOSM, but it is based upon linear analysis only which makes its predictions less accurate than those of ADAMS.

In 1989 Bakr, Gastouniotis and Shabana [Ref 13], presented a new method for the dynamic analysis of multi-body walking vehicles that consist of interconnected rigid and flexible components. The system differential equations of motion were solved by a direct numerical integration method. They concluded that the numerical experimentations indicate that the flexibility of the walking vehicle components does have a significant effect on the overall dynamic response of the system. This kind of models is not general and requires some effort to represent a specific Vehicle.

2.2 MOBILITY OF THE OFF-ROAD VEHICLES:

In the field of mobility and comfort, the interaction between vehicles and terrain is quite important. On rigid soils, there is no significant problem with the mobility as well as the comfort of the vehicles, but for unprepared terrains (off-road) the behaviour of vehicles is different than on rigid terrains. This field of study is called "Terramechancis", and its aim is to provide guiding principles for the rational design, testing, selection, and evaluation of off-road vehicles and terrain working machinery.

In 1969, the Waterway Experiment Station (WES) of the US army has developed a simulation model, and they called it the "AMC 71" model [Ref. 14]. The model is used to predict the maximum cross country speed of tracked or wheeled vehicles. In the model the vehicle vibrations due to ground influences and accelerations while crossing single obstacles are treated in two dimensions only. Within the vertical centreline plane, longitudinal vibrations and accelerations are not considered and motions are not included. This causes inaccurate predictions because the vibratory power absorbed by the driver due to roll motion and longitudinal impacts is significant. The soil submodel is based on an empirical system which has been verified to have an acceptable accuracy for a variety of soil conditions. No tyre or suspension compliance is considered in calculating obstacle interference. Although ground roughness to cause severe vibrations, is usually hard, neglecting soil deformation and its smoothing effect on ride may result in predictions which are too conservative. A mathematical system based on fundamental soil properties and on the differential equations of soil-equilibrium and yield conditions would be more general, accurate and flexible.

A useful technique for measuring the soil properties was introduced, together with some tables about relevant soil parameters, in [Ref. 15].

A book on the theory of ground vehicles was written by Wong, [Ref. 16], where it was mentioned that the characteristics of a ground vehicle may be described in terms of its performance characteristics including the ability of the vehicle to accelerate, to develop drawbar pull to overcome obstacles, and to decelerate.

Various methods of approach to the analysis of wheel-soil interaction are reviewed and examined and their applications were discussed in 1989 by Wong [Ref. 17], such as the prediction of the performance of a wheel in relation to its design parameters and terrain conditions, and the prediction of the changes of soil conditions caused by the passage of the wheel. He concluded that the behaviour of the soil and the pertinent design parameters of the wheel are the basic input and must, therefore, be quantitatively defined.

A study of the track-soil interaction was carried out by Yong in 1984 [Ref 18]. Depending on existing research, he concluded that proper tools are needed to provide the kinds of measurements required to develop realistic analysis which correctly model the actual interaction performance between track and soil. Until more realistic information from actual track studies in the field become available, it is necessary for analysts to exercise proper judgment and caution in modelling for analytical predictions.

Marinshaw [Ref. 19] outlined the basic requirements, for dealing with mobility of a tracked vehicle. First, parameters necessary to define mobility should be identified. Second, analytical methods and evaluation criteria necessary to assess mobility are to be established. Finally, the obtained results should be validated by means of vehicle testing. He also suggested a systematic analytical method as a means for achieving tracked vehicle mobility requirements.

A model called Carleton Tracked vehicle Performance Model(CTVPM), was published in 1984 by Wong et al [Ref. 20]. In this model the effects of all major vehicle design parameters are taken into consideration, such as the number of road wheels, road wheel spacing and dimensions, track dimensions, initial track tension, suspension heave stiffness, and location of the centre of gravity of the vehicle. The pressure-sinkage and shearing characteristic of the terrain, as well as its response to the repetitive normal and shear loading are considered in the analysis of the mechanics of track-terrain interaction. The track is modelled as a flexible belt and in determining the sinkage of the track the effects of the independent suspensions of the road-wheels are neglected.

In 1986 [Ref. 21] a new model was developed by Wong and Preston-Thomas, and it was called Nepean Tracked Vehicle Performance Model-85 (NTVPM-85). This model has overcome some problems which they had not been taken into consideration in CTVPM model. It considers the sinkage of the vehicle till the belly (or hull) becomes in contact with some types of terrain such as deep snow, soft muskeg, or mud.

In 1987 [REf. 22] a third model known as (NTVPM-86) was developed by the same authors. In this model the road wheel centre was no longer assumed to be rigidly connected and the characteristics of the track link were also taken into consideration.

An experimental work to analyse the viscoelastic behaviour of soil and compare it with the results obtained by means of a finite element method program, was carried out by Oida in 1984 [Ref. 23]. In this work the author presented the time-dependent sinkage of rigid wheel and the soil as one mechanical system, and setting the axial load of the wheel as the load boundary condition. He concluded that the simulated sinkage coincided well with the measured one.

2.3 REVIEW OF HUMAN VIBRATION TOLERANCE CRITERIA:

In 1966 Pradko, Lee, and Kaluza [Ref. 24], studied the whole-body human response to mechanical vibration below 60 Hz. The theoretical considerations in this work are based on the view that man's response in a vibratory environment can be determined through measurement of input conditions only, and they end up by producing a new parameter, for measuring the amount of vibration which can be absorbed by the body of the humanbeing, identified as the "absorbed power".

In 1968 Lee, and Pradko [Ref. 25], introduced analytical expressions for transfer functions required to calculate the absorbed power term, and they concluded that the absorbed power can be evaluated in three directions, fore-aft, vertical, side to side, depending on the transfer function known at each direction and the frequency.

A comparison of time domain and frequency domain analysis of off-road vehicles was done in 1969 [Ref. 26], by Lins, Hoogterp, and Pradko. The difference between the two techniques to analyse the dynamic response of a vehicle travelling on a non-deformable off road terrain, together with a comparison between the computed results, the computation times, and the costs were investigated. It was concluded that the time domain analysis is the best for accurate results if the time and the costs are not at premium and the system nonlinearities have little or no effect.

In 1972 Lins, and Dugoff [Ref. 27], carried out an experimental investigation using two motion simulators, one has four degrees-of-freedom, and the other has a single degree-of-freedom. Both simulators were used to acquire information on the whole-body and visual response to vibration. Useful empirical expressions of vertical, fore-aft, and side to side human response transfer functions were achieved.

A brief literature review and analysis of the subjective tolerance question together with a study of vehicle vibration and the importance of seating systems which attenuate vehicle vibration was demonstrated by Stikeleather, Hall and Radke in 1972 [Ref 28]. They concluded that the subjective criteria could be applied with full knowledge of the vibration levels which are being satisfactorily tolerated under actual vehicle operating conditions.

Criteria of vibration acceleration versus frequency for ride comfort, which approximated the absorbed power characteristics of Pradko and Lee [Ref. 25], were recommended by Janeway [Ref 29]. Ride evaluation guidelines were given for instrumentation in keeping with the recommended criteria, and for the ISO (International Standard organization) indicated vertical comfort level at 4-8 Hz, and 8 hours exposure time.

In 1976 Stikeleather [Ref. 30], reviewed a three ride vibration standard and tolerance criteria, which are the ISO 2631, the American absorbed power, and the German " K " factor. He summerised the basic aspects of these criteria, and he concluded that there is enough similarity between existing criteria to assume each has a certain validity for predicting human responses.

An analysis was carried out in 1984 by Newell and Murrphy [Ref.31], in the ride quality assessment employing two widely used criteria, which are the absorbed power and the ISO. They concluded that for short distance travel and limits based on safety and health, both the absorbed power and ISO produce similar ride performance relations.

Hohl [Ref. 32], did an experimental and theoretical analysis for a proposed model of a human body using four types of off-road vehicles to judge the ride comfort. Using the existing criteria such as the K-values, and the ISO, he concluded that the main factor which can be influenced by the user of a vehicle system is the speed, other factors are spring system and seat construction which can be altered by the designer. These components should also be considered in vehicle tests.

2.4 NUMERICAL INTEGRATION METHODS:

The numerical solution of ordinary differential equations (ODE's) is an old topic and, perhaps surprisingly, methods discovered around the turn of the century are still the basic of the most effective, widely used codes for this purpose. Great improvements in efficiency have been made, but it is probably fair to say that the most significant achievements have been in reliability, convenience, and diagnostic capabilities. Typical scientific problems can be solved by casual users of these codes both easily and cheaply. Nevertheless there are several kinds of problems which classical methods do not handle very efficiently, such as the problems called "stiff". By a stiff problem we mean the one for which no solution component is stable (no eigenvalue has a real part which is at all large and positive) and at least some component is very stable (at least one eigenvalue has a real part which is large and negative). Further, a problem is not considered stiff unless its solution is slowly varying with respect to the most negative real part of the eigenvalues [Ref. 33], [Ref. 34].

With reference to an ODE, it becomes stiff when there are severe restrictions on the time step size as employed by the classical solver. The use of stiff ODE solvers is advisable in the event of failure of classical solvers [Ref. 35].

In recent years a series of step-by-step integration methods are developed to deal with linear and nonlinear stiff ODE, such as a new scheme developed by the Applied Mechanics Group of Cranfield Institute of Technology, based upon a Hermitian weighted residual method [Ref. 36].

A computational procedure of some numerical integration methods , such as the Wilson θ method, the Houbolt method, and the Central difference method, was demonstrated by Bathe in 1982 [Ref.37]. These direct integration methods show a reasonable accuracy but they may require more investigation to prove their numerical stability, for stiff problems.

A new generalized algorithm in the class of single step time marching schemes was developed for the solution of dynamic equation of motion by Hoff and Pahl in 1988 [Ref 38]. The algorithm includes various known methods, such as the Newmark-β method, and the Collocation method. After theoretical investigation of the spectral stability, the truncation error, and overshooting behaviour of the new algorithm, they concluded that it can yield good results because the numerical dissipation is not associated with disadvantages, such as the decrease in accuracy, and a final test of the method must consist of practical calculations for real systems, especially the overshooting effects must be investigated for real systems.

The same scheme using a proposed method called θ_1-method in structural dynamics was presented by the same authors in 1988 [Ref. 39]. They concluded that the θ_1-method shows some advantages over other known methods, especially in accuracy and overshooting behaviour.

By means of the weighted residual method a general form of linear multi-step method is developed for time dependent vibrating systems by Gao and Zhang in 1988 [Ref. 40]. They concluded that the two-step method obtained from the multi-step method can be used not only to solve initial value problems of time-dependent systems, but also to seek the steady-state solution of periodically time-dependent systems.

An explicit-explicit sub-cycling procedure for the finite element analysis of structural dynamics is developed by Neal and Belytschko in 1989 [Ref. 41]. They concluded that it has a flexibility in exploiting the increased stability of domains with larger or more flexible elements.

A survey of some of direct time integration methods and computational solution procedures was carried out in two parts by Subbaraj and Dokainish, where the explicit methods such as Central difference methods, Runge-kutta method, and stiffly stable methods are in the first part [Ref. 42], whilst part two [Ref. 43] covers the Newmark method, the Wilson θ method, and the Houbolt method, the

numerical stability of which has been investigated, and useful results were achieved.

Some of the above methods can be applied to solve linear and nonlinear problems others are suitable for linear only, but all together need a deep investigation and validation to check their numerical stability. The nature of the problem plays a significant key rule in this case.

2.5 CONCLUSIONS:

It is clear from the literature that the basic aspects in the subject of ride analysis for off-road vehicles can be divided into four basic topics:

a) The off-road suspension models
b) The vehicle-terrain interactions
c) The ride tolerance criteria, and
d) The numerical solution methods.

Considering the suspension modelling, most of the models demonstrated in the literature are based upon classical suspension elements (lumped masses, springs, dashpots), which are limited in theory for dealing with general types of suspension elements for off-road vehicles, and can not yield an accurate ride analysis.

It is obvious that very few models employ the finite element method, and this may be due to the fact that the finite element method is new compared with other known methods.

It can also be observed that many of those models have limited objectives in dealing with the analysis of specific phenomena and they lack experimental validation. Few non-linear aspects, such as non-linear spring and damper characteristics have been covered in the literature. However, there is a very little published on dealing with other sources of non-linearity such as wheel separation, bump stops, and soil effects. The track effect on ride analysis and limiting

speed of the vehicle over different types of terrain has not been fully investigated.

Generally speaking, it can be said that most of the models found in the literature, although limited to the analysis of few vehicle characteristics, they are advantageous in providing a means for an approximate estimation of the effects of some critical parameters on the dynamic characteristics of the vehicle such as the effects of hull flexibility and track stiffness. With the development of experimental work, it becomes possible to design and validate computer simulation modules based on theoretical methods.

The second ride analysis aspect, the vehicle terrain interaction, is the one on which there are many publications. Unfortunately, most of the published work has considered rigid soil terrain with standard test courses. This is far from establishing a general theory for ride analysis of off-road vehicles which are expected to be operating on a variety of soils and unprepared terrains. Although it seems that some researchers have tried to deal with soil properties but the connection between the soil and the ride of suspension systems is obviously missing.

As for ride tolerance criteria, a limited amount of research has been carried out, and most of which concentrated on the relation between vibrations and their effect on humanbeings; the driver or the crew of the vehicle. It is clear from the literature that there are only three different criteria for ride tolerance. This shortage of work could be due to the complexity of the analysis of the physical response of humanbeings to different types of vibration, and it may require a sophisticated non-destructive experimentation.

Finally, with regard to numerical solution methods, it was observed that most of the ordinary methods suffer from numerical instability problems due to the fact that the differential equations of motion for off-road vehicle suspension systems, are classified as stiff equations which have specific requirements for stable time-marching schemes. Most of the available techniques have failed to handle this type of equations and their numerical stability is extremely

conditional.

In the light of the above conçlusions, the objectives of this work have been emphasized. It is clear that a comprehensive system capable of dealing with the ride analysis of off-road suspension vehicles, based upon an accurate representation of different types of suspension elements will be extremely useful. The developed system should contain its own complete library of routines to allow the user to be able to control the numerical stability of time marching schemes. The author has decided to use the finite element method due to its flexibility and reliability.

CHAPTER THREE

MODELLING OF GENERAL OFF-ROAD VEHICLES

3.1 INTRODUCTION:

In the modelling of the suspension systems of general off-road vehicles the spring and damper assemblies connecting the unsprung mass to the main frame describe the suspension compliance, while the spring and damper assemblies below the unsprung masses serve to describe the tyre compliance. The mass elements are assumed to be rigid bodies, and the spring elements possessing elasticity are assumed to be of negligible mass.

There are two common types of damping which occur in vehicle suspensions. The first one is the Coulomb damping, sometimes called frictional damping, in which the damping force is a function of the normal force between the sliding bodies as well as the material involved (as in leaf springs). The other type, which is used most often in modelling, is that which is characterized by dashpot action in which the damping force depends on the relative velocity of the deformation. The most popular damper of this kind is the telescopic damper which is used in the majority of the commercial vehicles as well as in modern military tracked vehicles for example the British Challenger tank.There is also the rotary-vane damper in which the force is transmitted from the road wheel by means of a four bar mechanism, which aims at gaining some mechanical advantages . This type is used in the Scorpion tank. A schematic digram of different types of dampers is shown in Figure 3.1.

Coil and leaf springs are the most popular types of springs used in suspension systems, also torsion bars acting as springs are employed in most of the military tracked vehicles.

In the following items general off-road vehicle models are described and the characteristic equations of different types of suspension elements are derived.

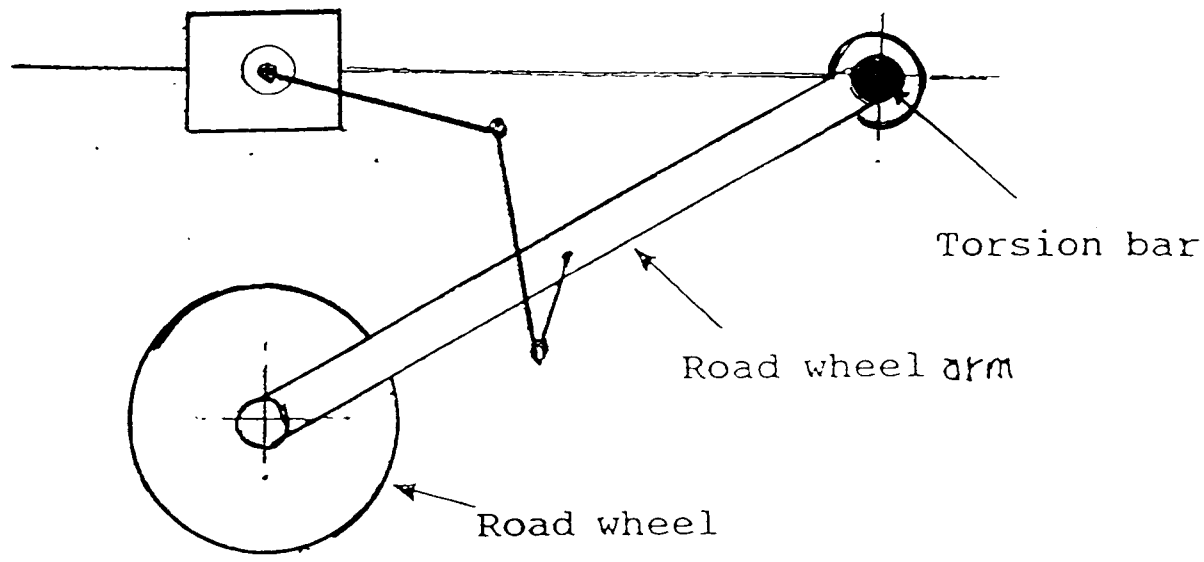

Rotary-vane damper

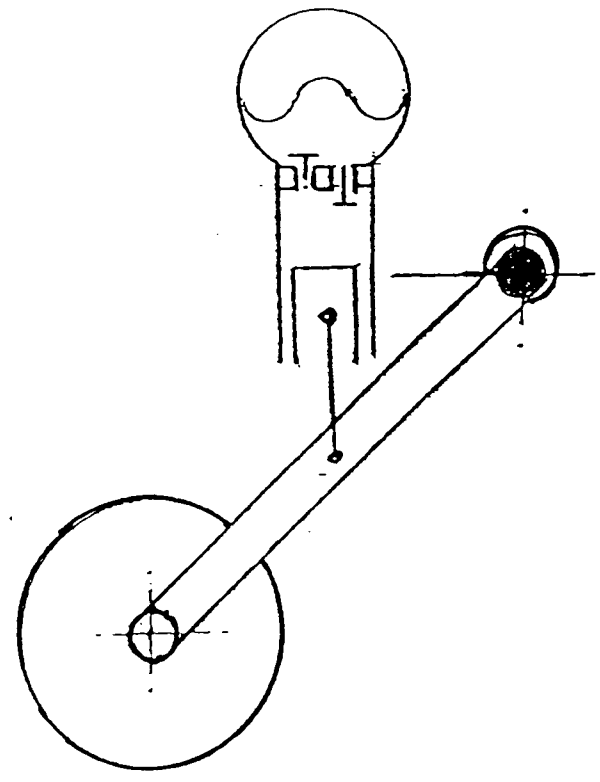

Hydrogas unit damper

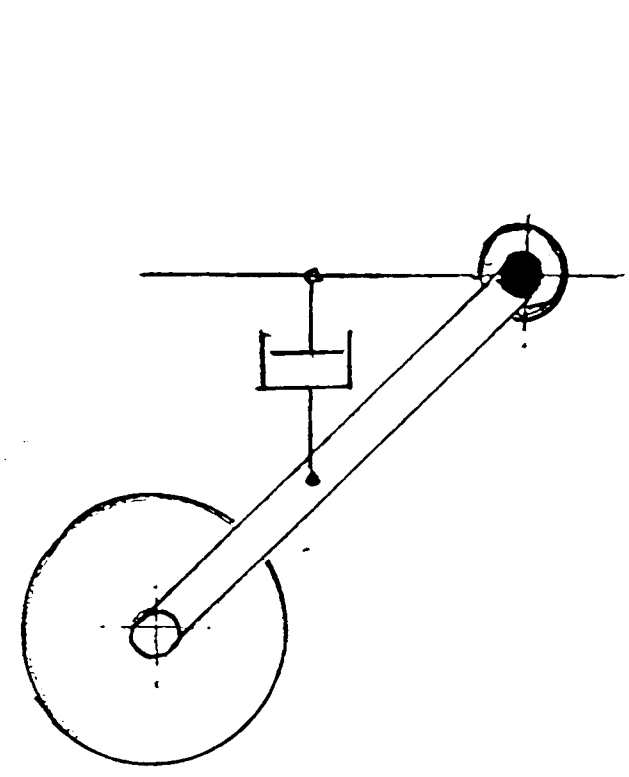

Telescopic damper

Fig (3.1) Types of Off-Road Vehicle Dampers.

3.2 COORDINATE SYSTEMS:

The number of degree of freedom of any system is determined by the number of independent coordinates required to describe the configuration of each mass of the system. Generally, three coordinates are required to describe the configuration of the spring mass (bounce, pitch, and roll).

Four separate coordinate systems are used in the present work as shown in Figure(3.2), and are summarised as follows:

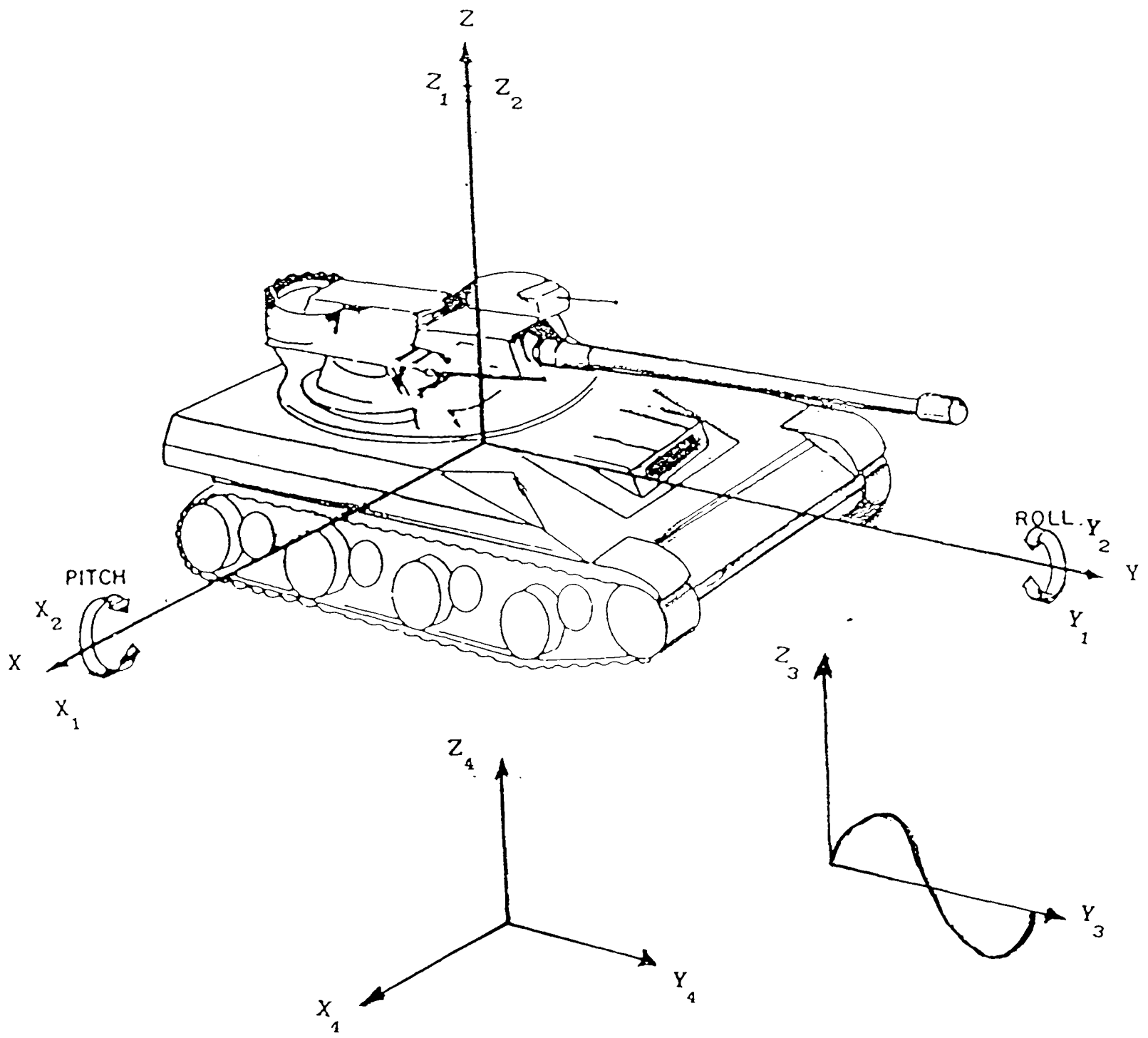

Fig (3.2) Off-Road Vehicle Different Coordinate Systems.

a) Vehicle Input Coordinate System:

This coordinate system is centred at the vehicle C.G. when the vehicle is resting on a hard flat surface and facing the right hand side of the observer. The X-axis and Y-axis are parallel to the surface, while the Z-axis is perpendicular to it. The axes of this system are denoted as X_1, Y_1, Z_1 axes.

b) Vehicle Coordinate System:

This system is centred at the vehicle C.G. and moves with the vehicle. In fact, the initial position of the axes is the same as the vehicle input data coordinate system. The axes of this second system are represented as X_2, Y_2, Z_2 axes.

c) Ground-Vehicle Coordinate System:

This system is assumed to remain fixed to the ground and is centred at the starting point of the surface profile of the specified terrain. It is denoted by Y_3, Z_3axes.

d) Vehicle Fixed-Ground Parallel Coordinate System:

This coordinate system is centred at the C.G. and moves with the vehicle, however it remains parallel to the ground fixed coordinate system. Initially it coincides with the vehicle coordinate system when the vehicle is at rest on hard, flat ground. This system is represented by X_4, Y_4, Z_4 axes.

The motion of the C.G. is restricted to the Z_4 direction (bounce), rotation about X_4-axis (pitch), and rotation about Y_4-axis (roll).

Effect of a Rotation About the X-Axis:

Consider a rigid rotation of the hull with respect to the X-axis by an angle θ_o. For a point P which is initially at or (r,α), as shown

in Figure 3.3 a, and moves to P′ due to that rotation, then it can be proved that its movement in the Z direction is:

$$\Delta D_\theta = r \sin(\theta_o + \alpha) - r \sin \alpha$$
$$= r(\sin \theta_o \cos \alpha + \cos \theta_o \sin \alpha) - r \sin \alpha$$

Using

$$r \sin \alpha = Z - Z_o$$
$$r \cos \alpha = Y - Y_o$$

it can be deduced that

$$\Delta D_\theta = (Y - Y_o) \sin \theta_o - (Z - Z_o)(1 - \cos \theta_o)$$

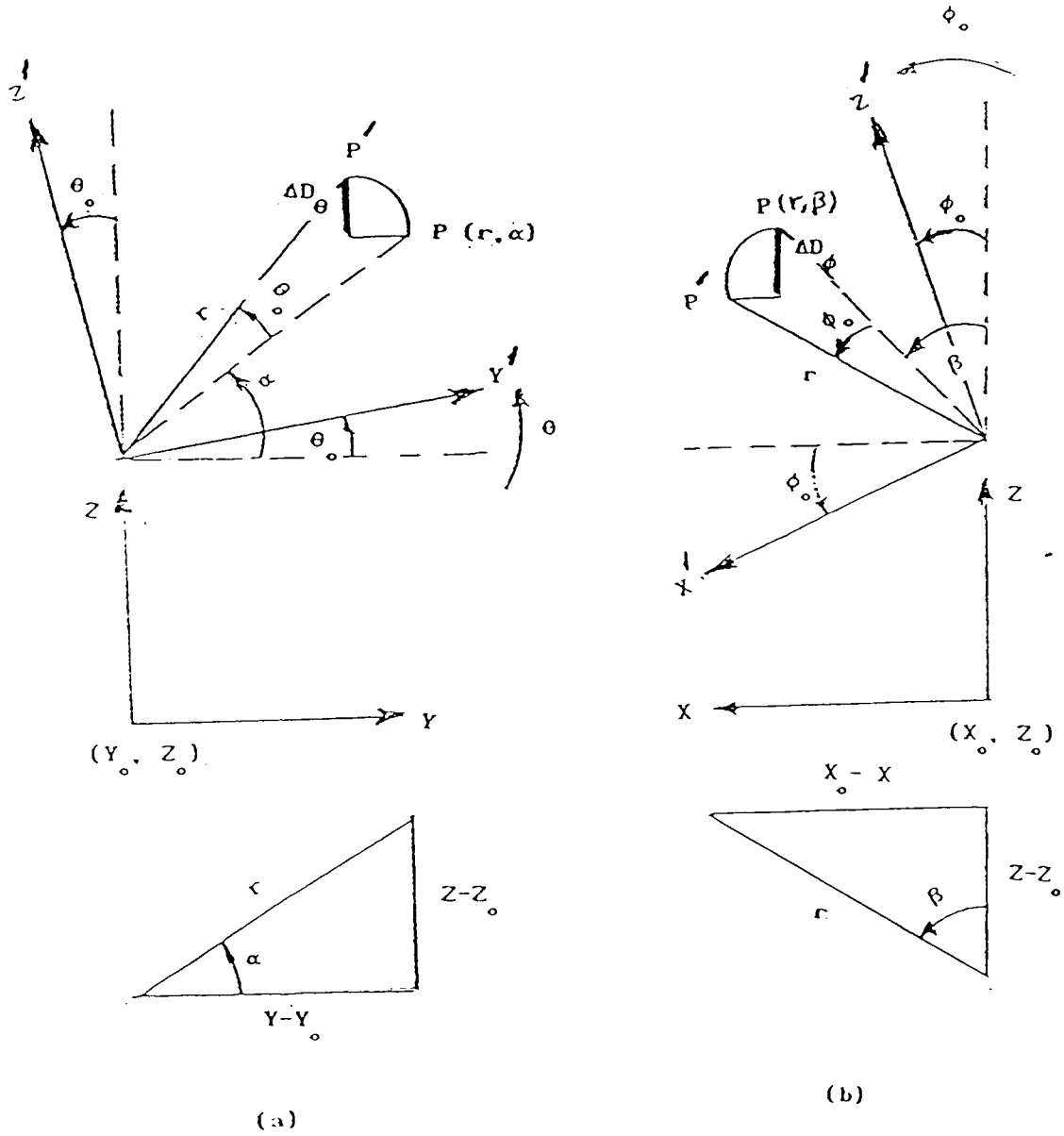

Fig (3.3) Effect of Rotations About the X and Y Axes.

Effect of a Rotation About the Y-Axis:

In this case if the hull rotation is assumed to be with respect to Y-axis by an angle ϕ_o. For P (r,β) moves to P' as shown in Figure 3.3b, and it can be proved that the movement in Z direction is:

$$\begin{aligned}\Delta D_\phi &= r\cos(\phi_o + \beta) - r\cos\beta \\ &= r\cos\phi_o\cos\beta - r\sin\phi_o\sin\beta - r\cos\beta \\ &= -r\sin\phi_o\sin\beta - r\cos\beta\,(1-\cos\phi_o)\end{aligned}$$

using

$$r\cos\beta = Z - Z_o$$
$$r\sin\beta = X - X_o$$

it can be proved that

$$\Delta D_\phi = (X_o - X)\sin\phi_o - (Z - Z_o)(1-\cos\phi_o)$$

Effect of the C.G. Bounce δ_o, Pitch θ_o, and Roll ϕ_o:

The contribution of all movements in Z direction to the hull C.G.can be expressed as follows:

$$\begin{aligned}\delta(x,y,z,t) &= \delta_o + (Y - Y_o)\sin\theta_o - (Z - Z_o)(1-\cos\theta_o) \\ &\quad + (X_o - X)\sin\phi_o - (Z - Z_o)(1-\cos\phi_o)\end{aligned}$$

$$\begin{aligned}&= \delta_o + (Y - Y_o)\sin\theta_o + (X_o - X)\sin\phi_o \\ &\quad - (Z - Z_o)(2 - \cos\theta_o - \cos\phi_o) \qquad (3.1)\end{aligned}$$

Equation (3.1) gives the contribution of the vertical displacement δ_o to the pitch and roll. The velocity $\dot{\delta}$ is :

$$\begin{aligned}\dot{\delta}(x,y,z,t) &= \dot{\delta}_o + [(Y - Y_o)\cos\theta_o - (Z - Z_o)\sin\theta_o]\,\dot{\theta}_o \\ &\quad + [(X_o - X)\cos\phi_o - (Z - Z_o)\sin\phi_o]\,\dot{\phi}_o \qquad (3.2)\end{aligned}$$

and the acceleration $\ddot{\delta}$ is :

$$\ddot{\delta}(x,y,z,t) = \ddot{\delta}_o + [(Y - Y_o)\cos\theta_o - (Z - Z_o)\sin\theta_o]\,\ddot{\theta}_o$$

$$- [(Z - Z_o)\cos\theta_o + (Y - Y_o)\sin\theta_o]\left[\dot{\theta}_o\right]^2$$

$$+ [(X_o - X)\cos\phi_o - (Z - Z_o)\sin\phi_o]\,\ddot{\phi}_o$$

$$- [(Z - Z_o)\cos\phi_o + (Y - Y_o)\sin\phi_o]\left[\dot{\phi}\right]^2 \qquad (3.3)$$

3.3 SIMULATION OF SUSPENSION SYSTEMS USING THE FINITE ELEMENT METHOD:

Element matrices are obtained by considering the equations of motion of the hull and every road wheel. However, only the contributions of an element to such equations define element matrices.

The vector of the total degrees of freedom can be defined as follows:

$$\underline{\delta} = \left\{ \delta_o \;\; \theta_o \;\; \Phi_o \;\; \delta^{(1)} \;\; \delta_T^{(1)} \;\; \delta^{(2)} \;\; \delta_T^{(2)} \;\; \ldots\ldots\ldots \right\}$$

where

$\left\{ \delta_o \;\; \theta_o \;\; \Phi_o \right\}$ are displacement, and rotations for the hull, at its C.G.,

$\left\{ \delta^{(e)} \;\; \delta_T^{(e)} \right\}$ are the displacements of the e^{th} road wheel, at the wheel centre and the point of contact with the ground, etc.

For the e^{th} Suspension element, the element displacement vector is defined as follows:

$$\underline{\delta}^{(e)} = \left\{ \delta_o \;\; \theta_o \;\; \Phi_o \;\; \delta^{(e)} \;\; \delta_T^{(e)} \right\}$$

The superscripts will not be written unless more than one element are considered.

The hull is considered as a rigid mass element, the $zero^{th}$ element, with:

$$\underline{\delta}^{(0)} = \left\{ \delta_o \;\; \theta_o \;\; \Phi_o \;\; 0 \;\; 0 \right\}$$

$$\underline{M} = \begin{bmatrix} M & I_x & I_y & 0 & 0 \end{bmatrix}$$

$$\underline{K} = \begin{bmatrix} \underline{0} \end{bmatrix}$$

$$\underline{C} = \begin{bmatrix} \underline{0} \end{bmatrix}$$

3.3.1 Simple Suspension Element.

This element is used to demonstrate the method of derivation and assembly, so superscripts are kept.

A schematic diagram of the e^{th} element is shown in Figure 3.4, where the following notations are employed:

$K^{(e)}$ = The stiffness of torsion bar (spring) of the element.
$C^{(e)}$ = The damping coefficient of the element damper.
$m^{(e)}$ = The mass of road wheel (or tyre) of the element.
$K_T^{(e)}$, $C_T^{(e)}$ = Equivalent stiffness and damping for the road wheel (or tyre).

$\delta^{(e)}$ = Vertical displacement of the C.G. of the wheel.

$\delta_T^{(e)}$ = Vertical displacement at the point of contact with soil (may be restrained or prescribed).

From the rigidity of the hull and for the special case of small deflection,

$$\frac{\partial \delta_{hull}}{\partial x} \simeq - \Phi_o \quad , \quad \frac{\partial \delta_{hull}}{\partial y} \simeq \theta_o$$

i.e. for any point on the hull at (x,y,z)

$$\delta(x,y,z,t) \simeq \delta_o + (y - y_o)\, \theta_0 + (x_o - x)\, \phi_o \qquad (3.4)$$

$$\dot{\delta}(x,y,z,t) \simeq \dot{\delta}_o + (y - y_o)\, \dot{\theta}_0 + (x_o - x)\, \dot{\phi}_o \qquad (3.5)$$

$$\ddot{\delta}(x,y,z,t) \simeq \ddot{\delta}_o + (y - y_o)\, \ddot{\theta}_0 + (x_o - x)\, \ddot{\phi}_o \qquad (3.6)$$

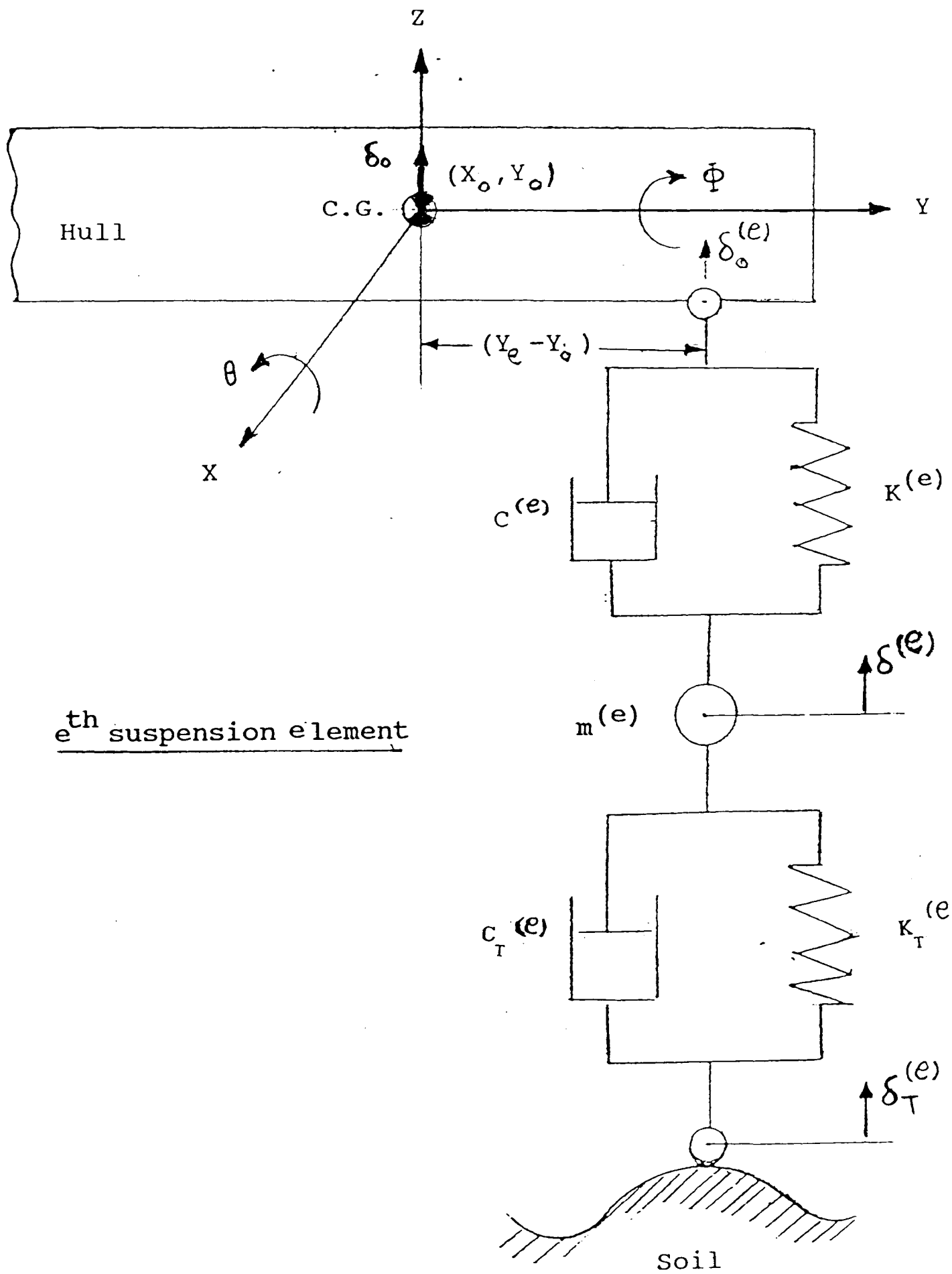

e^{th} suspension element

Fig (3.4) Simple Type of Suspension Elements

The equations of motion of the suspension system can be summarised as follows:

First Equation:

This is the hull equation of motion in the Z-direction. The total force acting on the hull at Z direction:

$$(F_z)_o = \sum (F_z)_{hull}$$

$$= \sum_{e=o}^{n_e} \left[C^{(e)} \left[\dot{\delta}_o^{(e)} - \dot{\delta}^{(e)} \right] + K^{(e)} \left[\delta_o^{(e)} - \delta^{(e)} \right] \right] + M \ddot{\delta}_o$$

where

n_e ....The number of element.

The contribution of the e^{th} element can be expressed as follows:

$$(F_z)_o = \sum_{e=1}^{n_e} F_z^{(e)}$$

where

$$F_z^{(e)} = C^{(e)} \left[\dot{\delta}_o^{(e)} - \dot{\delta}^{(e)} \right] + K^{(e)} \left[\delta_o^{(e)} - \delta^{(e)} \right] \qquad (3.7)$$

Substituting equations (3.4), and (3.5) in to equation (3.7) it can be deduced that:

$$F_z^{(e)} = C^{(e)}\left[\dot{\delta}_o + (y_e - y_o)\,\dot{\theta}_0 + (x_o - x_e)\,\dot{\phi}_o - \dot{\delta}^{(e)}\right]$$

$$+ K^{(e)}\left[\delta_o + (y_e - y_o)\,\theta_0 + (x_o - x_e)\,\phi_o - \delta^{(e)}\right] \qquad (3.8)$$

$$e > 0$$

and the hull force is

$$F_z^{(o)} = M\,\ddot{\delta}_o$$

Second Equation

This equation represents the angular equation of motion with respect to the X direction.

The total moment acting on the hull at X direction is given by:

$$M_x = \sum (M_x)_{hull}$$

$$= I_x\,\ddot{\theta}_o + \sum_{e=1}^{n_e}\left[C^{(e)}\left(\dot{\delta}_o^{(e)} - \dot{\delta}^{(e)}\right)(y_e - y_o)\right.$$

$$\left. + K^{(e)}\left(\delta_o^{(e)} - \delta^{(e)}\right)(y_e - y_o)\right]$$

$$= \sum_{e=o}^{n_e} M_x^{(e)}$$

where

$$M_x^{(o)} = I_x \ddot{\theta}_o$$

and the contribution of the e^{th} element is:

$$M_x^{(e)} = C^{(e)}(y_e - y_o)\left[\dot{\delta}_o + (y_e - y_o)\dot{\theta}_0 + (x_o - x_e)\dot{\phi}_o - \dot{\delta}^{(e)}\right]$$

$$+ K^{(e)}(y_e - y_o)\left[\delta_o + (y_e - y_o)\theta_0\right.$$

$$\left. + (x_o - x_e)\phi_o - \delta^{(e)}\right] \qquad (3.9)$$

$$e > 0$$

Third Equation

The total moment acting on the hull at Y direction is:

$$M_y = I_y \ddot{\Phi}_o + \sum_{e=1}^{n_e}\left[C^{(e)}\left(\dot{\delta}_o^{(e)} - \dot{\delta}^{(e)}\right)(x_o - x_e)\right.$$

$$\left. + K^{(e)}\left(\delta_o^{(e)} - \delta^{(e)}\right)(x_o - x_e)\right]$$

$$= \sum_{e=o}^{n_e} M_y^{(e)}$$

where

$$M_y^{(o)} = I_y \ddot{\Phi}_o$$

and the contribution of the e^{th} element is:

$$M_y^{(e)} = C^{(e)} (x_o - x_e) \left[\dot{\delta}_o + (y_e - y_o) \dot{\theta}_0 + (x_o - x_e) \dot{\phi}_o - \dot{\delta}^{(e)} \right]$$

$$+ K^{(e)} (x_o - x_e) \left[\delta_o + (y_e - y_o) \theta_0 \right.$$

$$\left. + (x_o - x_e) \phi_o - \delta^{(e)} \right] \qquad (3.10)$$

$$e > 0$$

Equation (2e+2) $\quad e = 1,2,..,n_e$

This equation represents the equation of motion of the e^{th} road wheel in the Z direction.

The force acting on the e^{th} road wheel is:

$$(F_z)_e = \sum (F_z)_e$$

$$= m^{(e)} \ddot{\delta}^{(e)} + C^{(e)} \left[\dot{\delta}^{(e)} - \dot{\delta}_o^{(e)} \right]$$

$$+ K^{(e)} \left[\delta^{(e)} - \delta_o^{(e)} \right]$$

$$+ C_T^{(e)} \left[\dot{\delta}^{(e)} - \dot{\delta}_T^{(e)} \right]$$

$$+ K_T^{(e)} \left[\delta^{(e)} - \delta_T^{(e)} \right] \qquad (3.11)$$

Substituting equations (3.4), and (3.5) in to equation (3.11), and rearranging the terms it can be proved that:

$$(F_z)_e = m^{(e)} \ddot{\delta}^{(e)} + \left[C^{(e)} + C_T^{(e)} \right] \dot{\delta}^{(e)}$$

$$- C^{(e)} \left[\dot{\delta}_o + (y_e - y_o) \dot{\theta}_0 + (x_o - x_e) \dot{\phi}_o \right]$$

$$- C_T^{(e)} \dot{\delta}_T^{(e)} + \left[K^{(e)} + K_T^{(e)} \right] \delta^{(e)}$$

$$- K^{(e)} \left[\delta_o + (y_e - y_o) \theta_0 + (x_o - x_e) \phi_o \right]$$

$$- K_T^{(e)} \delta_T^{(e)} \qquad (3.12)$$

Equation (2e + 3) $e = 1,2,..,n_e$

This equation is based upon the equilibrium of the e^{th} road wheel contact point with the ground, and the force acting on the e^{th} contact point is:

$$(R_z)_e = C_T^{(e)} \left[\dot{\delta}_T^{(e)} - \dot{\delta}^{(e)} \right]$$

$$+ K_T^{(e)} \left[\delta_T^{(e)} - \delta^{(e)} \right] \qquad (3.13)$$

The total equations of the hull and the suspension system can be represented by means of the following matrix form:

$$\begin{bmatrix} (F_z)_o \\ M_x \\ M_y \\ (F_z)_1 \\ (R_z)_1 \\ (F_z)_2 \\ (R_z)_2 \\ \cdot\ \cdot \end{bmatrix} = \underline{M}\,\ddot{\underline{\delta}} + \underline{C}\,\dot{\underline{\delta}} + \underline{K}\,\underline{\delta}$$

where

$$\underline{\delta} = \left\{ \delta_o \;\; \theta_o \;\; \Phi_o \;\; \delta^{(1)} \;\; \delta_T^{(1)} \;\; \delta^{(2)} \;\; \delta_T^{(2)} \;\; \cdots\cdots\cdots \right\}$$

If the assembly rules of the FEM are applied such that:

$$\underline{\delta}^{(e)} = \left\{ \delta_o \;\; \theta_o \;\; \Phi_o \;\; \delta^{(e)} \;\; \delta_T^{(e)} \right\}$$

$$\underline{F}^{(o)} = \left\{ (F_z)_o \;\; M_x \;\; M_y \;\; 0 \;\; 0 \right\}$$

$$\underline{F}^{(e)} = \left\{ 0 \;\; 0 \;\; 0 \;\; (F_z)_e \;\; (R_z)_e \right\} \quad e > 0$$

$$\underline{F} = \sum_{e=0}^{n_e} \underline{F}^{(e)}$$

one can write:

$$\underline{F} = \sum_{e=0}^{n_e} \underline{F}^{(e)}$$

$$= \sum_{e=o}^{n_e} \left[\underline{M}^{(e)} \ \ddot{\underline{\delta}}^{(e)} + \underline{C}^{(e)} \ \dot{\underline{\delta}}^{(e)} + \underline{K}^{(e)} \ \underline{\delta}^{(e)} \right] \qquad (3.14)$$

where the summations are carried out according to the FEM assembly rules. For the simple suspension element, defining:

$$\Delta y_e = y_e - y_o \ , \qquad \Delta x_e = x_o - x_e$$

and dropping the superscripts in the RHS terms, the element matrices may be defined as follows:

$$\underline{M}^{(e)} = \begin{bmatrix} 0 & 0 & 0 & m & 0 \end{bmatrix}$$

$$\underline{C}^{(e)} = \begin{bmatrix} C & \Delta y_e C & \Delta x_e C & -C & 0 \\ \Delta y_e C & (\Delta y_e)^2 C & \Delta y_e \Delta x_e C & -\Delta y_e C & 0 \\ \Delta x_e C & (\Delta y_e \Delta x_e) C & (\Delta x_e)^2 C & -\Delta x_e C & 0 \\ -C & -\Delta y_e C & -\Delta x_e C & C + C_T & -C_T \\ 0 & 0 & 0 & -C_T & C_T \end{bmatrix}$$

$$\underline{K}^{(e)} = \begin{bmatrix} K & \Delta y_e K & \Delta x_e K & -K & 0 \\ \Delta y_e K & (\Delta y_e)^2 K & \Delta y_e \Delta x_e K & -\Delta y_e K & 0 \\ \Delta x_e K & (\Delta y_e \Delta x_e) K & (\Delta x_e)^2 K & -\Delta x_e K & 0 \\ -K & -\Delta y_e K & -\Delta x_e K & K + K_T & -K_T \\ 0 & 0 & 0 & -K_T & K_T \end{bmatrix}$$

3.3.2 Second Type of Suspension Elements

This element represents the hydrogas unit used sometimes in the suspension system of off-road vehicles, and schematic diagram for it is shown in Figure 3.5. The derivation of the equations of this element can be carried out in a way similar to that employed for previous element and the contribution of the Coulomb friction (α) is included with the damping force.

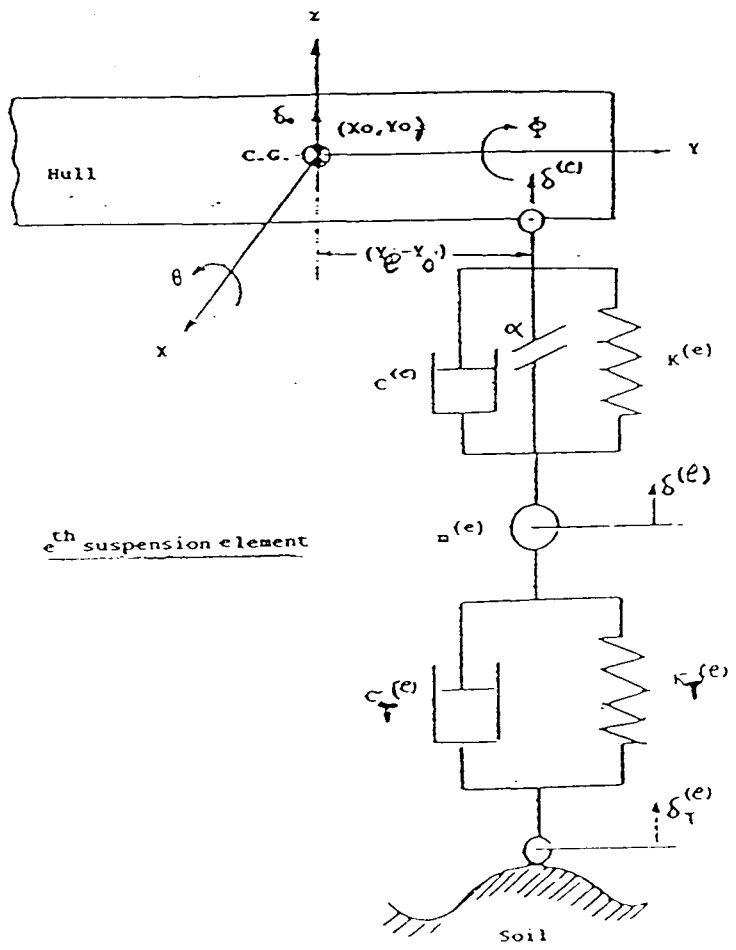

Fig (3.5) Second Type of Suspension Elements.

The element matrices can be expressed as follows:

$$\underline{M}^{(e)} = \begin{bmatrix} 0 & 0 & 0 & m & 0 \end{bmatrix}$$

$$\underline{C}^{(e)} = \begin{bmatrix} \mu C & \mu\Delta y_e C & \mu\Delta x_e C & -\mu C & 0 \\ \mu\Delta y_e C & \mu(\Delta y_e)^2 C & \mu\Delta y_e \Delta x_e C & -\mu\Delta y_e C & 0 \\ \mu\Delta x_e C & \mu(\Delta y_e \Delta x_e) C & \mu(\Delta x_e)^2 C & -\mu\Delta x_e C & 0 \\ -\mu C & -\mu\Delta y_e C & -\mu\Delta x_e C & \mu C + C_T & -C_T \\ 0 & 0 & 0 & -C_T & C_T \end{bmatrix}$$

$$\underline{K}^{(e)} = \begin{bmatrix} K & \Delta y_e K & \Delta x_e K & -K & 0 \\ \Delta y_e K & (\Delta y_e)^2 K & \Delta y_e \Delta x_e K & -\Delta y_e K & 0 \\ \Delta x_e K & (\Delta y_e \Delta x_e) K & (\Delta x_e)^2 K & -\Delta x_e K & 0 \\ -K & -\Delta y_e K & -\Delta x_e K & K + K_T & -K_T \\ 0 & 0 & 0 & -K_T & K_T \end{bmatrix}$$

where

$$\mu = (1 + \alpha) \quad , \ \alpha < 1$$

3.3.3 Third Type of Suspension Elements

This element represents the standard system for spring and wheel location on modern military tracked vehicles. It consists of a transverse torsion bar directly operated by a longitudinal wheel arm. One end of a telescopic damper is fixed to the vehicle body while the other is attached somewhere between the wheel centre and the torsion bar on the wheel arm, as shown in Figure 3.6.

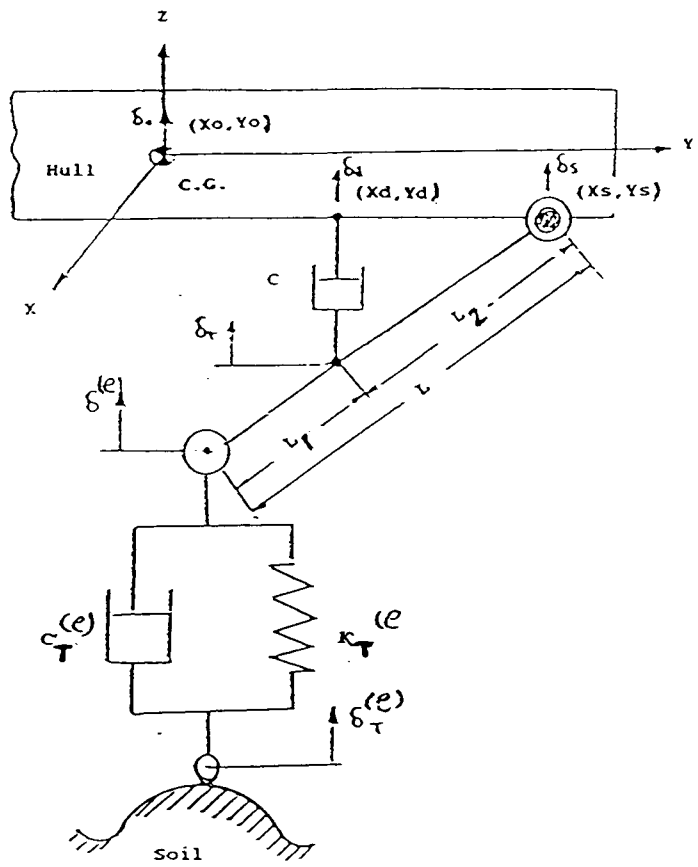

(x_o, y_o) = The x-y Coordinates of the hull.

(x_d, y_d) = The x-y Coordinates of the damper attached point on the hull.

(x_s, y_s) = The x-y Coordinates of the spring attached point on the hull

δ_d = Hull vertical deformation at (x_d, y_d).

δ_s = Hull vertical deformation at (x_s, y_s).

δ_r = Road wheel arm deformation at damper point of fixation.

Fig (3.6) Third Type of Suspension Elements.

Modelling of Torsion Bar Spring

Torsion bars are used in many off-road tracked vehicles, usually the torsion bar is fixed with one end and the other end is connected to the road wheel by an arm called the road wheel arm, which is responsible to transmit the force caused by the ground surface and acting on the road wheel, to the torsion bar. This force will twist the torsion bar, which is usually made of spring steel, by a angle θ, as schematic shown schematically in Figure (3.7).

Applying a force F at the end of the arm to produce vertical displacement δ and rotation θ, then due to the resistance of the torsion bar, a torque M_s is generated such that:

$$M_s = K\,\theta = F\,L\cos\alpha$$

An equivalent stiffness $\bar{K}$ can be defined such that: ($\delta_s = 0$)

$$F = \bar{K}\,\delta$$

$$\therefore \quad K\,\theta = \bar{K}\,\delta\,L\cos\alpha$$

Assuming θ to be very small, then

$$\theta \simeq \delta / L \quad \text{or} \quad \delta = L\,\theta$$

$$K\,\theta = \bar{K}\,L^2\cos\alpha\,\theta$$

or

$$\bar{K} = \left(\frac{K}{L^2\cos\alpha} \right) \tag{3.15}$$

and

$$M_s = \frac{K\,\delta}{L} = \frac{L^2 \cos\alpha\ \bar{K}\,\delta}{L}$$

$$= (\ L \cos\alpha\ )\ \bar{K}\,\delta \qquad (3.16)$$

If the point of fixation on the hull has a vertical deformation δ_s, then, the force acting on the road wheel:

$$F = \bar{K}\ (\ \delta - \delta_s\ )$$

and on the hull:

$$F_s = \bar{K}\ (\ \delta_s - \delta\ )$$

$$M_s = K\ (\ \delta_s - \delta\ )/\ L$$

$$= (\ L \cos\alpha)\ \bar{K}\ (\ \delta_s - \delta\ )$$

The torsion bar spring can now be dealt with in a way similar to that used with simple springs, except the moment M_s should be added to $\sum M_x$ equation. In the following analysis, only the contributions of the element will be considered.

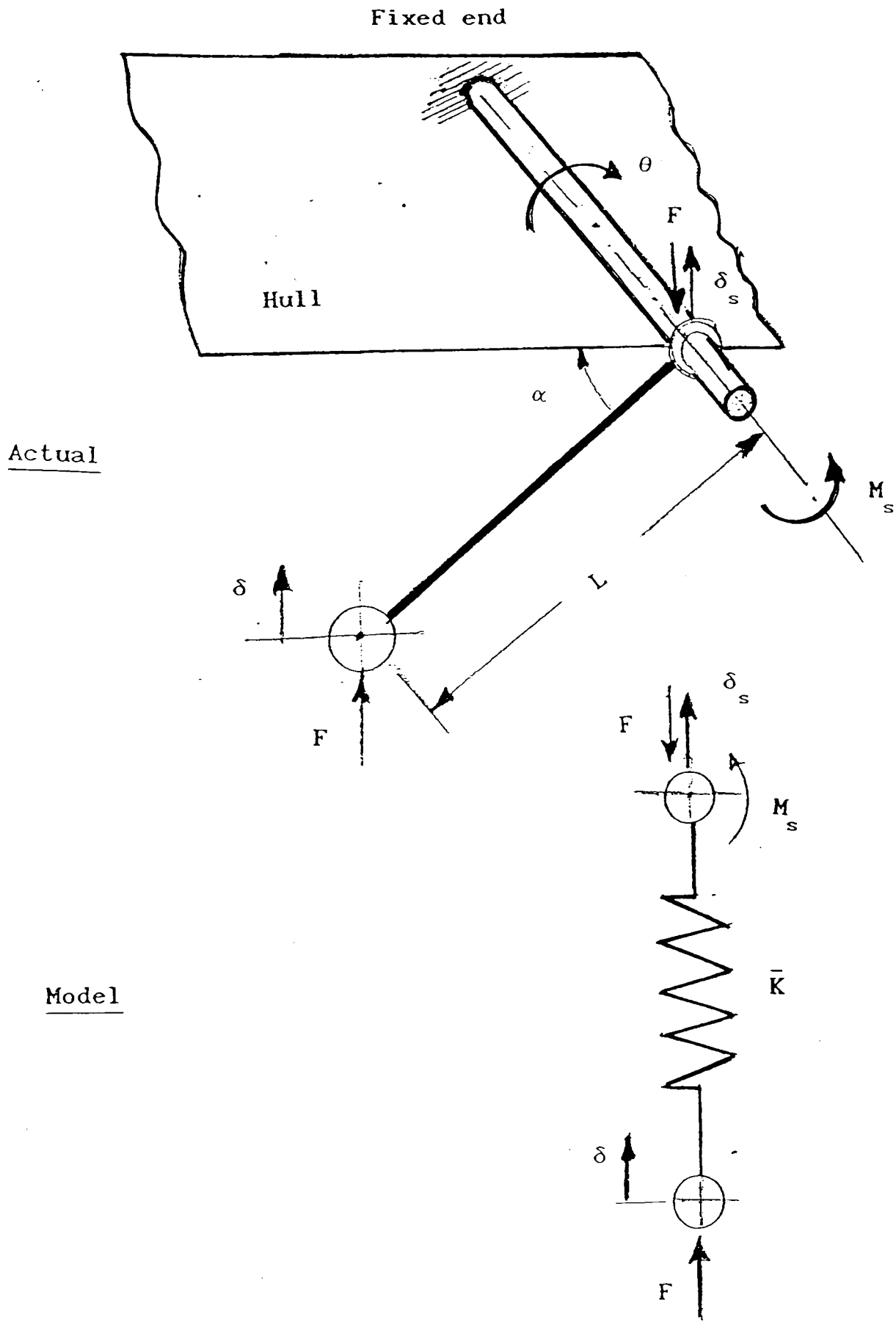

Fig(3.7) A Torsion Bar Model.

$(F_z)_o$ Equation:

This equation represents the force acting on the hull in the Z direction:

$$F_z^{(e)} = C (\dot{\delta}_d - \dot{\delta}_r) + \bar{K} (\delta_s - \delta)$$

Notice that, from the rigidity of the hull, it can be deduced that:

$$\delta_d = \delta_o + (y_d - y_o)\, \theta_0 + (x_o - x_d)\, \phi_o$$

$$\delta_s = \delta_o + (y_s - y_o)\, \theta_0 + (x_o - x_s)\, \phi_o$$

Also, the road wheel arm will be assumed rigid, i.e.

$$\frac{\delta_r - \delta_s}{\delta - \delta_s} = \frac{L_2}{L} = \beta$$

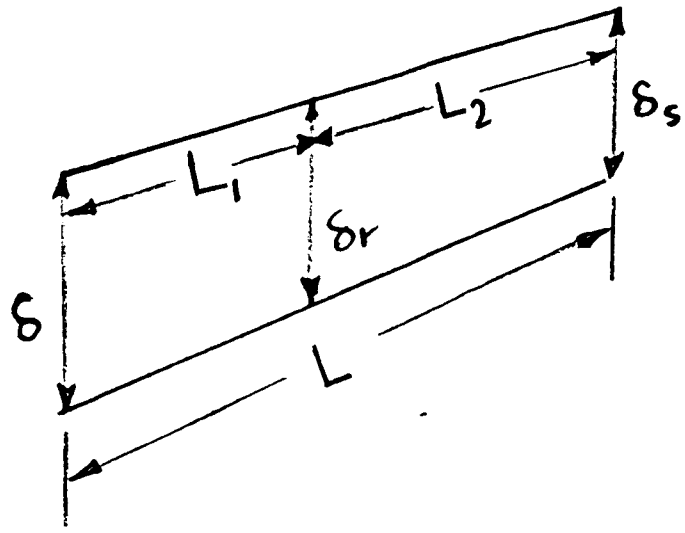

where

$$\beta = L_2 / L$$

i.e.

$$(\delta_r - \delta_s) = \beta (\delta - \delta_s)$$

or

$$\delta_r = (1 - \beta) \left[\delta_o + (y_s - y_o)\, \theta_0 + (x_o - x_s)\, \phi_o \right] + \beta\, \delta$$

Hence it can be deduced that

$$\delta_d - \delta_r = \beta\,\delta_o + \left[(y_d - y_o) - (1 - \beta)(y_s - y_o) \right] \theta_o$$

$$+ \left[(x_o - x_d) - (1 - \beta)(x_o - x_s) \right] \phi_o - \beta\,\delta$$

Substituting in $F_z^{(e)}$ equation, it can be shown that:

$$F_z^{(e)} = C \left\{ \beta (\dot{\delta}_o - \dot{\delta}) \right.$$

$$+ \left[(y_d - y_o) - (1 - \beta)(y_s - y_o) \right] \dot{\theta}_o$$

$$\left. + \left[(x_o - x_d) - (1 - \beta)(x_o - x_s) \right] \dot{\phi}_o \right\}$$

$$+ \bar{K} \left[(\delta_o - \delta) + (y_s - y_o)\,\theta_o \right.$$

$$\left. + (x_o - x_s)\,\phi_o \right] \qquad (3.17)$$

M_x Equation

This equation is defined as the angular equation of motion with respect to the X direction:

$$M_x^{(e)} = M_s + C (\dot{\delta}_d - \dot{\delta}_r) (y_d - y_o) + \bar{K} (\delta_s - \delta)(y_s - y_o)$$

$$= (L \cos \alpha)\bar{K} (\delta_s - \delta)$$

$$+ C (y_d - y_o) \left\{ \beta (\dot{\delta}_o - \dot{\delta}) \right.$$

$$+ \left[(y_d - y_o) - (1 - \beta)(y_s - y_o) \right] \dot{\theta}_o$$

$$+ \left[(x_o - x_d) - (1 - \beta)(x_o - x_s) \right] \dot{\phi}_o \Big\}$$

$$+ \bar{K} (y_s - y_o) \left[(\delta_o - \delta) + (y_s - y_o) \theta_0 \right.$$

$$\left. + (x_o - x_s) \phi_o \right]$$

Rearranging the terms it can be deduced that:

$$M_x^{(e)} = C (y_d - y_o) \Big\{ \beta (\dot{\delta}_o - \dot{\delta})$$

$$+ \left[(y_d - y_o) - (1 - \beta)(y_s - y_o) \right] \dot{\theta}_o$$

$$+ \left[(x_o - x_d) - (1 - \beta)(x_o - x_s) \right] \dot{\phi}_o \Big\}$$

$$+ \bar{K} \left[L \cos \alpha + (y_s - y_o) \right] \left[(\delta_o - \delta) \right.$$

$$\left. + (y_s - y_o) \theta_0 + (x_o - x_s) \phi_o \right] \qquad (3.17)$$

Similarly, it can be proved that:

$$M_y^{(e)} = C (x_o - x_d) \Big\{ \beta (\dot{\delta}_o - \dot{\delta})$$

$$+ \left[(y_d - y_o) - (1 - \beta)(y_s - y_o) \right] \dot{\theta}_o$$

$$+ \left[(x_o - x_d) - (1 - \beta)(x_o - x_s) \right] \dot{\phi}_o \Big\}$$

$$+ \bar{K} (x_o - x_s) \left[(\delta_o - \delta) + (y_s - y_o) \theta_0 \right.$$

$$\left. + (x_o - x_s) \phi_o \right] \qquad (3.18)$$

Wheel Equation:

To avoid any unknown reaction force at the point of fixation of arm wheel pin, with the hull, the moment of all forces acting on the arm will be taken about the X-axis at that point, i.e.

$$(F_z^{(e)})\ L \cos\alpha = -\ C\ (\dot{\delta}_d - \dot{\delta}_r)\ L_2 \cos\alpha - M_s$$
$$+ \left[m\ \ddot{\delta} + K_T\ (\delta - \delta_T) \right.$$
$$\left. + C_T\ (\dot{\delta} - \dot{\delta}_T) \right] L \cos\alpha$$

where

$$-\ M_s = L \cos\alpha\ \bar{K}\ (\delta - \delta_s)$$

Hence, it can be shown that:

$$F_z^{(e)} = -\ \beta\ C\ (\dot{\delta}_d - \dot{\delta}_r) + \bar{K}\ (\delta - \delta_s) + m\ \ddot{\delta}$$
$$+ K_T\ (\delta - \delta_T) + C_T\ (\dot{\delta} - \dot{\delta}_T)$$

or

$$F_z^{(e)} = -\ C\ \beta \left\{ \beta\ (\dot{\delta}_o - \dot{\delta}) \right.$$
$$+ \left[(y_d - y_o) - (1 - \beta)(y_s - y_o) \right] \dot{\theta}_o$$
$$\left. + \left[(x_o - x_d) - (1 - \beta)\ (x_o - x_s) \right] \dot{\phi}_o \right\}$$
$$+ (\bar{K} + K_T)\ \delta - K_T\ \delta_T + C_T\ (\dot{\delta} - \dot{\delta}_T)$$

$$- \bar{K} \left[\delta_o + (y_s - y_o)\, \theta_0 + (x_o - x_s)\, \phi_o \right]$$

$$+ m \ddot{\delta}$$

Rearranging the terms, it can be proved that:

$$F_z^{(e)} = m \ddot{\delta} - \beta^2 C \dot{\delta}_o$$

$$- C \beta \left\{ \left[(y_d - y_o) - (1 - \beta)(y_s - y_o) \right] \dot{\theta}_o \right.$$

$$\left. + \left[(x_o - x_d) - (1 - \beta)(x_o - x_s) \right] \dot{\phi}_o \right\}$$

$$+ (\beta^2 C + C_T)\, \dot{\delta} - C_T \dot{\delta}_T - \bar{K} \left[\delta_o + (y_s - y_o)\, \theta_0 \right.$$

$$\left. + (x_o - x_s)\, \phi_o \right] + (\bar{K} + K_T)\, \delta$$

$$- K_T \delta_T \qquad (3.19)$$

Equation at Point of Contact:

$$R_z^{(e)} = C_T (\dot{\delta}_T - \dot{\delta}) + K_T (\delta_T - \delta) \qquad (3.20)$$

Element Matrices:

Defining

$$\underline{\delta}^{(e)} = \left\{ \delta_o \quad \theta_o \quad \Phi_o \quad \delta \quad \delta_T \right\}$$

and from the following element matrix equation:

$$\underline{M}^{(e)} \ \ddot{\underline{\delta}}^{(e)} + \underline{C} \ \dot{\underline{\delta}}^{(e)} + \underline{K} \ \underline{\delta}^{(e)} = \underline{F}^{(e)}$$

the element matrices can be deduced as follows:

$$\underline{M}^{(e)} = \begin{bmatrix} 0 & 0 & 0 & m & 0 \end{bmatrix}$$

$$\underline{K}^{(e)} = \begin{bmatrix} \bar{K} & \Delta y_e \bar{K} & \Delta x_e \bar{K} & -\bar{K} & 0 \\ \bar{K}_y & \Delta y_e \bar{K}_y & \Delta x_e \bar{K}_y & -\bar{K}_y & 0 \\ \bar{K}_x & \Delta y_e \bar{K}_x & \Delta x_e \bar{K}_x & -\bar{K}_x & 0 \\ -\bar{K} & -\Delta y_e \bar{K} & -\Delta x_e \bar{K} & \bar{K} + K_T & -K_T \\ 0 & 0 & 0 & -K_T & K_T \end{bmatrix}$$

$$\underline{C}^{(e)} = \begin{bmatrix} \beta C & \Delta y C & \Delta x\ C & -\beta\ C & 0 \\ \beta \Delta y_d C & \Delta y_d \Delta y C & \Delta y \Delta x\ C & -\beta\ \Delta y_d C & 0 \\ \beta \Delta x_d C & \Delta y \Delta x_d C & \Delta x_d \Delta x\ C & -\beta\ \Delta x_d C & 0 \\ -\beta^2 C & -\beta \Delta y_d \Delta y C & -\beta \Delta x C & \beta^2 C + C_T & -C_T \\ 0 & 0 & 0 & -\ C_T & C_T \end{bmatrix}$$

where

$$\bar{K} = \frac{K}{L^2 \cos \alpha}\ , \qquad \bar{K}_y = \bar{K} \left[L \cos \alpha + \Delta y_e \right] ,$$

$$\bar{K}_x = \bar{K}\ \Delta x_e\ , \qquad \Delta y_e = (y_s - y_o), \qquad \Delta x_e = (x_o - x_s),$$

$$\Delta x = \Delta x_d - (1-\beta) \Delta x_e\ , \qquad \Delta y = \Delta y_d - (1-\beta) \Delta y_e\ ,$$

$$\beta = L_2 / L$$

3.3.4 Fourth Type of Suspension Elements

The rotary-vane damper is used in this element, and it is assumed to be connected to the road wheel arm by a four-bar linkage. The derivation of the equations of this element can be carried out similarly to the previous element except including the four-bar linkage transmission ratio, where the mechanical advantage of the four-bar linkage λ is defined as the ratio of the input torque caused by the terrain irregularity to the output torque developed by the damper. A computer program is built to calculate the values of λ depending on known dimensions of the four-bar linkage. A schematic diagram of this element is given in Figure 3.8.

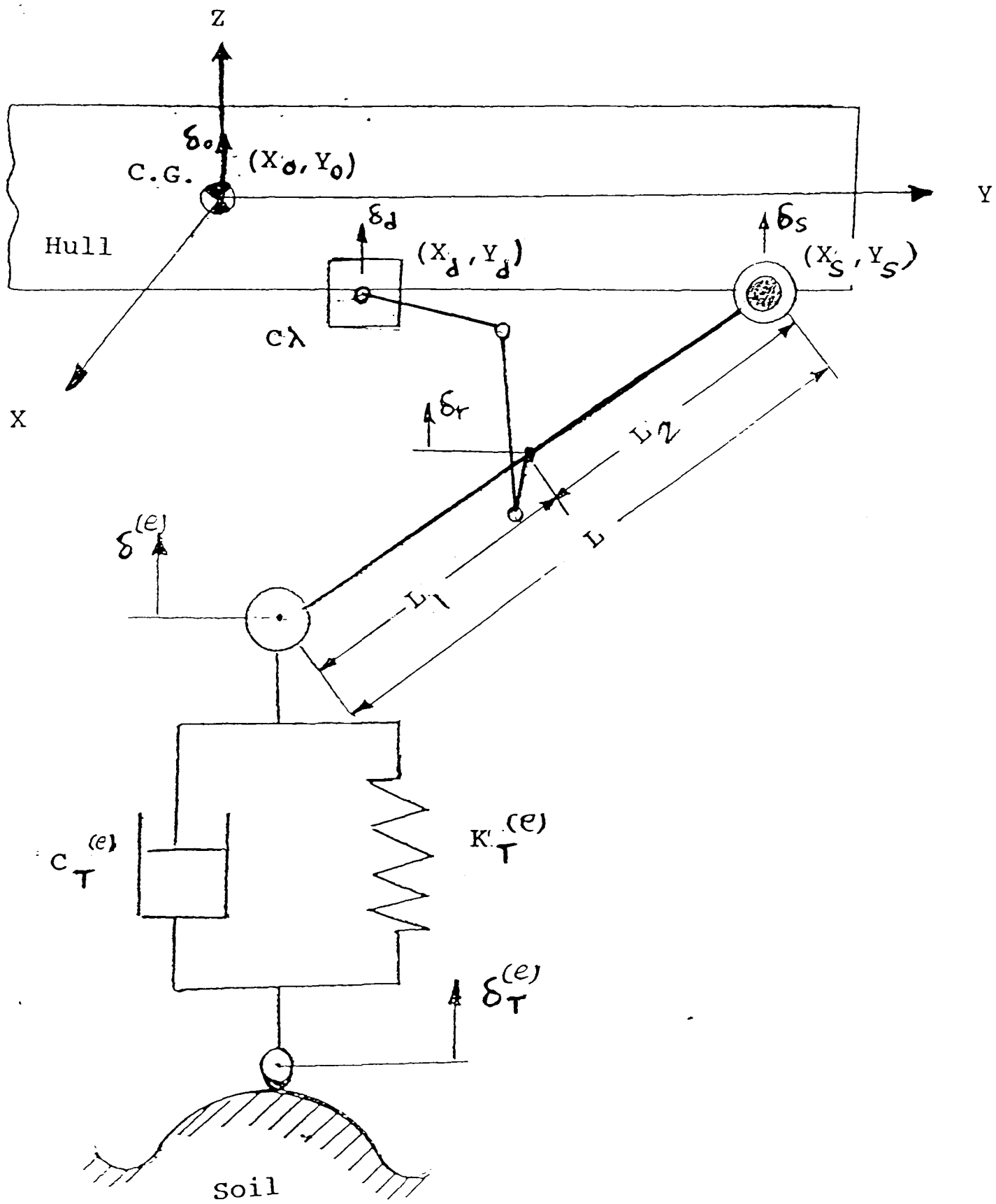

Fig (3.8) Fourth Type of Suspension Elements.

The element matrices can be expressed as follows:

$$\underline{M}^{(e)} = \begin{bmatrix} 0 & 0 & 0 & m & 0 \end{bmatrix}$$

$$\underline{K}^{(e)} = \begin{bmatrix} \bar{K} & \Delta y_e \bar{K} & \Delta x_e \bar{K} & -\bar{K} & 0 \\ \bar{K}_y & \Delta y_e \bar{K}_y & \Delta x_e \bar{K}_y & -\bar{K}_y & 0 \\ \bar{K}_x & \Delta y_e \bar{K}_x & \Delta x_e \bar{K}_x & -\bar{K}_x & 0 \\ -\bar{K} & -\Delta y_e \bar{K} & -\Delta x_e \bar{K} & \bar{K} + K_T & -K_T \\ 0 & 0 & 0 & -K_T & K_T \end{bmatrix}$$

$$\underline{C}^{(e)} = \begin{bmatrix} \beta C\lambda & \Delta y C\lambda & \Delta x\, C\lambda & -\beta\, C\lambda & 0 \\ \beta \Delta y_d C\lambda & \Delta y_d \Delta y C\lambda & \Delta y \Delta x\, C\lambda & -\beta\, \Delta y_d C\lambda & 0 \\ \beta \Delta x_d C\lambda & \Delta y \Delta x_d C\lambda & \Delta x_d \Delta x\, C\lambda & -\beta\, \Delta x_d C\lambda & 0 \\ -\beta^2 C\lambda & -\beta \Delta y_d \Delta y C\lambda & -\beta \Delta x C\lambda & \lambda\beta^2 C + C_T & -C_T \\ 0 & 0 & 0 & -C_T & C_T \end{bmatrix}$$

where

$$\bar{K} = \frac{K}{L^2 \cos \alpha} \quad , \qquad \bar{K}_y = \bar{K} \left[L \cos \alpha + \Delta y_e \right] ,$$

$$\bar{K}_x = \bar{K}\, \Delta x_e \quad , \qquad \Delta y_e = (y_s - y_o), \qquad \Delta x_e = (x_o - x_s),$$

$$\Delta x = \Delta x_d - (1-\beta)\Delta x_e \quad , \qquad \Delta y = \Delta y_d - (1-\beta)\Delta y_e \quad ,$$

$\beta = L_2 / L$, λ ... Four bar transmission ratio

3.3.5 The Track Element Simulation.

The aim of using the track in the tracked vehicle is to fulfill a large and rigid contact area between the road wheels and the ground, and to insure a uniform distribution of the cross weight of the vehicle on the ground, the other purpose for using the track is to transmit the engine power between the sprocket and the idler wheels. Hence the track is an important element in the off-road tracked vehicles. From the modelling point of view, the track physics is still of great complexity, and for this reason most of the researchers are avoiding the modelling of the track, and they employ smooth terrains on which the dynamics do not limit the mobility of the vehicles. However this approach does not simulate the practical off-road which contains a variety of surface roughness.

Recently an experimental work [Ref. 2] proves that the track has a significant effect on ride dynamics. The track compliance is represented by interconnecting linear springs between adjacent road wheels. From the experimental work available in the literature, it is found that when the tracked vehicle approaching an obstacle with height greater than the road wheel radius, the initial track-obstacle contact tends to lift the front road wheel and guide it over the obstacle. This lifting has a significant effect on the longitudinal motion. To simulate this effect, massless feelers are positioned in front of the first road wheel by a stiff spring. The equivalent spring stiffness of the track can be determined approximately by observing photographs of the vehicle in different positions on an obstacle (see Refs [1,2]).

In the case of a semi tracked vehicle with a suspension system being a combination of any two types of the previous elements, its differential equations are as derived in the previous sections, mainly the front two wheel assemblies are the same as for the simple or the second type of suspension elements, while the remaining wheel assemblies are the same as for the third or the forth type of suspension elements with track. Because the finite element method is

employed in this work, all that is required for the assembler is to recognise the type of an element used in the assembly, in this case the same library routines will be implemented without any modification. A schematic diagram representing the tracked and the semi tracked elements is shown in Figure 3.9.

3.4 TWO DIMENSIONAL VEHICLE SIMULATION:

The two dimensional(2-D) approach has been employed in the literature, by many authors either because of its simplicity or because of the symmetry of the vehicle suspension systems with respect to the centre of gravity. The 2-D model reduces the number of the necessary degrees of freedom of the system to about half of those required for the three dimension model 3-D for the same vehicle, and it will save the computer CPU time as well as the human effort. But for the case of unsymmetrical suspension systems, which is usually found in most of the tanks, the 3-D modelling is required so as to yield an accurate representation of such vehicles.

In this work the 2-D model is represented by means of all the previous elements in the Y-Z plane. The three dimensional modelling is always assumed initially. For the case of 2-D analysis, the 2-D equations are obtained from 3-D ones by eliminating the contributions of M_y and Φ_o.

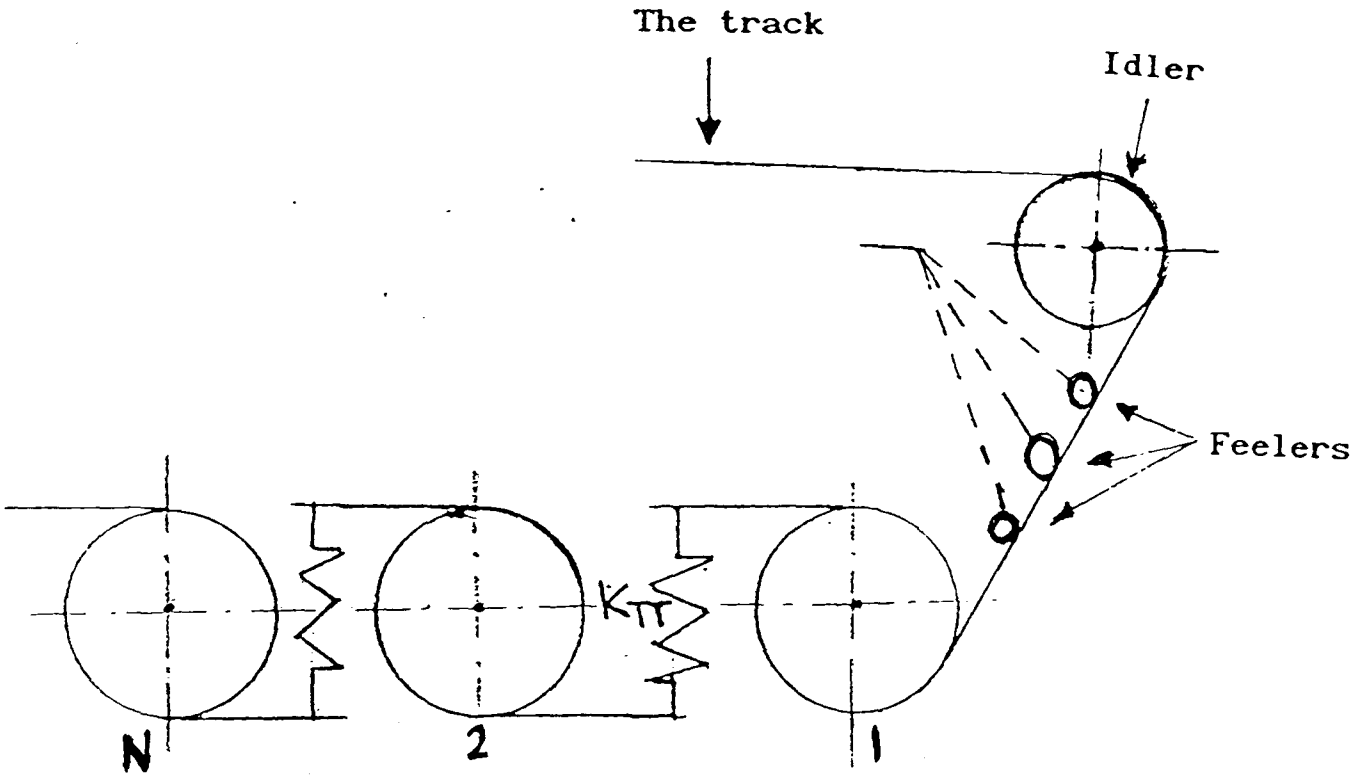

Tracked element

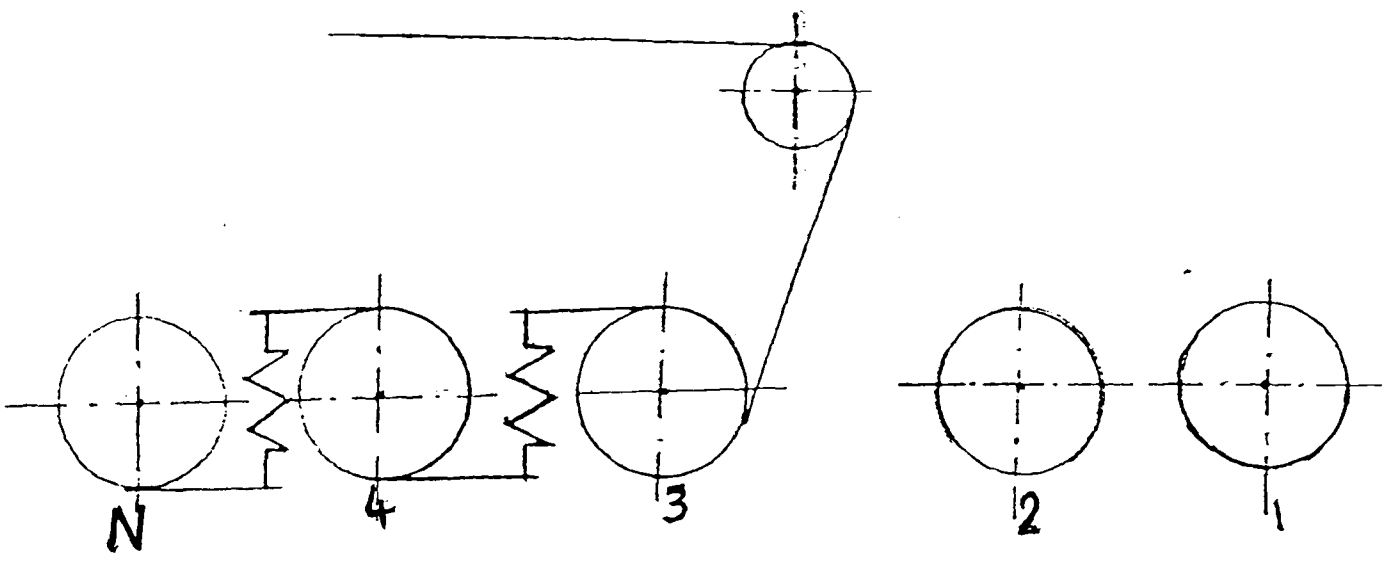

Semi-tracked element

Fig (3.9) Types of Tracked and Semi-Tracked Elements.

CHAPTER

FOUR

VEHICLE TERRAIN-INTERACTION

4.1 INTRODUCTION:

There are two prime objectives of the study of vehicle terrain interaction. One is to establish the functional relationship between the performance of an off-road vehicle and its design parameters and terrain characteristics. The other objective is to establish a procedure with which the changes in terrain conditions caused by the passage of an off-road vehicle or soil working machinery may be predicted.

The mechanical properties of the terrain quite often impose severe limitations to the mobility and performance of cross-country vehicles. An adequate knowledge of the mechanical properties of the terrain and an understanding of the mechanics of vehicle-terrain interaction are therefore, essential for the proper design, selection, and operation of off- road vehicles. The study of the relationship between the performance of an off-road vehicle and its physical environment (terrain) has now become known as "Terramechanics". A brief review of this subject can be found in Refs.[15,16,45].

4.2 TYRE MODELLING:

Due to the characteristics of the tyres or the road wheels, which consist of combinations of two or three materials, mainly, rubber, fibres, and steel subjected to nonuniform force caused by the terrain profile (specially for the off-road),accurate mathematical modelling of them is not possible.

The tyre models available are reviewed to justify the selection of appropriate alternatives for the ride model, (see Crolla [Ref. 46], and Captain [Ref. 47]).

a) The Point Contact Tyre Model:

This model represents the tyre by means of a spring and damper connected in parallel, and this combination is responsible for transmitting the support forces from the terrain to the vehicle through the point contact with the ground. The tyre mass is assumed to be concentrated at the wheel centre, and the relative motion between the free end of the contact with the ground and the terrain profile will cause a deflection of the spring, which will create a dynamic force in the vertical direction, see Figure 4.1a.

b) Rigid Tread Band Tyre Model:

The difference between this model and the above one is that the point follower is replaced by a roller follower of diameter equal to the tyre diameter, see Figure 4.1b.

c) Fixed Foot Print Tyre Model:

In this model more than one point contact are used and the interaction between the tyre and the terrain profile is assumed to be a constant size foot print, as shown in Figure 4.1c and it is similar to the point contact model if the linear characteristics of the tyre are considered.

The first model can be used for linear simulation in terms of an equivalent constant spring rate and a coefficient of damping. It has been used in some studies without mentioning its advantages or disadvantages. The second model is unable to simulate fully the dominant footprint characteristics of a real tyre, unless a modified input terrain profile is used.

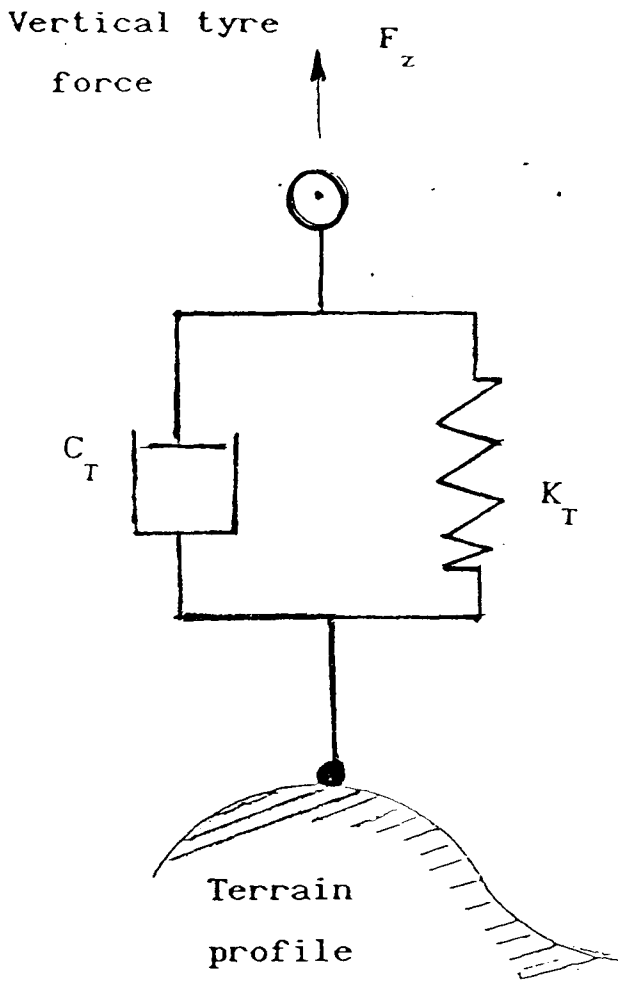

a) point contact

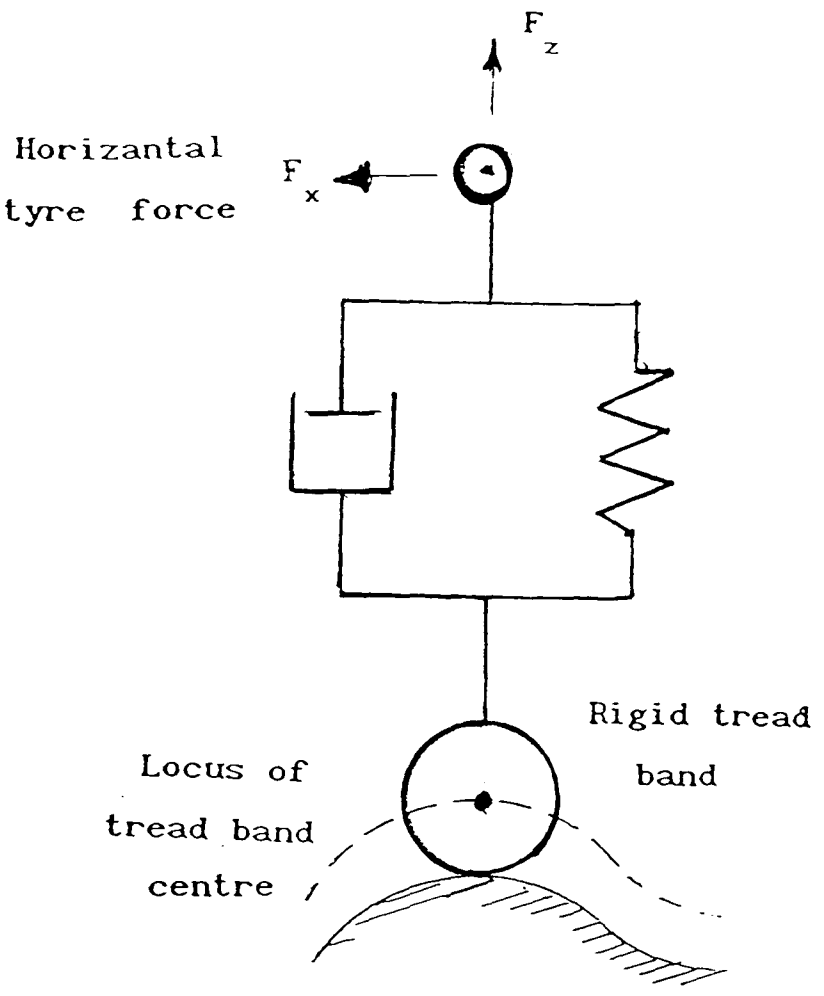

b) Rigid tread band

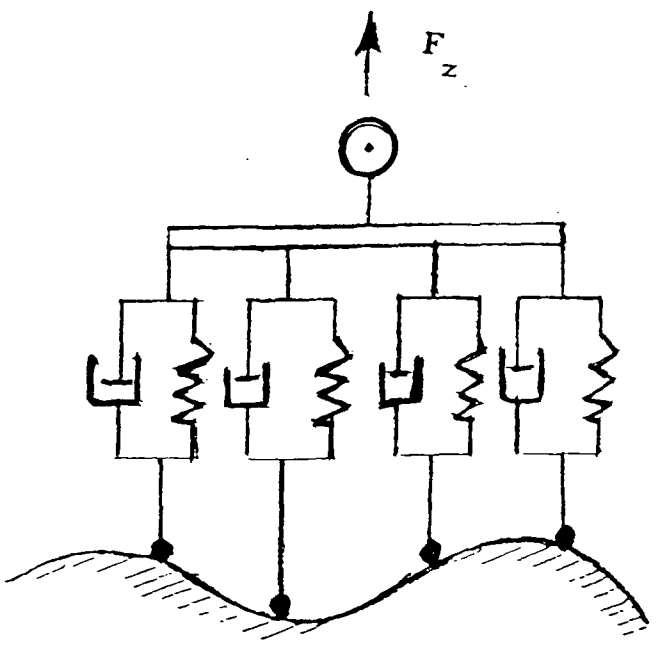

c) Fixed footprint

Fig (4.1) Various Tyre Models.

4.3 SOIL EFFECTS AND THE TYPES OF SOIL USED IN THIS WORK:

In cross-country operations, various types of terrain with different soil characteristics, ranging from desert sand through deep mud to snow-covered soils, may be facing the vehicles.

The mechanical behaviour of the terrain can be measured under loading conditions similar to those exerted by the vehicle. One of the various techniques for measuring terrain parameters is the load sinkage relationship technique, which depends on the penetration test. The test procedure is explained by Bekker [Ref. 15], where, a plate simulating the contact area of a track or a tyre is forced vertically into the ground, the pressure P and the sinkage Z are measured, and a family of pressure-sinkage curves are obtained from penetration tests in various homogeneous soils.

Based upon experimental data, Bekker proposed the following pressure-sinkage relationship for homogeneous soils.

$$P = \left(\frac{K_c}{b} + K_\varphi \right) Z^n \qquad (4.1)$$

where **n** is the exponent of deformation, **b** is the smaller dimension of the loading area, and K_c, K_φ are cohesive and frictional moduli of deformation, respectively.

The values of K_c, K_φ, and **n** can be obtained using two tests at least. The procedure for obtaining these values is shown in Appendix (A).

Generally, there are two types of soil, the rigid soil, and the soft soil (deformable soil). For the case of rigid soil there is no need to redrive new equations because all system equations derived in chapter three are applicable. However for the case of soft soil the equation which describes the force at the contact point between the terrain and the wheel should be modified as explained below.

Consider a road wheel on soft soil as shown in Figure 4.2, it can deduced from soil equilibrium that:

$$K_s \delta_s = K_T(\delta_1) + C_T(\dot{\delta}_1)$$

or

$$\delta_s = \frac{1}{K_s}\left[K_T \delta_1 + C_T \dot{\delta}_1 \right] \qquad (4.2)$$

where

K_s is the equivalent stiffness of soil,

δ_s is soil sinkage.

Hence the equation of motion of the road wheel in the vertical direction can be expressed as follows:

$$m \ddot{\delta} + C (\dot{\delta} - \dot{\delta}_o) + K (\delta - \delta_o) + C_T(\dot{\delta} - \dot{\delta}_1)$$

$$+ K_T(\delta - \delta_1 - \delta_s) = F_z$$

Comparing this equation with equations (3.12) and (3.13), the reaction force acting on the road wheel can be expressed as follows:

$$R_z = C_T(\dot{\delta}_1 - \dot{\delta}) + K_T(\delta_1 + \delta_s - \delta)$$

$$\equiv F_m - C_T\dot{\delta} - K_T\delta$$

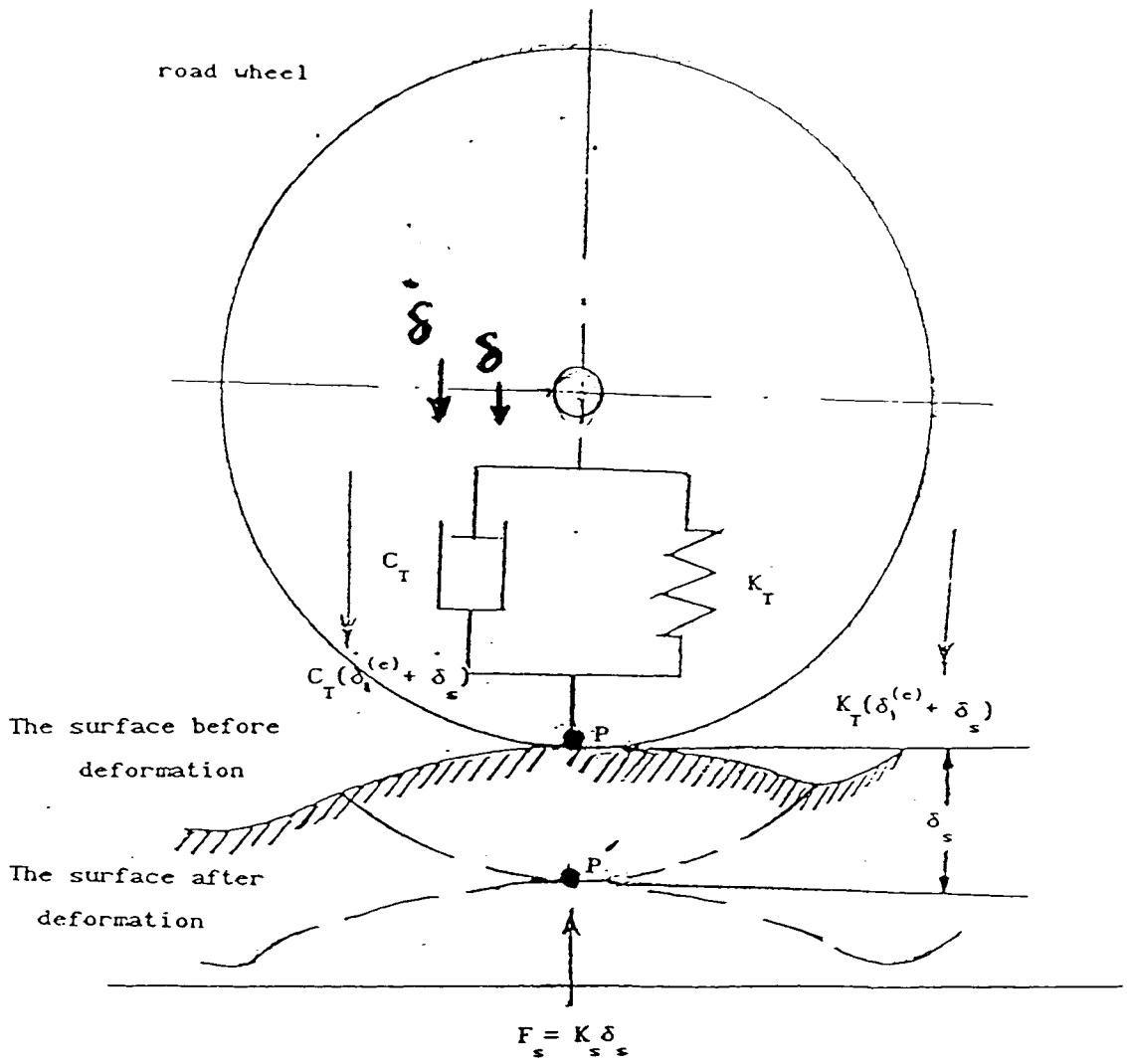

Fig(4.2) Soft Soil Road Wheel (Tyre) Model.

Hence, the equation describing the force caused by the road wheel or tyre on a soft soil can be expressed by:

$$F_m = C_T \dot{\delta}_1 + K_T \delta_1 + K_T \delta_s$$

Substituting for δ_s from equation (4.2) it can be shown that:

$$F_m = C_T \dot{\delta}_1 + K_T \delta_1 + \frac{K_T}{K_S}\left[K_T \delta_1 + C_T \dot{\delta}_1 \right]$$

$$= \left(1 + \frac{K_T}{K_S} \right)\left[K_T \delta_1 + C_T \dot{\delta}_1 \right] \qquad (4.3)$$

4.3.1 The Calculation of the Soil Equivalent Stiffness K_s:

For a homogeneous soil Bekker's equation (4.1), can be applied, i.e.

$$P = K Z^n = \frac{F}{A} \qquad (4.4)$$

where

$$K = \left(\frac{K_c}{b} + K_\varphi \right)$$

Hence

$$P A = \left(K Z^n A \right)$$

or

$$F = \left(K Z^{n-1} A \right) Z = K_{eqv.} Z$$

and the force per unit length is

$$F/ Z = K Z^{n-1} A = K_{eqv.}$$

To obtain the sinkage Z and the contact area A the following procedure could be used:

Consider a road wheel which has a contact area as shown in Figure 4.3

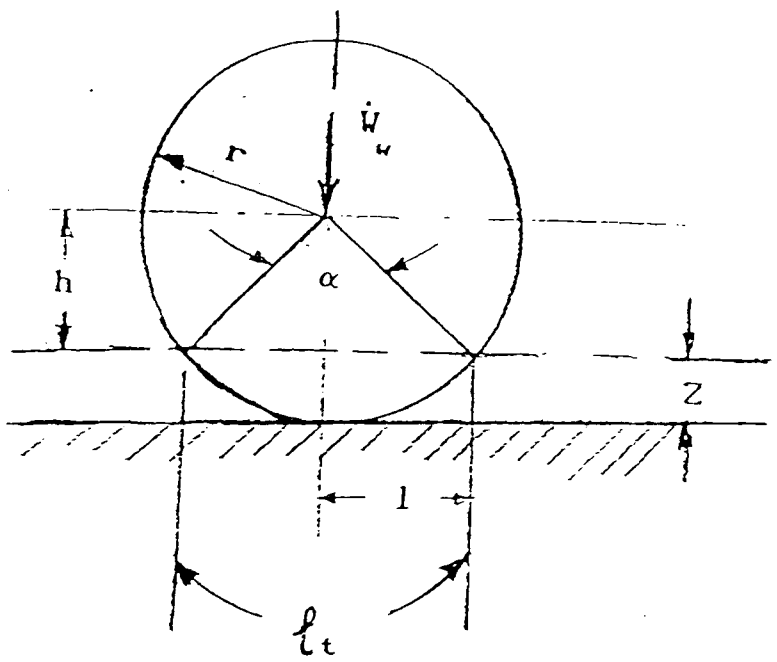

Fig (4.3) Untracked Road Wheel Contact Area.

From simple geometrical relationships, it can be shown that:

$$\ell^2 = r^2 - h^2$$

and

$$h = r - Z \quad , \text{ i.e}$$

$$h^2 = (r - Z)^2 = r^2 - 2rZ + Z^2$$

$$\therefore \ell = \sqrt{2rZ - Z^2} \qquad ..(a)$$

The soil pressure acting on the wheel can be expressed from equation (4.4) as:

$$P = K Z^n = \frac{W_w}{\ell . B} \qquad (b)$$

where

B.....is the tyre or road wheel width

W_w....is the tyre or road wheel load.

Substituting from equation (a) into equation (b), it can be deduced that

$$\frac{W_w}{B\sqrt{2rZ - Z^2}} = K Z^n$$

Using an iterative approach such as Newton-Raphson method the sinkage Z can be determined. Then the effective angle α also can be calculated by:

$$r \sin\frac{\alpha}{2} = \ell$$

or

$$\alpha = 2 \sin^{-1}\left(\frac{\ell}{r}\right) \qquad ..(c)$$

and the contact area A for one road wheel can be obtained as follows:

a) **For Wheeled Vehicles:**

The footprint of a tyre is almost likely to be an ellipse, with axes B and ℓ_t, where

$$\ell_t = r\,\alpha \qquad ..(d)$$

Hence, the contact area of one tyre can be approximated as follows:

$$A = \frac{\Pi}{4}\,\ell_t . B$$

and the total contact area A_t of the vehicle is

$$A_t = A \,.\, N$$

where

N.... is the number of tyre.

b) For Tracked Vehicles:

Consider a tracked vehicle on a soft soil where the contact area of the track with the ground is as shown in Figure 4.4. For simplicity assume that:

$\alpha_1 = \alpha_2 = \alpha$

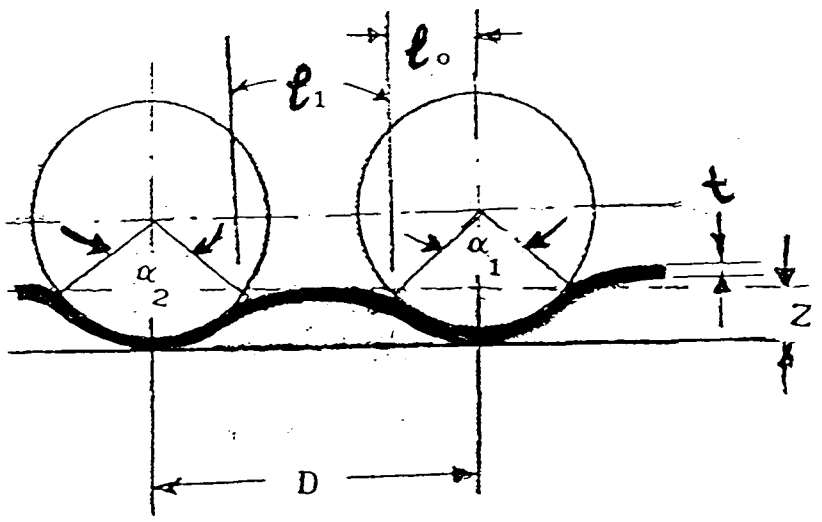

Fig (4.4) Tracked Vehicle Contact Area.

Hence, it can be proved that:

$$\ell_o = r \sin\left(\frac{\alpha}{2}\right) \equiv \ell$$

$$\ell_1 = D - 2\ell$$

Notice that:

$$\ell = (r + t) - Z$$

where

t....is the track thickness

Using equation (c) to obtain α, and equation (d) to obtain ℓ_t then, the contact area caused by one road wheel is:

$$A = \ell_t B_T$$

where

B_T.....is the track width.

and the total contact area can be expressed as follows:

$$A_t = A.N + \ell_1 (N - 1)\ B_T$$

Then the equivalent stiffness K_s can be determined from:

$$K_s = K\ Z^{n-1}\ A_t \qquad (4.5)$$

Two types of soft soil are implemented in this work, the sandy soil , and the organic soil, which are the most popular types of soil. Each type has its own parameters, the value of which are shown in Appendix A, more terrain data can be found in Refs.[15,16,45,48]

4.3.2 Obstacles Types:

The off-road vehicles are expected to operate on a wide variety of surfaces, and such unprepared terrains consist of different kinds of obstacles. Two types of obstacles are used, in the computer simulation of such terrains.

a) Trapezoidal Obstacle:

Usually the square shape obstacle is used in the literatures to check the reliability of the models, but it is very important that the data file describing the obstacle should be in an accepted form, so it is essential that the square obstacle will be modified to a suitable trapezoidal shape. See Figure 4.5a.

b) Semicircular Obstacle:

This is another proposed obstacle used in the simulation, and for such a case the data file describing this obstacle should be carefully formatted. It should be noted that the vehicle is automatically positioned, so that the axle of the first wheel coincides with the first profile point. For this reason the obstacle data file should be created with a reasonable level approach to permit an acceptable wheel-obstacle impact, see Figure 4.5b.

4.4 FORCE FUNCTIONS:

In ride analysis, the exiting force is assumed to be generated from the movement of the vehicle on the terrain, and it is considered in the vertical direction. The terrain surface roughness can be represented in terms of a series of elevations which are functions of the vertical amplitude of the terrain profile, and may be expensed by:

$$Z_3 = f (Y_3)$$

Taking the vehicle velocity into consideration Z_3 becomes a function of time t also, i.e.

$$Z_3 = f (Y_3 , t)$$

The terrain elevation can be measured at equal distances along the Y_3- axis or unequal distances according to the shape of the terrain surface or data available. A tabulated data can be used as input terrain elevation data, an interpolation formula is employed to find the mid points of the elevation, which may not be included in the data table given. Once the function Z_3 is determined, the velocity $\dot{Z}_3$ can be derived by means of numerical differentiation, then the force function can easily be obtained by means of previous analysis.

4.4.1 Harmonic Force Function:

The sine wave terrain profile is used in many test courses for vehicles, for example in Maclaurine's paper [Ref. 49], three sinewave test courses are demonstrated; 0.05 m amplitude and 4.5 m wavelength, 0.1 m amplitude and 7 m wavelength, and 0.1 m amplitude 12 m wavelength. The first is suitable for medium sized vehicles (e.g. Reconnaissance vehicles), the second course is suitable for a typical sized main battle tanks, it is useful for checking resonance frequencies, degree of damping, and adequacy of idler and sprocket clearances, and the 12 m wavelength course is useful to excite resonance at high vehicle speeds.

Referring to Figure 4.6, and starting with the front wheel lying on the origin, at time t = 0 Sec, $C_o = 0$, the distance between the i^{th} wheel and $(i-1)^{th}$ wheel is C_i. After time t, the vehicle moves a distance d, with respect to the terrain, and taking the distance between wheels into consideration, all wheels will be shifted by the same distance d, where d = V t, and V is the speed of the vehicle.

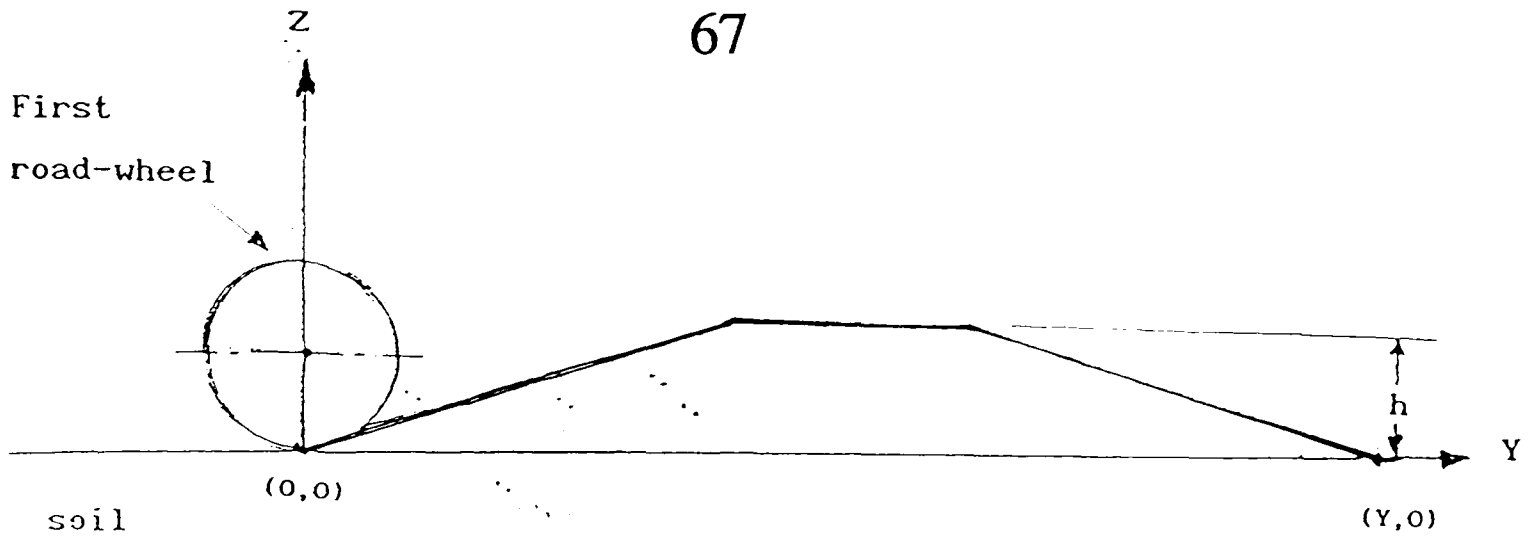

a) Trapezoidal obstacle

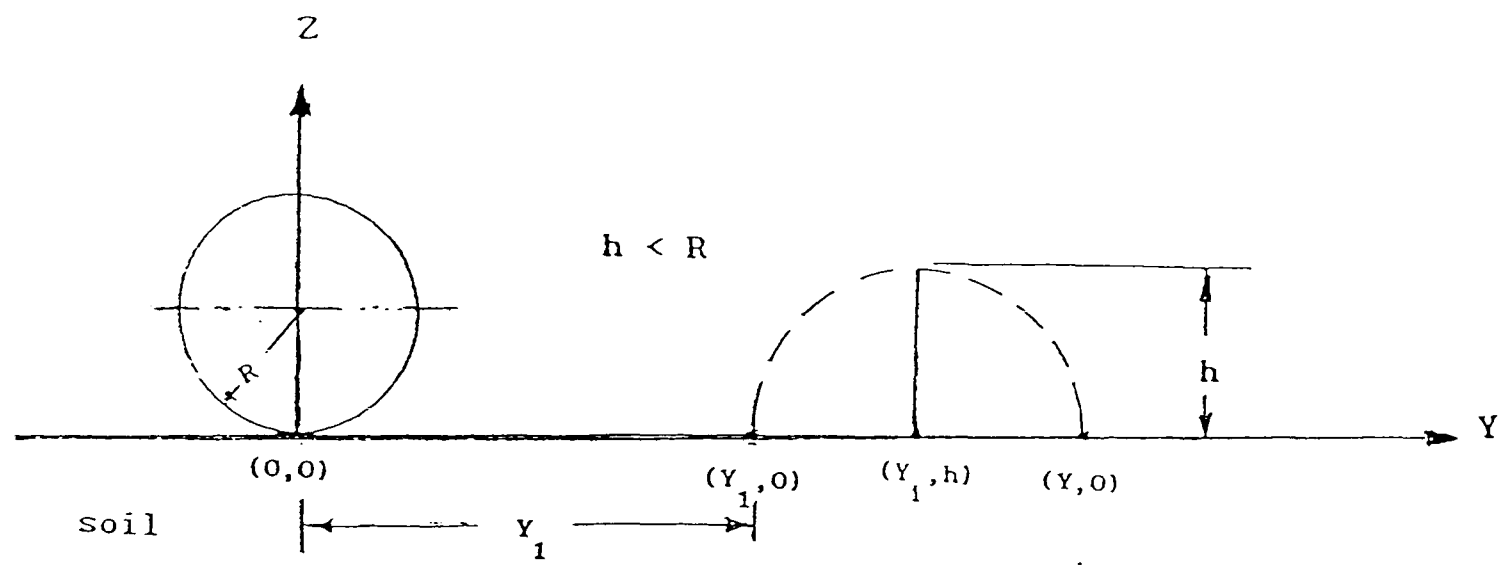

b) Semi-circular obstacle

Fig (4.5) Two Obstacles Types

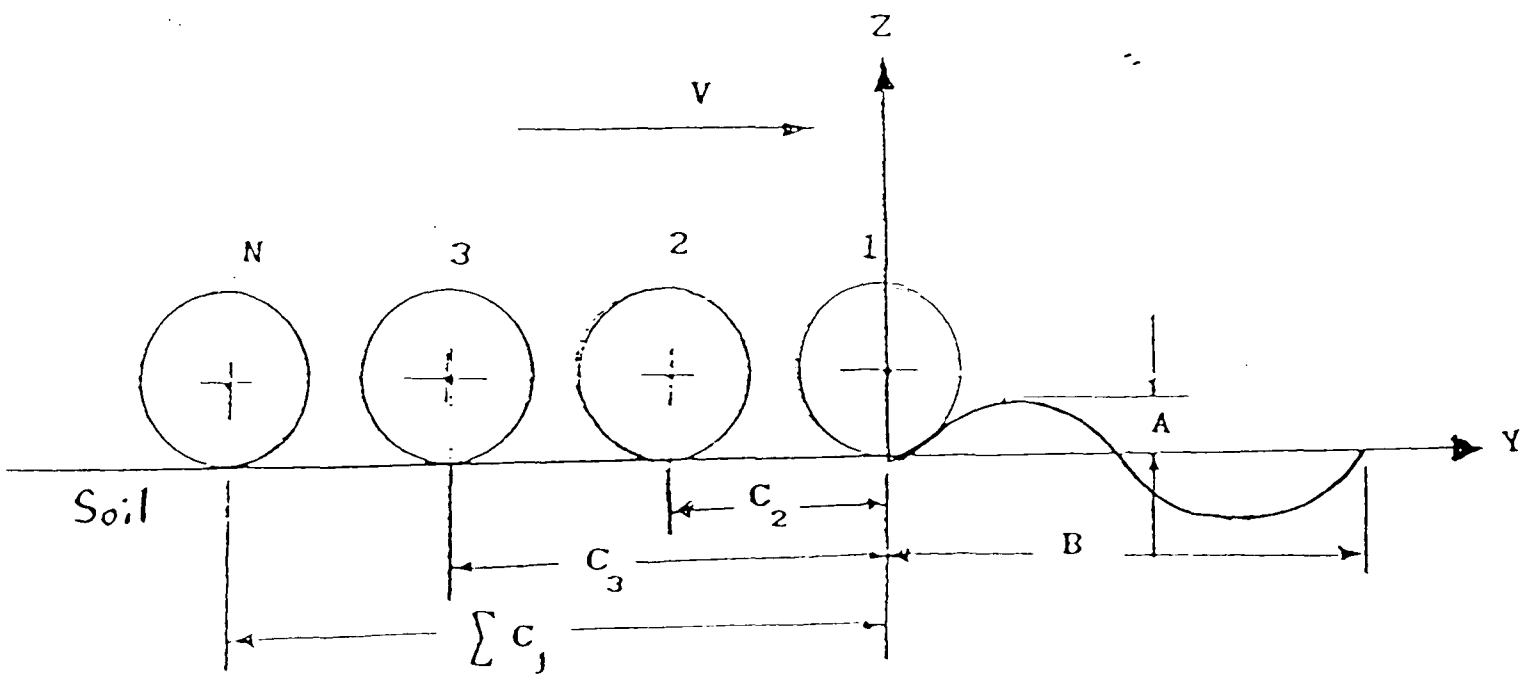

Fig (4.6) Sinewave Force Function.

To obtain the elevation of the terrain which produces the displacement of wheels, the following procedure could be used:

(i) The sine wave function may be expressed by:

$$Z(y) = A \sin (C\, y) \qquad (4.6)$$

At $y = B$, the wavelength,

$$C = \frac{2\,\Pi}{B}$$

hence

$$Z(y) = A \sin \left(\frac{2\,\Pi}{B}\, y \right) \qquad (4.7)$$

(ii) At time t:

$$Y_k(t) = V \,.\, t - C_{(k-1)} + C_o$$

or

$$Y_k(t) = V.t - \sum_{j=1}^{k} C_j \qquad (4.8)$$

where

$k = 1,2 \ldots\ldots N$

N is the number of wheels.

(iii) Substituting from equation (4.8) into equation (4.7), and considering the i^{th} point it can be deduced that:

$$Z(y_i) = A \sin \left[\frac{2\,\Pi}{B} \left(V.t - \sum_{j=1}^{k} C_j \right) \right] \qquad (4.9)$$

and

$$\dot{Z}(y_i) = \frac{2\,\Pi}{B}\, A.V \cos\left[\frac{2\,\Pi}{B}\left(V.t - \sum_{j=1}^{k} C_j\right)\right] \qquad (4.10)$$

(iv) Then the force function can be calculated by multiplying the displacement Z by the wheel or tyre stiffness, and the velocity $\dot{Z}$ by the wheel or tyre coefficient of damping.

4.4.2 Arbitrary Force Function:

The off-road vehicle is expected to face the kind of terrain which generates arbitrary forces. There are two ways to obtain this type of excitation which could be used in the simulation of the arbitrary force function.

a) Analytical Expression:

In this case a direct equation which represents an arbitrary terrain profile can be implemented in the simulation program, and such equation may be described as:

$$Z = Z(y)$$

and for the k^{th} wheel at time t_i ,

$$y_i = V.t_i - C_k$$

i.e.

$$Z(t_i) = Z(y_i)$$

$$= Z(V.t_i - C_k) \qquad (4.11)$$

b) Tabulated Values:

This is the popular form of terrain input elevation, and in this case the procedure employed to obtain the force function can be as follows:

(i) The arbitrary function may expressed by:

$$y_i = V.t_i - C_k$$

Such that $y_j < y_i < y_{j+1}$

where

$$j = 1,2,\ldots,N_p$$

N_p...is the number of input elevation points.

(ii) Generally the value of the corresponding y_i should be interpolated using an interpolation formula such as the three point Lagrangian polynomial. Then the displacement can be described by:

$$Z = V_1 \left[(y_i - y_{j+1})\,(y_i - y_{j+2}) \right] + V_2 \left[(y_i - y_j)\,(y_i - y_{j+2}) \right] + V_3 \left[(y_i - y_j)\,(y_i - y_{j+1}) \right] \qquad (4.12)$$

where

$$V_1 = Z_j \,/\, \left[(y_j - y_{j+1})\,(y_j - y_{j+2}) \right]$$

$$V_2 = Z_{j+1} \,/\, \left[(y_{j+1} - y_j)\,(y_{j+1} - y_{j+2}) \right]$$

$$V_3 = Z_{j+2} \Big/ \left[(y_{j+2} - y_j)\ (\ y_{j+2} - y_{j+1}) \right]$$

(iii) To obtain the vertical velocity:

$$\frac{dZ}{dt} = \frac{dZ}{dy}\ \frac{dy}{dt} = \frac{dZ}{dy}\ .\ V$$

and from equation (4.12), it can be shown that:

$$\frac{dZ}{dy} = 2\ [V_1 + V_2 + V_3]\ y_i - [V_1 + V_2]\ y_{j+2}$$

$$- [V_2 + V_3]\ y_j - [V_1 + V_3]\ y_{j+1}$$

CHAPTER

FIVE

RIDE ANALYSIS

5.1 RIDE TOLERANCE CRITERIA:

Because of the roughness of the terrain they encounter, cross country vehicles experience more shock and vibration than ordinary road vehicles, hence the off-road speed is usually limited by the ability of the operator to withstand these vibrations to negotiate and to retain adequate control of the vehicle. The ride comfort is considered in this work, in addition to other factors. The weakest link in the performance of vehicle systems is usually the operator, and to measure the operator (driver) tolerance, a ride tolerance criterion could be used. In fact there are three criteria employed in this work, namely, the absorbed power (A.P.), the International Standard Organization criterion (ISO 2631), and the German 'K' factor. In this chapter, these criteria with their computer algorithms will be reviewed.

5.1.1 The Absorbed Power Criterion:

The absorbed power is the measure of the rate at which vibrational energy is absorbed by the human body, and is the quantity used to determine human tolerance to vibration when a vehicle crosses rough terrains.

The absorbed power for a given input depends on input intensity and frequency content. At any given frequency the energy absorbed by the body depends upon the real component of the mechanical impedance of the body for that particular mode or body orientation. The absorbed power parameter was introduced by Lee, and Pradko [Ref. 24]. In the frequency domain the average absorbed power is defined as:

$$A.P = \sum_{i=1}^{m} K_i \, A_i^{\,2} \qquad (5.1)$$

where

A_i^2 ...is the mean square acceleration at frequency "i"
K_i ...is a coefficient depending on body orientation with respect to the input and frequency "i"
m ... is the number of data points

and in time domain:

$$A.P = \lim_{t \Rightarrow \infty} \frac{1}{t} \int_0^t F(t)\, V(t)\, dt \qquad (5.2)$$

where

F(t) ...is the instantaneous force at the point of applied input motion.

V(t) ...is the instantaneous velocity at the point of applied input motion.

As a scalar quantity, the A.P. can be summed in complex multiple-degrees of freedom systems to determine human response.

The Absorbed Power Computational Algorithm:

The total absorbed power, is the summation of the power at each frequency. The power can be computed by multiplying the acceleration root mean square (RMS), by its corresponding constant coefficient K_i, as follows:

(i) The accelerations in different directions, i.e. vertical, side-to- side, and fort-after, are the outcome from the program in (m/s^2), and to be converted to (ft/s^2), so as to suit the given units of K_i then the root mean square of which is to be obtained.

(ii) The coefficient K_i as a function of the frequency is to be obtained from the empirical transfer functions shown in Appendix B. Figure 5.1, shows the transfer functions in different orientations, where the Laplace operator frequency S is in (rad/ s), and for the i^{th} frequency:

$$S_i = 2 \Pi f_i$$

$$K_i = \left[G(S_i) \right]^2$$

(iii) Then the absorbed power can be calculated in each direction, using equation (5.1).

5.1.2 The International Standard Organization Criterion (ISO 2631):

This criterion is given in ISO 2631 which is titled as "Guide for the elevation of human exposure to whole body vibration". The definition and numerical values given in the ISO 2631 are only valid in the frequency range (1 to 80 Hz). This standard which was developed by the World Federation on National Standards Institutes, is based on the research carried out by Hohl in 1982, [Ref. 32].

For the assessment of mechanical vibration transmitted from a solid surface to the human body, four physical factors should be considered.

(i) Intensity (acceleration RMS).
(ii) Frequency (1-80 Hz).
(iii) Direction.
(iv) Duration (exposure time).

RATS SYSTEM

Run on

Fri Aug 2 16:37:16 1991

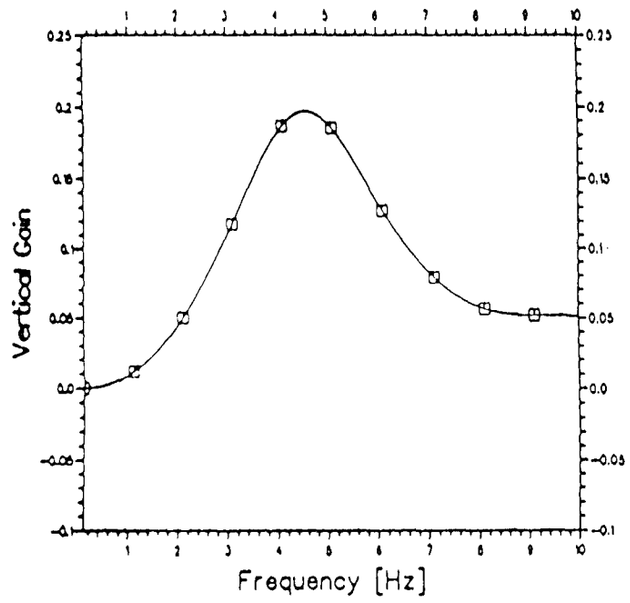

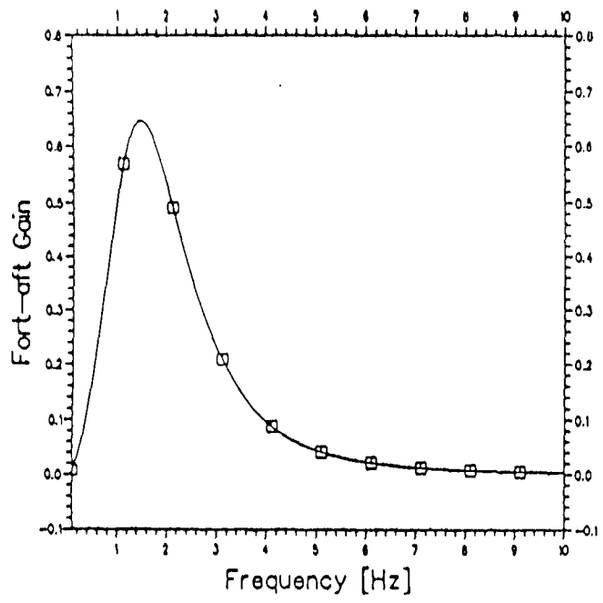

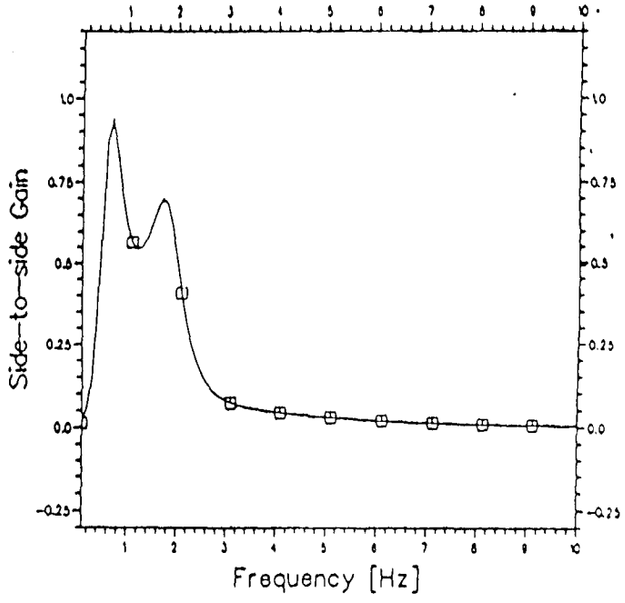

Fig (5.1) Human Response Characteristics.

The fact that the human body has high sensitivity to vertical vibrations in the range (4-8 Hz) is proved by an experimental work in Reference 32. The following procedure is employed to obtain the information published in the ISO 2631:

a. The accelerations in direction (foot-to-head) are $\mp a_z$, in direction (chest-to-back) are $\mp a_x$, and the lateral direction (right-to-left side) are $\mp a_y$.

b. A curve is then plotted between the acceleration a_z (m/s^2) and the frequency of (1/3) octave band (Hz).

c. It is shown in Appendix (B) in Figures B.1, and B.2 , and tables (B.1), and (B.2), that the minimum frequency tolerance of the human body is in the range of (4-8 Hz) for a_z, and (1-2 Hz) for a_y, a_x.

d. For the evaluation of human exposure to whole body vibration , three criteria can be distinguished:

   (i) The preservation of comfort " reduced comfort boundary".

   (ii) The preservation of working efficiency "fatigue-decreased proficiency boundary"

   (iii) The preservation of health or safety "exposure limit".

These criteria are intended only for average people considered fit for normal living routines and the stress of an average working day.

For "reduced comfort boundary", the acceleration values are divided by 3.15 (10 dB lower), and for "exposure limits", above which the health cannot be assured, the acceleration values are to be multiplied by 2 (6 dB higher), this recommendation is given in Reference 50. The allowable daily exposure times corresponding to the exposure limit and to the fatigue-decreased proficiency boundary are

about 8 hours and 2 hours 30 minutes respectively [Ref. 51].

The ISO Computer Algorithm:

The maximum allowable exposure time is considered as a measure for ride comfort criteria. The allowable exposure time is determined for each axis of vibration if there is more than one, and each third of an octave, separately, and the one of these which gives the shortest time is the one to use.

The following procedure could be used to compute the exposure time:

(i) Since the one-third octave band analysis is recommended, and according to the limitation of this standard (1-80 Hz), the centre frequency of third octave band filter can be defined as:

$$f_3 = \sqrt{32} \; / \; T_{total} \quad >1$$

where

T_{total} ....is the total time of the simulation.

(ii) The exposure time limits are given in the standard from 1 minute to 24 hours with irregular acceleration and time steps. Tables (B.1, B.2), and Figures B.1, and B.2 in Appendix (B) show the standard values.

An interpolation is necessary in order to obtain the corresponding exposure time T. A linear interpolation will be possible for accurate evaluation of time at the specified limits of the standard. An interpolation process including frequency, acceleration, and time interpolation can be carried out as follows:

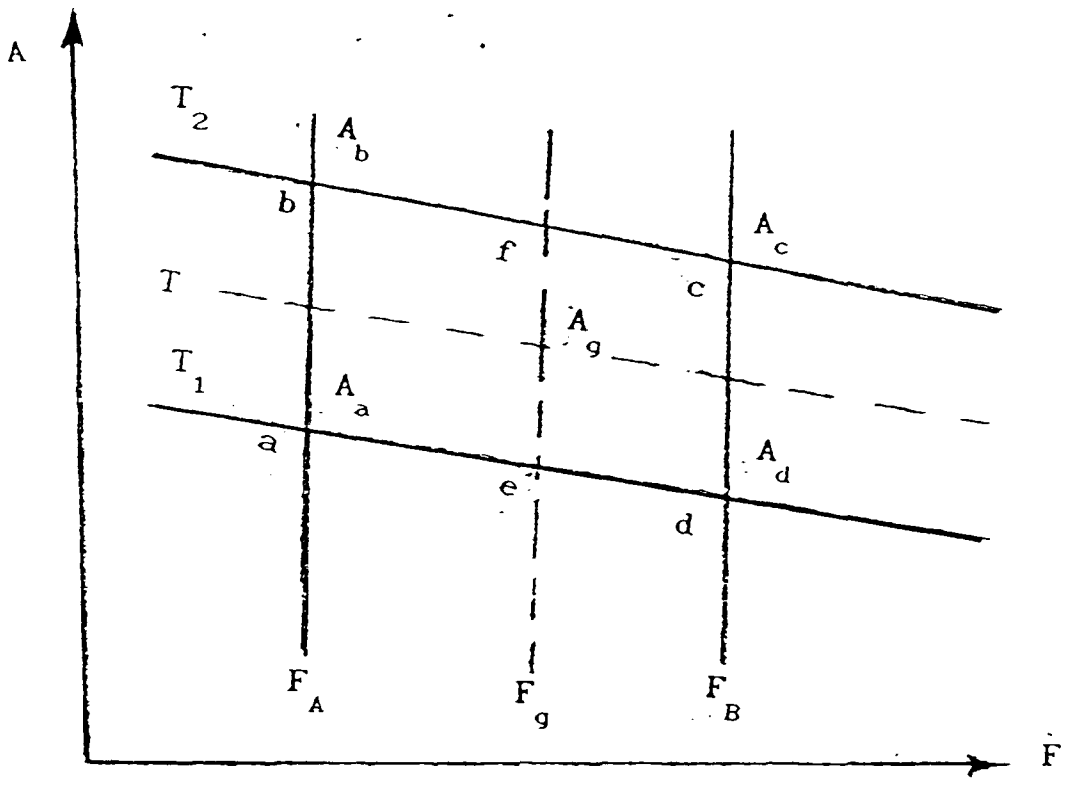

Fig (5.2) ISO Interpolation.

Referring to Figure 5.2 if the RMS acceleration A_g and frequency F_g are defined in such a way that,

$$A_d < A_g < A_b$$

and

$$F_A < F_g < F_B ,$$

the following interpolation can be carried out:

a) **Acceleration Interpolation, at $T=T_1$:**

The equation of the straight line ad at $T=T_1$ is

$$A = m_1 F + C_1$$

where

A, F ...are the acceleration and the frequency variables respectively.

$$m_1 = (A_a - A_d) / (F_A - F_B)$$

$$C_1 = A_a - m_1 F_a \quad \text{or} \quad C_1 = A_d - m_1 F_B$$

Hence, it can be proved that:

$$A_1 = m_1 F_g + C_1 \text{ at } T=T_1 \qquad (5.3)$$

b) Acceleration Interpolation at $T=T_2$:

Similar to the previous case it can be shown that,

$$A_2 = m_2 F_g + C_2 \text{ at } T=T_2 \qquad (5.4)$$

where

$$m_2 = (A_b - A_c) / (F_B - F_A)$$

$$C_2 = A_b - m2 F_B$$

c) Time Interpolation:

Using the previous values, a linear relation is assumed between the exposure time and acceleration as follows:

$$T = m_3 A + C_3 \qquad (5.5)$$

where

$$m_3 = (T_2 - T_1) / (A_2 - A_1)$$

$$C_3 = T_1 - m_3 A_1$$

Hence the required Time is given by :

$$T = m_3 A_g + C_3$$

The same procedure could be repeated for the three direction (i.e vertical, side-to-side, and fort-aft).

(iii) Finally, the minimum value of the time T is to be chosen and used as maximum allowable exposure time for such simulation.

5.1.3 The German "K" Factor:

This criterion is defined as a measure of the observed vibration strength or intensity. It is based on the following formula proposed by Dieckmann in Germany (see Ref. 29):

$$A = \frac{K \sqrt{1 + \left[\frac{f}{f_o}\right]}}{18}$$

where

A ... acceleration m/s^2 (RMS)

$f_o = 5$

f ... frequency Hz.

This formula is entirely empirical, and is calculated to give a substantially constant acceleration criterion up to 5 Hz.

The limitation of application of this criterion is similar to the one in ISO 2631 with respect to the values of the frequency, where the range (1-80 Hz) can only be covered. Recently three formulas for the K-value in the vertical direction in the corresponding frequency ranges are proposed by Hohl [Ref. 32], as follows:

$$\left.\begin{array}{ll} \text{For} \quad 1 \le f \le 4 \text{ Hz} & K_z = 10.\ a\sqrt{f} \\ \text{For} \quad 4 \le f \le 8 \text{ Hz} & K_z = 20.\ a \end{array}\right\} \qquad (5.6)$$

$$\text{For} \quad 8 \le f \le 80 \text{ Hz} \qquad K_z = 160.\ a\ /\ f$$

And the third octave band analysis filter is to be used in a way similar to that used with ISO 2631. The difference between these ranges is made in words as not, little, normal, great, maximum.

K Factor Computer Algorithm:

The K-values calculation can be carried out as follows:

(i) A third octave band filter similar to the one used with ISO 2631 can be employed.

(ii) Calculate K-values according to the corresponding frequency and the values of acceleration, using equation (5.6).

(iii) The total K-value can be calculated as the root of the sum of the squared partial K-values as:

$$K_{totl} = \sqrt{K_1^2 + K_2^2 + K_n^2} = \sqrt{\sum K_i^2} \qquad (5.7)$$

5.2 DRIVER SEATS:

The seat or operator/vehicle interface is responsible for the amount of vehicle vibration transmitted to the operator. Recently many attempts to reduce the vibration transmitted to the driver have been made, such developments however should not be on the expense of the driver's ability to "feel" the terrain, but usually the driver should be in better situation than the other crew members to enable him to control speed, and to observe obstacles in front of the vehicle.

5.2.1 Rigid Seat Link:

For a case of a vehicle with rigid body, and to transfer the acceleration, displacement, velocity from the vehicle's C.G. to the driver or any of the crew members position, the rigid link formula of relative speed suggested by [Ref.52], could be used.

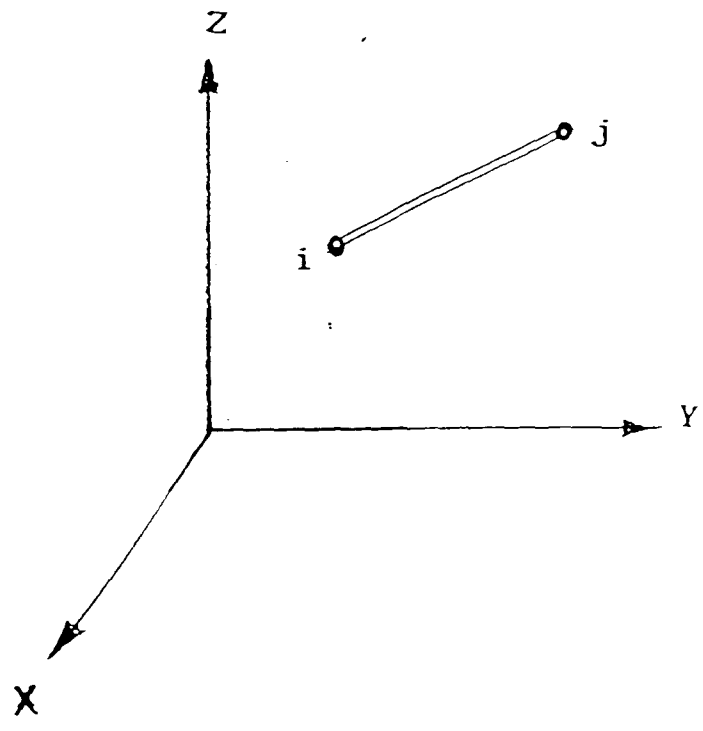

Fig (5.3) Rigid Link

From Figure 5.3 the relative velocity between point j and point i, could be expressed as follows:

$$\dot{\vec{q}}_j = \dot{\vec{q}}_i + \omega \wedge \vec{ij}$$

Defining

$$\mathbf{f}_{ij} = \mathbf{f}_j - \mathbf{f}_i$$

the components of the previous equation can be expressed as follows:

$$\dot{u}_j = \dot{u}_i + (\omega_y z_{ij} - \omega_z y_{ij})$$

$$\dot{v}_j = \dot{v}_i + (\omega_z x_{ij} - \omega_x z_{ij})$$

$$\dot{w}_j = \dot{w}_i + (\omega_x y_{ij} - \omega_y x_{ij})$$

Thus the effect of a rigid link element, can be obtained as:

$$\underline{\delta}_j = \underline{R}\ \underline{\delta}_i$$

$$\dot{\underline{\delta}}_j = \underline{R}\ \dot{\underline{\delta}}_i$$

$$\ddot{\underline{\delta}}_j = \underline{R}\ \ddot{\underline{\delta}}_i$$

where

$$\underline{R} = \begin{bmatrix} u & v & w & \theta_x & \theta_y & \theta_z \\ 1 & 0 & 0 & 0 & Z_{ij} & -y_{ij} \\ 0 & 1 & 0 & -Z_{ij} & 0 & X_{ij} \\ 0 & 0 & 1 & y_{ij} & -X_{ij} & 0 \\ 0 & 0 & 0 & 1 & 0 & 0 \\ 0 & 0 & 0 & 0 & 1 & 0 \\ 0 & 0 & 0 & 0 & 0 & 1 \end{bmatrix}$$

$$\underline{\delta} = \{ u\ v\ w\ \theta_x\ \theta_y\ \theta_z \}$$

$$\underline{\delta} = \{ u\ v\ w\ \omega_x\ \omega_y\ \omega_z \}$$

$$\underline{\delta} = \{ \ddot{u}\ \ddot{v}\ \ddot{w}\ \dot{\omega}_x\ \dot{\omega}_y\ \dot{\omega}_z \}$$

For a rigid seat connected to the body of the vehicle, the following vectors can be defined to obtain the driver seat displacement, velocity, and acceleration.

$$\vec{\delta}_d = \vec{\delta}_o + \vec{\theta} \wedge \vec{R}$$

$$\dot{\vec{\delta}}_d = \dot{\vec{\delta}}_o + \vec{\omega} \wedge \vec{R}$$

$$\ddot{\vec{\delta}}_d = \ddot{\vec{\delta}}_o + \dot{\vec{\omega}} \wedge \vec{R} + \vec{\omega} \wedge (\vec{\omega} \wedge \vec{R})$$

where subscript o represents the origin of Cartesian coordinates. Defining the position vector $\overrightarrow{R}$ as

$$\overrightarrow{R} = X_d \hat{i} + Y_d \hat{j} + Z_d \hat{k}$$

then, it can be shown that:

$$\overrightarrow{\omega} \wedge \overrightarrow{R} = \begin{vmatrix} \hat{i} & \hat{j} & \hat{k} \\ \dot{\theta} & \dot{\phi} & 0 \\ X_d & Y_d & Z_d \end{vmatrix}$$

$$= Z_d \dot{\phi}\, \hat{i} - Z_d \dot{\theta}\, \hat{j} + \left[Y_d \dot{\theta} - X_d \dot{\phi} \right] \hat{k} \qquad (5.8)$$

and

$$\overrightarrow{\omega} \wedge (\overrightarrow{\omega} \wedge \overrightarrow{R}) = \begin{vmatrix} \hat{i} & \hat{j} & \hat{k} \\ \dot{\theta} & \dot{\phi} & 0 \\ Z_d \dot{\phi} & -Z_d \dot{\theta} & Y_d \dot{\theta} - X_d \dot{\phi} \end{vmatrix}$$

$$= \left[Y_d \dot{\theta}\, \dot{\phi} - X_d \dot{\phi}^2 \right] \hat{i} + \left[X_d \dot{\theta}\, \dot{\phi} - Y_d \dot{\theta}^2 \right] \hat{j}$$

$$- \left[Z_d \dot{\phi}^2 + Z_d \dot{\theta}^2 \right] \hat{k} \qquad (5.9)$$

Hence the driver-seat displacement in the X, Y, and Z directions can be expressed as:

$$\begin{bmatrix} \delta_x \\ \delta_y \\ \delta_z \end{bmatrix}_d = \begin{bmatrix} \delta_x \\ \delta_y \\ \delta_z \end{bmatrix}_{C.G.} + \begin{vmatrix} \hat{i} & \hat{j} & \hat{k} \\ \theta & \phi & 0 \\ X_d & Y_d & Z_d \end{vmatrix}$$

Since the vertical displacement (δ_z) is only considered for the C.G. it can be proved that:

$$(\delta_x)_d = \phi\, Z_d \tag{5.10}$$

$$(\delta_y)_d = -\,\theta\, Z_d \tag{5.11}$$

$$(\delta_z)_d = \delta_z + \theta\, Y_d - \phi\, X_d \tag{5.12}$$

Similarly, it can be deduced that the driver-seat velocities are:

$$(\dot{\delta}_x)_d = \dot{\phi}\, Z_d \tag{5.13}$$

$$(\dot{\delta}_y)_d = -\,\dot{\theta}\, Z_d \tag{5.14}$$

$$(\dot{\delta}_z)_d = \dot{\delta}_z + \dot{\theta}\, Y_d - \dot{\phi}\, X_d \tag{5.15}$$

and the driver-seat accelerations are:

$$(\ddot{\delta}_x)_d = \ddot{\phi}\, Z_d + Y_d \dot{\theta}\, \dot{\phi} - X_d \dot{\phi}^2 \tag{5.16}$$

$$(\ddot{\delta}_y)_d = -\,\ddot{\theta}\, Z_d + X_d \dot{\theta}\, \dot{\phi} - Y_d \dot{\theta}^2 \tag{5.17}$$

$$(\ddot{\delta}_z)_d = \ddot{\delta}_z + \ddot{\theta}\, Y_d - \ddot{\phi}\, X_d - Z_d \dot{\phi}^2 - Z_d \dot{\theta}^2 \tag{5.18}$$

5.2.2 Elastic Seat Link:

If it is necessary to protect the driver or the crew members from high vibration intensity which can not be avoided, an elastic seat link may be used, but the seat deformation should be controlled in order to prevent any damaging effect from vehicle vibration. In 1972 an experimental study carried out by Stikeleather [Ref. 28] showed that foam and spring cushions tend to amplify the input motion at low frequencies to which man is most sensitive and where terrain induced vehicle vibration tends to be concentrated. So properly-suspended seats, are suggested to overcome such a problem, where elastic coupling of the cushion and the vehicle by means of mechanical, pneumatic, or hydropneumatic springs incorporates viscous damping. Also the seats can attenuate both vertical and fore-aft vibration simultaneously.

For a suspended seat as shown in Figure 5.4, the differential equation of motion of a person of mass M_d can be expressed as:

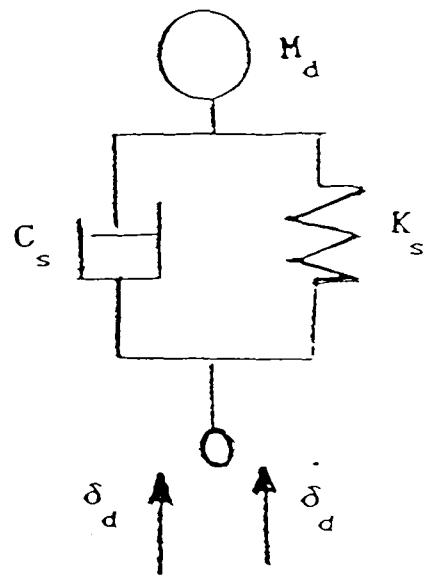

Fig (5.4) Driver Suspension Seat Model.

$$M_d \ddot{\delta}_d(t) + C_s \dot{\delta}_d(t) + K_s \delta_d(t) = F(t) \qquad (5.19)$$

where

C_s... is the seat coefficient of damping.

K_s... is the seat spring stiffness.

$\dot{\delta}_d$, δ_d... are the excitation velocity, displacement, which can be obtained from rigid seat link.

F....is the excitation force.

$$F = C_s \dot{\delta}_d + K_s \delta_d$$

Equation (5.19) is a non-homogeneous second order differential equation, which can be solved by any of the methods discussed in chapter 6.

CHAPTER

SIX

DYNAMIC ANALYSIS OF SUSPENSION SYSTEMS

6.1 INTRODUCTION:

The main objective of dynamic analysis is to enable the vehicle designer or the package user to make a successful assessment of the dynamic characteristics of suspension systems and to produce data relevant for ride analysis.

The basic types of dynamic analysis carried out by means of the programming package presented in this work are as follows:

1. **Steady State Response Analysis:**

   which is forced vibration analysis or the analysis of system response to periodic excitations.

2. **Natural Frequency Analysis:**

   This can be carried out in two stages:

   (i) The solution of the undamped dynamic value problem to provide approximate estimation of natural modes of vibration and natural frequencies.

   (ii) Analysis of resonance frequencies taking damping into consideration.

3. **Transient Response Analysis:**

   which is general dynamic analysis due to any excitation.

The previous types of analysis are introduced for the solution of the assembled finite element equation of the suspension system i.e.

$$\underline{M}\,\ddot{\underline{\delta}}(t) + \underline{C}\,\dot{\underline{\delta}}(t) + \underline{K}\,\underline{\delta}(t) = \underline{F}(t) \qquad (6.1)$$

and most of them can be carried out with the presence of one or more sources of non-linearities, as explained in this chapter.

6.2 STEADY STATE RESPONSE:

In this case the force vector $\underline{F}(t)$ in equation (6.1) is based upon a periodic excitation, i.e. $\underline{F}(t)$ repeats itself after every period of time T. The steady state response usually represents the response of the system after a considerable time, i.e. ignoring the transient effect. An efficient way of dealing with this analysis mathematically is based upon complex variables, and any periodic force can be represented in terms of Fourier series as follows:

$$\underline{F}(t) = \frac{\underline{A}_o}{2} + \sum_{n=1}^{\infty} \left[\underline{A}_n \cos(n\,\omega\,t) + \underline{B}_n \sin(n\,\omega\,t) \right] \qquad (6.2)$$

where

$$\omega = 2\Pi \,/\, T$$

$$\underline{A}_n = \frac{2}{T} \int_0^T \underline{F}(t) \cos(n\,\omega\,t)\, dt$$

$$\underline{B}_n = \frac{2}{T} \int_0^T \underline{F}(t) \sin(n\,\omega\,t)\, dt$$

Equation (6.2) may be rewritten as follows:

$$\underline{F}(t) = \underline{F}_o + \sum_{n=1}^{\infty} \underline{F}_n \qquad (6.3)$$

where

$$\underline{F}_n(t) = \underline{A}_n \cos(n\,\omega\,t) + \underline{B}_n \sin(n\,\omega\,t) \qquad (6.4)$$

$$\underline{F}_o = \frac{1}{2} A_o$$

and the effect of $\underline{F}_o$ can be dealt with by means of static analysis, i.e. solve,

$$\underline{\underline{K}}\ \underline{\delta}_o = \underline{F}_o \qquad (6.5)$$

Hence, it is required then to solve the following systems of equations:

$$\underline{\underline{M}}\ \ddot{\underline{\delta}}_n(t) + \underline{\underline{C}}\ \dot{\underline{\delta}}_n(t) + \underline{\underline{K}}\ \underline{\delta}_n(t) = \underline{F}_n(t) \qquad (6.6)$$

where

$$n = 1, 2, \ldots.$$

And the overall answer is given by:

$$\underline{\delta}(t) = \sum_{n=0}^{\infty} \underline{\delta}_n(t) \qquad (6.7)$$

6.2.1 **The Steady State Solution:**

The system of equations (6.6) can be dealt with using complex variables, and it can be shown that:

$$\underline{F}_n = R\left\{ (\underline{A}_n + j\underline{B}_n)\, e^{-jn\omega t} \right\}$$

$$= R\left\{ \hat{\underline{F}}_n\, e^{-jn\omega t} \right\} \qquad (6.8)$$

where

$$\hat{\underline{F}}_n = \underline{A}_n + j\underline{B}_n \ ,$$

$$e^{-j\theta} = \cos\theta - j\sin\theta \ ,$$

$$j = \sqrt{-1} \ , \text{ and}$$

$R(z) \equiv$ Real part of (z).

A solution to the system defined by equation (6.4) can be assumed as follows:

$$\underline{\delta}_n(t) = \underline{\alpha}_n \cos(n\,\omega\,t) + \underline{\beta}_n \sin(n\,\omega\,t)$$

$$= R\left\{ \hat{\underline{\delta}}_n\, e^{-jn\omega t} \right\} \qquad (6.9)$$

where

$$\hat{\underline{\delta}}_n = \underline{\alpha}_n + j\,\underline{\beta}_n$$

Hence it can be deduced that:

$$\dot{\underline{\delta}}_n(t) = -n\omega \left[\underline{\alpha}_n \cos(n\omega t) + \underline{\beta}_n \sin(n\omega t) \right]$$

$$= R\left\{ - jn\omega \hat{\underline{\delta}}_n e^{-jn\omega t} \right\} \qquad (6.10)$$

and

$$\ddot{\underline{\delta}}_n(t) = -(n\omega)^2 \left[\underline{\alpha}_n \cos(n\omega t) + \underline{\beta}_n \sin(n\omega t) \right]$$

$$= R\left\{ - (n\omega)^2 \hat{\underline{\delta}}_n e^{-jn\omega t} \right\} \qquad (6.11)$$

Substituting equations (6.8), (6.9), (6.10), and (6.11) into equation (6.6) it can be proved that:

$$R\left\{ \left[- (n\omega)^2 \underline{M} - j(n\omega) \underline{C} + \underline{K} \right] \hat{\underline{\delta}}_n e^{-jn\omega t} \right\}$$

$$= R\left\{ \hat{\underline{F}}_n e^{-jn\omega t} \right\} \qquad (6.12)$$

The solution of the above equation is equivalent to the solution of the following system:

$$\left[- (n\omega)^2 \underline{M} - j(n\omega) \underline{C} + \underline{K} \right] \hat{\underline{\delta}}_n = \hat{\underline{F}}_n \qquad (6.13)$$

which represents a linear system of simultaneous complex equations, which can be solved using Gauss-elimination or any other method.

6.3 NATURAL FREQUENCY ANALYSIS:

6.3.1 **Frequency Analysis of Undamped Systems:**

The natural frequency analysis of a real damped system is very time consuming and based upon complex variables. Since, the damping may have little effect on the natural modes of vibration, an analysis can be carried out neglecting damping and solving the dynamic eigenvalue problem governed by:

$$\underline{M}\,\ddot{\underline{\delta}} + \underline{K}\,\underline{\delta} = \underline{0} \qquad (6.14)$$

This analysis has may systematic direct algorithms [see Ref. 56], and it will provide the user with approximate values of natural frequencies which can be improved by carrying out an analysis as suggested by section 6.3.2.

An extensive explanation to the solution of the problem was given in references [53,55], and the solution of which can also be found in references [54,58].

6.3.1.1 **Formulation of the Dynamic Eigenvalue Problem:**

If there are no external forces, and if the initial condition are properly imposed, it is possible to induce vibration in any one of several natural modes which are characteristic of the structure. In a natural mode, each point of the structure executes harmonic motion about the position of static equilibrium at the same frequency. So it can be assumed that, at a natural mode of vibration, for undamped system:

$$\underline{\delta}(t) = \underline{\delta}\cos\omega t \qquad (6.15)$$

where

$\underline{\delta}$ .... is the vector of displacement amplitude.

Differentiating equation (6.15) with respect to time, it can be shown that:

$$\dot{\underline{\delta}}(t) = - \omega \, \underline{\delta} \sin \omega \, t \qquad (6.16)$$

$$\ddot{\underline{\delta}}(t) = - \omega^2 \, \underline{\delta} \cos \omega \, t \qquad (6.17)$$

Substituting from equations (6.15-6.17), into equation (6.14), and dividing by cos ω t, it can be deduced that,

$$| \underline{K} - \lambda \underline{M} | \, \underline{\delta} = 0 \qquad (6.18)$$

where

$$\lambda = \omega^2$$

Equation (6.18) is a polynomial equation in λ which is known as the characteristic equation. Its roots λ_1, λ_2 are called the eigenvalues, for each root λ_i, there exists a vector $\underline{\delta}_i$ known as the eignvector, such that

$$| \underline{K} - \lambda_i \, \underline{M} | \, \underline{\delta}_i = 0$$

where the components of the eignvector $\underline{\delta}_i$ can be obtained as ratios to the value of one of them.

6.3.1.2 **The Eigenvalues Simple Iteration Algorithm:**

There are many algorithms available in the literature for the solution of eigenvalue problems, and some of them are capable of handling large finite element systems of equations such as the dynamic condensation algorithm [Ref. 54], and the subspace iteration algorithm [Ref. 53].

Due to the limited number of equations generated for suspension systems, it was decided to develop an algorithm based on direct iterations, and it is referred to as the simple iteration algorithm, which is summarised in this section.

The equation of dynamic eigenvalue problem can be written as follows:

$$\underline{M}\ \underline{\delta} = \frac{1}{\lambda}\ \underline{K}\ \underline{\delta}$$

Multiplying both sides by $\underline{K}^{-1}$, the problem can be expressed as a standard eigenvalue problem.

$$\underline{H}\ \underline{\delta} = \frac{1}{\lambda}\ \underline{I}\ \underline{\delta}$$

where

$$\underline{H} = \underline{K}^{-1}\underline{M}$$

a) Iteration For the Lowest Eigenvalue:

The following iterative steps can be employed and they converge to the minimum eigenvalue.

(i) Start by an assumed value of $\underline{\delta}$, a vector of ones can be used.

(ii) Calculate the following vector:

$$\underline{b} = \underline{H}\ \underline{\delta}$$

(iii) The eigenvalue can be estimated as follows:

$$\lambda = (\underline{b}^T\ \underline{b}) \ / \ (\ \underline{b}^T \underline{H}\ \underline{b}\ )$$

where

$\underline{b}^T$... is the transpose of the vector $\underline{b}$.

(iv) An updated value of $\underline{\delta}$ is $\underline{\delta} = \underline{b} \ / \ \sqrt{\underline{b}^T \underline{M}\ \underline{b}}$

(v) If $| \lambda_{new} - \lambda_{old} | > \varepsilon$ a permissible error, then go to step (ii).

b) Sweeping of λ_j:

Defining

$$\underline{H}_1 = \underline{K}^{-1}\underline{M}$$

then

$$\underline{H}_1\ \underline{\delta} = \frac{1}{\lambda}\ \underline{I}\ \underline{\delta}$$

will converge to λ_1.

From the orthogonality of eigenvectors, it can be proved that:

$$\underline{H}_{j+1}\ \underline{\delta} = \frac{1}{\lambda}\ \underline{I}\ \underline{\delta}$$

converges to λ_{j+1}

where

$$\underline{H}_{j+1} = \underline{H}_{j} - \frac{1}{\lambda_j}\ \underline{\delta}_j^T\ \underline{M}$$

$$\lambda_1 \leq \lambda_2 \leq \lambda_3 \ldots..$$

6.3.2 Frequency Analysis of Damped Systems:

In this analysis, it is required to find the natural frequencies of vibration for the damped system, i.e. to find the resonance frequencies for a system governed by the following differential equation.

$$\underline{M}\ \ddot{\underline{\delta}}\ (t) + \underline{C}\ \dot{\underline{\delta}}(t) + \underline{K}\ \underline{\delta}(t) = \underline{0} \qquad (6.19)$$

The natural mode of vibration can be assumed as:

$$\underline{\delta}(t) = \underline{\delta}\ e^{j\omega t}$$

where

$$j = \sqrt{-1}$$

Differentiating with respect to time t, then it can be shown that:

$$\dot{\underline{\delta}}(t) = j\,\omega\,\underline{\delta}\,e^{j\omega t}$$

$$\ddot{\underline{\delta}}(t) = -\,\omega^2\,\underline{\delta}\,e^{j\omega t}$$

Substituting $\underline{\delta}(t)$, $\dot{\underline{\delta}}(t)$, $\ddot{\underline{\delta}}(t)$ into equation (6.19) it can be deduced that:

$$-\,\omega^2\,\underline{M}\,\underline{\delta} + j\,\omega\,\underline{C}\,\underline{\delta} + \underline{K}\,\underline{\delta} = 0$$

or

$$\left[\underline{K} - \omega^2\,\underline{M} + j\,\omega\,\underline{C}\right]\underline{\delta} = 0 \qquad (6.20)$$

The non-trivial solution to equation (6.20) is obtained by finding the real values ω_n $(n = 1,2,\ldots)$, which make the real part of the complex residual function $\mathrm{Res}(\omega)$ equal to zero, where,

$$\mathrm{Res}(\omega) = \left|\,\underline{K} - \omega^2\,\underline{M} + j\,\omega\,\underline{C}\,\right| \qquad (6.21)$$

The technique employed in this work is based on "the determinant search technique". Using the undamped eigenvalue solver discussed in section 6.3.1, one could estimate the ranges of values for the resonance frequencies. Then the residual function $\mathrm{Res}(\omega)$ will be evaluated within such ranges in order to find ω such that $R\left[\mathrm{Res}(\omega)\right] = 0$ whenever the sign of $R\left[\mathrm{Res}(\omega)\right]$ changes (either from positive to negative or vice versa) a critical ω can be found at the point where $R\left[\mathrm{Res}(\omega)\right] = 0$, using the false position rule, illustrated in Figure 6.1.

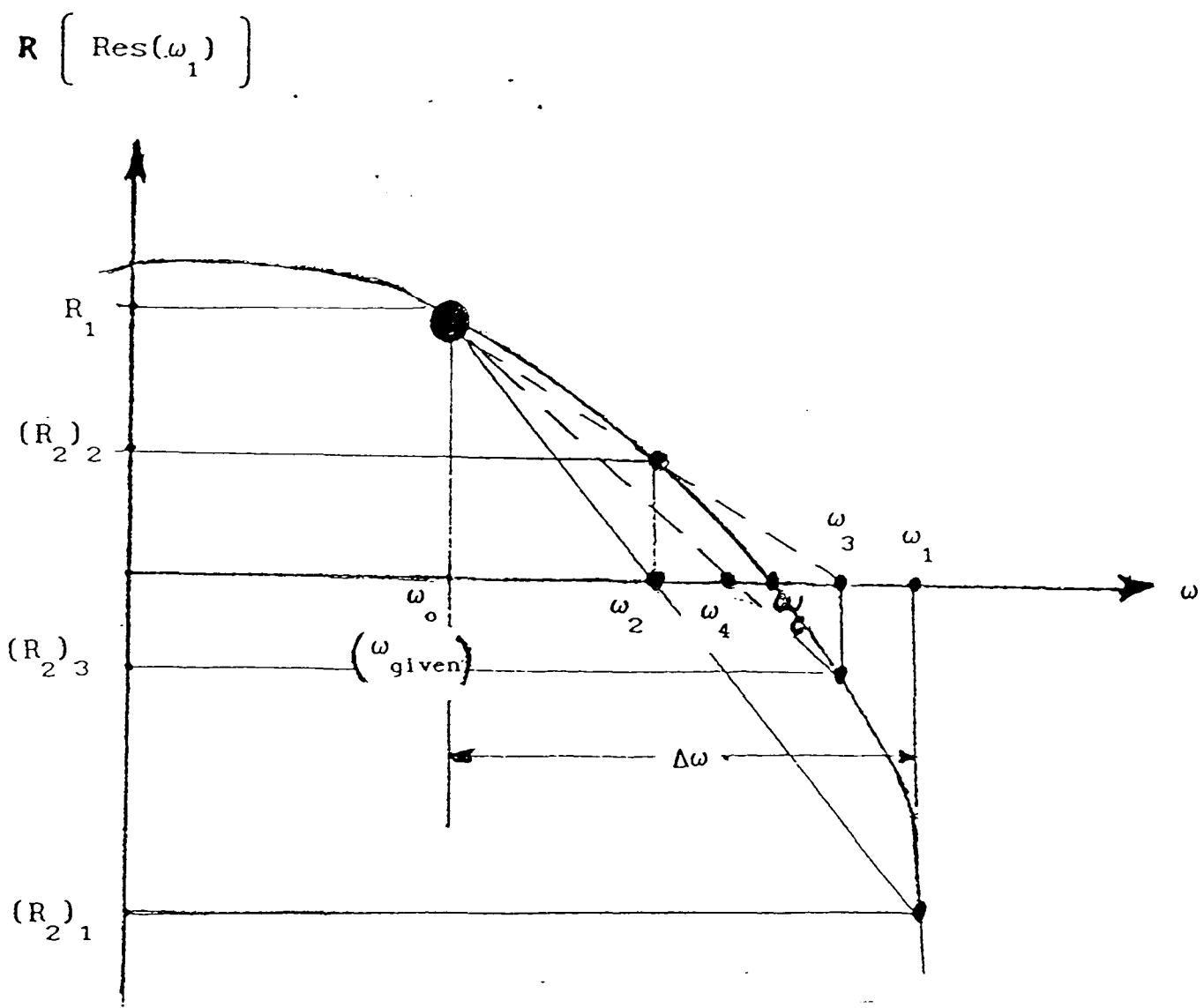

Fig (6.1) Illustration of False Position Iterations.

i.e

$$\frac{\omega_c - \omega_1}{\omega_2 - \omega_1} = \frac{0 - R_1}{R_2 - R_1}$$

or

$$\omega_c = \omega_1 - R_1\left[\frac{\omega_2 - \omega_1}{R_2 - R_1}\right] \qquad (6.22)$$

For a large system of equation an overflow problem may occur which can be dealt with as follows [Ref. 55]:

a) The complex logarithm of the residual function Res(ω) is calculated in terms of summation of logarithms of Gaussian-elimination pivots, found in determinant expansion.

b) Before restoring the value of Res(ω) from its logarithm a scale factor will be used. The division by this implies a subtraction of its logarithm from that of Res(ω). The value of this factor depends on the range of ω used, and it can be estimated automatically at the start of the search algorithm.

6.3.2.1 **Resonance Frequencies Computer Algorithm:**

An analytical solution algorithm to be used for determining the critical frequency, can be carried out as follows:

Given the search range starting from ω_s and ending with ω_e, and increment of $\Delta\omega$, then,

Step (1)

Assume an initial value of ω and calculate $R_1 = R\left[\text{Res}(\omega)\right]$
Check that $R_1 \neq 0$, otherwise ω_c equal to the assumed ω.

Step (2)

Update ω by a given increment $\Delta\omega$, i.e.

$$\omega_{new} = \omega_{old} + \Delta\omega$$

and calculate the real value of the corresponding residual function, i.e.

$$R_2 = \mathbf{R}\left[\mathrm{Res}(\omega_{new})\right]$$

Step (3)

If $|\ R_2\ | \leq \varepsilon$ a permissible error, then $\omega_c = \omega_{new}$ and go to step (1) to search for another value of ω_c.

Step (4)

If $R_1 R_2 > 0$
this means that both R_1 and R_2 have the same sign, then go to step (2).

Step (5)

If $R_1 R_2 < 0$ then there exists an ω_c, such that

$$\omega_1 < \omega_c < \omega_2$$

The search can now be improved by invoking the false position rule given by equation (6.22),

i.e.

$$\omega_{new} = \omega_1 - R_1\left[\frac{\omega_2 - \omega_1}{R_2 - R_1}\right] \qquad (6.23)$$

Step (6)

Calculate $R_2 = \mathbf{R}\left[\mathrm{Res}(\omega_{new})\right]$

and check the absolute value of R2, if $| R_2 | > \varepsilon$ use equation (6.23) for more refinement of ω_{new}. Repeat the iteration until $| R_2 | \leq \varepsilon$ then ω_c = the last value of ω, and go to step (1) to search for another value of ω_c.

6.4 TRANSIENT RESPONSE ANALYSIS:

For the case of the exciting force vector $\underline{F}(t)$ being a general function of time, and in order to carry out a ride analysis for an off-road vehicle, it is essential to estimate the displacement, velocity and acceleration as functions of time by finding the transient solution of the dynamic equations of the off-road vehicle suspension system. Due to the characteristics of such vehicles (very heavy structures moving on nonuniform terrains), the integration of their dynamic equations is very sensitive and requires special schemes, and such equations are known in the literature as "stiff equations", which characterise a structure whose highest frequencies are much greater than the lowest [Ref. 42].

Techniques for obtaining transient solutions for such dynamic equations are usually known as time marching techniques, which can generally be defined in terms of a step-by-step integration of the system dynamic equations with respect to time, starting from known initial conditions.

Practical time marching schemes for large systems of equations, as in the case of finite element derivations have been reviewed by Zienkiewicz [Ref. 57], and Bathe [Ref. 37]. A new scheme was developed by the finite element group at Cranfield Institute of Technology based upon the Hermitian weighted residual method [Ref.36], and it has been successfully used for the transient response analysis of "stiff" equations for off-road vehicles [Ref. 59].

The methods employed in this work can be summarised as follows:

6.4.1 **The Central Difference Method:**

The derivation of this method is shown in Appendix C, and to solve the system dynamic equations by means of this method [Ref 53], the following time marching algorithm could be used:

a) **Calculation of Basic Parameters.**

These are defined as follows:

$$a_o = \frac{1}{(\Delta t)^2}$$

$$a_1 = \frac{1}{2\Delta t}$$

$$a_2 = 2\, a_o$$

$$a_3 = \frac{1}{a_2}$$

and from which the following matrices are calculated:

$$\underline{Q}_1 = a_o \underline{M} - a_1 \underline{C}$$

$$\underline{Q}_2 = \underline{K} - a_2 \underline{M}$$

$$\hat{\underline{M}} = a_o \underline{M} - a_1 \underline{C}$$

b) **Initiation At t = 0.**

(i) Given $\underline{\delta}_o$, $\dot{\underline{\delta}}_o$ at t = 0

(ii) Given the equation which defines $\underline{F}(t)$, then calculate

$$\underline{F}_o = \underline{F}(0)$$

(iii) From the original dynamic equations.

$$\underline{M}\,\ddot{\underline{\delta}}_o + \underline{C}\,\dot{\underline{\delta}}_o + \underline{K}\,\underline{\delta}_o = \underline{F}_o$$

Evaluate $\ddot{\underline{\delta}}_o$

(iv) From $\underline{\delta}_{n-1} = \underline{\delta}_n - \Delta t\,\dot{\underline{\delta}}_n + a_3\,\ddot{\underline{\delta}}_n$

Find $\underline{\delta}_{-1} = \underline{\delta}_o - \Delta t\,\dot{\underline{\delta}}_o + a_3\ddot{\underline{\delta}}_o$

c) **For every Δt** , n = 0, 1, 2, ...

Given $\underline{\delta}_n$, $\underline{\delta}_{n-1}$, $t_n = n\Delta t$

Solve:

(i) $\hat{\underline{M}}\ \underline{\delta}_{n+1} = \underline{F}_n - \underline{Q}_2\underline{\delta}_n - \underline{Q}_1\underline{\delta}_{n-1}$

where:

$$\underline{F}_n = \underline{F}(t_n)$$

(ii) $\dot{\underline{\delta}}_n = a_1\left[\underline{\delta}_{n+1} + \underline{\delta}_{n-1}\right]$

(iii) $\ddot{\underline{\delta}}_n = a_o\left[\underline{\delta}_{n+1} - 2\underline{\delta}_n + \underline{\delta}_{n-1}\right]$

6.4.2 **The Wilson θ Method:**

The mathematical derivation of this method is reviewed in Appendix C, and the following steps can be used in order to solve for the solution of the system dynamic equations using this method:

a) **Initial Values:**

Calculate the parameters:

a_i where i= 0,1,2, ...,8

(as defined in Appendix C)

hence calculate:

$$\hat{\underline{K}} = \hat{\underline{K}} + a_o \underline{M} + a_1 \underline{C}$$

From $\underline{\delta}_o, \dot{\underline{\delta}}_o$ find $\ddot{\underline{\delta}}_o$ by solving:

$$\underline{M}\,\ddot{\underline{\delta}}_o + \underline{C}\,\dot{\underline{\delta}}_o + \underline{K}\,\underline{\delta}_o = \underline{F}_o$$

b) **For each Δt:**

(i) Calculate:

$$\underline{F}(t+\theta\Delta t) = \underline{F}(t) + \theta \left[\underline{F}(t+\Delta t) - \underline{F}(t)\right]$$
$$+ \underline{M}\left[a_o\,\underline{\delta}(t) + a_2\,\dot{\underline{\delta}}(t) + 2\,\ddot{\underline{\delta}}(t)\right]$$
$$+ \underline{C}\left[a_1\,\underline{\delta}(t) + 2\,\dot{\underline{\delta}}(t) + a_3\,\ddot{\underline{\delta}}(t)\right]$$

(ii) To obtain $\underline{\delta}\,(t+\theta\Delta t)$ solve:

$$\hat{\underline{K}}\ \underline{\delta}\ (t+\theta\Delta t) = \underline{F}\ (t+\theta\Delta t)$$

(iii) To obtain $\ddot{\underline{\delta}}\ (t+\Delta t)$, $\dot{\underline{\delta}}\ (t+\Delta t)$, and $\underline{\delta}(t+\Delta t)$ the following equations are used :

$$\ddot{\underline{\delta}}\ (t+\Delta t) = a_4\left[\underline{\delta}\ (t+\theta\Delta t) - \underline{\delta}\ (t)\right] + a_5\dot{\underline{\delta}}\ (t) + a_6\ \ddot{\underline{\delta}}\ (t)$$

$$\dot{\underline{\delta}}\ (t+\Delta t) = \dot{\underline{\delta}}\ (t) + a_7\left[\ddot{\underline{\delta}}\ (t+\Delta t) + \ddot{\underline{\delta}}(t)\right]$$

$$\underline{\delta}\ (t+\Delta t) = \underline{\delta}\ (t) + \Delta t\ \dot{\underline{\delta}}\ (t) + a_8\left[\ddot{\underline{\delta}}\ (t+\Delta t) + 2\ \ddot{\underline{\delta}}(t)\right]$$

6.4.3 **The Houbolt Method:**

The Houbolt method is based upon the same difference equation in terms of four time nodes [Ref. 53] and its mathematical derivation is reviewed in Appendix C. The basic steps of this method can be summarised as follows:

a) Initiation:

Use central difference scheme (or any possible method) to define:

$\underline{\delta}_{-1}$, $\underline{\delta}_{o}$, $\underline{\delta}_{-1}$ in terms of initial conditions.

b) Initial Calculation:

(i) Calculate a_o, a_1, a_2,...,a_7 , as defined in Appendix C

(ii) $\hat{\underline{K}} = \underline{K} + a_o \underline{M} + a_1 \underline{C}$

c) At every Δt :

Solve:

$$\hat{\underline{K}}\ \underline{\delta}_{n+1} = \underline{F}_{n+1} + \underline{M}\left[a_2\ \underline{\delta}_n + a_4\ \underline{\delta}_{n-1} + a_6\ \underline{\delta}_{n-2}\right]$$

$$+ \underline{C}\left[a_3\ \underline{\delta}_n + a_5\ \underline{\delta}_{n-1} + a_7\ \underline{\delta}_{n-2}\right]$$

then to find $\ddot{\underline{\delta}}_{n+1}$, $\dot{\underline{\delta}}_{n+1}$ the following equations can be employed.

$$\ddot{\underline{\delta}}_{n+1} = a_o\ \underline{\delta}_{n+1} - a_2\ \underline{\delta}_n - a_4\ \underline{\delta} - a_6\ \underline{\delta}_{n-2}$$

$$\dot{\underline{\delta}}_{n+1} = a_1\ \underline{\delta}_{n+1} - a_3\ \underline{\delta}_n - a_5\ \underline{\delta}_{n-1} - a_7\ \underline{\delta}_{n-2}$$

6.4.4 Hermitian Weighted Residual Scheme:

This scheme is similar, in dealing with the time response problems to the previous methods, but based upon the Hermitian interpolation formula, a 2-node time element is defined in Appendix C for this scheme.

6.4.5 Lagrangian Weighted Residual Scheme:

This method is employed to solve the system governing equations, where the time steps are considered as time-nodes, a case of 3-time node element is reviewed in Appendix C.

6.4.6 Runge Kutta Scheme:

This is a fourth order Runge-Kutta scheme which is employed in this work, to solve the system of differential equations. The parameters $\underline{\delta}_o$, $\dot{\underline{\delta}}_o$ and $\underline{F}_o$ are assumed to be known at time $t = t_o$. The basic four steps in this method can be summarised as follows [Ref. 36]:

Step (1)

Defining $\underline{\delta}_{-1} = \underline{\delta}_o$, $\dot{\underline{\delta}}_{-1} = \dot{\underline{\delta}}_o$ and $\underline{F}_{-1} = \underline{F}_o$ at $t_1 = t_o$, the following equation is solved for $\ddot{\delta}_1$:

$$\underline{M}\,\ddot{\underline{\delta}}_{-1} = \underline{F}_{-1} - \underline{C}\,\dot{\underline{\delta}}_{-1} - \underline{K}\,\underline{\delta}_{-1}$$

then the vector $\underline{G}_1$ is obtained as follows:

$$\underline{G}_{-1} = \Delta t\,\ddot{\underline{\delta}}_{-1}$$

Step (2)

Calculate:

$$\underline{\delta}_{-2} = \underline{\delta}_o + \frac{\Delta t}{2}\left(\dot{\underline{\delta}}_o + \frac{1}{4}\underline{G}_{-1}\right)$$

$$\dot{\underline{\delta}}_{-2} = \dot{\underline{\delta}}_o + \frac{1}{2}\underline{G}_{-1}$$

$$\underline{F}_{-2} = \underline{F}(t_2) \ , \ \text{where} \ t_2 = t_o + \frac{\Delta t}{2}$$

and solve

$$\underline{M}\ \ddot{\underline{\delta}}_{-2} = \underline{F}_{-2} - \underline{C}\ \dot{\underline{\delta}}_{-2} - \underline{K}\ \underline{\delta}_{-2}$$

Hence, the following vector can be obtained:

$$\underline{G}_{-2} = \Delta t\ \ddot{\underline{\delta}}_{-2}$$

Step (3)

The same procedure as in step (2) is repeated using:

$$\underline{\delta}_{-3} = \underline{\delta}_{-o} + \frac{\Delta t}{2}\left[\dot{\underline{\delta}}_{-o} + \frac{1}{4}\underline{G}_{-2}\right]$$

$$\dot{\underline{\delta}}_{-3} = \dot{\underline{\delta}}_{-o} + \frac{1}{2}\underline{G}_{-2}$$

$$\underline{F}_{-3} = \underline{F}\left[t_o + \frac{\Delta t}{2}\right]$$

to obtain $\underline{G}_{-3}$

Step (4)

The same procedure as in step (3) is repeated with:

$$\underline{\delta}_{-4} = \underline{\delta}_{-o} + \Delta t\left[\dot{\underline{\delta}}_{-o} + \frac{1}{2}\underline{G}_{-2}\right]$$

$$\dot{\underline{\delta}}_{-4} = \dot{\underline{\delta}}_{-o} + \underline{G}_{-2}$$

$$\underline{F}_{-2} = \underline{F}(t_4) \ , \ \text{where} \ t_4 = t_o + \Delta t$$

to define $\underline{G}_4$

The final answers are obtained as follows:

$$\underline{\delta}(t_o + \Delta t) = \underline{\delta}_o + \Delta\underline{\delta}$$

$$\dot{\underline{\delta}}(t_o + \Delta t) = \dot{\underline{\delta}}_o + \Delta\dot{\underline{\delta}}$$

where:

$$\Delta\underline{\delta} = \Delta t \left[\dot{\underline{\delta}}_o + (\underline{G}_1 + \underline{G}_2 + \underline{G}_3)/ 6 \right]$$

$$\Delta\dot{\underline{\delta}} = (\underline{G}_1 + 2\underline{G}_2 + 2\underline{G}_3 + \underline{G}_4)/ 6$$

and

$$\ddot{\underline{\delta}} = \underline{M}^{-1} \left[\underline{F} - \underline{K}\,\underline{\delta} - \underline{C}\,\dot{\underline{\delta}} \right]$$

Notice that for more than one time step, the procedure from step (1) to the final should be repeated for each time step.

6.5 NON-LINEAR EFFECTS:

Some of the practical causes for non-linear behaviour of an off-road vehicle suspension system are when vehicle components or auxiliary devices are subjected to highly nonuniform forces causing an abrupt change of the system dynamic governing equations such as; a blow-off of a damper, wheels leaving the ground, or bump stops being in action, etc. In this work, most of these non-linearities have been considered within transient dynamic analysis. The types of non-linearities can be summarised as follows:

6.5.1 **Main Springs or Dampers Non-Linearity:**

This is the case when one or more of the main springs or dampers have non-linear characteristics. Due to the fact that off-road tracked vehicles have non pneumatic tyres to damping the effects of sharp edged obstacles, their main dampers may blow-off at such circumstances to avoid the possibility of being damaged, and the blow-off function leads to a non-linear behaviour of such dampers.

Springs and dampers non-linear characteristics are represented in terms of non-linear analytical expressions or graphs between forces and spring deflection and/or damper velocity. Such expressions can be employed in the differential equations during the steps of time-marching through updating the values of stiffness and damping matrices.

6.5.2 **The Bump Stop Non-Linearity:**

Due to the irregularity of the terrain, one or more of the road wheels may leave the ground when hitting a sharp edged obstacle, this behaviour sometimes leads to a heavy bottoming of the vehicle hull to the ground, and bump stops may be used for limiting the vertical travel path of such wheels to avoid such problem. The bump stop is made of rubber or steel springs located in a proper position above the road wheel centre, and it is considered in when the following relation applies:

$$\delta_p + P_T - \delta_1 < 0$$

where

δ_p is the displacement of point P on the hull which lies directly above the wheel centre.

P_T is the travel from the initial position to the bump stop.

It is clear that the bump stop spring stiffness should be added to that of the main spring and this effect should be included in the differential equations. For the case of the simple suspension element discussed in chapter three the bump stop effect is included by modifying equation (3.8) such that:

$$F_z^{(e)} = C^{(e)} \left[\dot{\delta}_o + (y_e - y_o)\,\dot{\theta}_o + (X_o - X_e)\,\dot{\phi}_o - \dot{\delta}^{(e)} \right]$$

$$+ \left[K^{(e)} + K_b^{(e)} \right] \left[\delta_o + (y_e - y_o)\,\theta_o + (X_o - X_e)\,\phi_o - \delta^{(e)} \right]$$

$$+ K_b^{(e)} \left[P_T^{(e)} - Z^{(e)} \right]$$

where

K_b is the bump stop spring stiffness.

Similar modifications have been considered for other types of suspension elements.

6.5.3 **Non-Linear Characteristics of the Tyre or the Road Wheel:**

The source of this nonlinearity is the kind of contact between the road wheel or tyre and the ground. In fact there are two types of contact, the point contact which was discussed in chapter four, and the extended contact. The equivalent stiffness coefficient of the road wheel or tyre has a significant effect on the overall dynamics of the vehicle. The second type of contact and the calculation of the equivalent stiffness of the road wheel or tyre will be discussed in this section.

The model employed in this case is the radial spring model as shown in Figure 6.2, a number of radial springs is selected to approximate the tyre compliance. The effective angle α, and the deflection Z are specified by the package user.

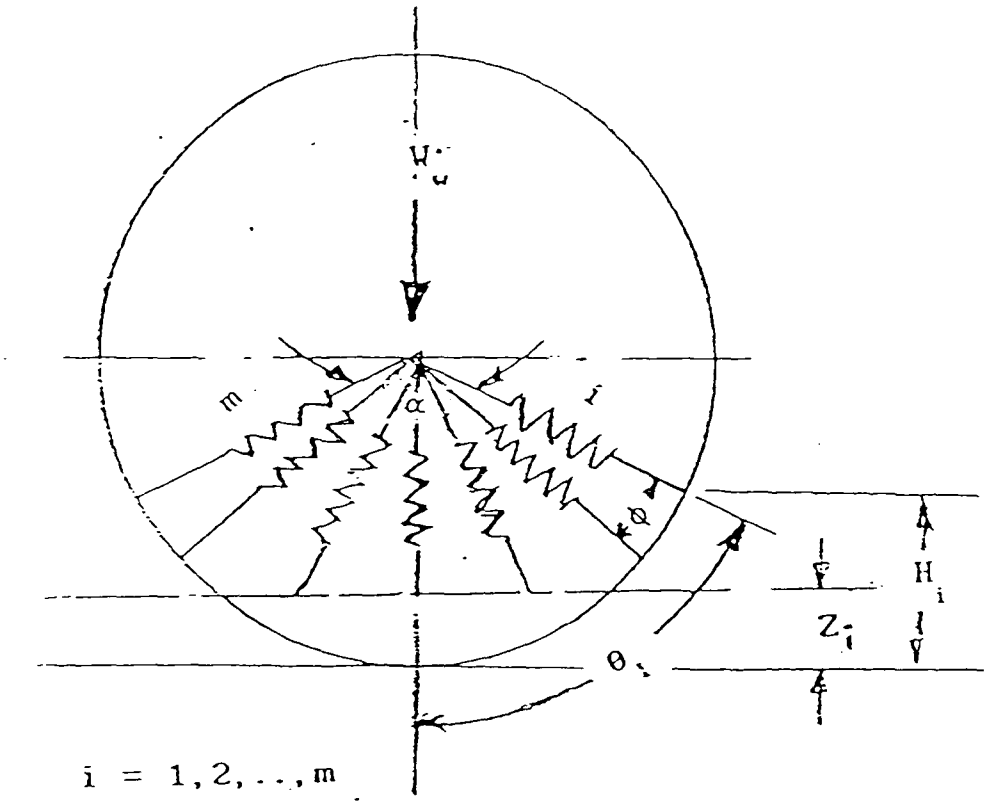

Fig (6.2) Radial Spring Road Wheel or Tyre Model.

The equivalent spring stiffness can be calculated by using the following static equation [Ref. 3].

$$W_w = K_w \sum_{i=1}^{m} \delta_i \cos \theta_i$$

where

W_w is the total load on the wheel,

K_w is the road wheel equivalent spring stiffness,

δ_i is the vertical deflection of the i^{th} spring as:

$$\delta_i = Z_i - H_i \quad \text{for} \quad Z_i - H_i \geq 0$$

$$\delta_i = 0 \quad \text{for} \quad Z_i - H_i < 0$$

Z_i is the vertical height of terrain profile beneath the i^{th} spring (given by the tabulated terrain data),

H_i is the height from the zero reference to the i^{th} spring of the undeflected wheel,

θ_i is the angle to the i^{th} spring measured from a vertical axis through the wheel centre, and

m is the total number of the segment springs.

6.5.4 Non-Linearity Resulting From Large Deflection Considerations:

This kind of nonlinearity is considered in the derivation of the equations of motion of the suspension systems when the pitch and roll angle can no longer be assumed small. With the large deflection assumption being taken into consideration, the general dynamic equations will include harmonic terms and the matrix form in chapter three is no longer suitable. A new derivation hence is necessary to include such nonlinearity.

The simple suspension element is used in this section to demonstrate such derivations, hence, when substituting equations (3.1), (3.2) into equations (3.8), (3.9), (3.10), (3.12), and (3.13), the nonlinear equations can be shown as:

First Equation:

$$F_z^{(e)} = C^{(e)} \left[\dot{\delta}_o + \left\{ (y_e - y_o) \cos\theta_o - (Z_e - Z_o) \sin\theta_o \right\} \dot{\theta}_o \right.$$

$$\left. + \left\{ (X_o - X_e) \cos - (Z_e - Z_o) \sin\phi_o \right\} \dot{\phi}_o - \dot{\delta}^{(e)} \right]$$

$$+ K^{(e)} \left[\delta_o + (y_e - y_o) \sin\theta_o + (X_o - X_e) \sin\phi_o \right.$$

$$\left. - (Z_e - Z_o)(2 - \cos\theta_o - \cos\phi_o) - \delta^{(e)} \right]$$

Second Equation:

$$M_x^{(e)} = C^{(e)}(y_e - y_o)\left[\dot{\delta}_o + \left\{(y_e - y_o)\cos\theta_o - (Z_e - Z_o)\sin\theta_o\right\}\dot{\theta}_o\right.$$

$$\left. + \left\{(X_o - X_e)\cos - (Z_e - Z_o)\sin\phi_o\right\}\dot{\phi}_o - \dot{\delta}^{(e)}\right]$$

$$+ K^{(e)}(y_e - y_o)\left[\delta_o + (y_e - y_o)\sin\theta_o + (X_o - X_e)\sin\phi_o\right.$$

$$\left. - (Z_e - Z_o)(2 - \cos\theta_o - \cos\phi_o) - \delta^{(e)}\right]$$

Third Equation:

$$M_y^{(e)} = C^{(e)}(X_o - X_e)\left[\dot{\delta}_o + \left\{(y_e - y_o)\cos\theta_o - (Z_e - Z_o)\sin\theta_o\right\}\dot{\theta}_o\right.$$

$$\left. + \left\{(X_o - X_e)\cos - (Z_e - Z_o)\sin\phi_o\right\}\dot{\phi}_o - \dot{\delta}^{(e)}\right]$$

$$+ K^{(e)}(X_o - X_e)\left[\delta_o + (y_e - y_o)\sin\theta_o + (X_o - X_e)\sin\phi_o\right.$$

$$\left. - (Z_e - Z_o)(2 - \cos\theta_o - \cos\phi_o) - \delta^{(e)}\right]$$

Equation (2e+2):

$$(F_z)_e = m^{(e)}\ddot{\delta}^{(e)} + \left[C^{(e)} + C_T^{(e)}\right]\dot{\delta}^{(e)}$$

$$- C^{(e)}\left[\dot{\delta}_o + \left\{(y_e - y_o)\cos\theta_o - (Z_e - Z_o)\sin\theta_o\right\}\dot{\theta}_o\right.$$

$$\left. + \left\{(X_o - X_e)\cos - (Z_e - Z_o)\sin\phi_o\right\}\dot{\phi}_o - \dot{\delta}^{(e)}\right]$$

$$- C_T^{(e)}\dot{\delta}_T^{(e)} + \left[K^{(e)} + K_T^{(e)}\right]\delta^{(e)}$$

$$- K^{(e)}\Big[\delta_o + (y_e - y_o)\sin\theta_o + (X_o - X_e)\sin\phi_o$$

$$- (Z_e - Z_o)(2 - \cos\theta_o - \cos\phi_o) - \delta^{(e)}\Big] - K_T^{(e)}\delta_T^{(e)}$$

Equation (2e + 3):

$$(R_z)_e = C_T^{(e)}\left[\dot{\delta}_T^{(e)} - \dot{\delta}^{(e)}\right] + K_T^{(e)}\left[\delta_T^{(e)} - \delta^{(e)}\right]$$

CHAPTER SEVEN

RESULTS AND DISCUSSIONS

7.1 INTRODUCTION:

This work, which started as a development to a project carried out at Cranfield [Ref. 59], has many novel points derived and employed for the ride analysis of off-road vehicles, such as; track modelling, vehicle-terrain interaction, non-linear effects, modified time marching schemes, etc., as described in previous chapters. Kamar's package is badly organised and with graphics being based upon GINO which is no longer supported. In the present work, a new programming package was developed using UNIRAS graphics. The package is simple, practical and easy to use, and its basic features are as summarised in Appendix E.

Different measures for validating the developed package have been considered. Two simple examples which may represent the simplest possible suspension element have been used for validating different package modules and they enable direct checking of every developed subroutine.

Of course, such examples can not represent realistic models which may have non-linear aspects or stiff equations but it is not possible to use a complex case without having its true data and some experimental results to compare with. Two case studies as such have been found and analysed.

The first case study is an off-road untracked vehicle which has published data and results based upon an analog computer simulation [Ref. 60]. The second case is a fully tracked vehicle, the Scorpion tank, which was provided together with some experimental results by the British Military Vehicle Engineering Establishment (MVEE).

It should be anticipated that accurate modelling of real off-road vehicles is far from being an easy task and many approximations are considered. The characteristics of springs and dampers for a vehicle in service may deviate from their estimated design values and up-to-date measurements of such characteristics may be required. Some

approximation techniques are often used for the calculation of mass and moments of inertia for existing vehicles [Ref. 49], etc. Hence, a limited deviation between theoretical and experimental results might be expected.

7.2 VALIDATION CASES:

7.2.1 **Free Vibration Analysis:**

To check the ability of the package to predict natural frequencies of vibration and vibration mode shapes, a simple one-dimensional case with two masses and springs, which has an analytical solution as shown in Appendix D has been employed. This case resembles a suspension system with two simple suspension elements, and more complex cases can, of course be analysed. The values of the two natural frequencies obtained by means of the package are compared with analytical values as shown in Table 7.1 which proves the complete agreement between the two sets of values.

Table(7.1) Natural Frequencies Results.

Natural frequencies	Analytical results	Package results
ω_1	2.79785	2.79419
ω_2	25265.0	25265.0

7.2.2 **Time-Marching Schemes:**

It is essential to test the accuracy of the derivation and programming of different time-marching schemes employed in this work, using a reliable source before using them for the transient analysis of any actual case.

A simple one degree of freedom case has been employed for this purpose with an analytical solution as shown in Appendix D, and the time-marching schemes investigated are:

(i) Wilson θ method

(ii) Houbolt method

(iii) Runge-Kutta scheme

(iv) Hermitian 2-point weighted residual approach

(v) Lagrangian 3-point weighted residual approach, and

(vi) Central difference method.

Displacement, velocity, and acceleration responses are plotted against analytical solutions as shown in Figures 7.1(a)- 7.3 (b). The group shown in Figures 7.1 (a), 7.2 (a), 7.3 (a) represent the first four time-marching solvers which are less sensitive to the value of the time step (Δt) compared with the other two solvers. Lagrangian and Central difference methods are shown in Figures 7.1(b), 7.2(b), 7.3 (b) with two different values of Δt, $\Delta t_1 = 0.01$, and $\Delta t_2 = 0.1$.

It is clear from those figures that, generally speaking, with the appropriate value of time step, the time-marching schemes can predict displacement, velocity and acceleration responses with a reasonable degree of accuracy. However, schemes such as the Central difference, and Lagrangian weighed-residual methods have proved to be sensitive to the value of Δt, even for the case of the simplest possible system. Hence, these two methods might not be suitable for the analysis of stiff equations expected for realistic cases.

7.3 CASE STUDY OF AN OFF-ROAD NON-TRACKED VEHICLE:

This case is employed for a more realistic validation of time-marching schemes available in the package. The case represents an off-road wheeled vehicle, excited by a bump of 0.152 m height and 0.71 m length. The vehicle data and analog computer results due to such an excitation are published by [Ref. 60].

The vehicle has the following data parameters:

The number of suspension elements	= 5
The sprung mass	= 435.3 kg
The unsprung mass	= 20.5 kg
The moment of inertia about X-axis	= 13500 $kg.m^2$
The undeflected tyre diameter	= 0.6096 m
The stiffness of the first and the fifth main springs	= 5216.3 kg/s^2
The stiffness of other main springs	= 3175.14 kg/s^2
The main dampers coefficient of damping	= 362.87 kg/s.
The tyre equivalent stiffness	= 181436.96 kg/s^2
The tyre equivalent coefficient of damping	= 181.43 kg/s
The distance from the vehicle C.G. [fixed in the origin (0,0)] to the tyres centres starting from the front leading tyre are	= 1.8288 m, 0.9144 m, 0.3048 m, -0.6096 m, -1.5224 m.

This case study was excited by a bump of 0.152 m height and 0.71 m length.

a) Transient Analysis:

The package was used for a linear transient analysis of the vehicle subjected to the same excitation as given in [Ref. 60]. Different solvers were tested and the transient response of the C.G. velocity and pitch angle are shown in Figures 7.4 and 7.5 respectively.

Initially, as predicted for the simple case, the Lagrangian and the central difference solvers require very small Δt for numerical stability. It is clear from Figures 7.4 and 7.5 that both the Wilson-θ and the Hermitian methods are giving identical results which are very closed to the analog computer results, but the Wilson-θ method uses less computer CPU time than that required by the Hermitian method.

To confirm the previous conclusions, the vehicle was tested with a higher speed at which no published results are available, and the package results given in Figures 7.6, 7.7, and 7.8 show some consistency between the results obtained by means of different solvers.

To show the ability of the package to predict an accurate response for every element of the suspension system, the displacement at the C.G. of the five rows of the vehicle due to for an excitation of a bump of 0.5 m height and 2.4 m length are plotted against time as shown in Figure 7.9 which shows the sequence of wheels crossing the obstacle.

b) Application For Shock Analysis:

Shock response is the reaction of the vehicle to a discrete obstacle. The shock criterion is the greatest peak vertical acceleration received at the driver location. The shock response limit can be used as 2.5g vertical acceleration [Ref. 3], and the shock limiting speed is that speed at which the 2.5g occurs. To determine this speed on a group of obstacles of representative heights, first the relation of the peak acceleration versus speed for each obstacle is as shown in figure 7.10, which represents a five different heights of a semicircular obstacle. Second the corresponding 2.5g speeds are obtained from the previous figure, and a new plot is developed between the 2.5g speeds and the obstacle height as shown in figure 7.11.

7.4 CASE STUDY OF AN OFF-ROAD TRACKED VEHICLE:

This case represents a real off-road tracked vehicle, the Scorpion Tank, and it has a significant importance since some experimental data are provided by the MVEE. The case was also used to demonstrate the use of the additional package facilities with a realistic vehicle.

a) Data Parameters:

The vehicle data employed in the analysis can be summarised as follows:

The number of suspension elements	= 5
The sprung mass	= 3750. kg
The unsprung mass	= 40.0 kg
The moment of inertia about X-axis	= 7500 $kg.m^2$
The road wheel diameter	= 0.58 m
The main springs stiffness	= 10599.72 kg/s^2
The main dampers coefficient of damping	= 17840. kg/s.
The road wheel equivalent stiffness	= 1×10^6 kg/s^2
The road wheel equivalent coefficient of damping	= 2000. kg/s
The distance from the vehicle C.G.[fixed in the organ (0,0)] to the road wheels centre starting from the front leading road wheel are	= 1.407 m, 0.782 m, 0.154 m, -0.467 m, -1.095 m.

Non-linear characteristic of spring, and damper are provided as shown in Figures 7.12, 7.13. The number of the bump stops are equal to the number of road wheels, they have the same stiffness which is based

upon force-deflection values, given as follows:

For force = 1×10^6 N on a bump stop, its deflection = 0.28 m

b) Transient Response:

An experimental analysis of the peak acceleration at the front of the vehicle as function of tank speed when the tank is moving on a rigid terrain and excited by a bump of 0.1 m height and 3.75 m length has been provided by the MVEE [Ref. 61], and used for this study. Two different type of analysis were carried out by means of the programming package developed in this work. The first was a linear analysis with average values for stiffness and damping coefficients. The second one was non-linear analysis considering the following aspects available in the package:

(i) Large deflection effect.

(ii) Non-linear characteristic of springs and dampers as given in Figures 7.12, 7.13.

(iii) The effect of the bump stop as provided in the tank data.

(iv) Wheel separation.

The results, were plotted against experimental results as shown in Figure 7.14 which proves that when the speed of the tank increases, i.e when non-linear phenomena become dominant, the linear analysis over estimates the acceleration whilst the non-linear analysis converges to experimental results with the increase of the tank speed. these logical results prove beyond any doubt, the ability of the package to handle realistic cases and the importance of

non-linear considerations developed in this work in yielding accurate answers.

Further analysis was carried out by means of the package. The displacement at the centre of every road wheel was plotted against time for linear and non-linear analysis as shown in Figures 7.15, and 7.16 respectively which agree with expected response and the non-linear displacement showing smooth change of displacement than the linear one. Similar phenomena were observed for road wheel arm angles plotted in Figures 7.17, and 7.18 respectively. The displacement of the tank C.G during bump excitation is shown in Figure 7.19.

c) Ride Analysis With Different Types of Soil:

This study was carried out to show how package facilities can help in the assessment of maximum vehicle speed which is safe for the driver when the vehicle is moving on different types of soil and to illustrate non-linear effects on such analysis.

The absorbed power criterion was used in this study where the recommended value of the power absorbed by the driver should be less than 6 watts for safe driving and controllabilty over vehicle [Ref. 29], whilst it should not exceed 10 watts otherwise the vehicle be dangerous for the crew and driver.

A linear and non-linear analysis was carried out assuming that the vehicle is moving on a rigid standard terrain, as specified by [Ref. 49], as shown in Figure 7.20, which proves that if the track is not considered in the analysis, the limiting speed will be underestimated by a factor of 23% for the case of linear analysis and 18% for the non-linear analysis.

Limiting speed as estimated by linear and non-linear analysis for rigid soil, sandy soil and organic soil are shown in Figures 7.21,

7.22, and 7.23 respectively which prove that linear analysis underestimate the limiting speeds because it overestimates the response, as proved when compared with experimental results in Figure 7.14.

Comparison between different types of soil for linear (untracked), and non-linear cases, are shown in Figures 7.24, and 7.25 respectively which prove that the track as expected, improves the limiting speed for the sandy soil which is near to that obtained for rigid soil. However, for organic soil the speed is reduced even with the presence of the track.

d) Effect of Suspension Component Failure:

The package developed in this work has the ability to consider the effect of the failure of any one or more of the components of the suspension system, at any specified instant of time, on the transient response and ride analysis of the off-road vehicle. This may be useful, if the vehicle is operating in different types of conditions where it is expected that failure may occur in one or more of the torsion bars or dampers, since it will provide the operator with an idea of the margin of safety available and to give him some necessary early warning for replacing the failed components before the vehicle become too dangerous to be used.

In order to demonstrate the ability of the package for predicting such an analysis, first the acceleration response, for a normal case, and case with one torsion bar failing and a third with one damper failing are shown in Figure 7.26 which shows the increase in acceleration for the case with a failed damper, and consequently on the limiting speed for the case of failed torsion bar and damper as shown in Figure 7.27. The displacement of the first wheel centre was plotted at the same conditions as shown in Figure 7.28 which illustrates the induced vibration due to such failure.

e) Two D and Three D Analysis:

If the vehicle is not symmetric w.r.t the Y-axis, then a full 3-D analysis should be carried out. Since the developed package is capable of such analysis, an example has been analysed using the full 3-D data of the Scorpion tank, and the C.G. peak acceleration is plotted against tank speed as shown in Figure 7.29 which proves that there is a significant difference between results for 2-D and 3-D cases.

7.5 GENERAL DISCUSSIONS:

It is clear from the examples and case studies analysed in this work that the developed package can provide a useful means for the ride analysis of off-road vehicles. The package is capable of predicting natural frequencies of vibration which may be required to define critical operating conditions with serious vibrations. The mode shapes of vibration can highlight components with damaging vibration amplitudes.

Although the time-marching schemes employed in this work have results in close agreement with analytical solutions, they can not all be used for the analysis of real off-road vehicles. Some methods such as the central difference and the Lagrangian methods are conditionally stable and may require a very small time step to yield acceptable answers. The Hermitian and Wilson-θ methods have proved to be numerically stable for the cases of real vehicles, and the Wilson-θ method requires computer CPU time and memory less than that required for the Hermitian method.

Non-linear aspects introduced in this work have proved useful and reliable and the non-linear ride analysis of the Scorpion tank carried out by the present package has results which agree well with the experimental results. Linear analysis may lead to an

overestimated response.

The package has proved useful for ride analysis of off road vehicles moving either on standard terrain or generalised terrain specified by the package user. The types of soil introduced in the package have been tested and proved that the limiting speed of a vehicle increases with the stiffness of the soil, as might be expected. The effects of the vehicle track on minimizing its sinkage and improving its ride characteristics is quite clear from the previous analysis.

The package has proved advantageous for the study of the effect of failure of one or more of the suspension components. Such a study may provide some useful measures for component maintenance or replacement.

Full three-dimensional analysis is available and may be employed for vehicles with distinguished asymmetry.

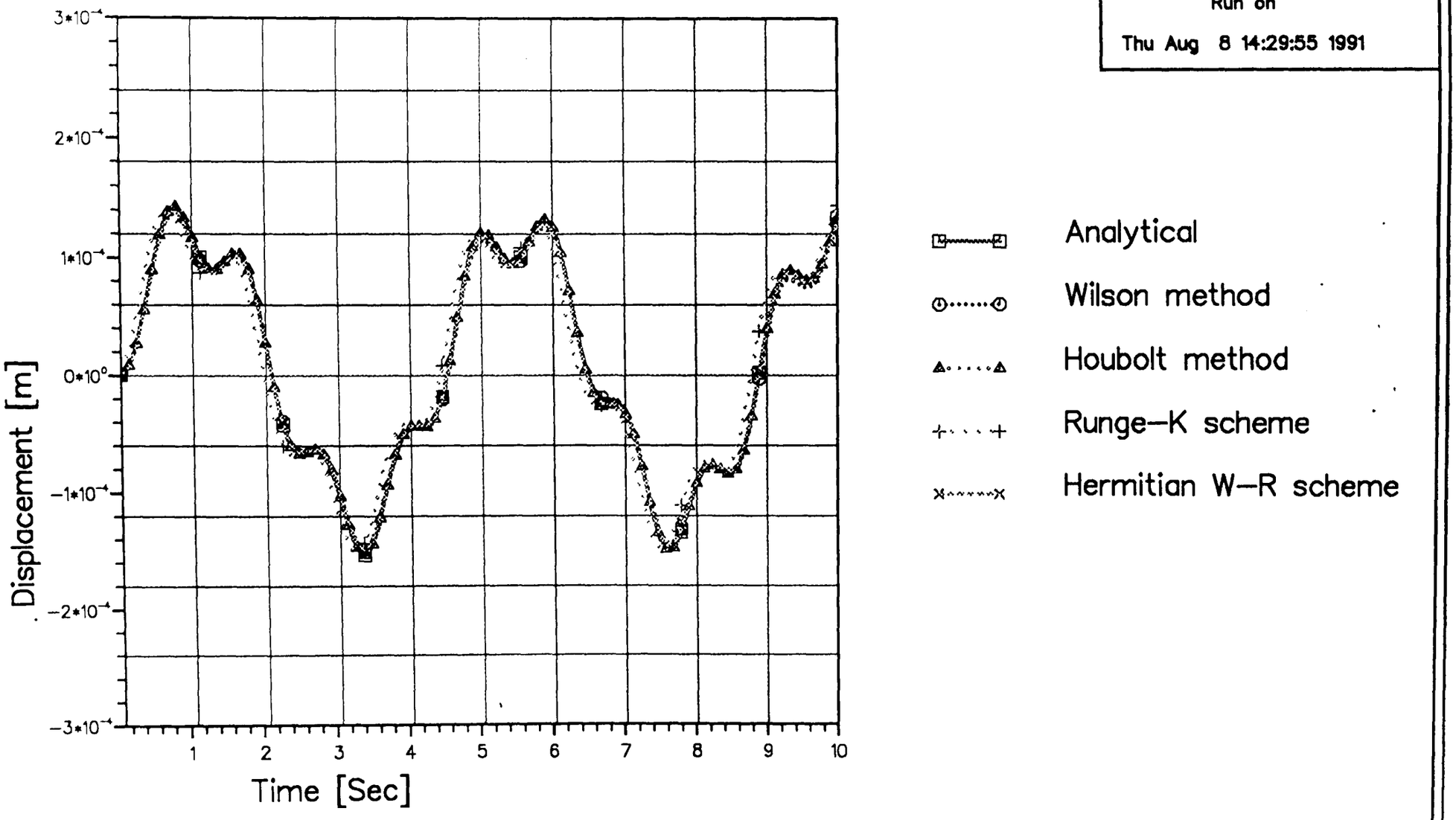

Fig (7.1 a) Displacement versus Time for One Degree of Freedom System Using Different Time Marching Schemes.

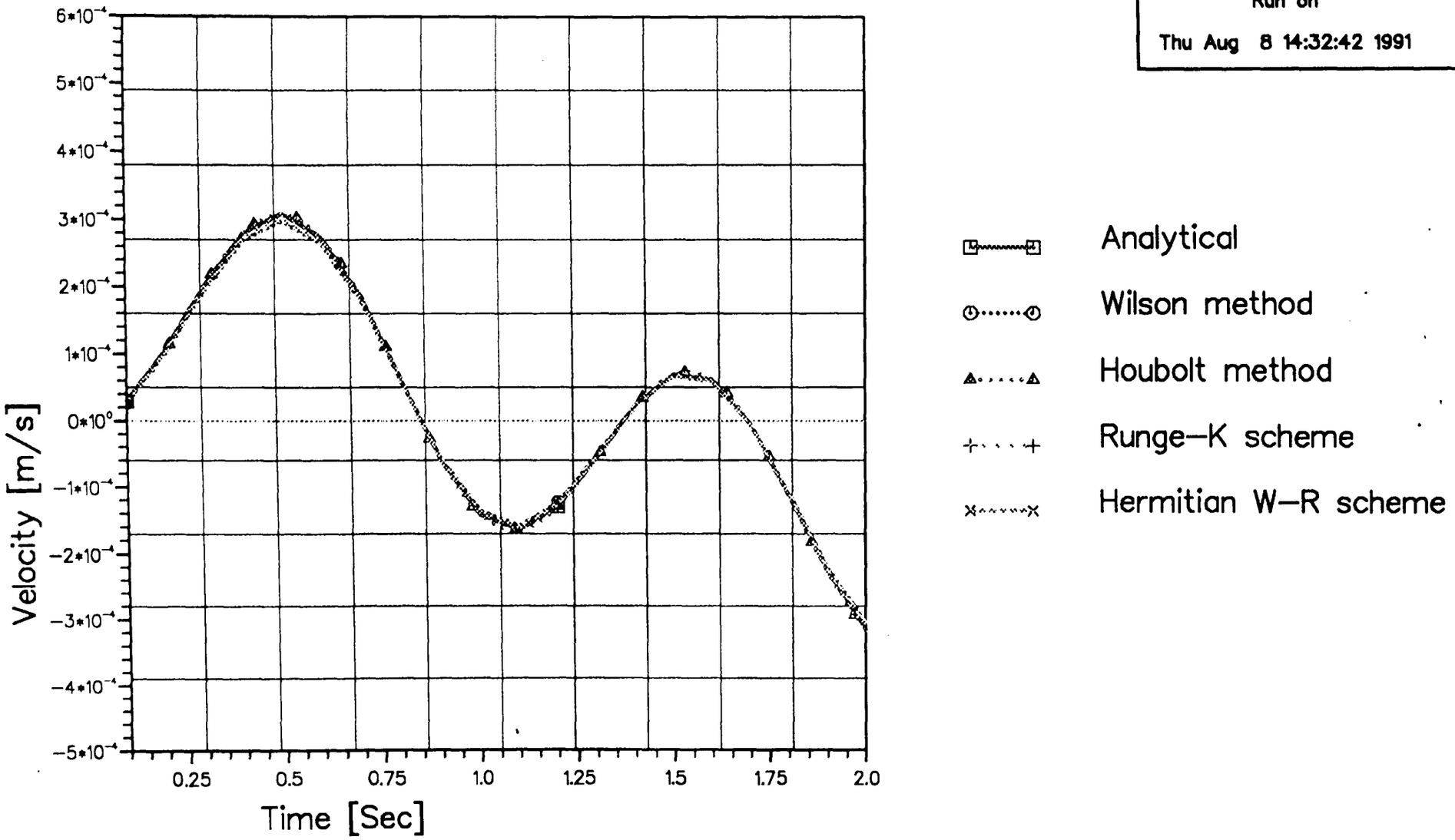

Fig (7.2 a) Velocity versus Time for One Degree of Freedom System Using Different Time Marching Schemes.

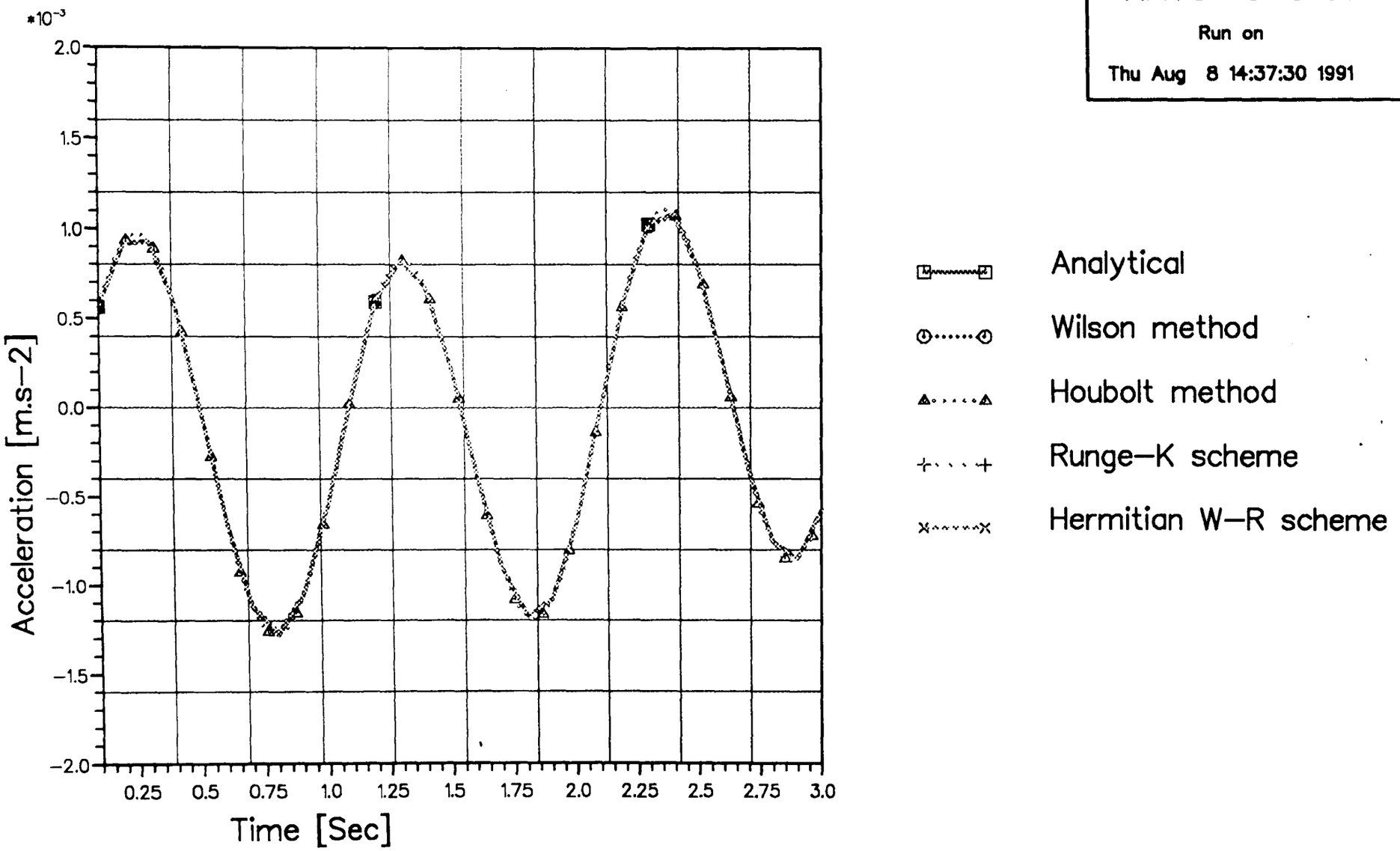

Fig (7.3 a) Acceleration versus Time for One Degree of Freedom System Using Different Time Marching Schemes.

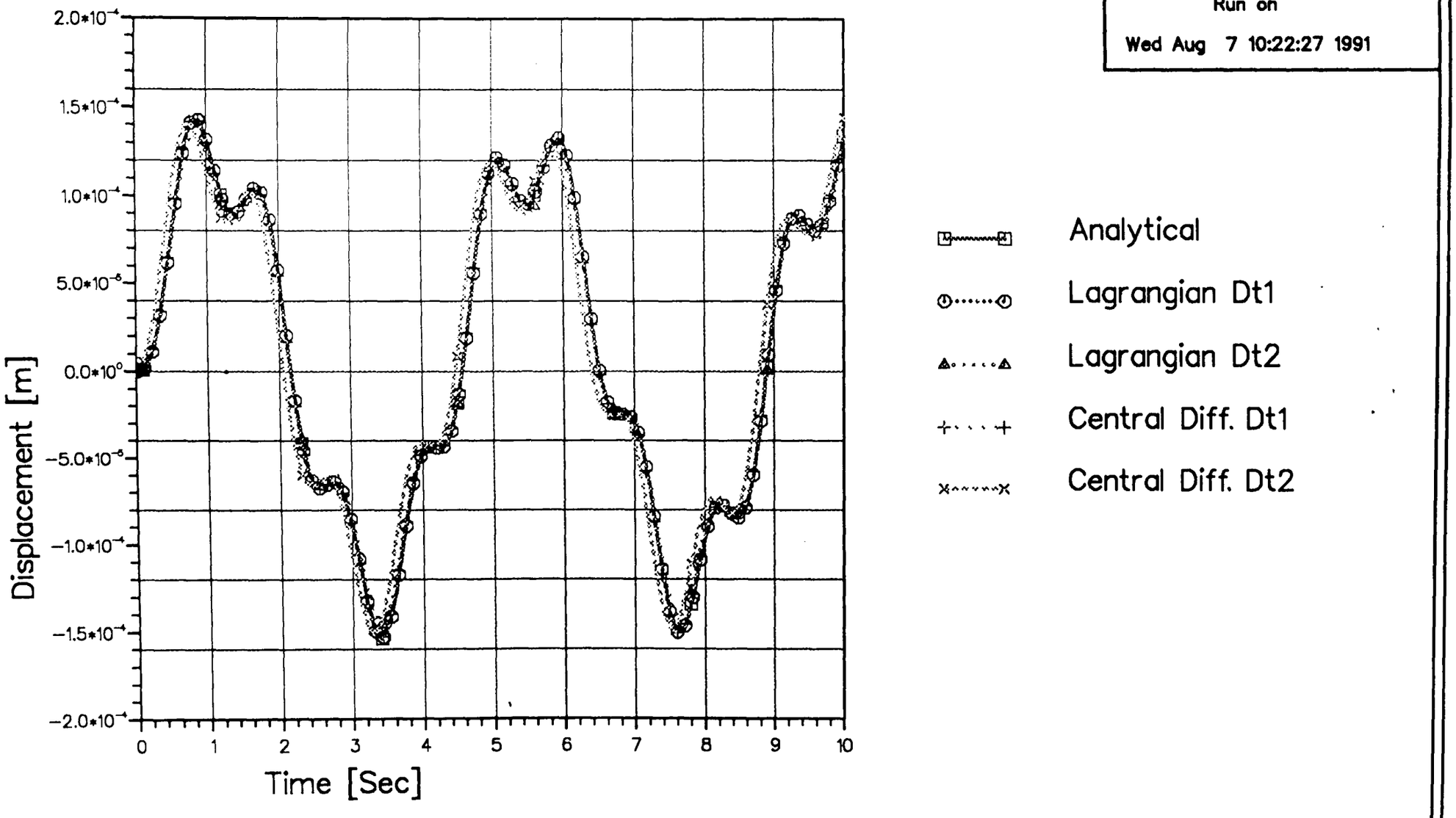

Fig (7.1 b) Displacement versus Time for One Degree of Freedom System
Using Central Difference and Lagrangian Methods.

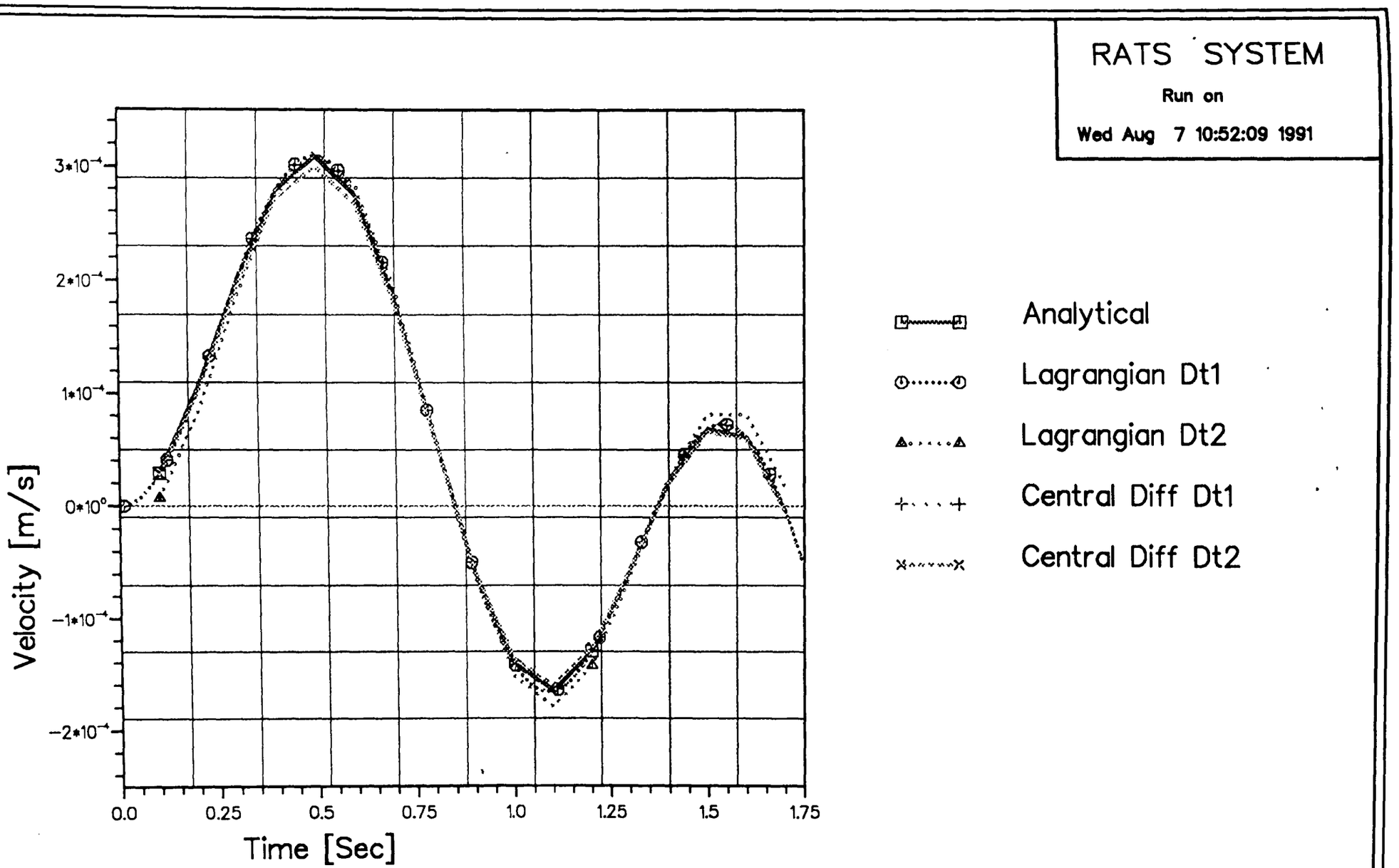

Fig (7.2 b) Velocity versus Time for One Degree of Freedom System
Using Central Difference and Lagrangian Methods.

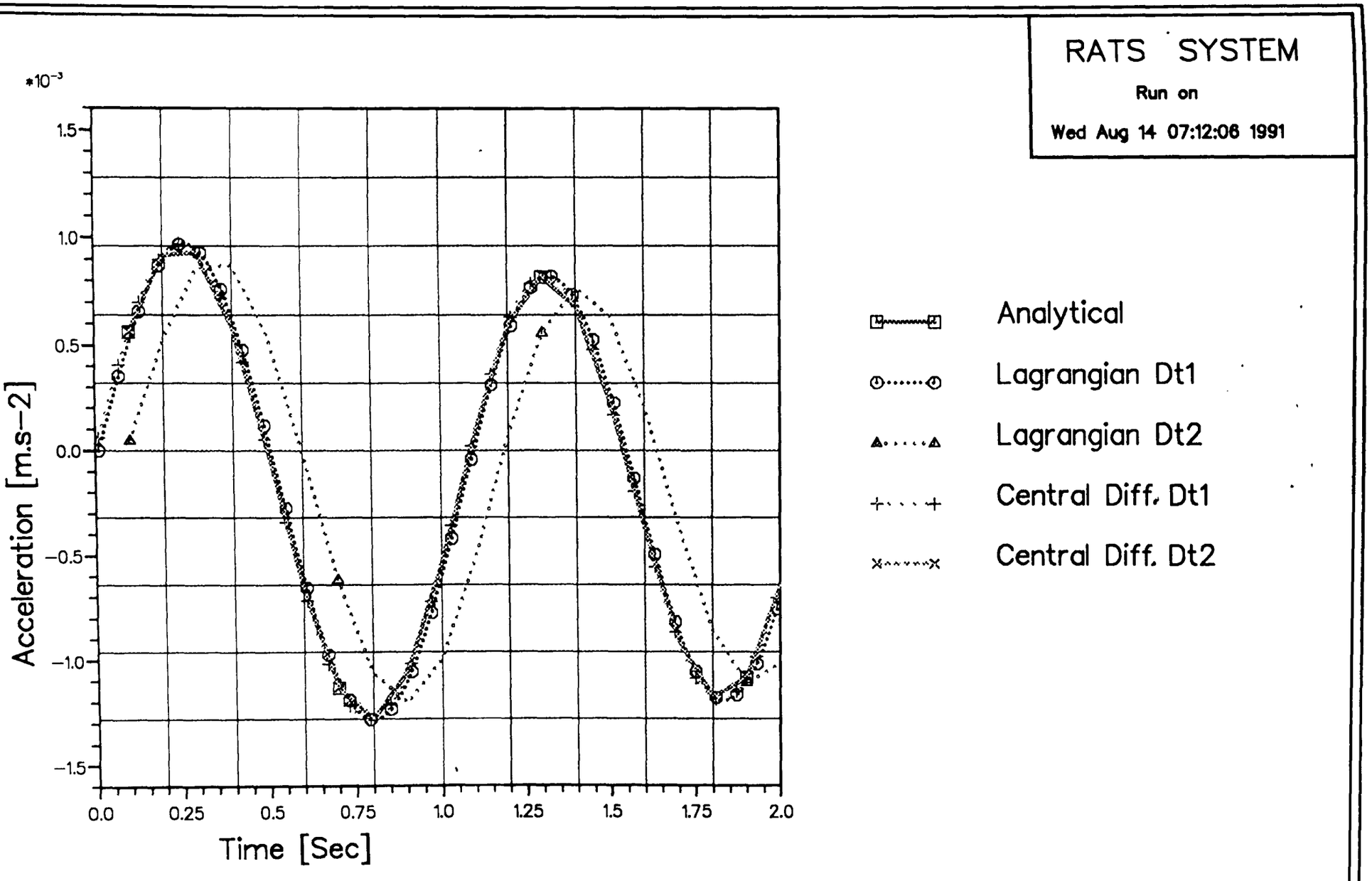

Fig (7.3 b) Acceleration versus Time for One Degree of Freedom System
Using Central Difference and Lagrangian Methods.

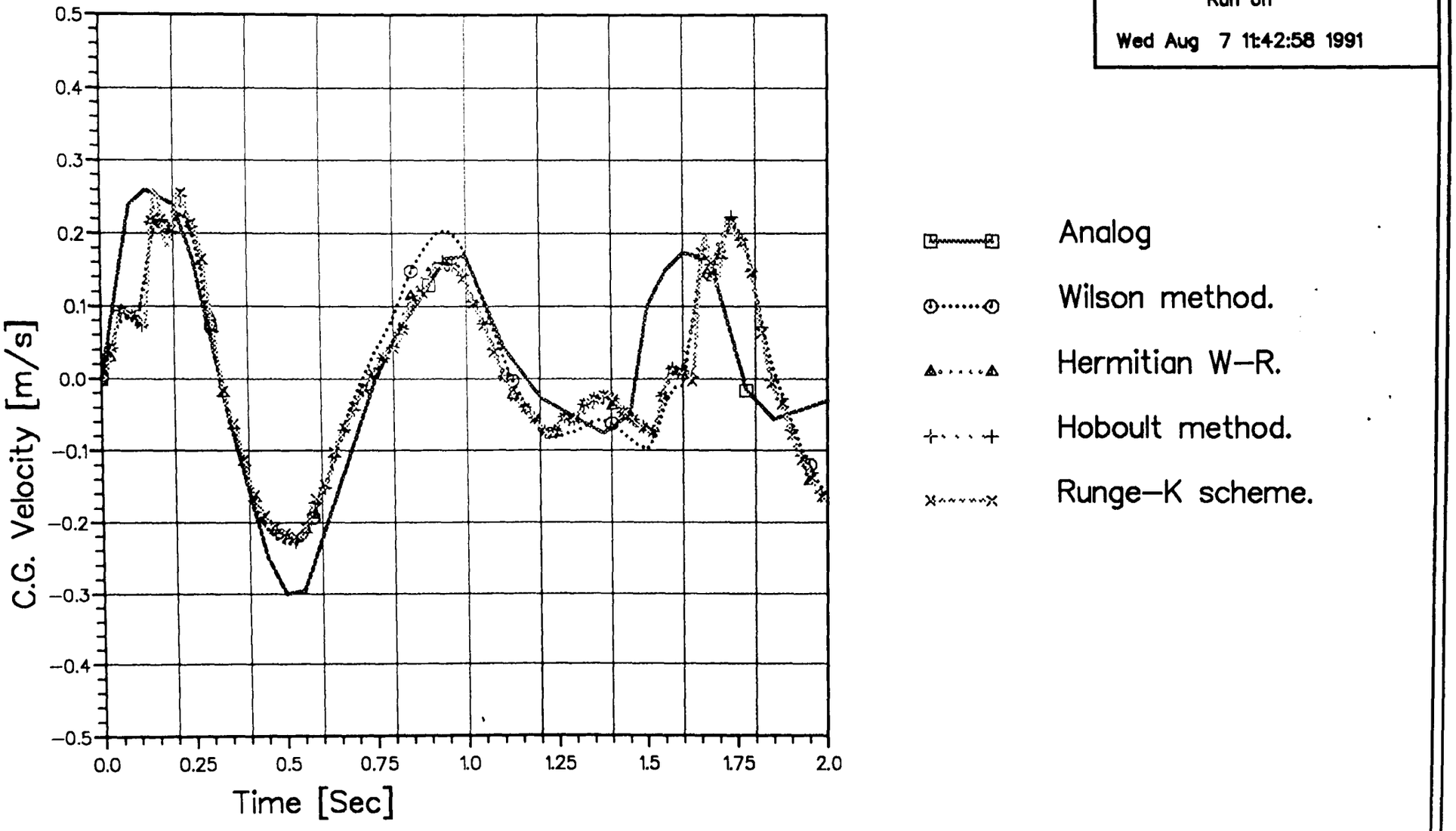

Fig (7.4) Comparison of C.G. Velocity versus Time with Analog Results For Untracked Vehicle at Speed of 8 km/h.

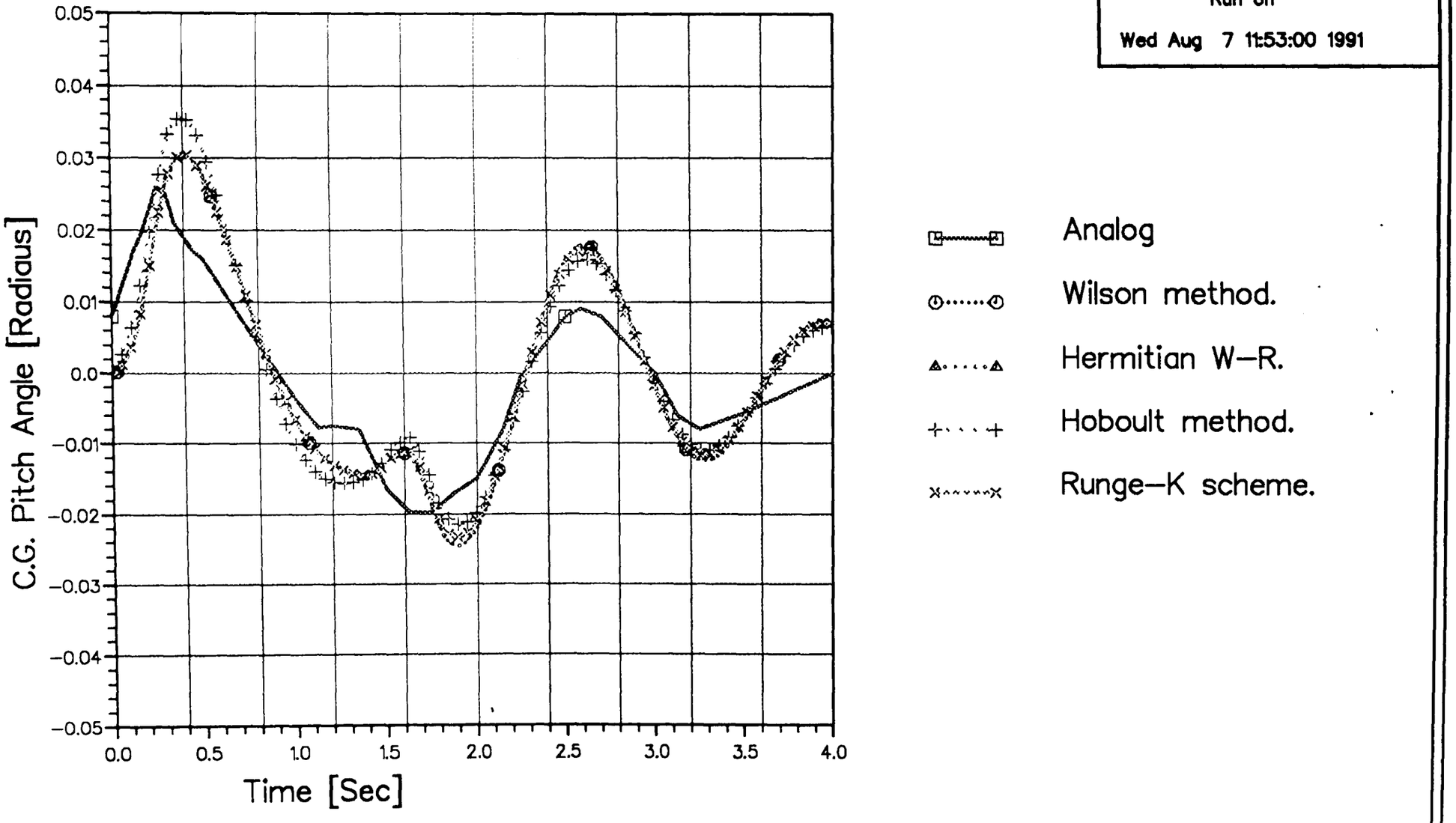

Fig (7.5) Comparison of C.G. Pitch Angle versus Time with Analog Results For Untracked Vehicle at Speed of 8 km/h.

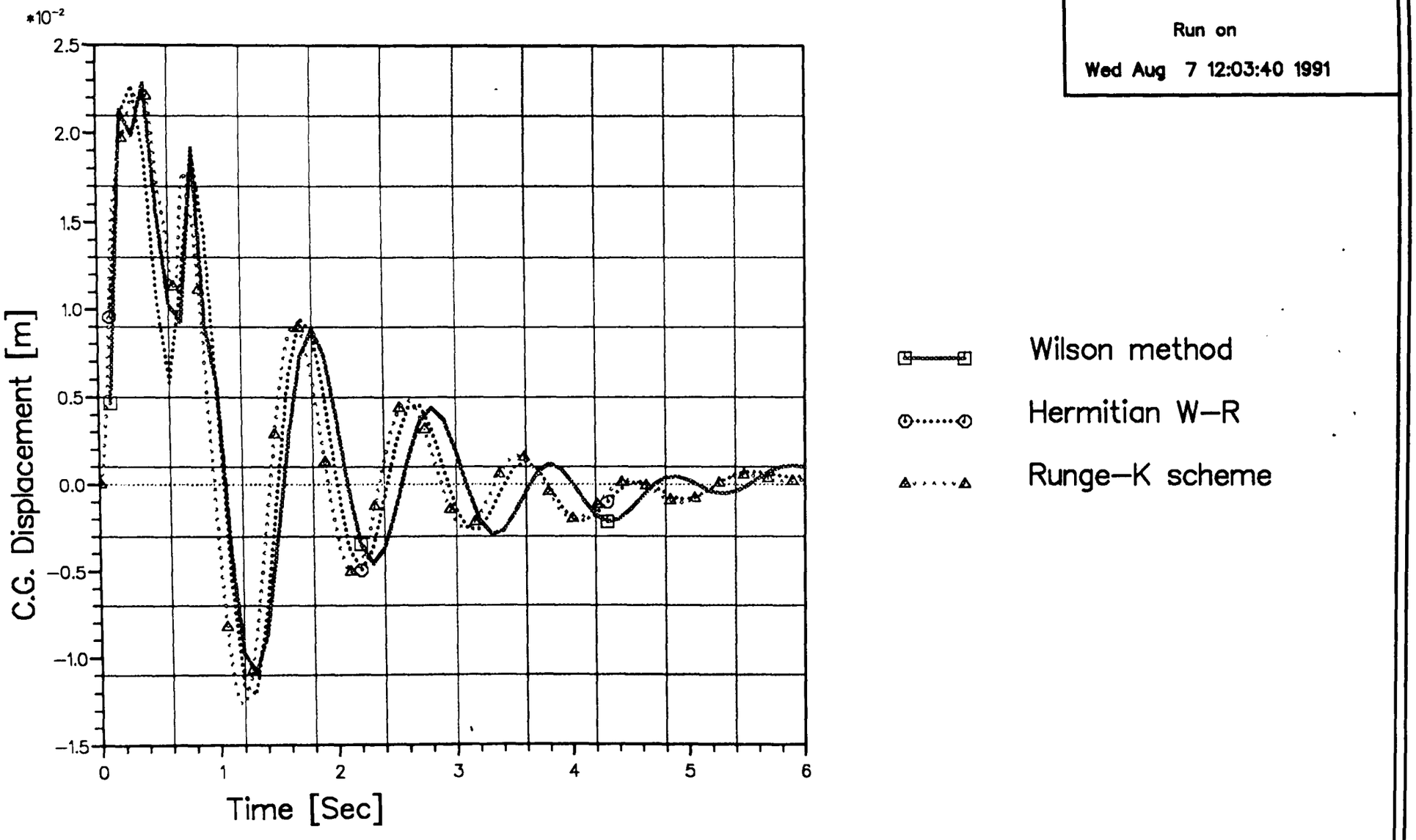

Fig (7.6) Displacemet versus Time of the C.G of the First Case Study at Speed of 20 km/h Using Different Integration Methods.

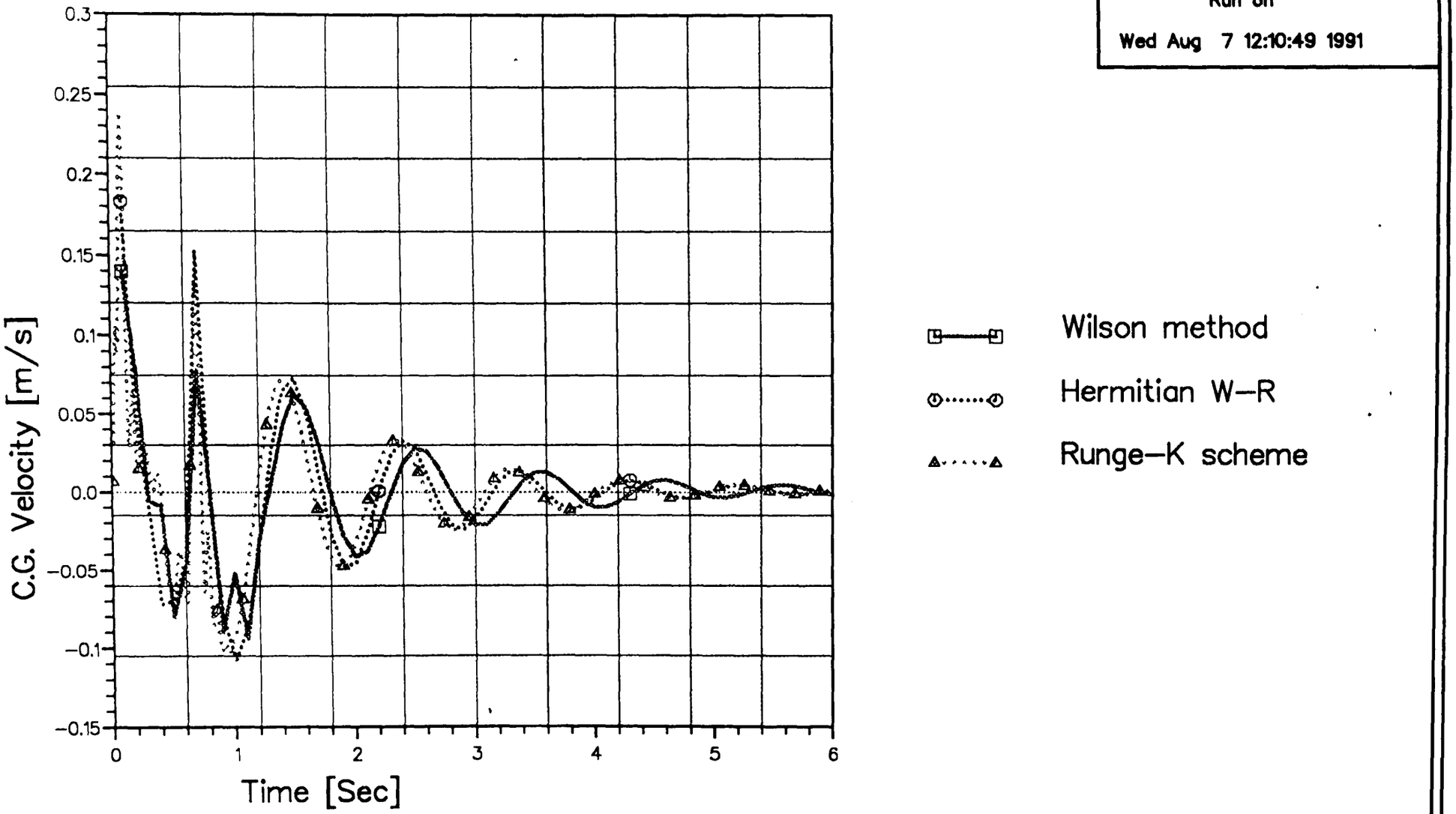

Fig (7.7) Velocity versus Time of the C.G of the First Case Study at Speed of 20 km/h Using Different Integration Methods.

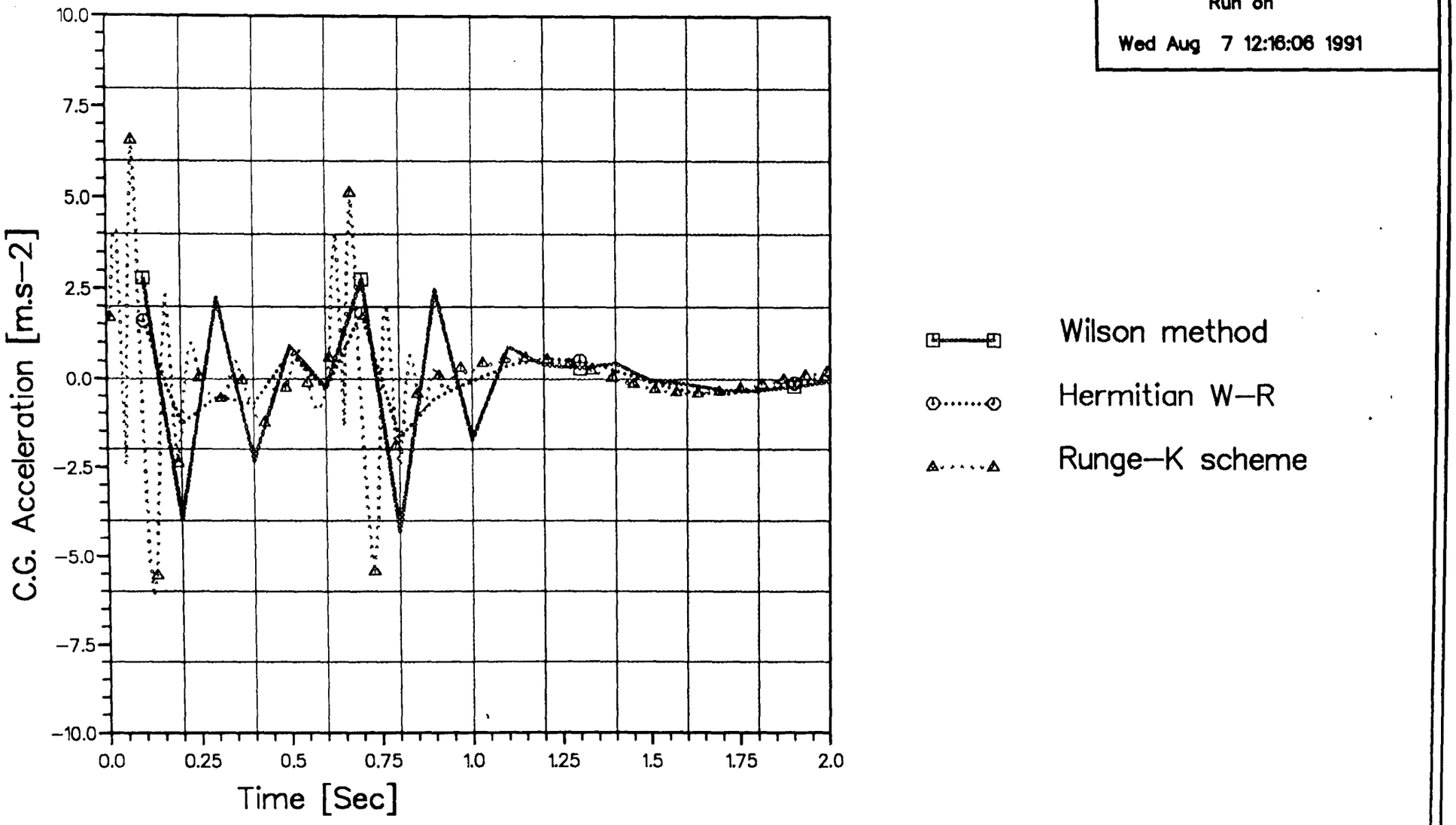

Fig (7.8) Acceleration versus Time of the C.G of the First Case Study at Speed of 20 km/h Using Different Intgration Methods.

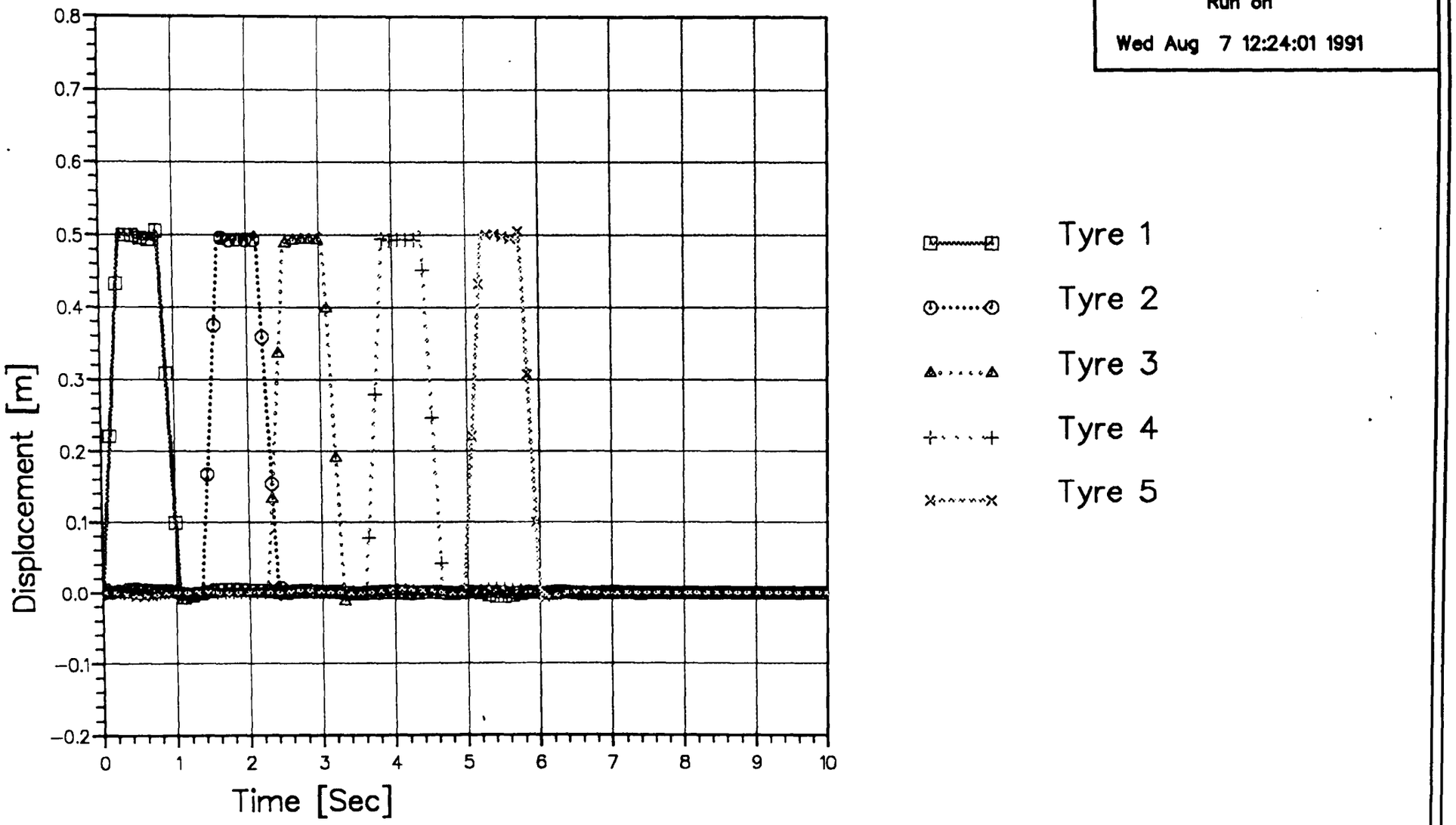

Fig (7.9) Displacement of Wheel Centres of the First Case Study
Excited by a Bump at Speed of 8 km/h.

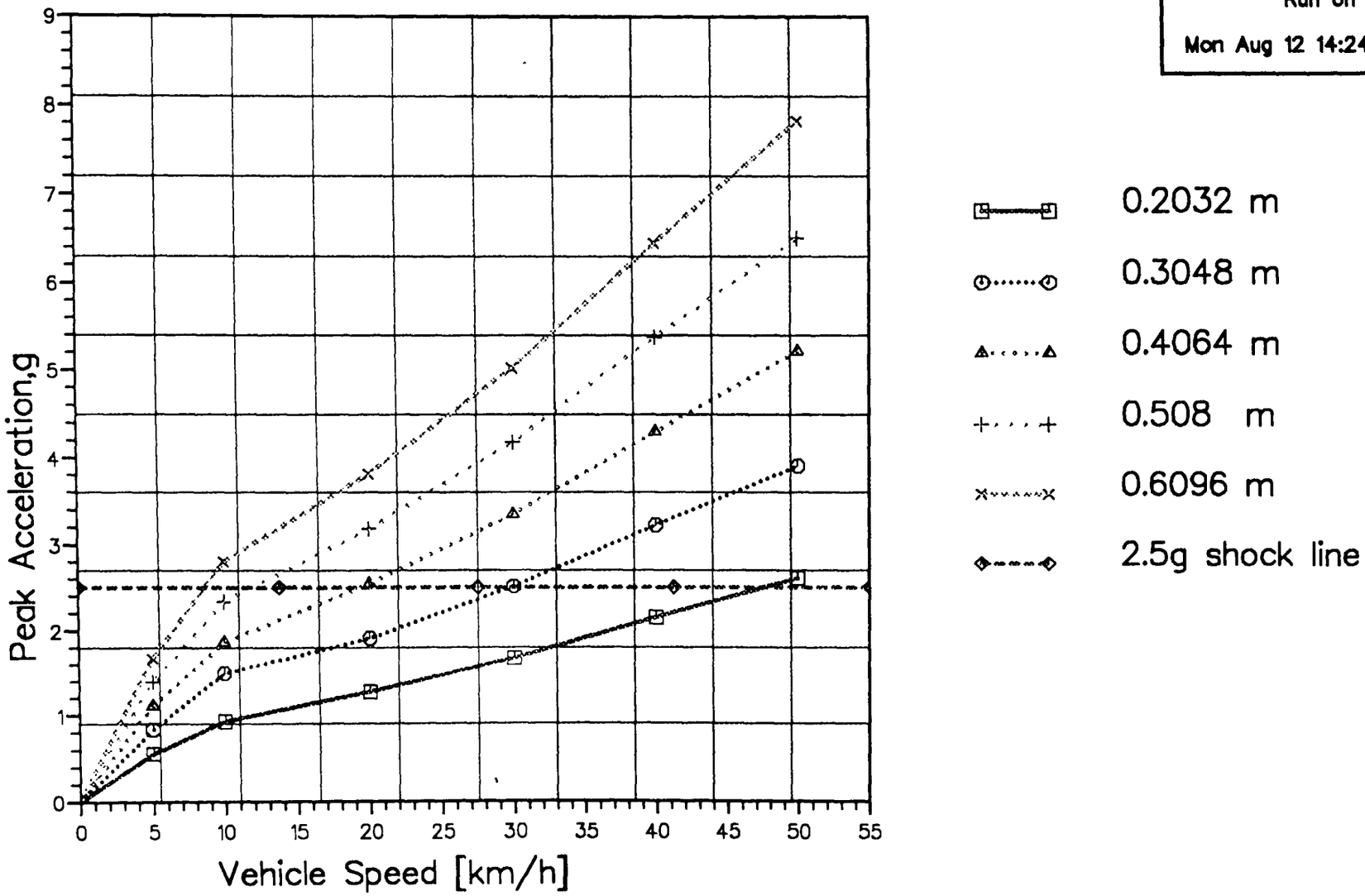

Fig (7.10) Peak Acceleration For First Case Study Excited by Different–Height Semicircular Obstacles at Variable Speed.

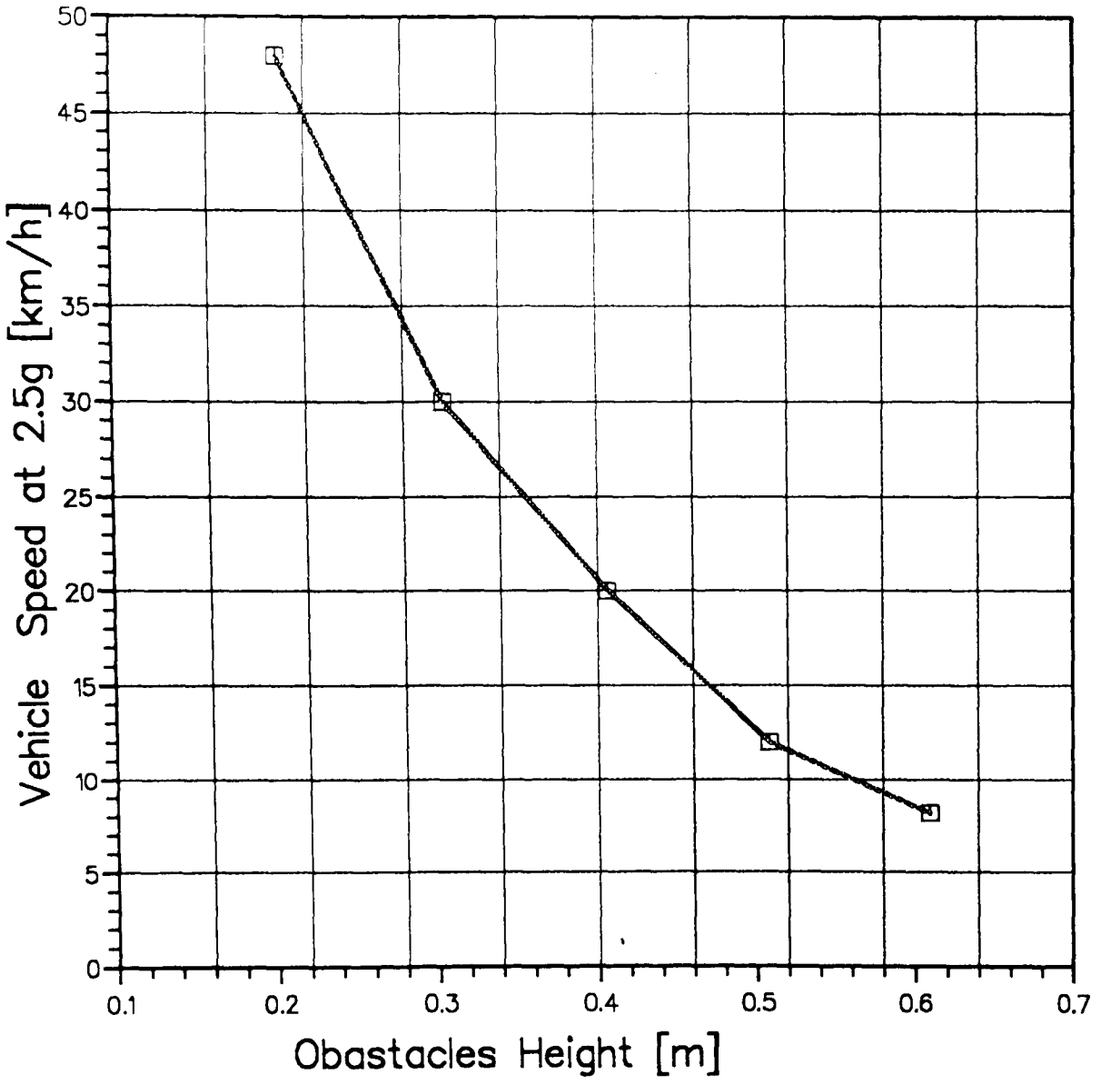

Fig (7.11) Vehicle Speed versus Obstacle Height For First Case Study.

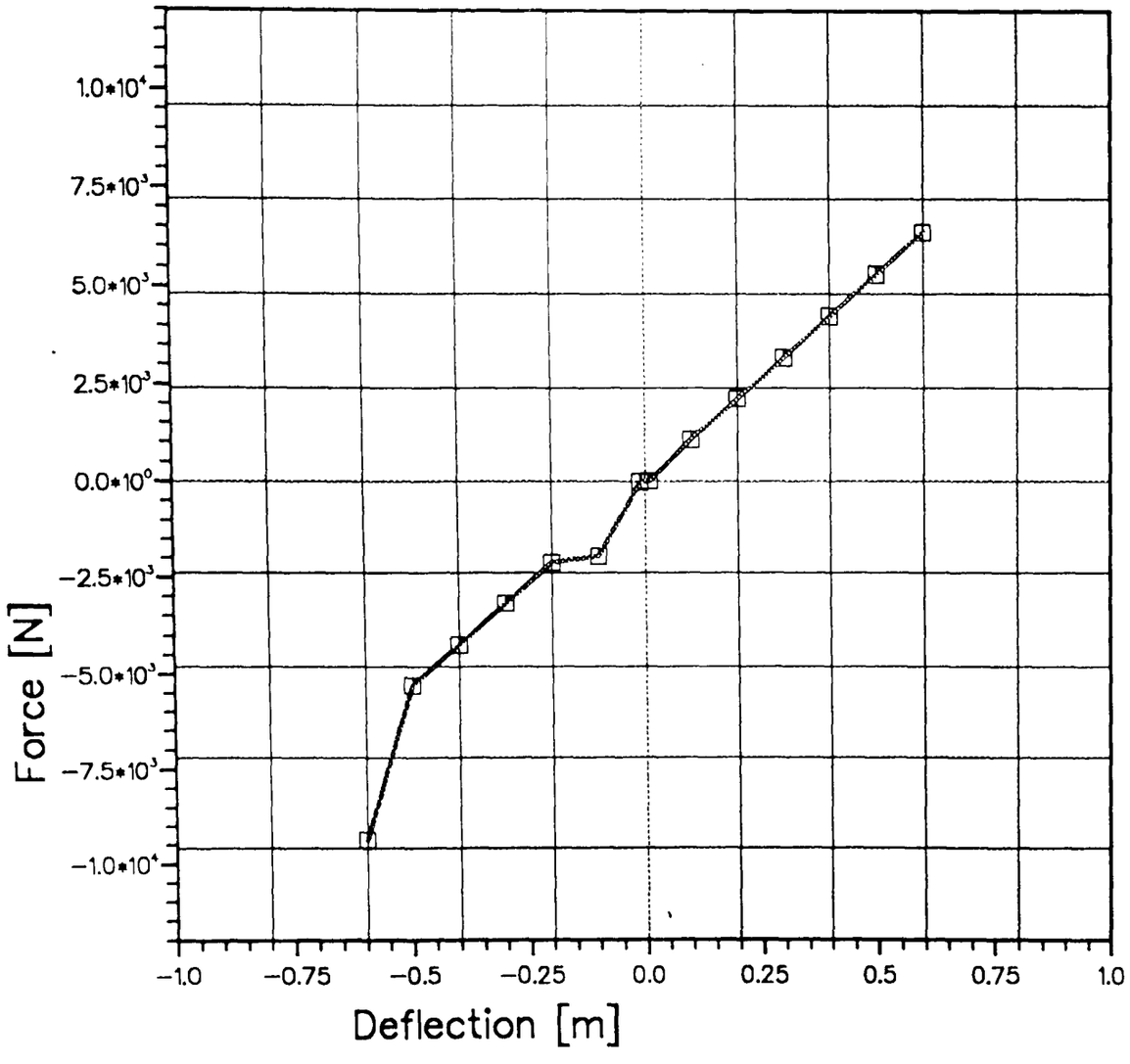

Fig (7.12) Spring Non−linear Characteristics For the Scorpion Tank.

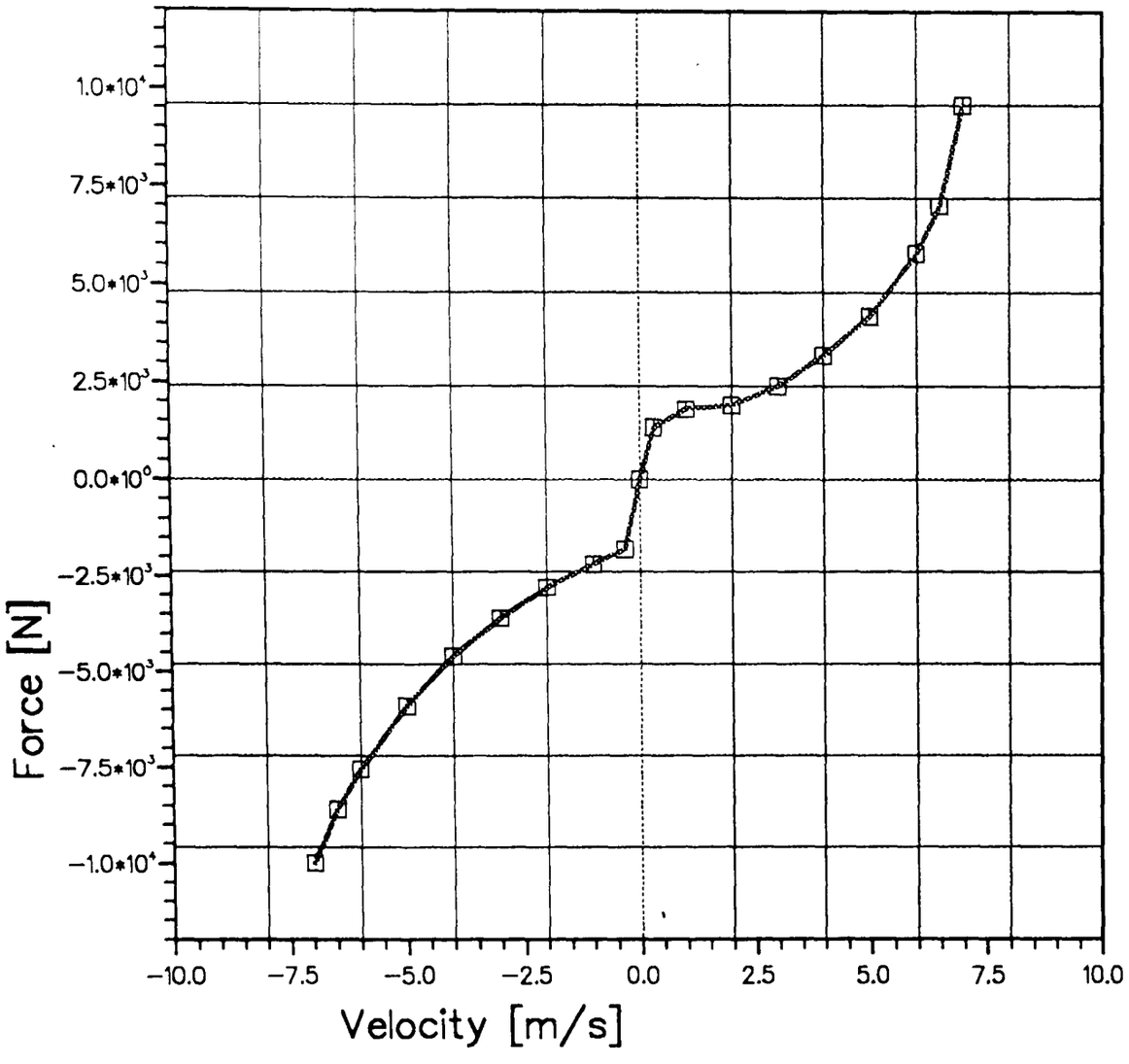

Fig (7.13) Damper Non−linear Characteristics For the Scorpion Tank.

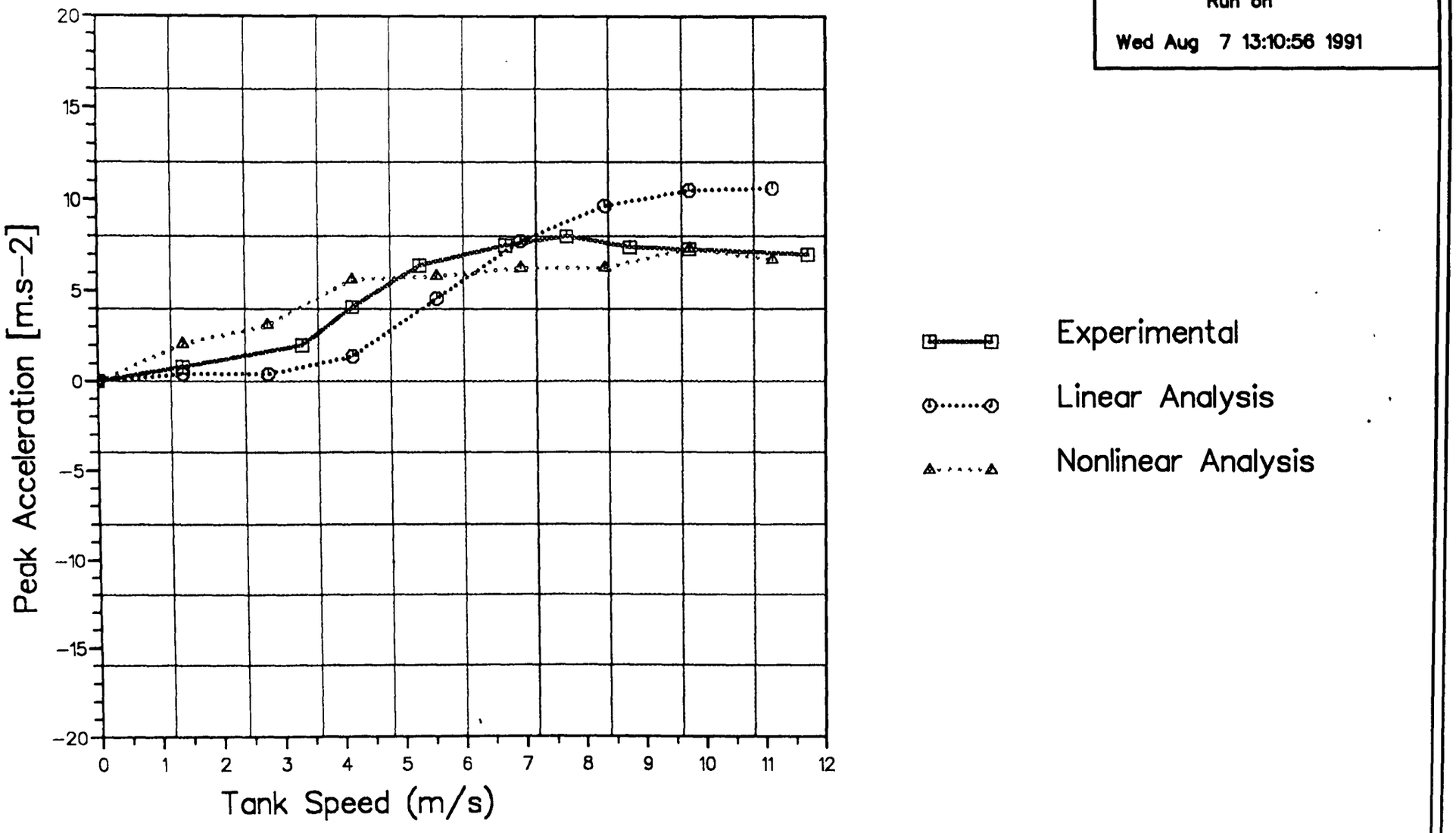

Fig (7.14) Comparison of Experimental and Theoretical Results
For the Second Case Study Excited by a Bump.

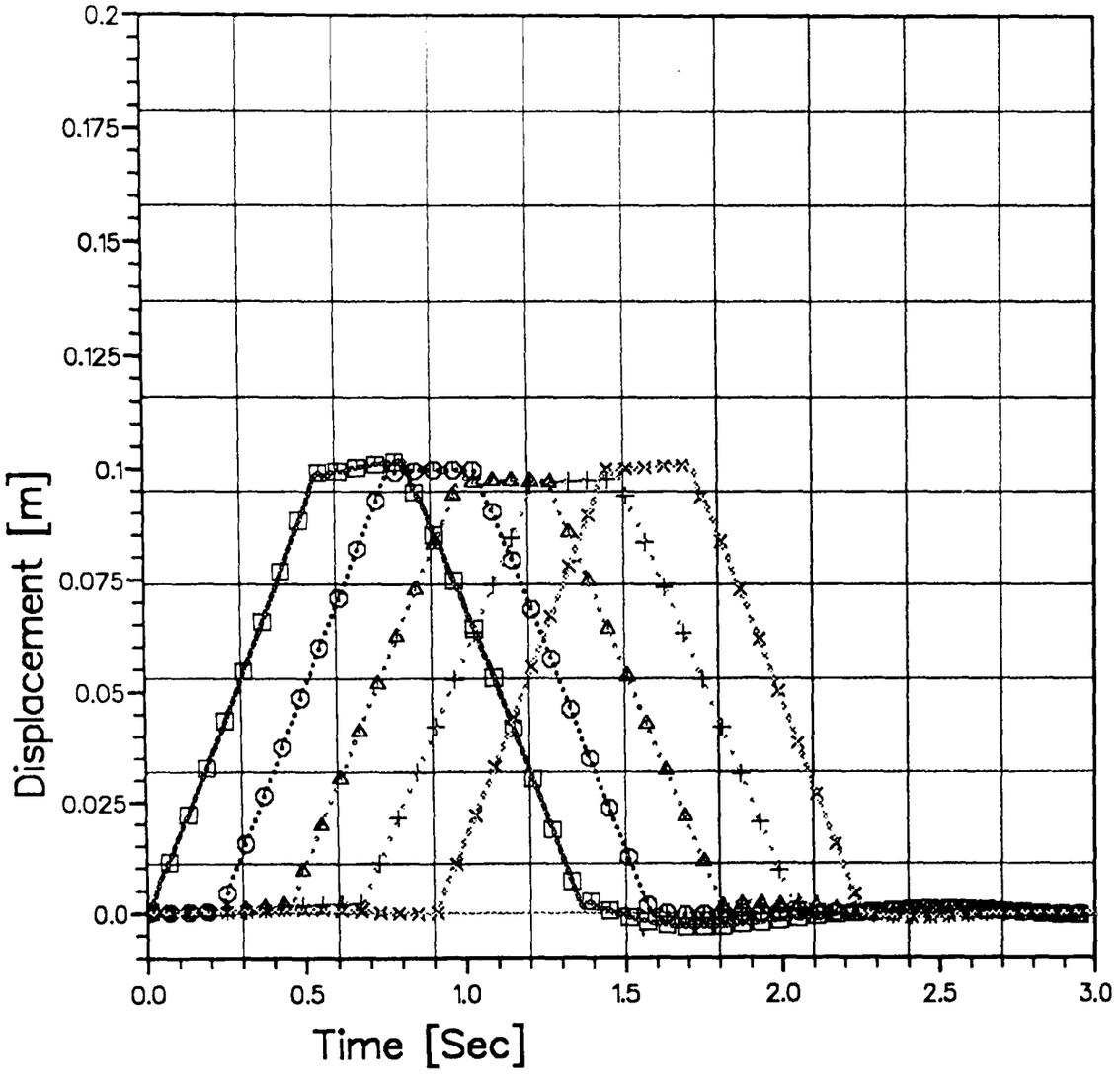

Fig (7.15) Displacement of Wheel Centres of a Scorpion Tank
For a Linear Model Excited by a Bump.

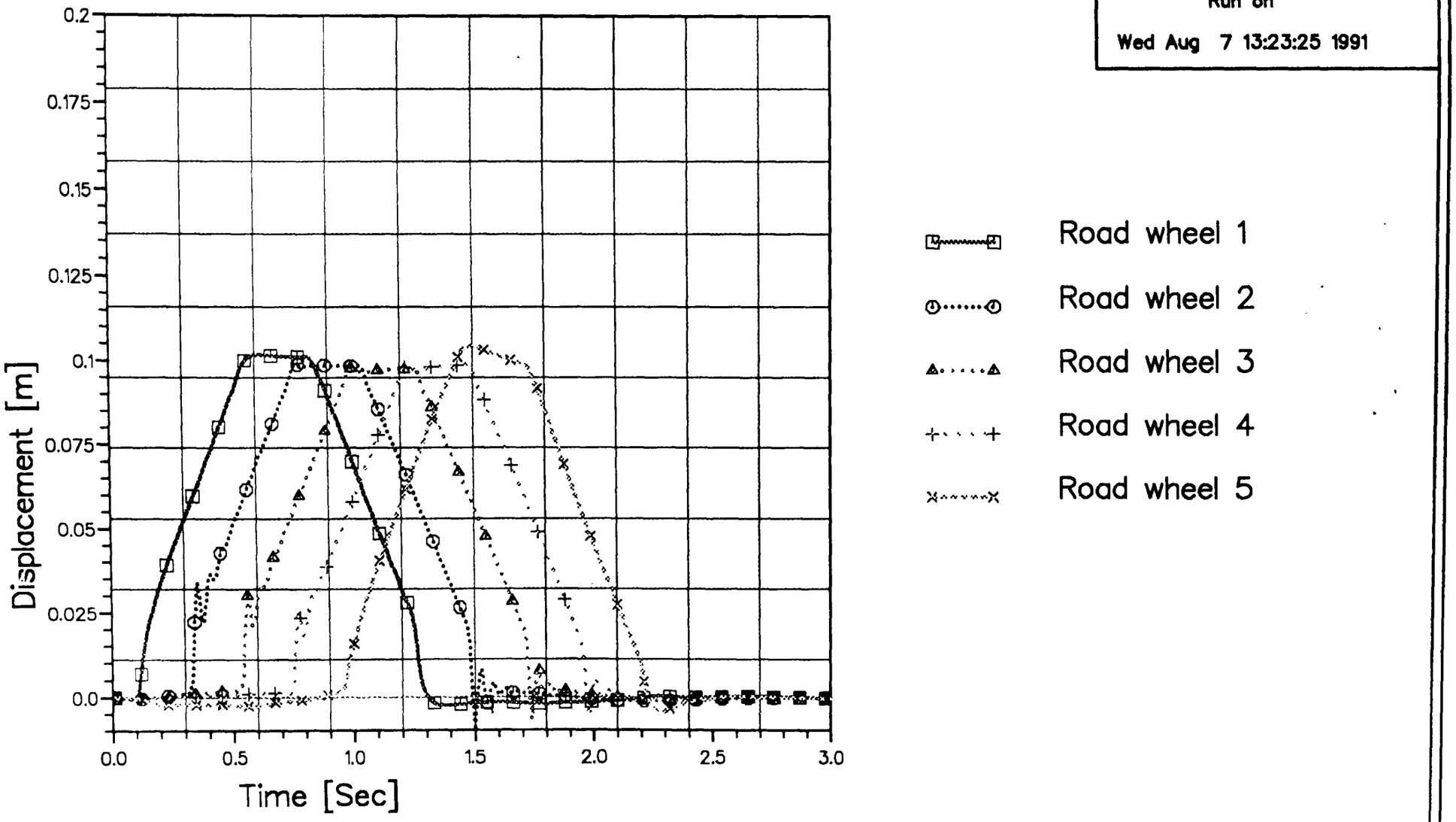

Fig (7.16) Displacement of Wheel Centres of a Scorpion Tank
For a Nonlinear Model Excited by a Bump.

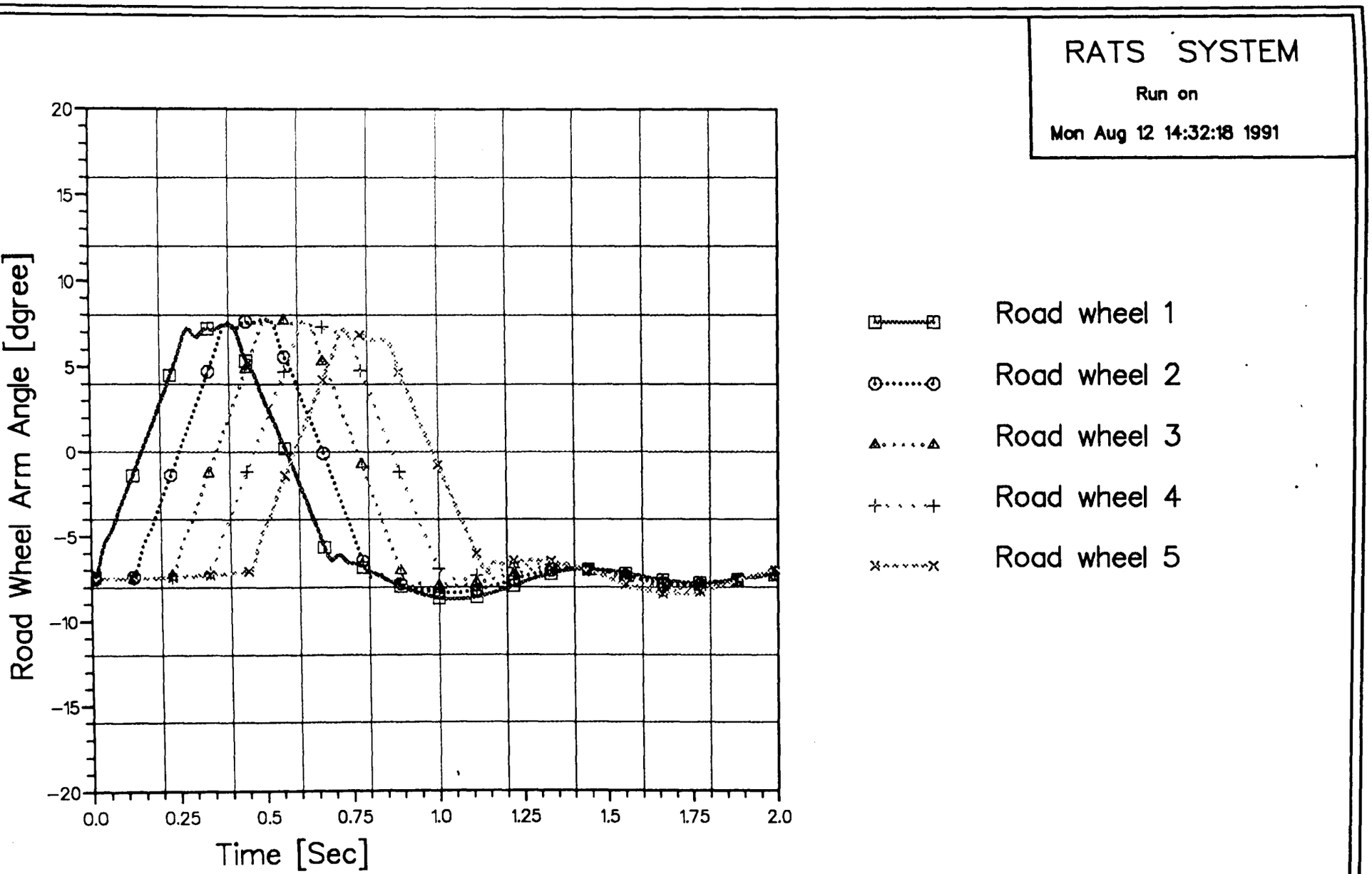

Fig (7.17) The Road Wheel Arm Angle vs Time For a Scorpion Tank Moving with 20 km/h and Excited by a Bump, Linear Model

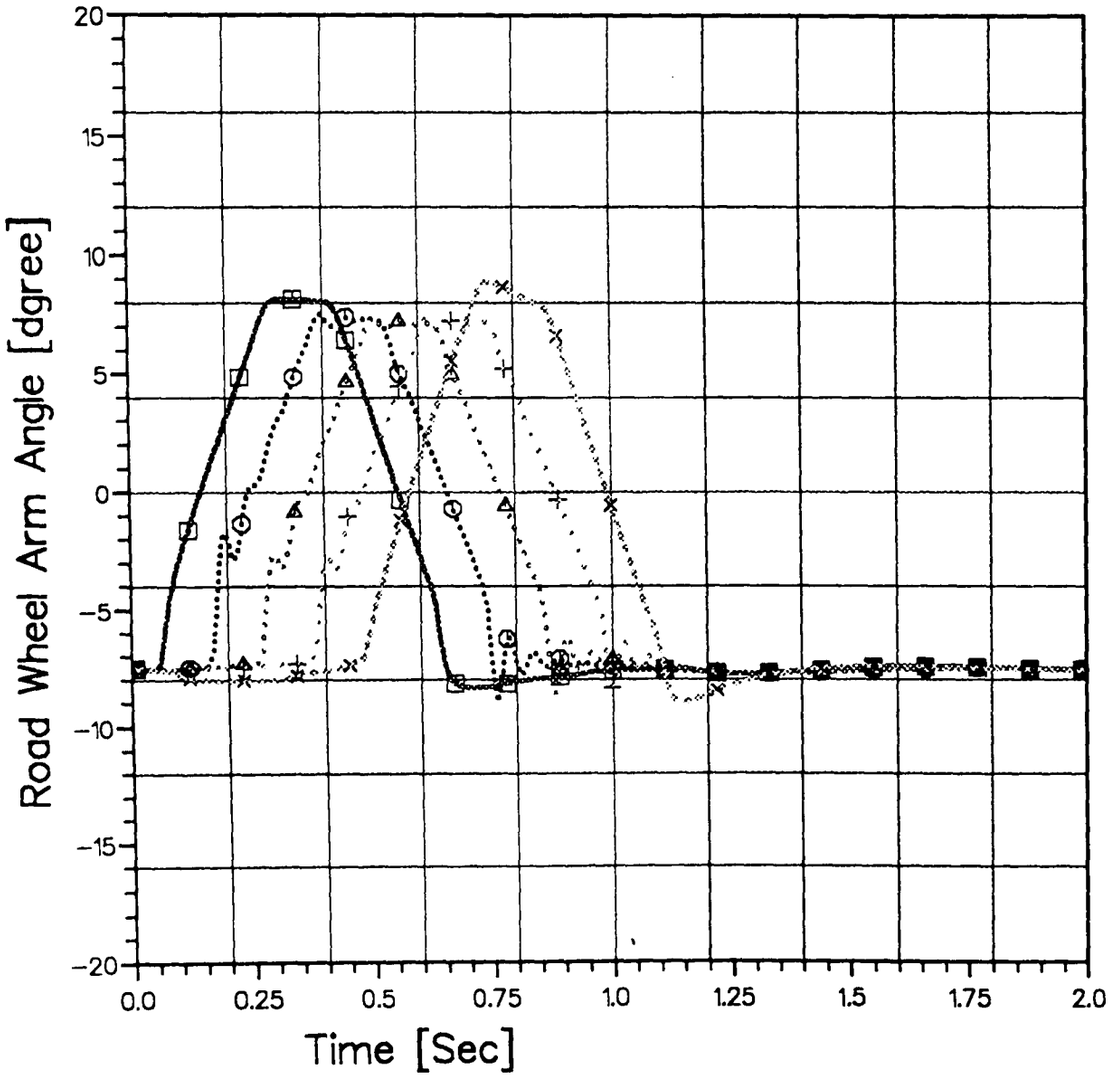

Fig (7.18) The Road Wheel Arm Anlge vs Time For a Scorpion Tank Moving with 20 km/h and Excited by a Bump, Nonlinear Model.

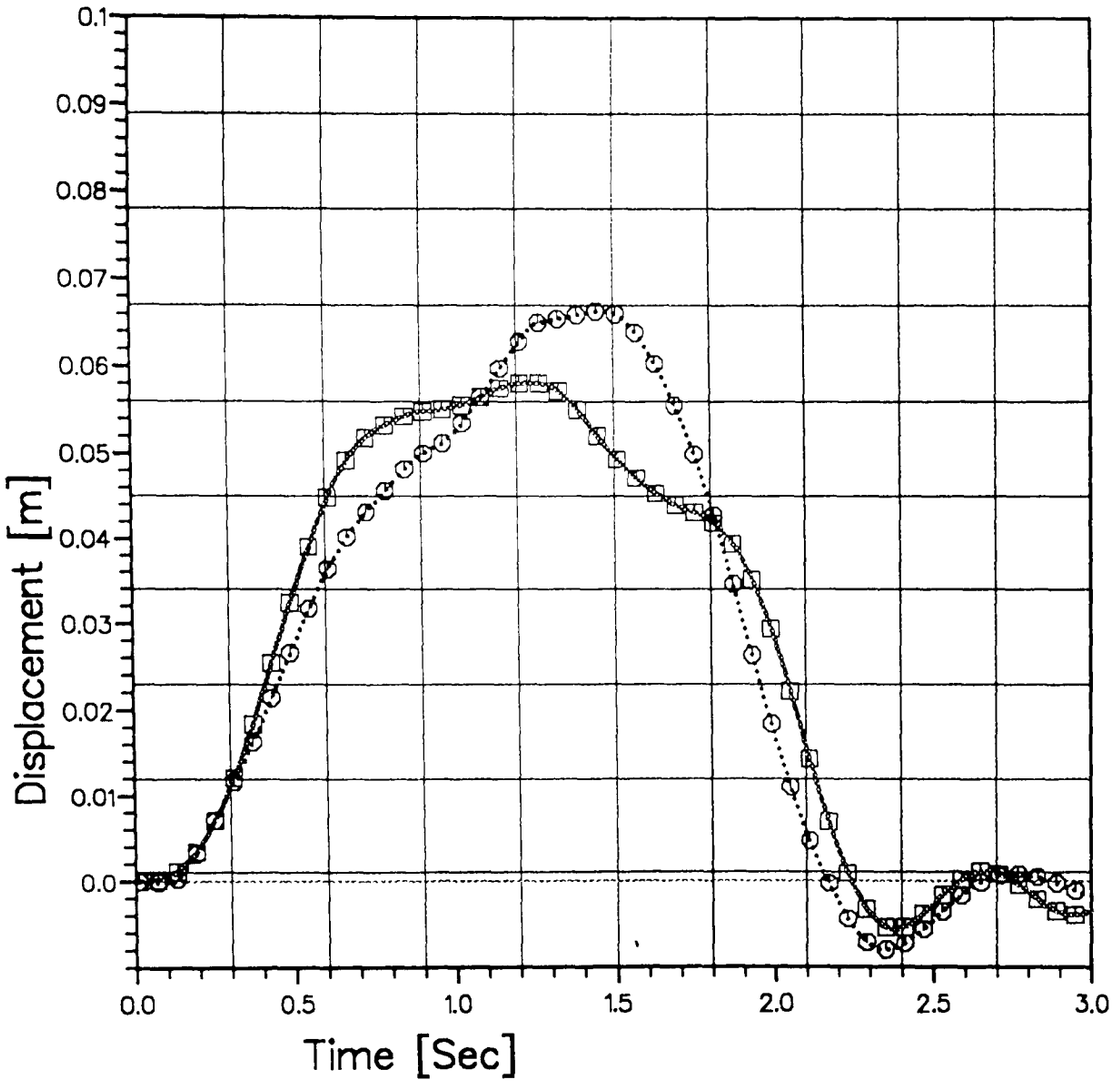

Fig(7.19) Displacement of C.G. of a Scorpion Tank Linear and Nonlinear Models Excited by a Bump.

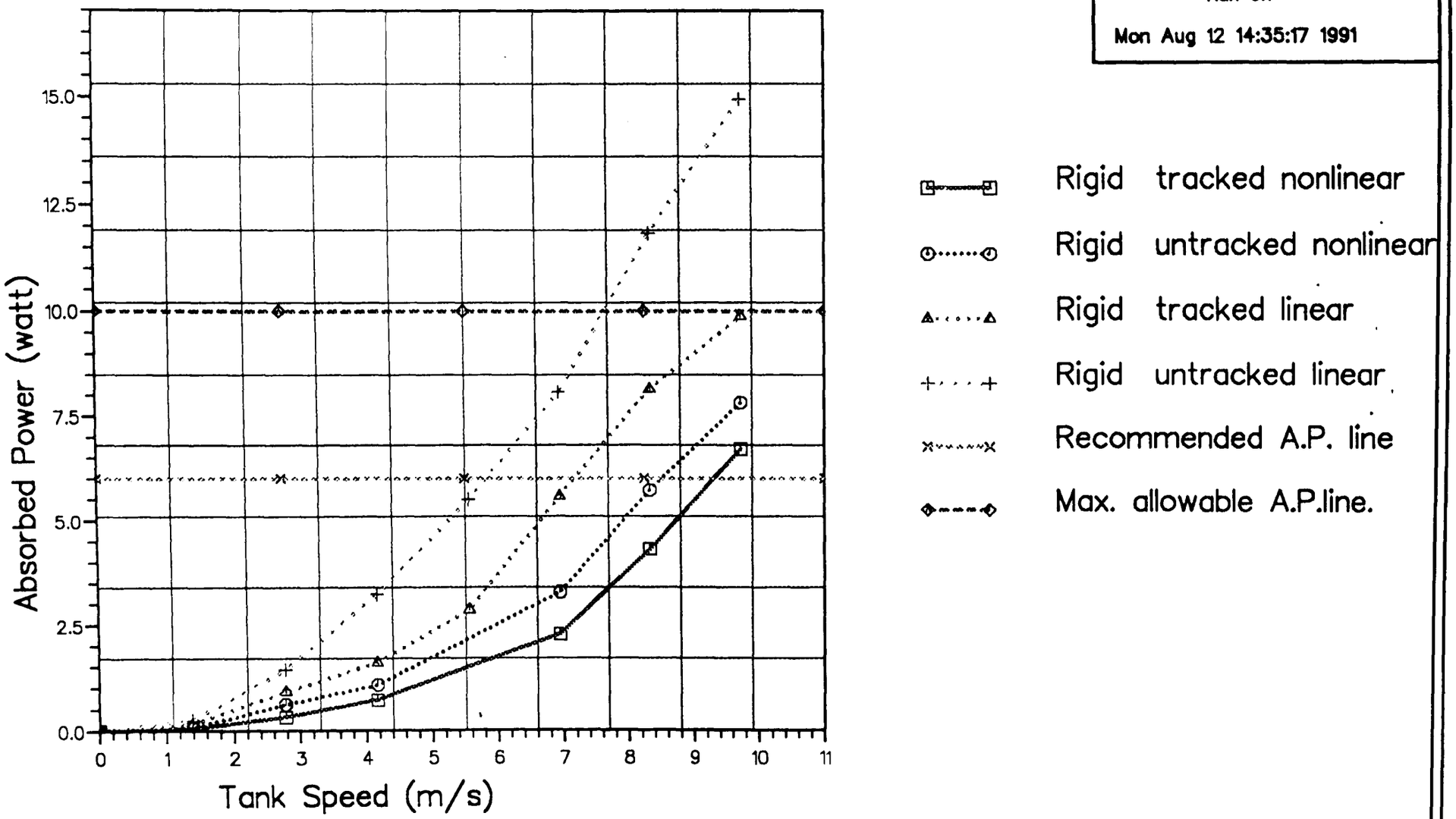

Fig (7.20) Absorbed Power versus Vehicle Speed For Scorpion Tank Linear and Nonlinear Models.

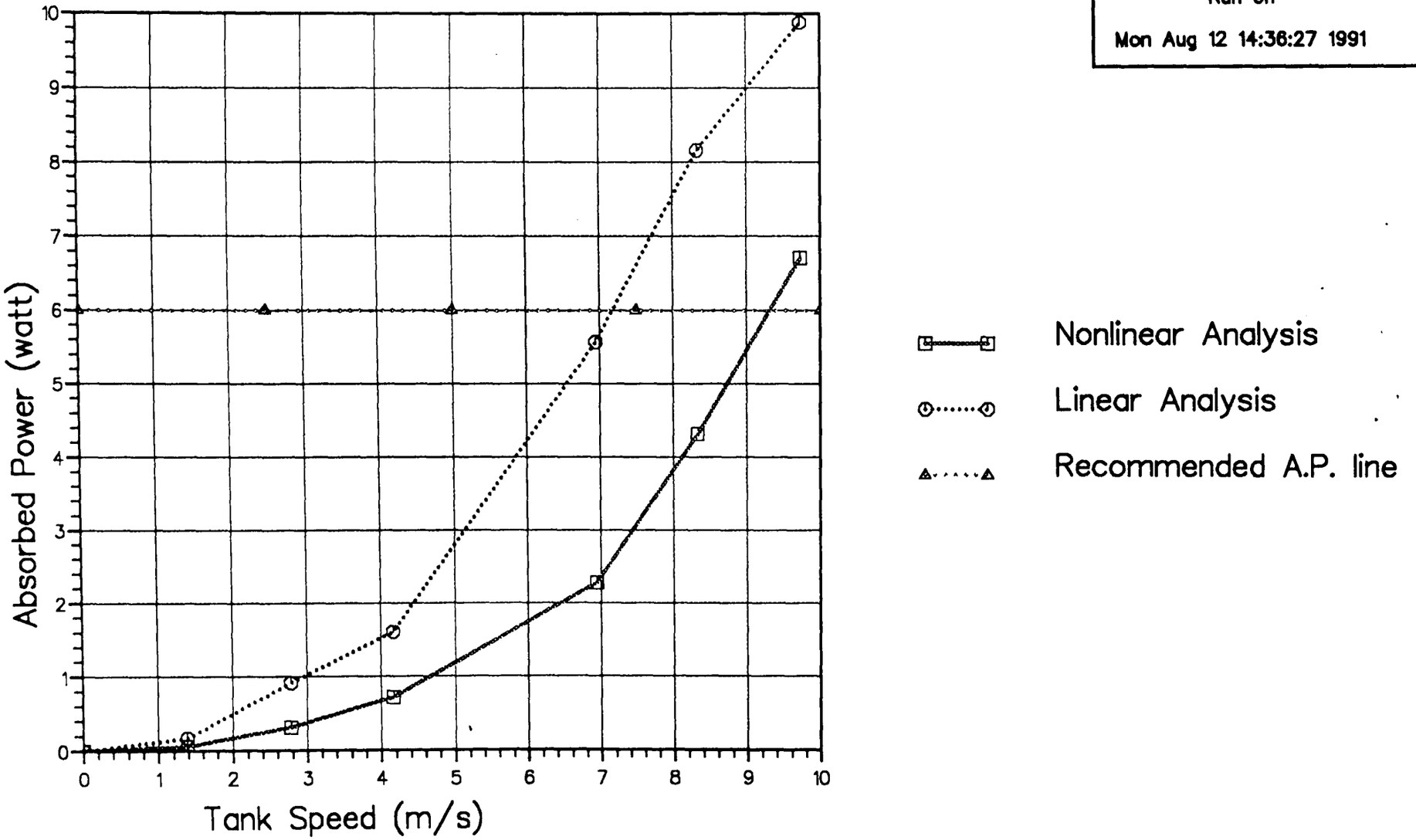

Fig (7.21) Comparison between Absorbed Power versus Vehicle Speed For Tracked Scorpion Tank Linear & Nonlinear Models on Rigid Soil

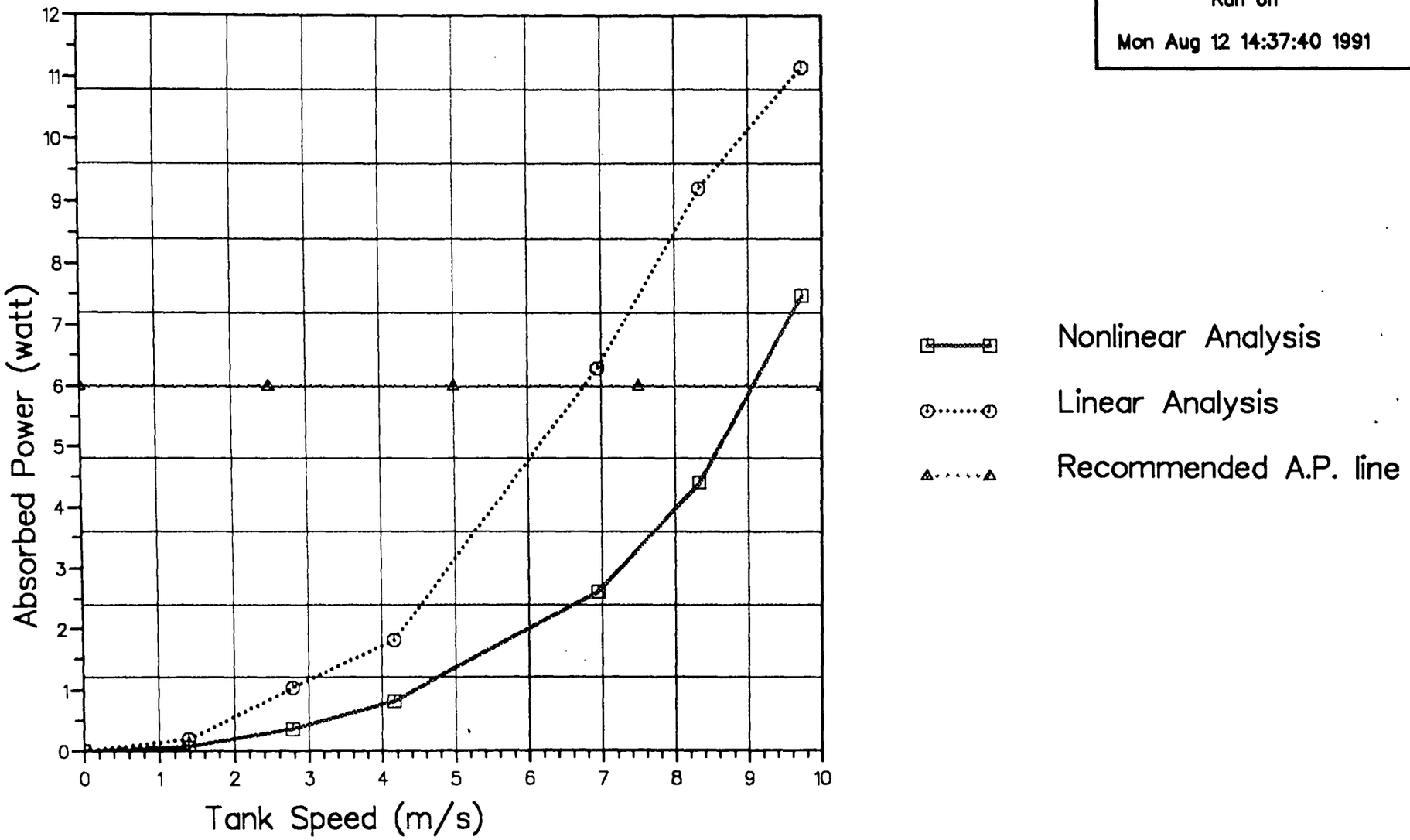

Fig (7.22) Comparison between Absorbed Power versus Vehicle Speed For Tracked Scorpion Tank Linear & Nonlinear models on Sandy Soil

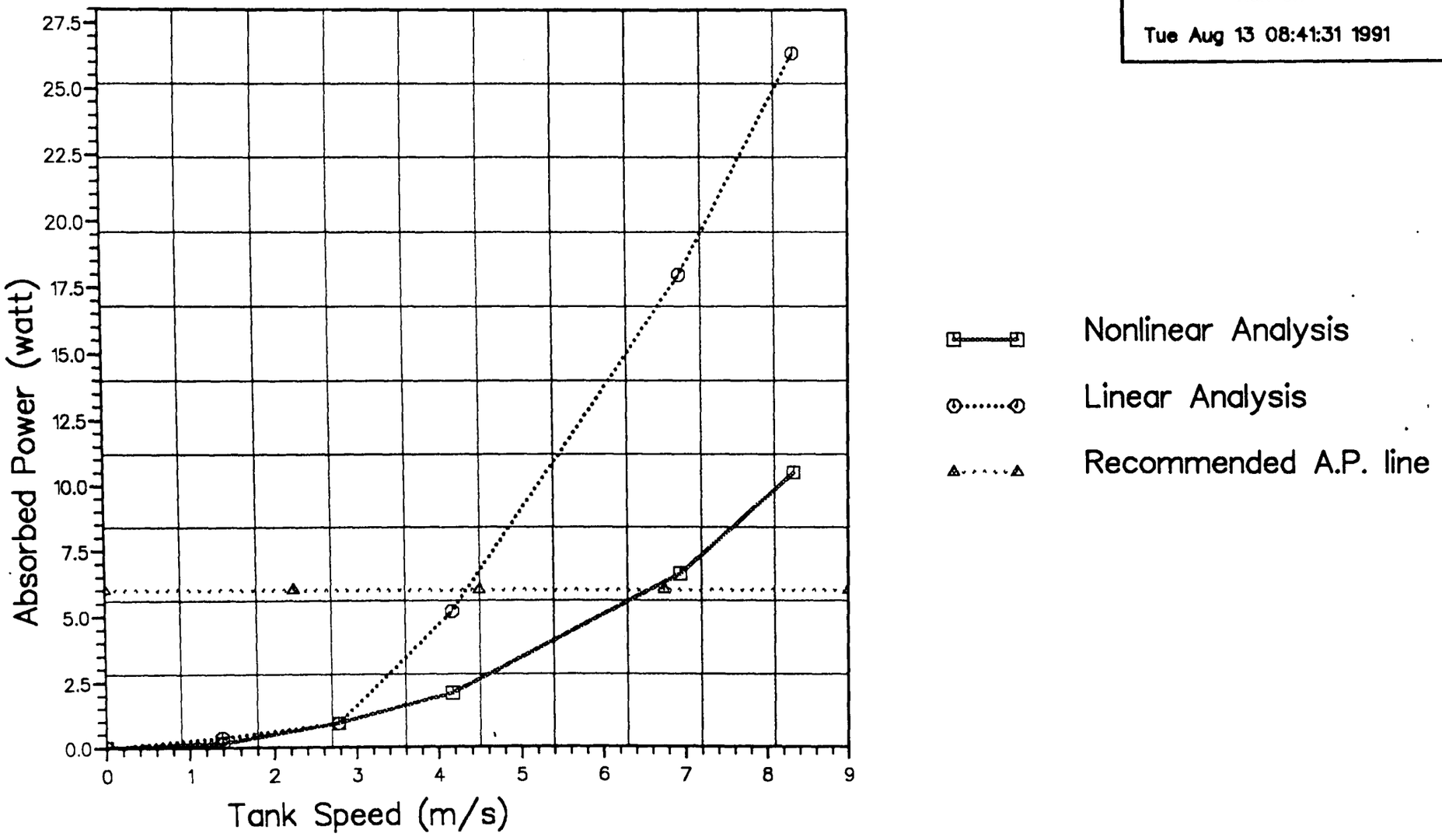

Fig (7.23) Comparison between Absorbed power versus Vehicle Speeds For Tracked Scorpion Tank Linear & Nonlinear Model on Organic Soil

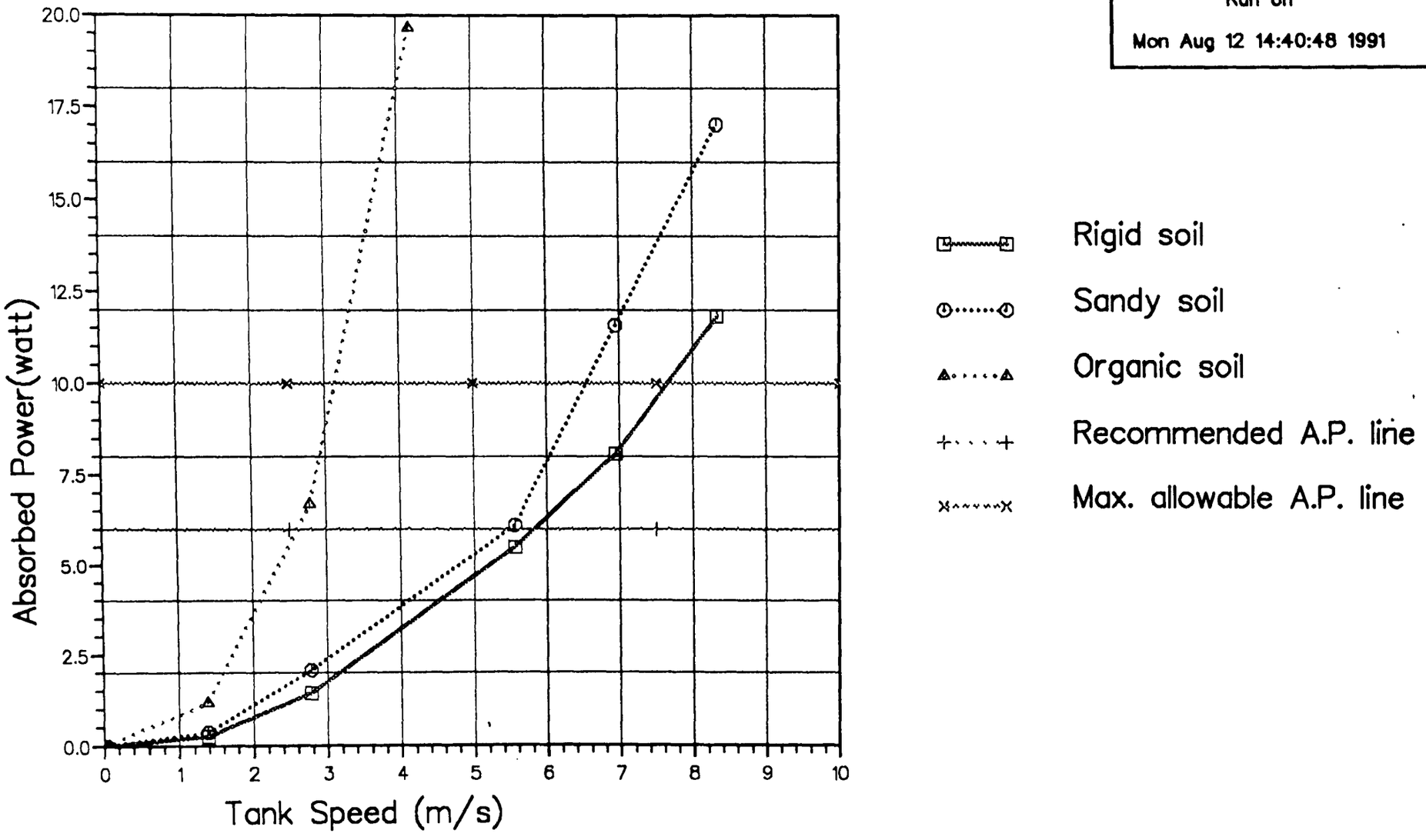

Fig (7.24) Comparison between Absorbed Power versus Vehicle Speed For Untracked Scorpion Tank Linear Model on Different Soils.

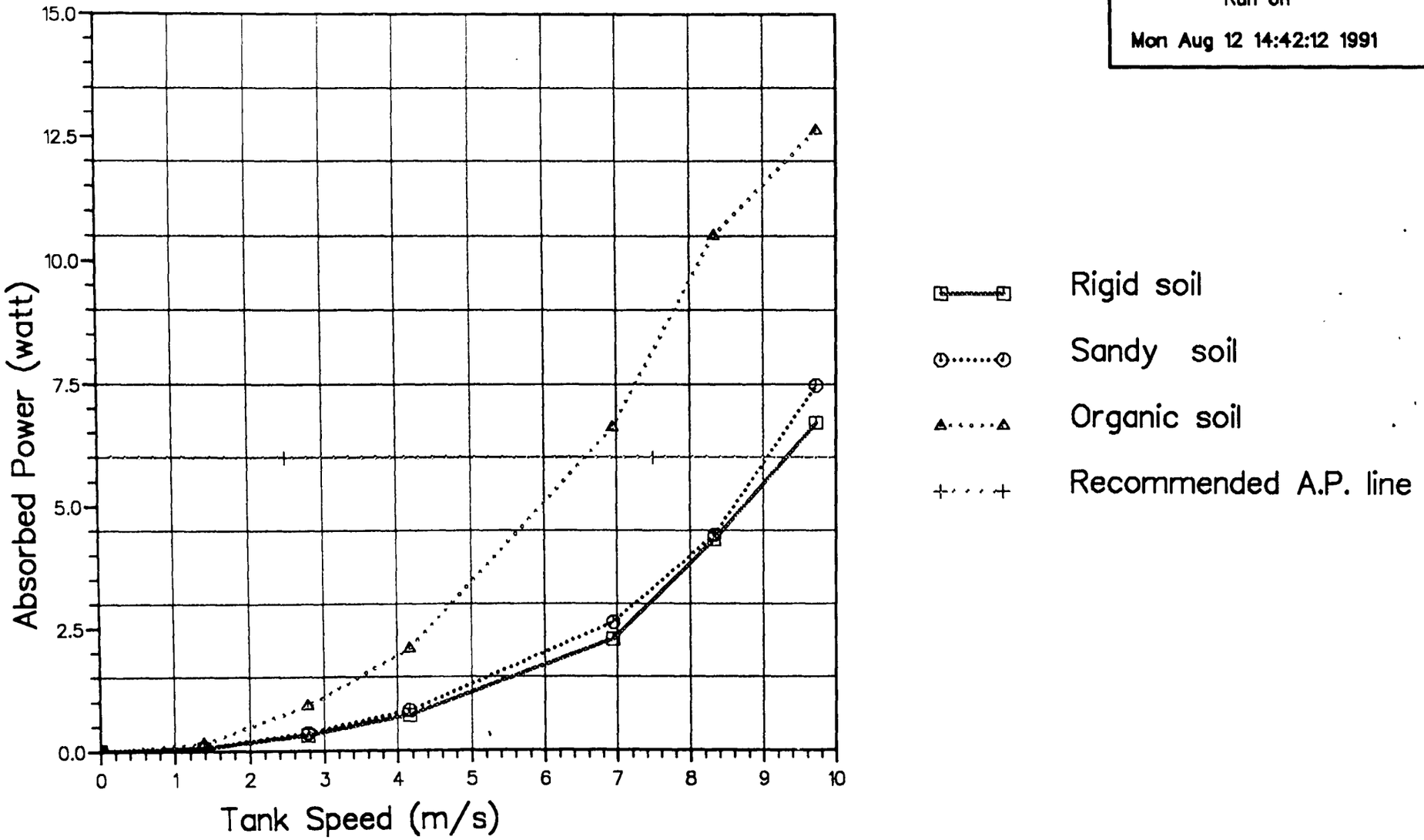

Fig (7.25) Comparison between Absorbed Power versus Vehicle Speed For Tracked Scorpion Tank Nonlinear Model on Different Soils.

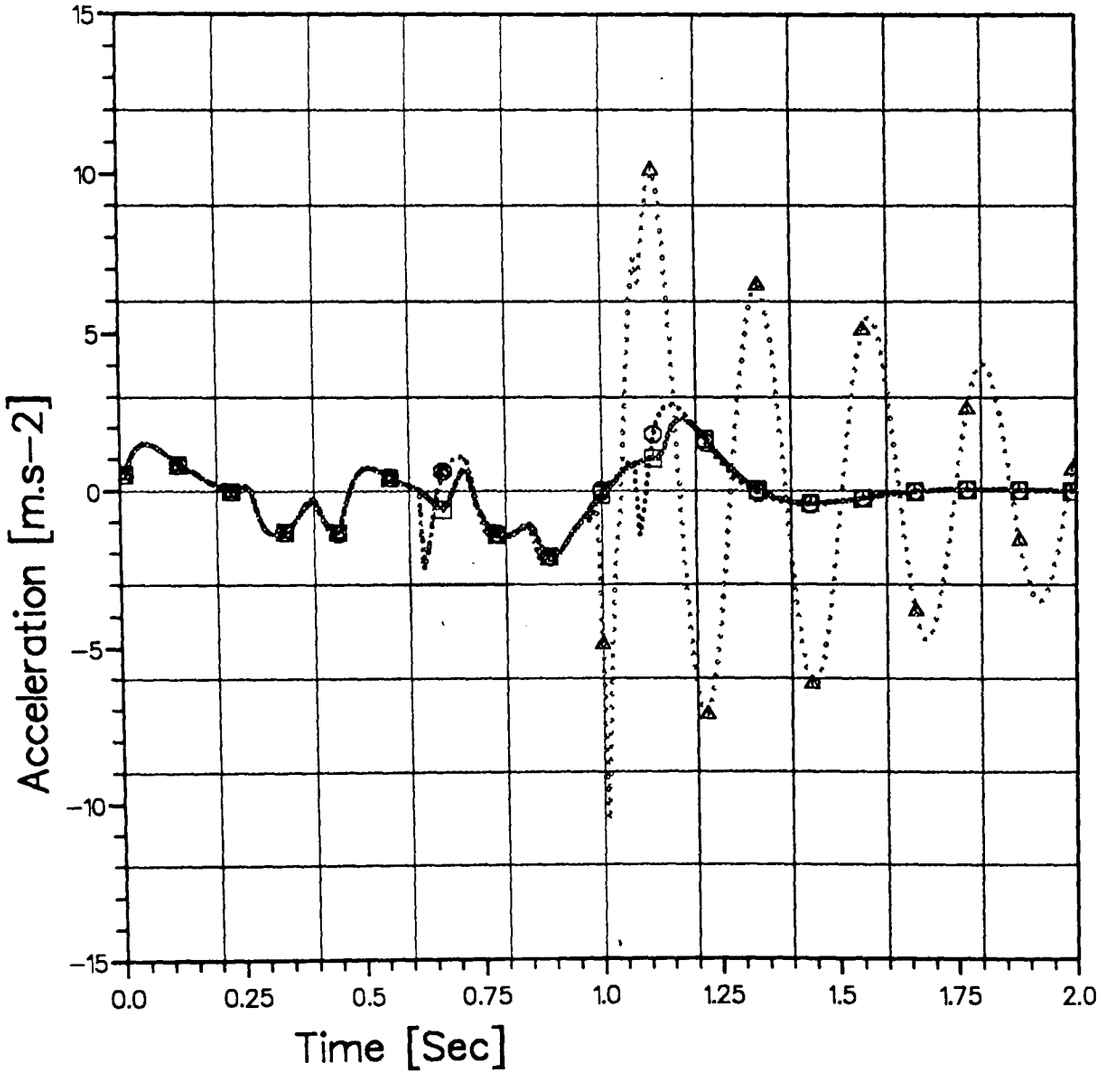

Fig (7.26) C.G. Acceleration versus Time with Failure of First Torsion Bar and Damper of the Scorpion Tank at Speed of 20 km/h.

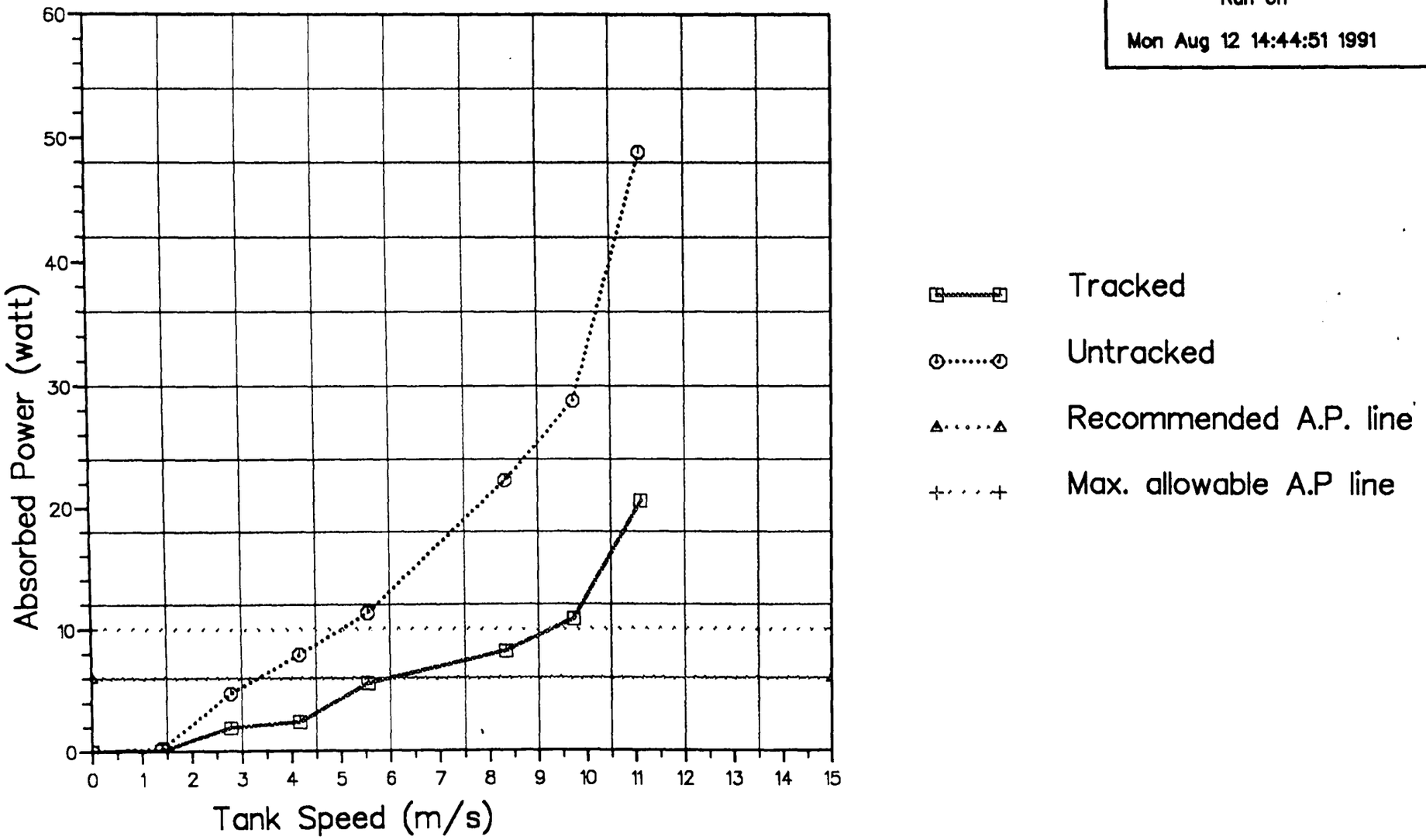

Fig (7.27) Absorbed Power versus Vehicle Speed For the Scorpion Tank, the First Torsion Bar and Damper Failed on Rigid Soil.

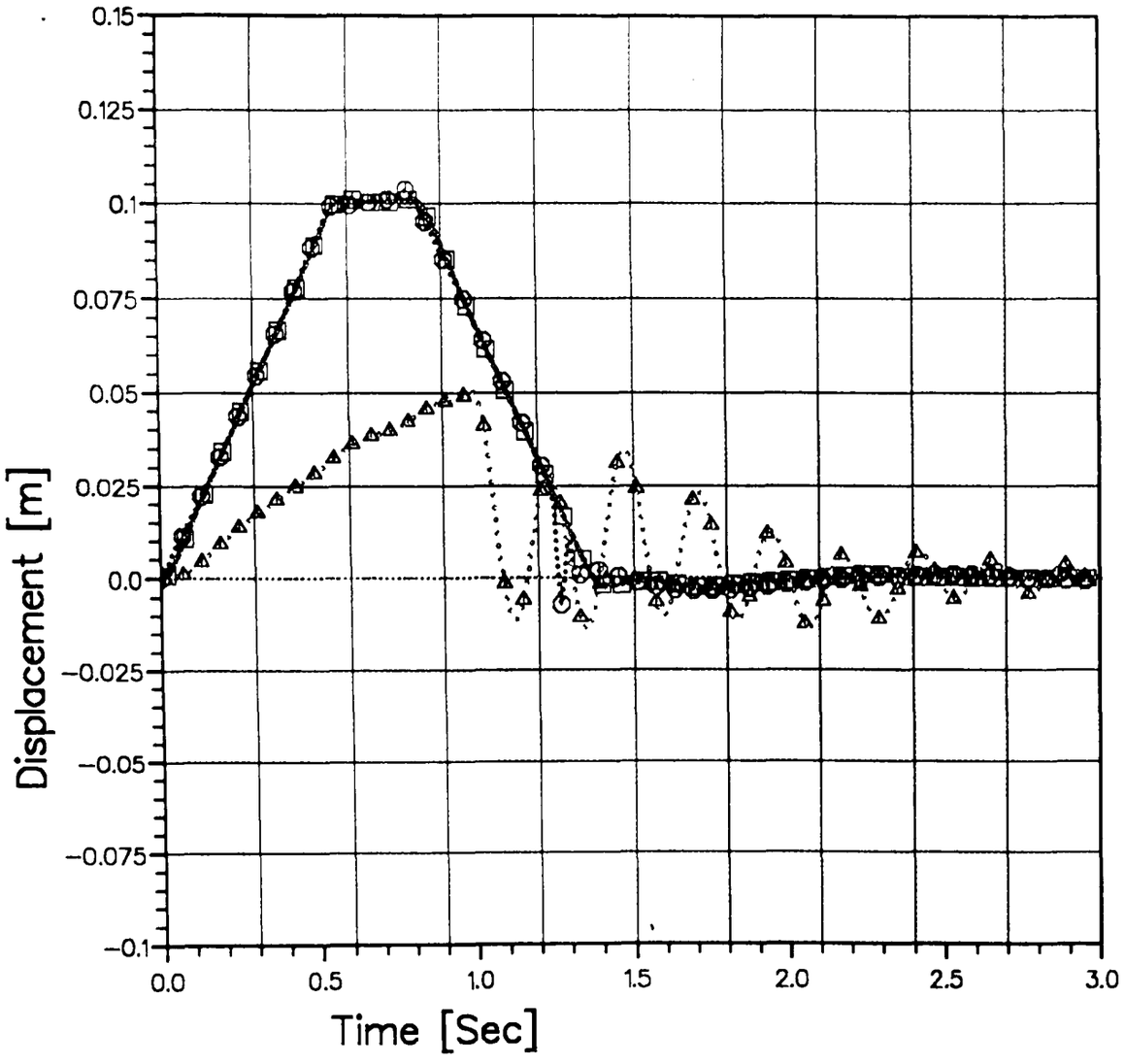

Fig (7.28) Displacement of First Wheel Centre versus Time of Normal and Failed, Scorpion Tank at Speed of 10 Km/h.

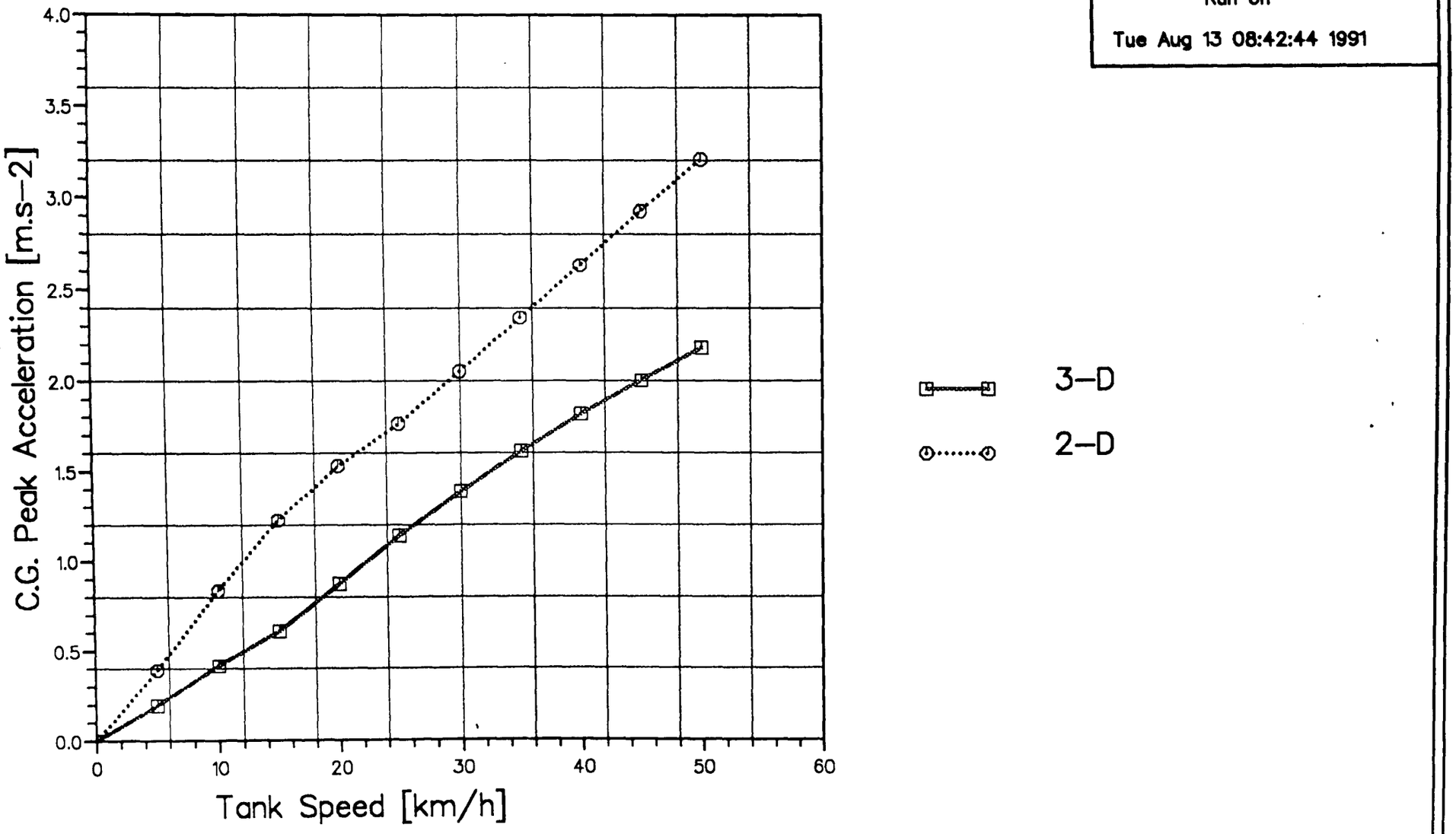

Fig (7.29) Comparison between C.G. Peak Acceleration of the Scorpion Tank 3–D and 2–D Models Excited by a Sinuosoidal Profile

CHAPTER EIGHT

CONCLUSIONS AND RECOMMENDATIONS

8.1 CONCLUSIONS:

It is clear that the author has managed to achieve his main objectives of designing a finite-element package for ride analysis of off-road vehicles with non-linear aspects been considered.

Novel points have been derived and implemented in the package such as, the mathematical modelling of generalised suspension systems of off-road vehicles using a modified finite-element method which will make it easy for future integration with hull structural stiffness parameters, several non-linear aspects such as large deflection, non-linear characteristics of springs and dampers, bump stops and wheel separation, and the analysis of different types of soil together with an appropriate modelling of vehicle tracks.

From the analysis of practical case studies several conclusions have been deduced and summarised as follows:

(i) The Wilson-θ and Hermitian time-marching schemes have proved to be numerically stable and reliable for the analysis of practical cases with stiff equations, and Wilson-θ, is more efficient than the Hermitian method from computational point of view.

(ii) Linear analysis may lead to an over estimation of vehicle response, and non-linear effects should be considered for ride analysis of real vehicles.

(iii) The limiting speed of a vehicle is function of soil stiffness and the existence of the track. Soft soil tends to lower the limiting speed as might be expected.

(iv) The package provides an efficient tool for the prediction of the effects failure of any element of the suspension system on ride and comfort of the vehicle.

8.2 RECOMMENDATIONS FOR FUTURE WORK:

It is advantageous if the study on different types of soil could be supported by some experimental investigation. Other types of soil such as snow-covered soil could be included. Ride analysis under a random excitation could be included and it may be useful for vehicles used on unspecified terrains. The finite-element analysis of suspension system will make it possible to include hull flexibility in the vehicle model which may lead to more accurate prediction of driver acceleration. More accurate modelling of tracks with the effect of friction and contact being considered could be dealt with using more sophisticated finite element analysis.

REFERENCES

REFERENCES

1. **CLARK, D. C.** — An Analysis of Track Mechanics to Improve the Simulations of Ride Dynamics of Track-Laying Vehicles. Report No. YM-1424-V-205, July 1961.

2. **LESSEM, A. S.** **MURPHY, N. R.** — Studies of the Dynamics of Tracked Vehicles. Technical report M-72-1, 1972, U.S. Army Engineer Waterways Experiment Station, CE, Vicksburg, Miss.

3. **MURPHY, N. R.** **AHLVIN, R. B.** — AMC-74 Vehicle Dynamic Module. Technical report M-76-1, 1976, U.S. Army Engineer Waterways Experiment Station.

4. **WHEELER, P.** — Tracked vehicle ride dynamics computer program. International Automotive engineering Congress and Exposition, cobo Hall, Deteroit, SAE paper No. 770048, 1977.

5. **DOYLE, G. R.** **WORKMAN, G. H.** — Prediction of track tension when traversing an obstacle. International Automotive engineering Congress and Exposition, cobo Hall, Deteroit, SAE paper No. 790416, 1979.

6. **GIANNOPOULOS, F.** **RAO, A. K.** — Dynamic loads on suspension components using mechanisms programs. SAE paper No. 811307, 1980.

7. **PETRICK, E. N.**
JANOSI, Z. J.
HALEY, P. W.
The use of the NATO reference mobility model in military vehicle procurement. SAE paper No. 810373. Int. Congress and Exposition Cobo Hall, Detroit. Michigan, Feb. 23-27, 1981.

8. **KIM, S. S.**
SHABANA, A. A.
HAUG., E. J.
Automated vehicle dynamic analysis with flexible component.
Journal of mechanism. Transition, and Automation in design, March, 1984 Vol. 106, pp 126-132.

9. **CRAIGHEAH, I. A.**
BROWN, P. R.
Vibration and dynamics of off-road vehicles.
IMechE 1984 C135/84, pp 65-76.

10. **BENNETT, M. D.**
PENNY, P. H. G.
Dynamic simulation of track laying vehicles.
RMCS Shrivenham, Swindon, Wilts UK.

11. **HORTON, D. N. L.**
CROLLA, D. A.
Designing off-road vehicles with good ride behaviour.
Dept of Mech. Engn., University of Leeds, Leeds, UK, 1983.

12. **ANDERSON, R. J.**
HANNA, D. M.
Comparison of three vehicle simulation methodologies.
Journal of Vehicles 1984.

13. **BAKR, E. M.**
GASTOUNIOTIS. I.
SHABANA, A. A.
Dynamic analysis of flexible legged vehicles using the finite element method.
Int. J. of Vehicle Design, Vol 10, 1989, No 1, pp 1-15.

14. **U.S. ARMY TANK AUTOMATIVE COMMAND**
The AMC-71 Mobility Model.
Technical Report 11789 (LL 143),
July 1973, Warren, Michigan.

15. **BEKKER, M. G.**
Introduction to Terrain-Vehicle Systems,
The University of Michigan press, 1969.

16. **WONG, J. Y.**
Theory of Ground Vehicles.
Carleto University, Ottawa, Ontario,
JOHN WILEY & SON, 1984.

17. **WONG, J. Y.**
On the study of wheel-soil interaction.
Journal of Terramechanics, Vol 21.,1984
No 2, pp. 117-131.

18. **YONG, R. N.**
Track-soil interaction.
Journal of Terramechanics, Vol 21,1984
No 2, pp. 133-152.

19. **MARINSHAW, J.**
Implementing tracked Vehicle mobility specifications.
Government/Industry meeting & Exposition,
Washington, D.C., May 21-24, 1984
SAE paper No. 840874

20. **WONG, J. Y.**
GARBER, M.
PRESTON-THOMAS, J.
Theoretical prediction and experimental substantiation of the ground pressure distribution and tractive performance of tracked vehicles.
Proceedings of the Institute of Mech. Engineers, Part D, 1984, Vol. 198(15), pp.265-285.

21. **WONG, J. Y.**
PRESTON-THOMAS, J.
Parametric analysis of tracked vehicle performance using an advanced computer simulation model.
Proceedings of the of the Institute of Mech Engineers, Part D, 1986, Vol.200(D2), pp 101-114.

22. **WONG, J. Y.**
PRESTON-THOMAS, J.
Further developments and applications of a computer simulation model for parametric evaluation of tracked vehicle design.
Proceedings of the 9th International Society for Terrain-Vehicle systems, 1987 pp 200-212.

23. **OIDA, A.**
Analysis of rheological deformation of soil by means of finite element method., Journal of Terramechanics, Vol 21, No 3, pp. 237-251, 1984.

24. **LEE, R. A.**
PRAKO, F.
KALUZA, V.
Theory of human vibration response.
ASME paper 66-WA/BHF-15, 1966.

25. **LEE, R. A.**
PRADKO, F.
Analytical analysis of human vibration.
SAE Transactions,Vol.77,paper No.680091, 1968.

26. **LINS, W. F.**
HOOGTERP, F. B.
PRADKO, F.
Comparison of time domain and frequency domain analysis of off road vehicles,
SAE paper No. 690353, April 1969.

27. **LINS, W. F.**
DUGOFF, H.
Motion simulation and its application to ride dynamics research. SAE paper No. 720003, 1972.

28. **STIKELEATHER, L. F.**
HALL, G. O.
RADKE, A. O.
A study of vehicle vibration spectra as related to seating dynamics. SAE paper No. 720001, January 1972.

29. **JANEWAY, R. N.**
Human vibration tolerance criteria and applications to ride evaluation. SAE paper no. 750166, 1975.

30. **STIKELEATHER, L.F.**
Review of ride vibration standards and tolerance criteria. SAE paper No. 760413, 1976.

31. **NEWELL, R.**
MURPHY, JR.
Further development in ride quality assessment. U.S. army engineer waterways experiment station, 8th Intentional conference, August 5-11, 1984, pp. 433-449.

32. **HOHL, G. H.**
Ride comfort of off road vehicles. 8th International conference, August 5-11, 1984, pp.413-433.

33. **SHAMPINE, L. F.**
GEAR. C. W.
A user's view of solving stiff ordinary differential equations. SIAM review, Vol. 21 No. 1,Jan. 1979. pp.1-17.

34. **SHAMPINE, L. F.**
What is stiffness. International conference on stiff computation, Vol. 1, 1982.

35. **AIKEN, R. C.**
Stiff review 1974-1982.
International conference on stiff computation, Vol. 1, 1982.

36. **EL-ZAFARANY, A.**
COOKSON, R. A.
Efficient schemes for transient dynamic analysis (To be published).

37. **BATHE, K. J.**
Finite Element Procedures in Engineering Analysis.
Prentice-Hill, Inc, Englewood cliffs, New Jersey 07632, TA 347.F5B36, ISBN 0-13-317305-4, 1982.

38. **HOFF, C.**
PAHL, P. J.
Development of an implicit method with numerical dissipation from a generalized single-step algorithm for structural dynamics.
Computer methods in applied mechanics engineering 67(1988).pp. 367-385.

39. **HOFF, C.**
PAHL, P. J.
Practical performance of the θ_1 method and comparison with other dissipative algorithms in structural dynamics.
Computer methods in applied mechanics engineering 67(1988).pp. 87-110.

40. **GAO, X.**
ZHANG, Q.
Multi-steps numerical integrations for time-dependent vibration systems.
Computer methods in applied mechanics engineering 69(1988).pp. 45-52.

41. **NEAL, M. O.**
BELYTSCHKO, T.
Explicit-explicit subcycling with nonlinear time step ratios for structural dynamic systems.
Computer & Structures, Vol. 31, NO. 6, pp. 871-880, 1989.

42. **SUBBARAJ, K.**
DOKAINISH, M. A.
A survey of direct time-integration methods in computational structural dynamics-I explicit methods.
Computers & Structures Vol. 32., No. 6, pp 1371-1386, 1989.

43. **SUBBARAJ, K.**
DOKAINISH, M. A.
Survey of direct time-integration methods in computational structural dynamics-II implicit methods.
Computers & Structures Vol. 32., No. 6, pp 1387-1401, 1989.

44. **CHADHA, B.**
AGRAWAL, O. P.
Dynamic analysis of flexible multi-body systems using mixed modal and tangent coordinates.
Computer & Structures Vol. 31 No.6, 1989 pp. 1041-1050.

45. **BEKKER, M. G.**
Theory of Land Locomotion.
University of Michigan, press,
Ann Arbon, MI 1956.

46. **CROLLA, D. A.**
DALE, A. K.
Off road vehicle ride vibration.
I Mech E conf. Publications 1984-5, 1984.

47. **CAPTAIN, K. M.**
BOGHANI, A. B.
WORMLEY, D. M.
Analytical tyre models for dynamic vehicle simulation.
J. of Vehicle System Dynamics,
Vol. 8, No. 1, 1979.

48. **WONG, J. Y.**
PRESTON, T. J.
Investigation into the effects of suspension characteristics and design parameters on the performance of tracked vehicles using an advanced computer simulation model.

49. **MACLAURIN, B.** Progress in British tracked vehicle suspension systems. SAE paper No. 830442, 1984.

50 **ISO PUBLICATION.** Guide for the evaluation of human exposure to whole-body vibration. International standard ISO 2631-1978/Amendment 1, 1983.

51. **BOULANGERE MISTROT** Valuation of Amount of Exposure to Vibrations Transmitted to The Whole Body. RAF, March 1978.

52. **COLLATZ, L.** The Numerical Treatment of Differential Equations. Springer-Verlay, 1960.

53. **BATHE, K. J. WILSON, E. L.** Numerical Methods in Finite Element analysis . Printice-Hall, TA347.F5B37, ISBN 0-13-627190-1, 1976.

54. **ZIENKIEWICZ, O. Z.** The Finite Element Method. McGraw-Hill, 1982.

55. **EL-ZAFARANY, A.** An Advanced Finite Element System for Engineering Analysis. Ph. D Thesis, Cranfield Institute of Technology, 1983.

56. **SPENCER, A. J. and et al** Engineering Mathematics. Vol. I. Van Nostrand Reinhold Company Ltd., 1981.

57. **ZIENKIEWICZ, O. Z.** The Finite Element. Third edition. McGraw-Hill, 1977.

58. **RAO, S. S.** The Finite Element Method in Engineering, Pergamon Press, 1982.

59. **KAMAR, E. A.**
EL-ZAFARANY, A.
COOKSON, R. A. Simulation of suspension system by the finite element method. IAVSD congress 3rd on Vehicle design and components, conf. D, pp 225-247, 1986.

60. **U.S Army** Automotive Suspenstions. Engineering Design Handbook (Automotive series), Headguarters, U.S Army Material Command, Report No. ADB17023, 1967.

61 **MACLAURIN, B.** Design of off-road vehicles for higher speeds. Conf. of off-highway vehicles, tractors and equipment, London, 28-29 Oct. Published by Mechanical Engineering Publications Ltd, 1975.

62. **WONG, J. Y.** Terramechanics and Off-Road Vehicle. Amsterdam., Elsevier, 1989.

APPENDICES

APENDIX (A)

THE SOIL PRESSURE-SINKAGE PARAMETERS

The values of K_c, K_φ, and n can be obtained by a minimum of two test with two plates having different widths. The tests produce two curves.

$$P_1 = \left(\frac{K_c}{b_1} + K_\varphi \right) Z^n$$

$$P_2 = \left(\frac{K_c}{b_2} + K_\varphi \right) Z^n$$

On the logarithmic scale, the above equations can be rewritten as follows:

$$log\ P_1 = log\left(\frac{K_c}{b_1} + K_\varphi \right) + n\ log\ Z$$

$$log\ P_2 = log\left(\frac{K_c}{b_2} + K_\varphi \right) + n\ log\ Z$$

They represent two parallel straight lines of the same slope on a *log-log* scale as shown in Figure.(A-1).

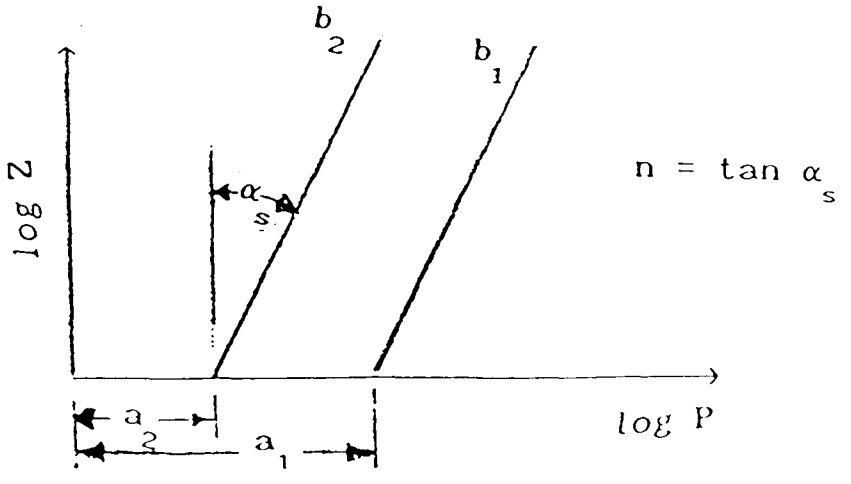

Fig.(A-1) Method For Determining Sinkage Moduli And Exponent.

Thus the exponent of deformation **n** can be determined from the slope of the straight lines. At sinkage Z=1, the values of the normal pressure for the two plates are:

$$P_{1(z=1)} = \frac{K_c}{b_1} + K_\varphi = a_1$$

$$P_{2(z=1)} = \frac{K_c}{b_2} + K_\varphi = a_2$$

In the above equations, $P_{1(z=1)}$ and $P_{2(z=1}$ are measured values, and the only unknowns are K_c and K_φ . Thus, the moduli of deformation can be determined by the following equations.

$$K_\varphi = \frac{a_2 b_2 - a_1 b_1}{b_2 - b_1}$$

$$K_c = \frac{(a_1 - a_2) b_1 b_2}{b_2 - b_1}$$

Owing to the non-homogeneity of soil and experimental errors, the pressure-sinkage lines may not be quite parallel on the *log-log* scale in some cases, Thus, two values of the exponent of deformation may be produced, Under these circumstances, the value of **n** is usually taken as the arithmetic mean of the two values obtained.

The values of K_c, K_φ , and **n** for various type of soils are given in table (A-1).

Table (A-1) Values of the pressure-sinkage parameters for sandy, and organic terrains.

Terrain type	n	K_c kN/m^{n+1}	K_ϕ kN/m^{n+2}
Sandy	0.793	102.	5301.
Organic	1.0	20.68	814.30

Source from [Ref. 62]

TABLES AND GRAPHS USED IN THE ISO AND HUMAN RESPONSE TRANSFER FUNCTIONS

Frequency (centre frequency of third-octave band)	Acceleration, m/s²								
	Exposure times								
Hz	24 h	16 h	8 h	4 h	2,5 h	1 h	25 min	16 min	1 min
1,0	0,280	0,425	0,63	1,00	1,40	2,36	3,55	4,25	6,60
1,25	0,250	0,375	0,56	0,95	1,20	2,12	3,15	3,75	5,00
1,6	0,224	0,335	0,50	0,85	1,12	1,90	2,80	3,35	4,50
2,0	0,200	0,300	0,45	0,75	1,00	1,70	2,50	3,00	4,00
2,5	0,160	0,265	0,40	0,67	0,90	1,50	2,24	2,65	3,55
3,15	0,100	0,235	0,355	0,60	0,80	1,32	2,00	2,35	3,15
4,0	0,140	0,212	0,315	0,53	0,71	1,18	1,80	2,12	2,80
5,0	0,140	0,212	0,315	0,53	0,71	1,18	1,80	2,12	2,80
6,3	0,140	0,212	0,315	0,53	0,71	1,18	1,00	2,12	2,80
8,0	0,140	0,212	0,315	0,53	0,71	1,10	1,80	2,12	2,80
10,0	0,180	0,265	0,40	0,67	0,90	1,50	2,24	2,65	3,55
12,5	0,224	0,335	0,50	0,85	1,12	1,90	2,80	3,35	4,50
16,0	0,280	0,425	0,63	1,06	1,40	2,36	3,55	4,25	5,60
20,0	0,355	0,530	0,80	1,32	1,80	3,00	4,50	5,30	7,10
25,0	0,450	0,670	1,0	1,70	2,24	3,75	5,60	6,70	9,0
31,5	0,560	0,850	1,25	2,12	2,80	4,75	7,10	8,50	11,2
40,0	0,710	1,060	1,60	2,65	3,55	6,00	9,00	10,6	14,0
50,0	0,900	1,320	2,0	3,35	4,60	7,50	11,2	13,2	18,0
63,0	1,120	1,700	2,5	4,25	5,60	9,50	14,0	17,0	22,4
80,0	1,400	2,120	3,15	5,30	7,10	11,8	18,0	21,2	28,0

Table (B.1) Numerical values for vibration acceleration in the longitudinal a_z direction.

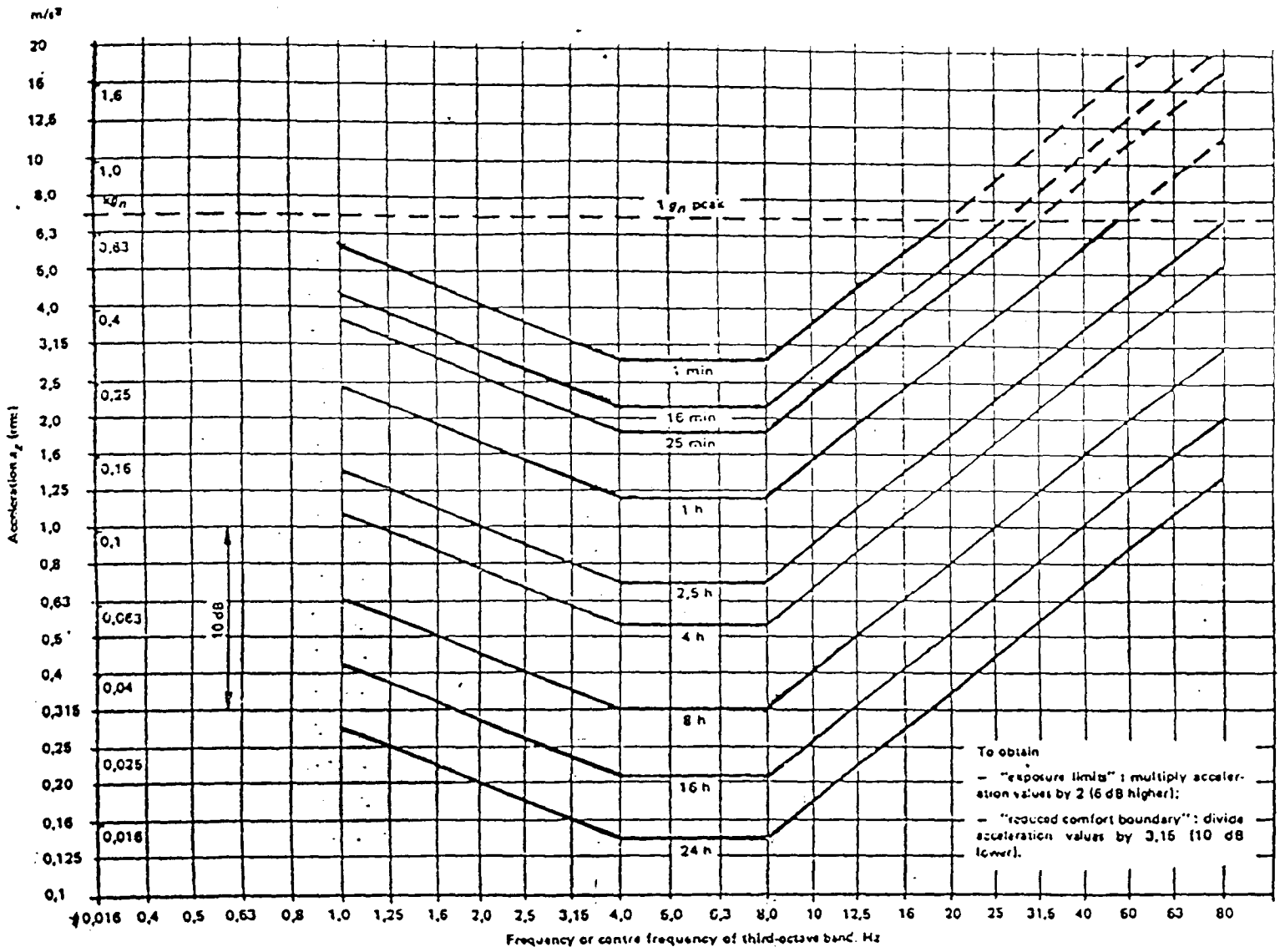

Fig (B.1) Longitudinal a_z acceleration limits as a function of frequency and exposure time.

Frequency (centre frequency of third-octave band)	Acceleration, m/s^2								
	Exposure times								
Hz	24 h	16 h	8 h	4 h	2,5 h	1 h	25 min	10 min	1 min
1,0	0,100	0,150	0,224	0,355	0,50	0,85	1,25	1,50	2,0
1,25	0,100	0,150	0,224	0,355	0,50	0,85	1,25	1,50	2,0
1,6	0,100	0,150	0,224	0,355	0,50	0,85	1,25	1,50	2,0
2,0	0,100	0,150	0,224	0,355	0,50	0,85	1,25	1,50	2,0
2,5	0,125	0,190	0,280	0,450	0,63	1,06	1,6	1,9	2,5
3,15	0,160	0,236	0,355	0,560	0,8	1,32	2,0	2,36	3,15
4,0	0,200	0,300	0,450	0,710	1,0	1,70	2,5	3,0	4,0
5,0	0,250	0,375	0,560	0,900	1,25	2,12	3,15	3,75	5,0
6,3	0,315	0,475	0,710	1,12	1,6	2,65	4,0	4,75	6,3
8,0	0,40	0,60	0,900	1,40	2,0	3,35	5,0	6,0	8,0
10,0	0,50	0,75	1,12	1,80	2,5	4,25	6,3	7,5	10
12,5	0,63	0,95	1,40	2,24	3,15	5,30	8,0	9,5	12,5
16,0	0,80	1,18	1,80	2,80	4,0	6,70	10	11,8	16
20,0	1,00	1,50	2,24	3,55	5,0	8,5	12,5	15	20
25,0	1,25	1,90	2,80	4,50	6,3	10,6	16	19	25
31,5	1,60	2,36	3,55	5,60	8,0	13,2	20	23,6	31,5
40,0	2,00	3,00	4,50	7,10	10,0	17,0	25	30	40
50,0	2,60	3,75	5,60	9,00	12,5	21,2	31,5	37,5	50
63,0	3,15	4,75	7,10	11,2	16,0	26,5	40	45,7	63
80,0	4,00	6,00	9,00	14,0	20	33,5	50	60	80

Table (B.2) Numerical values for vibration acceleration in the transverse a_x or a_y direction.

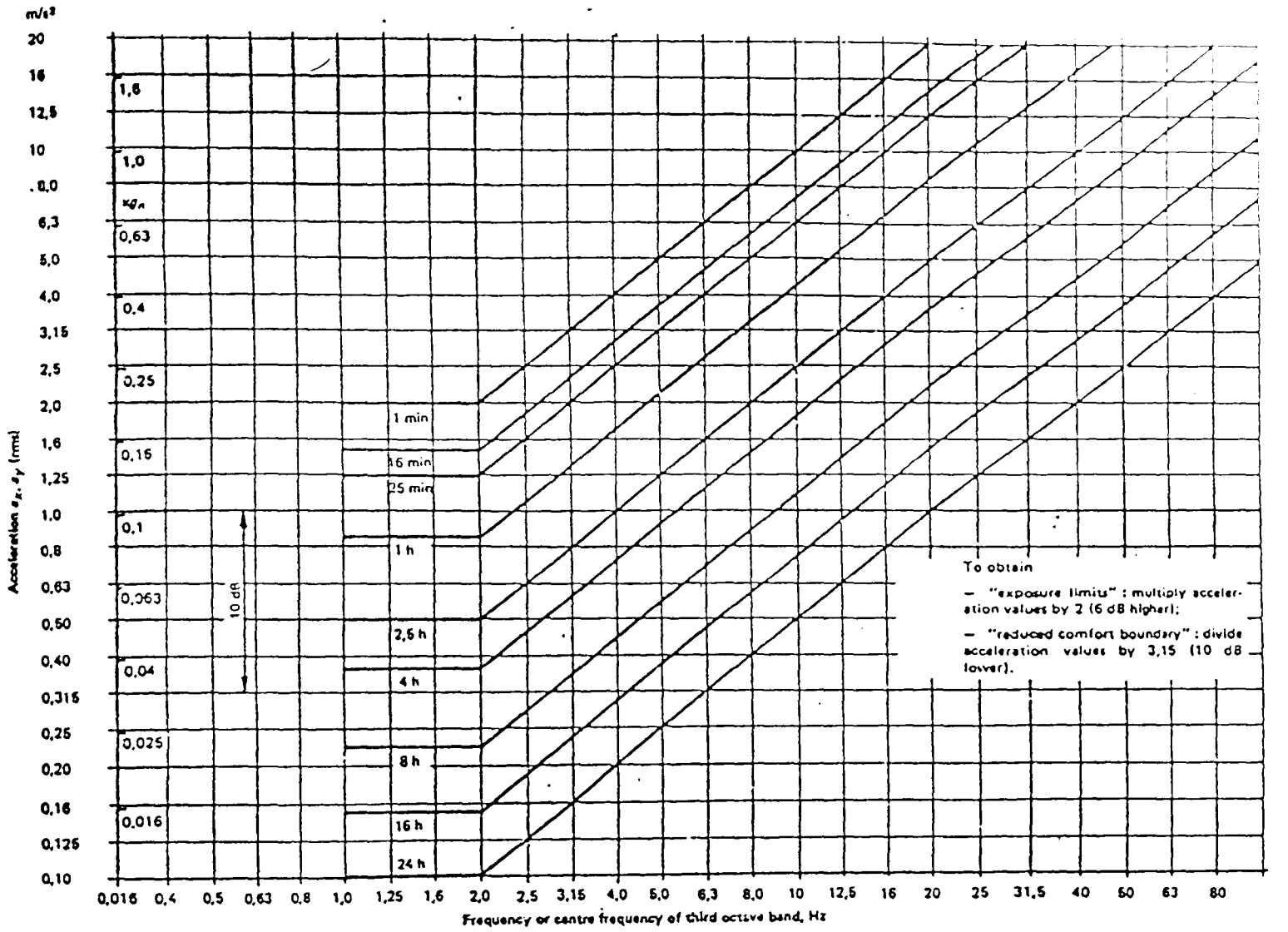

Fig (B-2) Transverse a_x , a_y acceleration limits as a function of frequency and exposure time.

Table (B.3) Human Response Transfer Functions

Vertical Gain:

$$G(S)_v = \frac{15.453\ S(S+5)(S^2+28.3S+2800)(S^2+105S+7570)}{(S+6)(S^2+29.8S+1000)(S^2+39.1S+3800)(S^2+125S+5180)}$$

Fore-aft Gain:

$$G(S)_f = \frac{209S(S+110)}{(S^2+17.6S+125)(S^2+110S+1300)}$$

Side-to-side Gain:

$$G(S)_s = \frac{478S(S+130)(S^2+11.2S+60)(S^2+14.2S+260)}{(S^2+3.33S+17)(S^2+5.5S+140)(S^2+44S+900)(S^2+255S+2500)}$$

where

S is the Laplace transform operator (frequency)

APPENDIX (C)

THE DERIVATION OF SOME OF THE INTEGRATION METHODS

C.1 Central Difference Method:

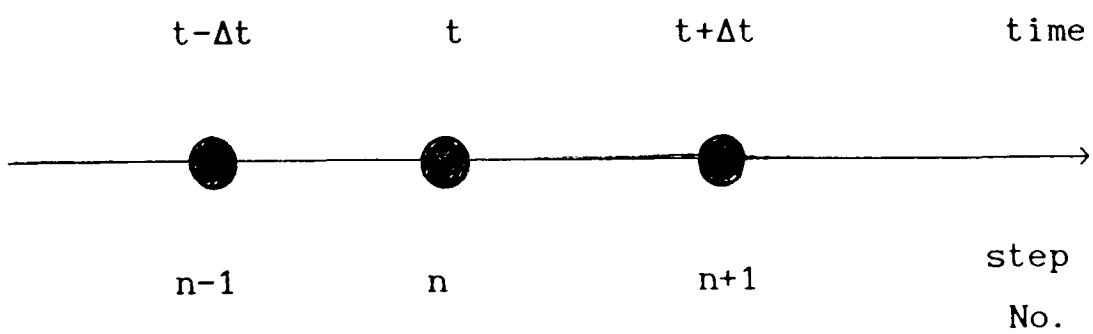

Theory:

Using Finite Difference Method.

$$\dot{\underline{\delta}}_{n-1/2} = \frac{\underline{\delta}_{n} - \underline{\delta}_{n-1}}{\Delta t}$$

$$\dot{\underline{\delta}}_{n+1/2} = \frac{\underline{\delta}_{n+1} - \underline{\delta}_{n}}{\Delta t}$$

Hence

a) $$\dot{\underline{\delta}}_{n} = \frac{\underline{\delta}_{n-1/2} + \underline{\delta}_{n+1/2}}{2}$$

$$= \frac{\underline{\delta}_{n+1} - \underline{\delta}_{n}}{2\Delta t}$$

b) $$\ddot{\underline{\delta}}_n = \frac{\underline{\delta}_{n+1/2} + \underline{\delta}_{n-1/2}}{\Delta t}$$

$$= \frac{\underline{\delta}_{n+1} - 2\underline{\delta}_n + \underline{\delta}_{n-1}}{(\Delta t)^2}$$

Substituting in the following dynamic equations:

$$\underline{M}\,\ddot{\underline{\delta}}_n + \underline{C}\,\dot{\underline{\delta}}_n + \underline{K}\,\underline{\delta}_n = \underline{F}_n$$

then:

$$\underline{M}\left[\frac{\underline{\delta}_{n+1} - 2\underline{\delta}_n + \underline{\delta}_{n-1}}{(\Delta t)^2}\right]$$

$$\underline{C}\left[\frac{\underline{\delta}_{n+1} - \underline{\delta}_n}{2\Delta t}\right] + \underline{K}\,\underline{\delta}_n = \underline{F}_n$$

i.e.

$$\left[\frac{1}{(\Delta t)^2}\underline{M} + \frac{1}{2\Delta t}\underline{C}\right]\underline{\delta}_{n+1}$$

$$+ \left[\underline{K} - \frac{2}{(\Delta t)^2}\underline{M}\right]\underline{\delta}_n$$

$$+ \left[\frac{1}{(\Delta t)^2}\underline{M} + \frac{1}{2\Delta t}\underline{C}\right]\underline{\delta}_{n-1} = \underline{F}_n$$

From

$$\dot{\underline{\delta}}_n = \frac{\underline{\delta}_{n+1} - \underline{\delta}_n}{2\Delta t}$$

$$\underline{\delta}_{n+1} - \underline{\delta}_{n-1} = (2\Delta t)\,\dot{\underline{\delta}}_n \qquad ..a$$

and from

$$\ddot{\underline{\delta}}_n = \frac{\underline{\delta}_{n+1} - 2\underline{\delta}_n + \underline{\delta}_{n-1}}{(\Delta t)^2}$$

$$\underline{\delta}_{n+1} + \underline{\delta}_{n-1} = (\Delta t)^2\,\ddot{\underline{\delta}}_n + 2\underline{\delta}_n \qquad ..b$$

Solving (a), (b) for $\underline{\delta}_{n-1}$, then:

$$\underline{\delta}_{n-1} = \underline{\delta}_{n} - \Delta t\, \dot{\underline{\delta}}_{n} + \frac{(\Delta t)^2}{2}\, \ddot{\underline{\delta}}_{n}$$

Defining:

$$a_o = \frac{1}{(\Delta t)^2}$$

$$a_1 = \frac{1}{2\Delta t}$$

$$a_2 = \frac{2}{(\Delta t)^2} = 2\, a_o$$

$$a_3 = \frac{(\Delta t)^2}{2} = \frac{1}{a_2}$$

then:

$$\underline{Q}_1 = a_o \underline{M} - a_1 \underline{C}$$

$$\underline{Q}_2 = \underline{K} - a_2 \underline{M}$$

$$\underline{Q}_3 = a_o + a_1 \underline{C}$$

$$\underline{\delta}_{n-1} = \underline{\delta}_{n} - \Delta t \dot{\underline{\delta}}_{n} + a_3 \ddot{\underline{\delta}}_{n} \qquad \text{at } n = 0$$

and the matrix equation reduces to:

$$\hat{\underline{M}}\ \underline{\delta}_{n+1} = \underline{F}_n - (\underline{K} - a_2 \underline{M})\underline{\delta}_n - (a_o \underline{M} - a_1 \underline{C})\ \underline{\delta}_{n-1}$$

or

$$\hat{\underline{M}}\ \underline{\delta}_{n+1} = \hat{\underline{F}}_n$$

C.2. The Houbolt Method:

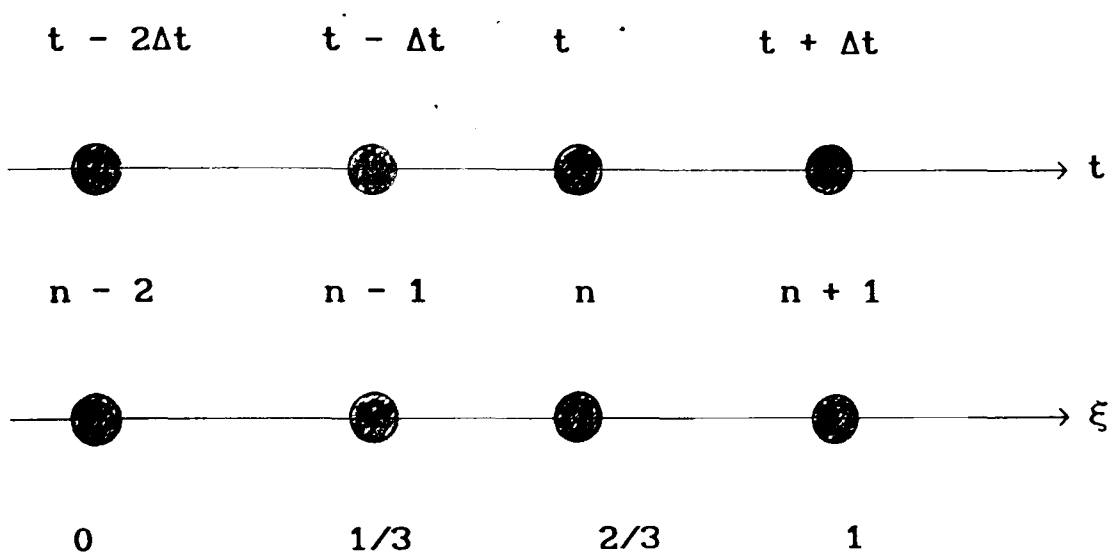

Theory:

Houbolt method is based upon 4 time nodes, as shown above. Instead of using difference equations, let us use intrinsic parameters ξ, where,

$$\xi = \frac{t - t_o}{3\Delta t} \equiv \frac{t_{n+1} - t_{n-2}}{3\Delta t}$$

From intrinsic shape functions, it can be deduced that:

$$f(\xi) = -\frac{1}{2}(\xi - 1)(3\xi - 1)(3\xi - 2)\, f_{n-2} + \frac{9}{2}\xi(\xi - 1)(3\xi - 2)\, f_{n-1} - \frac{9}{2}\xi(\xi - 1)(3\xi - 1)\, f_n + \frac{1}{2}\xi(\xi - 1)(3\xi - 2)\, f_{n+1}$$

i.e

$$f(\xi) = -\frac{1}{2}\left[9\xi^3 - 18\xi^2 + 11\xi - 2\right] f_{n-2}$$

$$+ \frac{9}{2}\left[3\,\xi^3 - 5\,\xi^2 + 2\,\xi\right] f_{n-1}$$

$$- \frac{9}{2}\left[3\,\xi^3 - 4\,\xi^2 + \xi\right] f_n$$

$$+ \frac{1}{2}\left[9\,\xi^3 - 9\,\xi^2 + 2\,\xi\right] f_{n+1}$$

Hence, it can be deduced that:

$$\dot{f}(\xi) = \frac{df}{dt} = \frac{1}{3\Delta t}\,\frac{df}{d\xi}$$

$$= \frac{1}{3\Delta t}\left[-\frac{1}{2}(27\xi^2 - 36\xi + 11)\, f_{n-2}\right.$$

$$+ \frac{9}{2}(9\,\xi^2 - 10\xi + 2)\, f_{n-1}$$

$$- \frac{9}{2}(9\,\xi^2 - 8\,\xi + 1)\, f_n$$

$$\left. + \frac{1}{2}(27\,\xi^2 - 18\xi + 2)\, f_{n+1}\right]$$

and

$$\ddot{f}(\xi) = \frac{d^2f}{dt^2} = \frac{1}{(3\Delta t)^2}\,\frac{d^2f}{d\xi^2}$$

$$= \frac{1}{9(\Delta t)^2}\left[-\frac{1}{2}(59\xi - 36)\, f_{n-2}\right.$$

$$+ \frac{9}{2}(18\xi - 10)\, f_{n-1}$$

$$- \frac{9}{2}(18\xi - 8)\, f_n$$

$$\left. + \frac{1}{2}(54\xi - 18)\, f_{n+1}\right]$$

At $t+\Delta t$, $\xi = 1$

$$\dot{f}(t+\Delta t) = \frac{1}{3\Delta t}\left[- f_{n-2} + \frac{9}{2} f_{n-1} - 9 f_n + \frac{11}{2} f_{n+1}\right]$$

i.e

$$\dot{f}_{n+1} = \frac{1}{6\Delta t}\left[- 2 f_{n-2} + 9 f_{n-1} - 18 f_n + 11 f_{n+1}\right]$$

also

$$\ddot{f}(t+\Delta t) = \frac{1}{9(\Delta t)^2}\left[- 9 f_{n-2} + 36 f_{n-1} - 45 f_n + 18 f_{n+1}\right]$$

i.e

$$\ddot{f}_{n+1} = \frac{1}{(\Delta t)^2}\left[- f_{n-2} + 4 f_{n-1} - 5 f_n + 2 f_{n+1}\right]$$

Similarly, the following approximations can be carried out in the dynamic equations of equilibrium:

$$\ddot{\underline{\delta}}_{n+1} = \frac{1}{(\Delta t)^2}\left[- \underline{\delta}_{n-2} + 4 \underline{\delta}_{n-1} - 5 \underline{\delta}_n + 2 \underline{\delta}_{n+1}\right]$$

$$\dot{\underline{\delta}}_{n+1} = \frac{1}{6\Delta t}\left[- 2 \underline{\delta}_{n-2} + 9 \underline{\delta}_{n-1} - 18 \underline{\delta}_n + 11 \underline{\delta}_{n+1}\right]$$

Substituting at $t+\Delta t$, in

$$\underline{M}\,\ddot{\underline{\delta}}_{n+1} + \underline{C}\,\dot{\underline{\delta}}_{n+1} + \underline{K}\,\underline{\delta}_{n+1} = \underline{F}_{n+1}$$

then

$$\frac{1}{(\Delta t)^2}\,[\underline{M}]\left[- \underline{\delta}_{n-2} + 4 \underline{\delta}_{n-1} - 5 \underline{\delta}_n + 2 \underline{\delta}_{n+1}\right]$$

$$+ \frac{1}{6\Delta t}\,[\underline{C}]\left[- 2 \underline{\delta}_{n-2} + 9 \underline{\delta}_{n-1} - 18 \underline{\delta}_n + 11 \underline{\delta}_{n+1}\right]$$

$$+ \underline{K}\,\underline{\delta}_{n+1} = \underline{F}_{n+1}$$

i.e

$$- \left[\frac{1}{(\Delta t)^2}\,\underline{M} + \frac{1}{6\Delta t}\,\underline{C}\right]\underline{\delta}_{n-2}$$

$$+ \left[\frac{1}{(\Delta t)^2}\,\underline{M} + \frac{3}{2\Delta t}\,\underline{C}\right]\underline{\delta}_{n-1}$$

$$- \left[\frac{5}{(\Delta t)^2}\,\underline{M} + \frac{3}{\Delta t}\,\underline{C}\right]\underline{\delta}_{n}$$

$$+ \left[\frac{2}{(\Delta t)^2}\,\underline{M} + \frac{11}{6\Delta t}\,\underline{C} + \underline{K}\right]\underline{\delta}_{n+1} = \underline{F}_{n+1}$$

Defining:

$$a_o = \frac{2}{(\Delta t)^2} \qquad a_1 = \frac{11}{6\Delta t}$$

$$a_2 = \frac{5}{(\Delta t)^2} \qquad a_3 = \frac{3}{\Delta t}$$

$$a_4 = -2\,a_o \qquad a_5 = -\frac{a_3}{2}$$

$$a_6 = \frac{a_o}{2} \qquad a_7 = \frac{a_3}{9}$$

then:

$$\ddot{\underline{\delta}}_{n+1} = a_o\,\underline{\delta}_{n+1} - a_2\,\underline{\delta}_n - a_4\,\underline{\delta}_{n-1} - a_6\,\underline{\delta}_{n-2} \qquad ..(a)$$

$$\dot{\underline{\delta}}_{n+1} = a_1\,\underline{\delta}_{n+1} - a_3\,\underline{\delta}_n - a_5\,\underline{\delta}_{n-1} - a_7\,\underline{\delta}_{n-2} \qquad ..(b)$$

and the dynamic equations at $t+\Delta t$ will be:

$$\underline{M}\left[a_o\,\underline{\delta}_{n+1} - a_2\,\underline{\delta}_n - a_4\,\underline{\delta}_{n-1} - a_6\,\underline{\delta}_{n-2}\right]$$

$$+\ \underline{C}\left[a_1\,\underline{\delta}_{n+1} - a_3\,\underline{\delta}_n - a_5\,\underline{\delta}_{n-1} - a_7\,\underline{\delta}_{n-2}\right]$$

$$+\ \underline{K}\ \underline{\delta}_{n+1} = \underline{F}_{n+1}$$

i.e

$$\left(\underline{K} + a_o\underline{M} + a_1\,\underline{C}\right)\underline{\delta}_{n+1}$$

$$= \underline{F}_{n+1} + \underline{M}\left(a_2\,\underline{\delta}_n + a_4\,\underline{\delta}_{n-1} + a_6\,\underline{\delta}_{n-2}\right)$$

$$+\ \underline{C}\left(a_3\,\underline{\delta}_n + a_5\,\underline{\delta}_{n-1} + a_7\,\underline{\delta}_{n-2}\right)$$

C.3 Wilson θ Method:

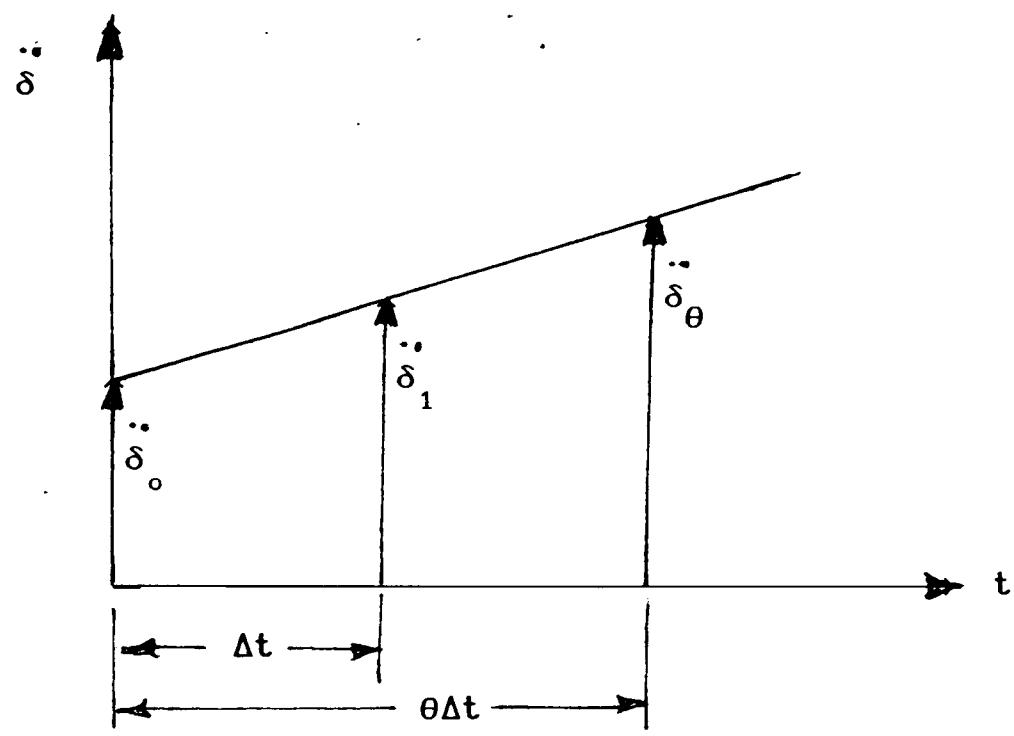

$t_o \qquad t_1 = t_o + \Delta t \qquad t_\theta = t_o + \theta\Delta t \qquad \theta \geq 1$

Theory:

This method is based upon assuming that the acceleration is linear within(t_o, t_θ) when

$$t_\theta = t_o + \theta\Delta t \qquad \theta \geq 1$$

i.e at any time t, where

$$t_o \leq t \leq t_\theta$$

$$\frac{\ddot{\underline{\delta}}(t) - \ddot{\underline{\delta}}(t_o)}{t - t_o} = \frac{\ddot{\underline{\delta}}(t_\theta) - \ddot{\underline{\delta}}(t_o)}{\theta\,\Delta t}$$

Defining $\tau = t - t_o$, then

$$\ddot{\underline{\delta}}(\tau) = \ddot{\underline{\delta}}_o + \frac{\tau}{\theta\Delta t}\left(\ddot{\underline{\delta}}_\theta - \ddot{\underline{\delta}}_o\right)$$

where:

$$\ddot{\underline{\delta}}_o \equiv \ddot{\underline{\delta}}(t_o)$$

$$\ddot{\underline{\delta}}_\theta \equiv \ddot{\underline{\delta}}(t_\theta)$$

Integrating the previous equation w.r.t time,

$$\dot{\underline{\delta}}(\tau) = \int_0^\tau \ddot{\underline{\delta}}(\tau)\, d\tau$$

$$= \dot{\underline{\delta}}_o + \tau\, \ddot{\underline{\delta}}_o + \frac{\tau^2}{2\theta\Delta t}\left(\ddot{\underline{\delta}}_\theta - \ddot{\underline{\delta}}_o\right)$$

Similarly

$$\underline{\delta}(\tau) = \underline{\delta}_o + \tau\, \dot{\underline{\delta}}_o + \frac{\tau^2}{2}\, \ddot{\underline{\delta}}_o + \frac{\tau^3}{6\theta\Delta t}\left(\ddot{\underline{\delta}}_\theta - \ddot{\underline{\delta}}_o\right)$$

i.e

$$\ddot{\underline{\delta}}(t+\tau) = \ddot{\underline{\delta}}(t) + \frac{\tau}{\theta\Delta t}\left[\ddot{\underline{\delta}}(t+\theta\Delta t) - \ddot{\underline{\delta}}(t)\right]$$

$$\dot{\underline{\delta}}(t+\tau) = \dot{\underline{\delta}}(t) + \tau\, \ddot{\underline{\delta}}(t) + \frac{\tau^2}{2\theta\Delta t}\left[\ddot{\underline{\delta}}(t+\theta\Delta t) - \ddot{\underline{\delta}}(t)\right]$$

$$\underline{\delta}(t+\tau) = \underline{\delta}(t) + \tau\, \dot{\underline{\delta}}(t) + \frac{\tau^2}{2}\, \ddot{\underline{\delta}}(t)$$

$$+ \frac{\tau^3}{6\theta\Delta t} \left[\ddot{\underline{\delta}}(t+\theta\Delta t) - \ddot{\underline{\delta}}(t) \right]$$

At $\tau = t + \theta\Delta t$:

$$\dot{\underline{\delta}}(t+\theta\Delta t) = \dot{\underline{\delta}}(t) + \frac{\theta\Delta t}{2} \left[\ddot{\underline{\delta}}(t) + \ddot{\underline{\delta}}(t+\theta\Delta t) \right]$$

and

$$\underline{\delta}(t+\theta\Delta t) = \underline{\delta}(t) + \theta\Delta t\, \dot{\underline{\delta}}(t) + \frac{\theta^2(\Delta t)^2}{6} \left[2\ddot{\underline{\delta}}(t) + \ddot{\underline{\delta}}(t+\theta\Delta t) \right]$$

From the last equation, it can be deduced that:

$$\ddot{\underline{\delta}}(t+\theta\Delta t) = \frac{6}{\theta^2(\Delta t)^2} \left[\underline{\delta}(t+\theta\Delta t) - \underline{\delta}(t) \right] - \frac{6}{\theta\Delta t} \dot{\underline{\delta}}(t) - 2\ddot{\underline{\delta}}(t)$$

and it can therefore be proved that:

$$\dot{\underline{\delta}}(t+\theta\Delta t) = \frac{3}{\theta\Delta t} \left[\underline{\delta}(t+\theta\Delta t) - \underline{\delta}(t) \right] - 2\dot{\underline{\delta}}(t) - \frac{\theta\Delta t}{2} \ddot{\underline{\delta}}(t)$$

Let us assume the load vector to be linearised in that interval,

$$\frac{\underline{F}(t+\theta\Delta t) - \underline{F}(t)}{\theta\Delta t} = \frac{\underline{F}(t+\Delta t) - \underline{F}(t)}{\Delta t}$$

i.e.

$$\boxed{\underline{F}(t+\theta\Delta t) = \underline{F}(t) + \theta \left[\underline{F}(t+\Delta t) - \underline{F}(t)\right]}$$

Substituting in the dynamic equations of equilibrium at $t+\theta\Delta t$

i.e.

$$\underline{M}\,\ddot{\underline{\delta}}\,(t+\theta\Delta t) + \underline{C}\,\dot{\underline{\delta}}\,(t+\theta\Delta t) + \underline{K}\,\underline{\delta}\,(t+\theta\Delta t) = \underline{F}\,(t+\theta\Delta t)$$

then

$$\underline{M}\left[\frac{6}{\theta^2(\Delta t)^2}\left[\underline{\delta}\,(t+\theta\Delta t) - \underline{\delta}\,(t)\right] - \frac{6}{\theta\Delta t}\,\dot{\underline{\delta}}(t) - 2\,\ddot{\underline{\delta}}(t)\right]$$

$$+ \underline{C}\left[\frac{3}{\theta\Delta t}\left[\underline{\delta}\,(t+\theta\Delta t) - \underline{\delta}\,(t)\right] - 2\,\dot{\underline{\delta}}(t) - \frac{\theta\Delta t}{2}\,\ddot{\underline{\delta}}(t)\right]$$

$$+ \underline{K}\,\underline{\delta}\,(t+\theta\Delta t) = \underline{F}\,(t+\theta\Delta t)$$

Let

$$a_o = \frac{6}{\theta^2(\Delta t)^2} \qquad a_1 = \frac{3}{\theta\Delta t}$$

$$a_2 = 2a_1 \qquad a_3 = \frac{\theta\Delta t}{2}$$

then

$$(\underline{K} + a_o\underline{M} + a_1\underline{C})\ \underline{\delta}(t+\theta\Delta t)$$

$$= \underline{F}\ (t+\theta\Delta t) + \underline{M}\left[a_o\ \underline{\delta}\ (t) + a_2\ \dot{\underline{\delta}}(t) + 2\ \ddot{\underline{\delta}}(t)\right]$$

$$+ \underline{C}\left[a_1\ \underline{\delta}\ (t)\right] + 2\ \dot{\underline{\delta}}(t) + a_3\ \dot{\underline{\delta}}(t)\Big]$$

or

$$\boxed{\hat{\underline{K}}\ \underline{\delta}\ (t+\theta\Delta t) = \underline{F}\ (t+\theta\Delta t)}$$

Evaluation of $\underline{\delta}\ (t+\Delta t), \dot{\underline{\delta}}\ (t+\Delta t), \ddot{\underline{\delta}}\ (t+\Delta t)$:

with $\tau = \Delta t$

$$\ddot{\underline{\delta}}\ (t+\Delta t) = \ddot{\underline{\delta}}\ (t) + \frac{1}{\theta}\left[\ddot{\underline{\delta}}\ (t+\theta\Delta t) - \ddot{\underline{\delta}}(t)\right]$$

$$= \ddot{\underline{\delta}}\ (t) + \frac{6}{\theta^3(\Delta t)^2}\left[\underline{\delta}\ (t+\theta\Delta t) - \underline{\delta}\ (t)\right]$$

$$- \frac{6}{\theta^2\Delta t}\ \dot{\underline{\delta}}(t) - \frac{3}{\theta}\ \ddot{\underline{\delta}}\ (t)$$

Defining:

$$a_4 = \frac{6}{\theta^3(\Delta t)^2} = \frac{a_o}{\theta}$$

$$a_5 = -\frac{6}{\theta^2\Delta t} = \frac{-a_2}{\theta} \qquad a_6 = 1 - \frac{3}{\theta}$$

then

$$\boxed{\ddot{\underline{\delta}}\,(t+\Delta t) = a_4\left[\underline{\delta}\,(t+\theta\Delta t) - \underline{\delta}\,(t)\right] + a_5\dot{\underline{\delta}}\,(t) + a_6\,\ddot{\underline{\delta}}\,(t)} \quad \ldots\ldots(a)$$

Similarly with $\theta = 1$, $\tau = \Delta t$:

$$\dot{\underline{\delta}}\,(t+\Delta t) = \dot{\underline{\delta}}\,(t) + \Delta t\,\ddot{\underline{\delta}}\,(t) + \frac{\Delta t}{2}\left[\ddot{\underline{\delta}}\,(t+\Delta t) - \ddot{\underline{\delta}}(t)\right]$$

$$= \dot{\underline{\delta}}\,(t) + \frac{\Delta t}{2}\left[\ddot{\underline{\delta}}\,(t+\Delta t) + \ddot{\underline{\delta}}(t)\right]$$

and

$$\underline{\delta}\,(t+\Delta t) = \underline{\delta}\,(t) + \Delta t\,\dot{\underline{\delta}}\,(t) + \frac{(\Delta t)^2}{6}\left[\ddot{\underline{\delta}}\,(t+\Delta t) + 2\,\ddot{\underline{\delta}}(t)\right]$$

Defining

$$a_7 = \frac{\Delta t}{2} \qquad a_8 = \frac{(\Delta t)^2}{6}$$

then

$$\boxed{\dot{\underline{\delta}}\,(t+\Delta t) = \dot{\underline{\delta}}\,(t) + a_7\left[\ddot{\underline{\delta}}\,(t+\Delta t) + \ddot{\underline{\delta}}(t)\right]} \quad \ldots\ldots\ldots(b)$$

$$\boxed{\underline{\delta}\,(t+\Delta t) = \underline{\delta}\,(t) + \Delta t\,\dot{\underline{\delta}}\,(t) + a_8\left[\ddot{\underline{\delta}}\,(t+\Delta t) + 2\,\ddot{\underline{\delta}}(t)\right]} \quad \ldots\ldots(c)$$

C.4 Lagrangian Weighted-Residual Scheme:

In this method we consider the time as time-nodes and by the following steps and for case of 3-time node element an intrinsic time coordinates (ξ) can be used, such that:

$$\xi = \frac{t - t_1}{t_3 - t_1} \qquad \frac{d\xi}{dt} = \frac{1}{t_3 - t_1}$$

Hence, any parameter f(t) can be interpolated in terms of its nodal values at the three time nodes as follows:

$$\underline{f}(t) = N_1(\xi)\ \underline{f}_1 + N_2(\xi)\ \underline{f}_2 + N_3(\xi)\ \underline{f}_3$$

where:

$$N_1(\xi) = (1-\xi)(1-2\xi)$$

$$N_2(\xi) = 4\xi(1-\xi)$$

$$N_3(\xi) = -\xi(1-2\xi)$$

Hence,

$$\underline{F}(t) = N_1(\xi)\ \underline{F}_1 + N_2(\xi)\ \underline{F}_2 + N_3(\xi)\ \underline{F}_3$$

and

$$\underline{\delta}(t) = N_1(\xi)\ \underline{\delta}_1 + N_2(\xi)\ \underline{\delta}_2 + N_3(\xi)\ \underline{\delta}_3 \qquad (1.C)$$

$$\dot{\underline{\delta}}(t) = \left[N_1'(\xi)\ \underline{\delta}_1 + N_2'(\xi)\ \underline{\delta}_2 + N_3'(\xi)\ \underline{\delta}_3\right] / 2\Delta t \qquad (2.C)$$

$$\ddot{\underline{\delta}}(t) = \left[N_1''(\xi)\ \underline{\delta}_1 + N_2''(\xi)\ \underline{\delta}_2 + N_3''(\xi)\ \underline{\delta}_3\right] / (2\Delta t)^2 \qquad (3.C)$$

Substituting equations (1.C), (2.C), and (3.C) in the dynamic equations:

$$\underline{M}\,\ddot{\underline{\delta}}(t) + \underline{C}\,\dot{\underline{\delta}}(t) + \underline{K}\,\underline{\delta}(t) = \underline{F}(t)$$

the following residual vector can be defined:

$$\underline{R}(\xi) = \underline{M}\,\ddot{\underline{\delta}}(t) + \underline{C}\,\dot{\underline{\delta}}(t) + \underline{K}\,\underline{\delta}(t) - \underline{F}(t)$$

Using the standard weighted-Residual expression:

$$\int_0^1 W(\xi)\,\underline{R}(\xi)\,d\xi = 0$$

i.e.

$$\underline{Q}_1\underline{\delta}_1 + \underline{Q}_2\underline{\delta}_2 + \underline{Q}_3\underline{\delta}_3 = \hat{\underline{F}} \qquad (4.C)$$

where:

$$\underline{Q}_i = \int_0^1 W(\xi)\,P_i\,d\xi$$

$$= \frac{1}{(\Delta t)^2}\,\alpha_i\underline{M} + \frac{1}{\Delta t}\,\beta_i\,\underline{C} + \gamma_i\underline{K}$$

and

$$\alpha_i = \frac{\int_0^1 W(\xi)\,N_i''\,d\xi}{2\int_0^1 W(\xi)}$$

$$\beta_i = \frac{\int_0^1 W(\xi)\, N_i'\, d\xi}{2\int_0^1 W(\xi)}$$

$$\gamma_i = \frac{\int_0^1 W(\xi)\, N_i\, d\xi}{2\int_0^1 W(\xi)}$$

$$\hat{\underline{F}} = \int_0^1 W(\xi)\left[N_1 \underline{F}_1 + N_2 \underline{F}_2 + N_3 \underline{F}_3 \right] d\xi$$

$$= \gamma_1 \underline{F}_1 + \gamma_2 \underline{F}_2 + \gamma_3 \underline{F}_3$$

The values of β, and γ are given in Table (1-C).

Table (1-C) Values of β, and γ.

NO.	1	2	3	4	5	6	7	8
β	0	0	1	1/6	1/10	4/5	1/12	1/4
γ	− 1/2	1/2	1/2	1/2	1/2	1/2	1/2	1/2

$$\alpha_1 = 1 \quad ; \quad \alpha_2 = -2 \quad ; \quad \alpha_3 = 1$$

$$\beta_1 = \gamma - 1 \quad ; \quad \beta_2 = 1 - 2\gamma \quad ; \quad \beta_3 = \gamma$$

$$\gamma_1 = 1/2 + \beta - \gamma \; ; \quad \gamma_2 = 1/2 - 2\beta + \gamma \quad ; \quad \gamma_3 = \beta$$

For a time marching scheme equation (4.C) forms the basic of the three-node recurrence formula. Hence δ at node (i+1) can be obtained from:

$$\underline{Q}_3 \, \underline{\delta}_{(i+1)} = \underline{F} - \underline{Q}_1 \underline{\delta}_{(i-1)} - \underline{Q}_2 \underline{\delta}_i$$

The following expressions can be employed to calculate $\dot{\underline{\delta}}_{(i+1)}$ and $\ddot{\underline{\delta}}_{(i+1)}$:

$$\dot{\underline{\delta}}_{(i+1)} = \frac{1}{2\,\Delta t} \left[\underline{\delta}_{(i-1)} - 4\,\underline{\delta}_i + 3\,\underline{\delta}_{(i+1)} \right] \qquad (5.C)$$

and

$$\ddot{\underline{\delta}}_{(i+1)} = \frac{1}{\Delta t^2} \left[\underline{\delta}_{(i-1)} - 2\,\underline{\delta}_i + \underline{\delta}_{(i+1)} \right]$$

At the start of the scheme, a fictitious node at $t = -\Delta t$ is assumed, such that:

$$\underline{\delta}(t) = N_1 \, \underline{\delta}_{-1} + N_2 \, \underline{\delta}_o + N_3 \, \underline{\delta}_1$$

$$\dot{\underline{\delta}}(t) = \frac{1}{2\,\Delta t} \left[N_1' \, \underline{\delta}_{-1} + N_2' \, \underline{\delta}_o + N_3' \, \underline{\delta}_1 \right]$$

$$= \frac{1}{2\,\Delta t} \left[(4\xi - 3) \, \underline{\delta}_{-1} + 4\,(1 - 2\xi) \, \underline{\delta}_o + (4\xi - 1) \, \underline{\delta}_1 \right]$$

Hence, for $\xi = 0.5$

$$\dot{\underline{\delta}}_o = \dot{\underline{\delta}}(0.5) = \frac{1}{2\,\Delta t}\left[\underline{\delta}_1 - \underline{\delta}_{-1}\right]$$

i.e.

$$\underline{\delta}_{-1} = \underline{\delta}_1 + 2\,\Delta t\,\dot{\underline{\delta}}_o$$

Substituting in equation (4.C), it can be deduced that:

$$\underline{Q}_3\underline{\delta}_3 = \hat{\underline{F}} - \underline{Q}_1\left(\underline{\delta}_1 - 2\,\Delta t\,\dot{\underline{\delta}}_o\right) - \underline{Q}_2\underline{\delta}_o$$

Hence,

$$\left(\underline{Q}_3 + \underline{Q}_1\right)\underline{\delta}_1 = \hat{\underline{F}} + 2\,\Delta t\,\underline{Q}_1\,\dot{\underline{\delta}}_o - \underline{Q}_2\underline{\delta}_o \qquad (6.C)$$

Usually, $\underline{\delta}_o$, $\dot{\underline{\delta}}_o$ are defined as the initial conditions, equation (6.C) can therefore be used for the starting of the scheme. Then equation (4.C) can further be employed for further time increments.

Notice that:

> *The Centeral Difference is the special case of Lagrangian method with* $\beta = 0$, $\gamma = 0.5$

C.5 Hermitian Weighted - Residual Sscheme:

The 2 - nodes time element can be defined as follows:

$$\underline{\delta}_t = g_1(t)\underline{\delta}_1 + h_1\,\underline{\delta}_1 + g_2(t)\underline{\delta}_2 + h_2\underline{\delta}_2$$

where:

$$g_1 = 2\,\xi^3 - 3\,\xi^2 + 1$$

$$g_2 = -\,2\,\xi^3 + 3\,\xi^2$$

$$h_1 = \Delta t\,(\xi^3 - 2\,\xi^2 + \xi) \qquad ;\ \xi = (t-t_1)/\Delta t$$

$$h_2 = \Delta t\,(\xi^3 - \xi^2) \qquad ;\ \Delta t = (t_2 - t_1)$$

and

$$\underline{F}_{(t)} = N_1\,\underline{F}_1 + N_2\,\underline{F}_2$$

$$= (1-\xi)\,\underline{F}_1 + \xi\,\underline{F}_2$$

N_1 , N_2... are the shape functions.

Hence, the residual vector can be expressed for such a case as:

$$\underline{R}(\xi) = \underline{P}_1\,\underline{\delta}_1 + \underline{P}_2\,\underline{\delta}_2 - \underline{Q}_1\,\underline{\delta}_1 + \underline{Q}_2\,\underline{\delta}_2 - \underline{F}$$

where:

$$\underline{P}_i = \frac{1}{\Delta t^2}\,g_i''\,\underline{M} + \frac{1}{\Delta t}\,g_i'\,\underline{C} + g_i\,\underline{K}$$

$$\underline{Q}_i = \frac{1}{\Delta t^2}\,h_i''\,\underline{M} + \frac{1}{\Delta t}\,h_i'\,\underline{C} + h_i\,\underline{K}$$

Using the Galerkin weighted-residual functions, it can be shown that:

$$\int_0^1 g_2(\xi)\,\underline{R}(\xi)\,d\xi = 0$$

$$\int_0^1 h_2(\xi)\ \underline{R}(\xi)\ d\xi = 0$$

By integrating the above Galerkin weighted-residual expression the following matrix equation are obtained:

$$\underline{R}_{11}\ \underline{\delta}_1 + \underline{R}_{12}\ \underline{\delta}_1 + \underline{S}_{11}\underline{\delta}_2 + \underline{S}_{12}\underline{\delta}_2 = \hat{\underline{F}}_1$$

$$\underline{R}_{21}\ \underline{\delta}_1 + \underline{R}_{22}\ \underline{\delta}_1 + \underline{S}_{21}\underline{\delta}_2 + \underline{S}_{22}\underline{\delta}_2 = \hat{\underline{F}}_2$$

where:

$$\underline{R}_{11} = \frac{1.2}{(\Delta t)^2}\ \underline{M} - \frac{0.5}{\Delta t}\ \underline{C} + \frac{9}{70}\ \underline{K}$$

$$\underline{S}_{11} = -\ \frac{1.2}{(\Delta t)^2}\ \underline{M} + \frac{0.5}{\Delta t}\ \underline{C} + \frac{13}{35}\ \underline{K}$$

$$\underline{R}_{12} = \Delta t\ \left[\ \frac{0.1}{(\Delta t)^2}\ \underline{M} - \frac{0.1}{\Delta t}\ \underline{C} + \frac{13}{420}\ \underline{K}\ \right]$$

$$\underline{S}_{12} = \Delta t\ \left[\ \frac{1.1}{(\Delta t)^2}\ \underline{M} + \frac{0.1}{\Delta t}\ \underline{C} - \frac{11}{210}\ \underline{K}\ \right]$$

$$\underline{R}_{21} = -\ \frac{0.1}{(\Delta t)^2}\ \underline{M} + \frac{0.1}{\Delta t}\ \underline{C} - \frac{13}{420}\ \underline{K}$$

$$\underline{S}_{21} = \frac{0.1}{(\Delta t)^2}\ \underline{M} - \frac{0.1}{\Delta t}\ \underline{C} - \frac{17}{210}\ \underline{K}$$

$$\underline{R}_{22} = \Delta t\ \left[\ \frac{1}{30(\Delta t)^2}\ \underline{M} + \frac{1}{60\ \Delta t}\ \underline{C} - \frac{1}{140}\ \underline{K}\ \right]$$

$$\underline{S}_{22} = \Delta t\ \left[-\ \frac{1}{15(\Delta t)^2}\ \underline{M} + \frac{1}{105}\ \underline{K}\ \right]$$

$$\hat{\underline{F}}_1 = \frac{3}{20}\ \underline{F}_1 + \frac{7}{20}\ \underline{F}_2$$

$$\hat{\underline{F}}_2 = -\frac{1}{20}\underline{F}_1 - \frac{1}{20}\underline{F}_2$$

Hence, the time marching equation can be written as follows:

$$\begin{bmatrix} \underline{S}_{11} & \underline{S}_{12} \\ \underline{S}_{21} & \underline{S}_{22} \end{bmatrix} \begin{bmatrix} \underline{\delta}_{p+1} \\ \underline{\delta}_{p+1} \end{bmatrix} = \begin{bmatrix} \hat{\underline{F}}_1 \\ \hat{\underline{F}}_2 \end{bmatrix} - \begin{bmatrix} \underline{R}_{11} & \underline{R}_2 \\ \underline{R}_{21} & \underline{R}_{22} \end{bmatrix} \begin{bmatrix} \underline{\delta}_p \\ \underline{\delta}_p \end{bmatrix}$$

where:

$$P = 0, 1, 2, \ldots\ldots$$

The above equations are solvable for initial conditions $\underline{\delta}_o$, $\dot{\underline{\delta}}_o$ without any modification.

APPENDIX (D)

THE DERIVATION OF TWO ANALYTICAL SOLUTION

D.1 The One Degree of Freedom Analytical Solution:

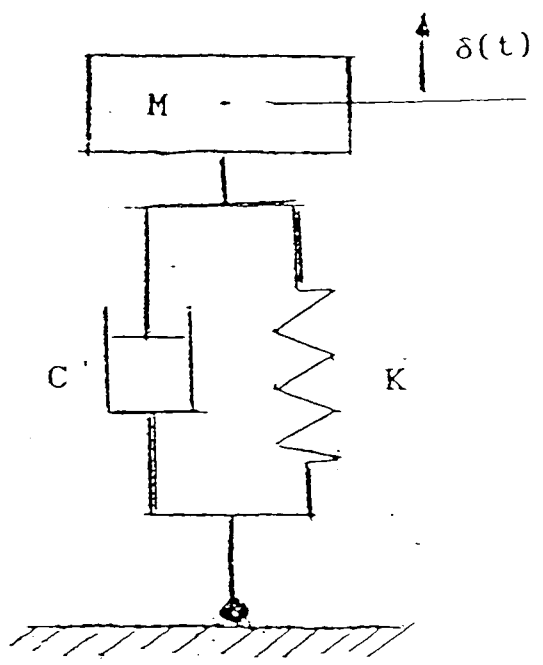

$F(t) = F_o \sin \omega t$

Defining:

$$\xi = \frac{C}{2M} / \omega_n = \frac{C}{2M} / \sqrt{\frac{K}{M}}$$

$$= \frac{C}{2\sqrt{KM}}$$

$$\frac{C}{2M} = \xi \omega_n$$

$$\delta(t)_{free} = e^{-\xi \omega_n t} \left[C_1 \sin \left(\sqrt{1-\xi^2}\ \omega_n t \right) + C_2 \cos \left(\sqrt{1-\xi^2}\ \omega_n t \right) \right]$$

For

$$M\ \ddot{\delta}(t) + C\ \dot{\delta}(t) + K\ \delta(t) = F_o \sin(\omega t)$$

$$\delta(t)_{forced} = \frac{F_o}{\sqrt{(K - M\omega^2)^2 + (C\omega)^2}} \sin(\omega t - \Phi)$$

$$\Phi = \text{ATAN2}\ (C\omega\ ,\ K - M\omega^2)$$

$$\Omega = \sqrt{1 - \xi^2}\ \omega_n$$

$$\delta(t) = e^{-\xi\omega_n t}\left[C_1 \sin(\Omega t) + C_2 \cos(\Omega t) \right] + \frac{F_o}{\sqrt{(K - M\omega^2)^2 + (C\omega)^2}} \sin(\omega t - \Phi) \quad ..a$$

$$\dot{\delta}(t) = -\xi\omega_n e^{-\xi\omega_n t}\left[C_1 \sin(\Omega t) + C_2 \cos(\Omega t) \right] + \Omega e^{-\xi\omega_n t}\left[C_1 \cos(\Omega t) + C_2 \sin(\Omega t) \right] + \frac{F_o}{\sqrt{(K - M\omega^2)^2 + (C\omega)^2}} \sin(\omega t - \Phi) \quad ..b$$

At $\delta(0) = 0$ equation (a) becomes:

$$C_2 + \frac{F_o}{\sqrt{(K - M\omega^2)^2 + (C\omega)^2}} \sin(-\Phi) = 0$$

$$C_2 = \frac{F_o}{\sqrt{(K - M\omega^2)^2 + (C\omega)^2}} \sin(\Phi)$$

$$= \delta_o \sin \Phi$$

where:

$$\delta_o = \frac{F_o}{\sqrt{(K - M\omega^2)^2 + (C\omega)^2}}$$

and at $\delta(0) = 0$ equation (b) becomes:

$$C_2(-\xi\omega_n) + C_1\Omega + \omega\delta_o \cos\Phi = 0 \qquad ..c$$

Substituting C_2 in (c) to obtain C_1:

$$C_1 = \frac{\delta_o}{\Omega}\left[\xi\omega_n \sin\Phi - \omega\cos\Phi\right]$$

For the special case of undamped system C = 0

$$\xi = 0$$

$$\Omega = \omega_n = \sqrt{\frac{K}{M}}$$

$$\Phi = \tan^{-1} 0 = 0$$

$$\delta_o = \hat{\delta}_o = \frac{F_o}{K - M\omega^2}$$

equation (a) becomes:

$$\delta(t) = C_1 \sin(\omega_n t) + C_2 \cos(\omega_n t) \qquad ..d$$

$$+ \hat{\delta}_o \sin(\omega t)$$

$$\dot{\delta}(t) = \omega_n C_1 \cos(\omega_n t) - \omega_n C_2 \sin(\omega_n t)$$

$$+ \omega \hat{\delta}_o \cos(\omega t) \qquad ..E$$

At $\delta(0) = 0$ from equation (d) :

$C_2 = 0$

Substituting in equation (E) to obtain C_1

$$C_1 = - \frac{\omega}{\omega_n} \delta_o$$

Hence

$$\delta(t) = \hat{\delta}_o \left[\sin(\omega t) - \frac{\omega}{\omega_n} \sin(\omega_n t) \right]$$

$$\dot{\delta}(t) = \omega \hat{\delta}_o \left[\cos(\omega t) - \cos(\omega_n t) \right]$$

$$\ddot{\delta}(t) = M^{-1} \left[F_o \sin(\omega t) - K \delta(t) \right]$$

D.2 The Two Degree of Freedom Analytical Solution:

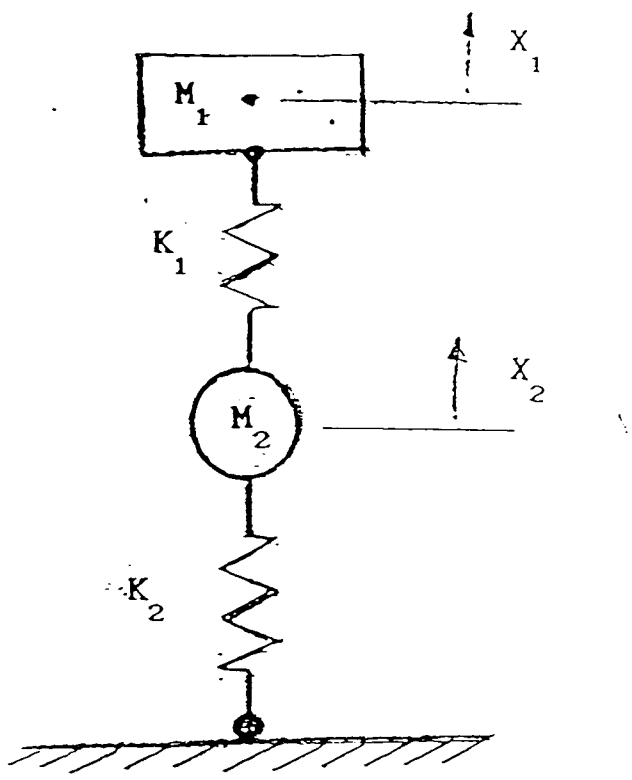

The system has two equations of motion can be shown as follows:

$$M_1 \ddot{X}_1 + K_1 (X_1 - X_2) = F_1 \qquad (a)$$

$$M_2 \ddot{X}_2 + K_1 (X_2 - X_1) + K_2 X_2 = F_2 \qquad (b)$$

Let

$$X = \hat{X} \cos \omega t \qquad (c)$$

hence

$$\ddot{X} = - \omega^2 \hat{X} \cos \omega t \qquad (d)$$

Substituting equations (c), and (d) into equations (a), and (b) it can be deduced that:

$$\left[K_1 - M_1 \omega^2 \right] \hat{X}_1 - K_1 \hat{X}_2 = \hat{F}_1 \qquad (e)$$

$$- K_1 \hat{X}_1 + \left[K_2 + K_1 - M_2 \omega^2\right] \hat{X}_2 = \hat{F}_2 \qquad (f)$$

Equations (e), and (f) can be written in the following matrix form:

$$\begin{bmatrix} K_1 - M_1\omega^2 & -K_1 \\ -K & K_2 + K_1 - M_2\omega^2 \end{bmatrix} \begin{bmatrix} \hat{X}_1 \\ \hat{X}_2 \end{bmatrix} = \begin{bmatrix} \hat{F}_1 \\ \hat{F}_2 \end{bmatrix}$$

Let $\omega^2 = \zeta$ it can be prove that:

$$M_1 M_2 \zeta^2 - \left[K_1 M_2 - M_1\left[K_1 + K_2\right]\right] \zeta + K_1 K_2 = 0$$

or

$$\zeta^2 - \left[\frac{K_1}{M_1} + \frac{K_1 + K_2}{M_2}\right] \zeta + \left[\frac{K_1 K_2}{M_1 M_2}\right] = 0$$

Hence

$$\zeta_{1,2} = \frac{1}{2}\left\{\left[\frac{K_1}{M_1} + \frac{K_1 + K_2}{M_2}\right] \pm \sqrt{\left[\frac{K_1}{M_1} + \frac{K_1 + K_2}{M_2}\right]^2 - 4\left[\frac{K_1 K_2}{M_1 M_2}\right]}\right\}$$

APPENDIX E

THE PROGRAMMING PACKAGE

E.1 INTRODUCTION:

The present package is entitled 'Ride Analysis of Tank Suspension System' (RATS SYSTEM). This system is designed to deal with the ride analysis of general off-road vehicles, which may be tracked, semi-tracked, or wheeled. Different types of suspension elements, such as the classical mass-spring-dashpot element, a torsion bar (spring) combined with rotary vane damper, telescopic damper, hydrogas unit damper can be analysed depending on the package own library routines. The ride analysis can be carried out on different types of soil; rigid, sandy, and organic soil. The main package structure is almost independent of computer type because of standard FORTRAN implementation. The package is working in the VAX computer, and it has already been converted to work on work stations such as Sun or Digital work stations.

The package facilities are summarised in the following sections.

E.2 THE PACKAGE STRUCTURE:

The package is built to be simple and user-friendly. The structure of the master command file is shown in Figure E.1. Once the command file is activated using RATS the first menu will be displayed. There is no possibility of accepting input data error, because the program will accept only the correct parameters suitable for the present menu before displaying the following menu. In Figure E.2 one of the solvers is selected to demonstrate other package menus.

The basic facilities of the package can be summarised as follows:

a) Vehicle Simulation:

Most of the widely used types of suspension systems have been modelled in this work. These types are used for tanks, cars, tractors, semi-tracked vehicles, earth moving machines, lorries, etc. The suspension assemblies and elements the models of which are available in the package are:

(i) A spring and damper colinear with the wheel centre.

(ii) A transverse torsion bar directly operated by a longitudinal wheel arm plus a telescopic damper.

(iii) A transverse torsion bar directly operated by a longitudinal wheel arm plus a rotary-vane damper.

(iv) Hydrogas units.

(vi) The track.

Both linear and non-linear modelling are available. The types of non-linearities existing in the package are:

1. Non-linear characteristics and/or blow-off function of the main dampers.

2. Non-linear characteristics of the main springs or torsion bars.

3. Non-linearity originating from the bump stop action.

4. Non-linear characteristics of the tyre or the road wheels.

5. Non-linearity resulting from large deflection consideration.

6. Non-linearity arising from wheel-ground separation.

b) Vehicle-Terrain Interaction:

The simplest and most accurate tyre models have been included in the programming package, namely, the point contact tyre model and the extended contact tyre model. Different kinds of soil are included such as sandy, organic in addition to the rigid soil.

C) Time Response:

To enable the user to control the numerical instability in the results which may occur during the simulation of the off-road vehicles, the package includes various numerical integration subroutines suitable for the solution of linear and non-linear systems of second order differential equations. The methods employed in the package can be summarised as follows:

1. The Wilson θ method.
2. The Houbolt method.
3. The Central difference method.
4. The Hermitian weighted residual method.
5. Lagrangian weighted residual method.
6. Runge-Kutta scheme.
7. Steady state solution.

d) Human Tolerance:

Three tolerance criteria have been employed to assess the ride performance or ride quality of vehicles. These three criteria are the absorbed power, the ISO 2631, and the 'K' factor.

e) Elements Library:

A comprehensive range of elements are used in the package, the description of the suspension system assemblies can be shown as:

Element Type No.	Description
1	Wheeled vehicles assembly.
2	Hydrogas assembly.
3	Tracked vehicles assembly (with telescopic dampers).
4	Tracked vehicles assembly(with rotary-vane dampers).

E.3 INPUT DATA FILE:

Three types of coordinate systems (illustrated in Figure 3.1) are used for the input of the necessary dimensions of the suspension system, and against which the output results can be obtained. Figure E.3 shows a general form of a 2-D data required for a tracked vehicle.

The general format of the input data can be summarised as follows:

E.3.1 Sprung Mass Data:

The sprung mass is the vehicle body or the main frame, and the necessary data of the sprung mass are:

1. Sprung mass M_s.
2. Sprung mass moment of inertia about the X-axis I_{xx}.
3. Sprung mass moment of inertia about the Y-axis I_{yy}.

4. Vehicle C.G. coordinate X_o, Y_o, Z_o (if X, Y, Z are based on C.G. X_o, Y_o, Z_o are zeros).

E.3.2 **Unsprung Mass Data:**

The unsprung mass consists of a number of wheel assemblies. The necessary data of the unsprung mass are:

1. Number of wheel assemblies N.

2. Coordinates of common points with the sprung mass. For the common point of the main spring or the torsion bar, the coordinates X, Y, Z, and the common point of the main damper, the coordinates X_C, Y_C, Z_C, the road wheel or tyre centre coordinate Z_T are required.

3. Linear main spring and damper coefficients K, C. For non-linear characteristics of the spring or damper, the data are in the form of force-displacement and force-velocity tables respectively.

4. Road wheel diameter D_T and width b, track thickness t, track width T_w, and the track stiffness K_{TT}.

5. Road wheel arm length L_o and distance of the torsion bar from the point of attachment of the damper linkage to the arm L_2.

6. Four-bar linkage transmission ratio λ, and feeler stiffness K_f, length L_f, and angle A_f.
7. Linear stiffness and damper coefficients of the tyre K_T, C_T.

E.3.3 **Terrain Data:**

The terrain profile data are required in the form of horizontal distance, and corresponding elevation. The number of data point is required, and any arbitrary tabulated terrain data are acceptable.

Figure E.4 shows the actual computer listing of the input data file, shown annotated in Figure E.3, which represents a 2-D case of an existing off-road tracked vehicle.

E.4 OUTPUT DATA:

The output data is available in analytical and/or graphical form. The displacement, velocity, and acceleration for each degree of freedom and the ride evaluation by the absorbed power, the ISO 2631, or 'K' factor are the output of the program. The output can be reduced to any degree, as required by the package user. A listing of an output file illustrated in Figure E.5.

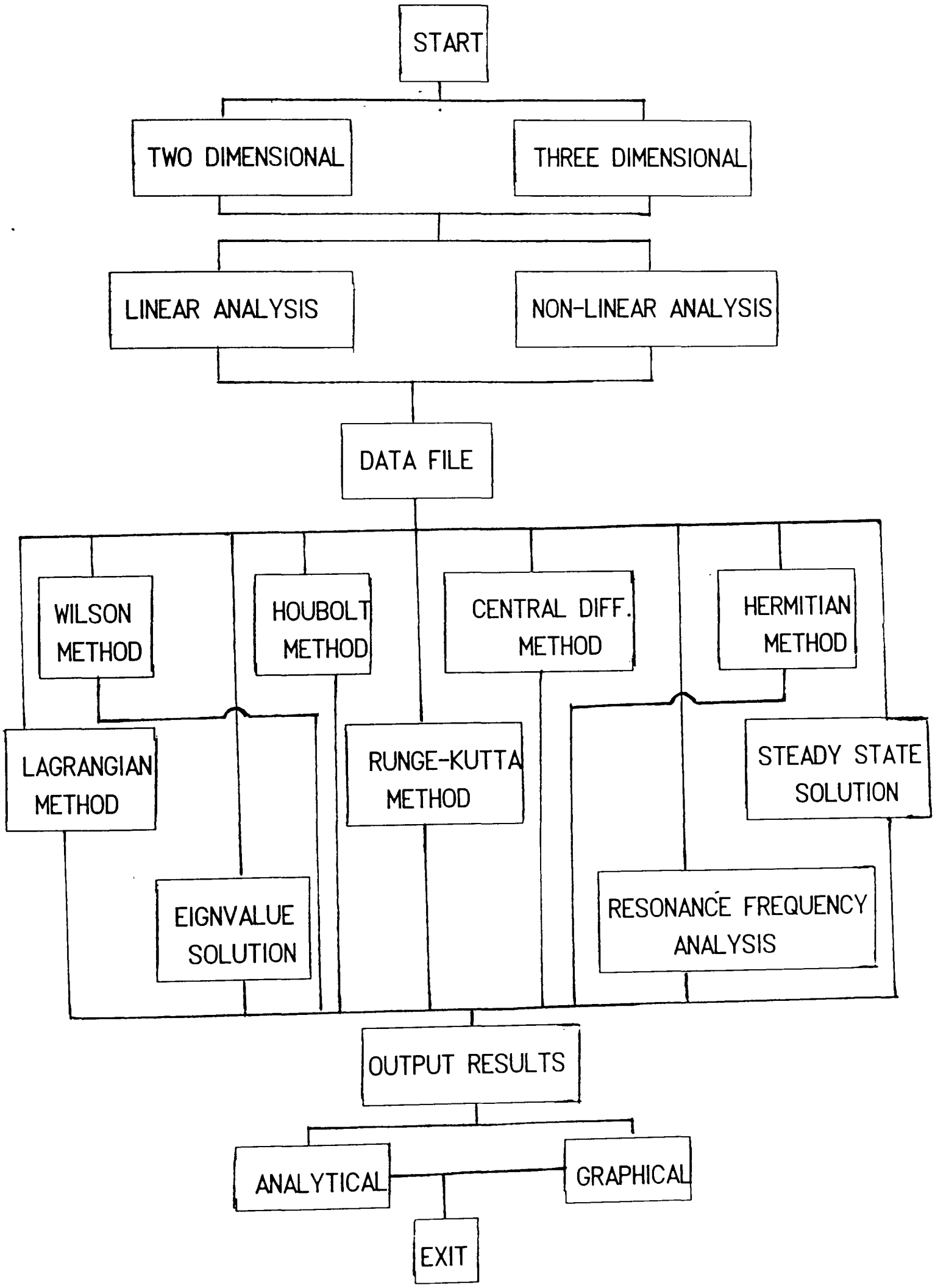

Fig (E.1) The Package Master Command File.

Fig (E.2) The Wilson θ Solver, Linear Analysis Fortran command File.

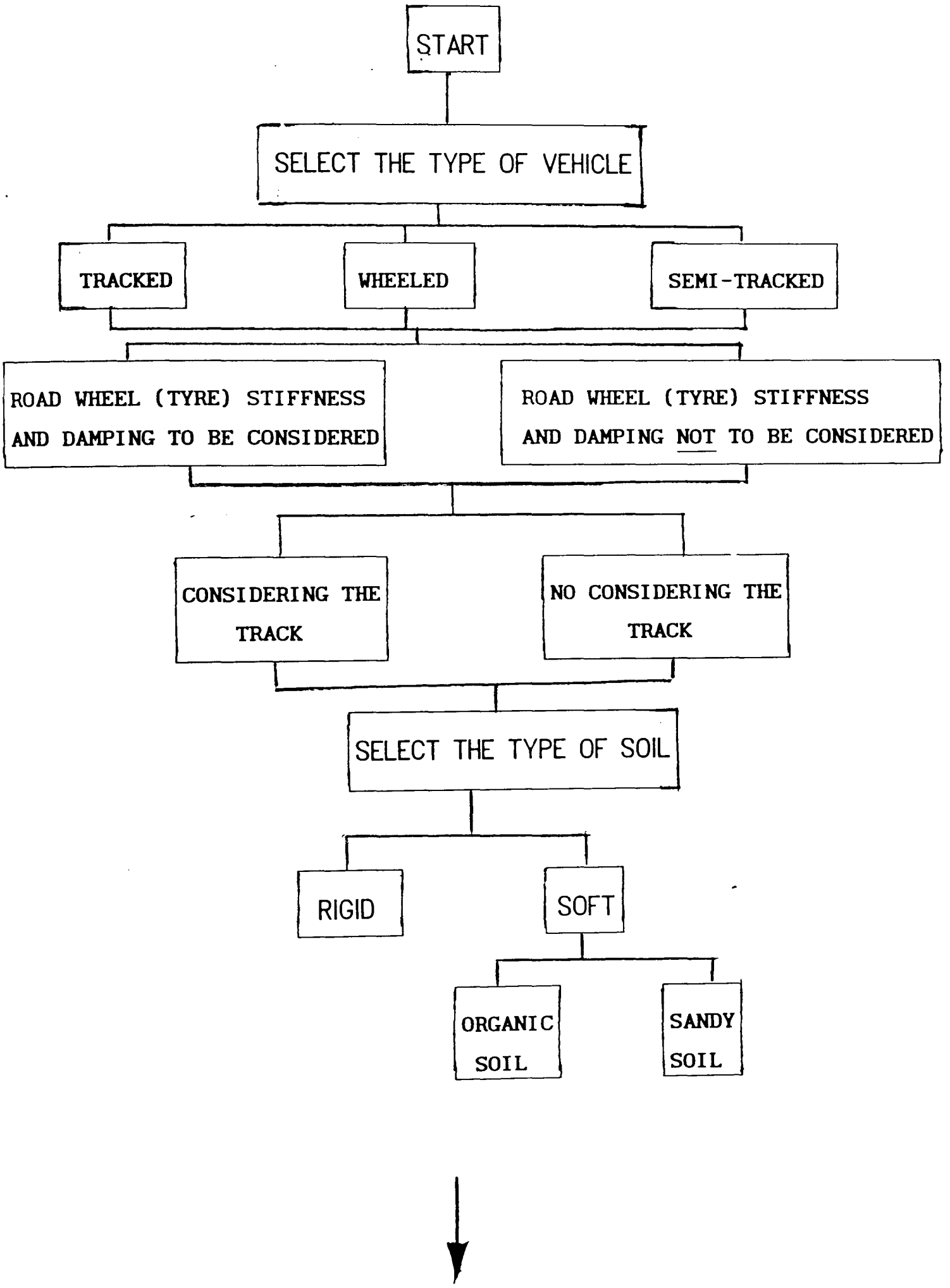

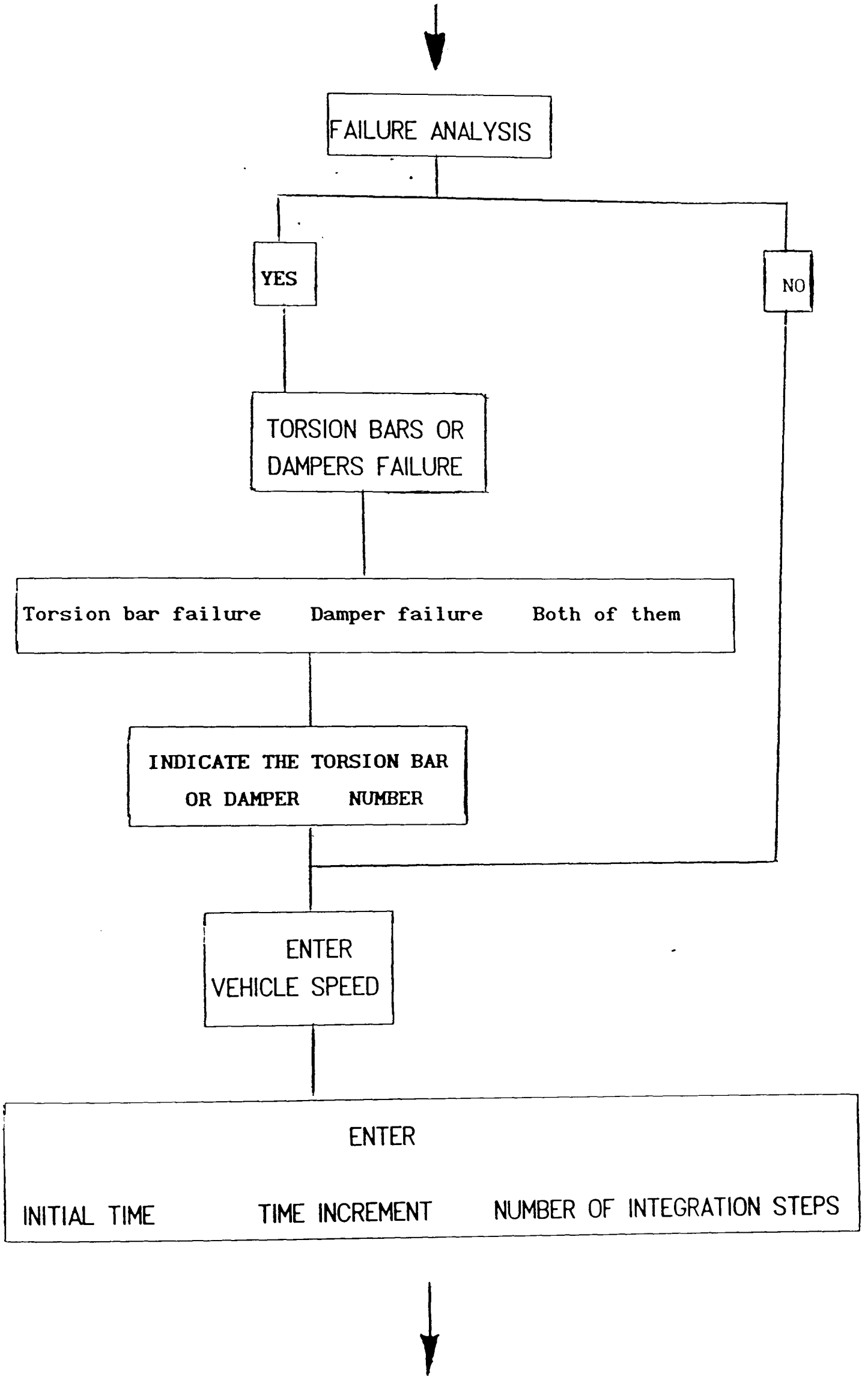
FAILURE ANALYSIS
YES
NO
TORSION BARS OR DAMPERS FAILURE
Torsion bar failure
Damper failure
Both of them
INDICATE THE TORSION BAR OR DAMPER NUMBER
ENTER VEHICLE SPEED
ENTER
INITIAL TIME
TIME INCREMENT
NUMBER OF INTEGRATION STEPS

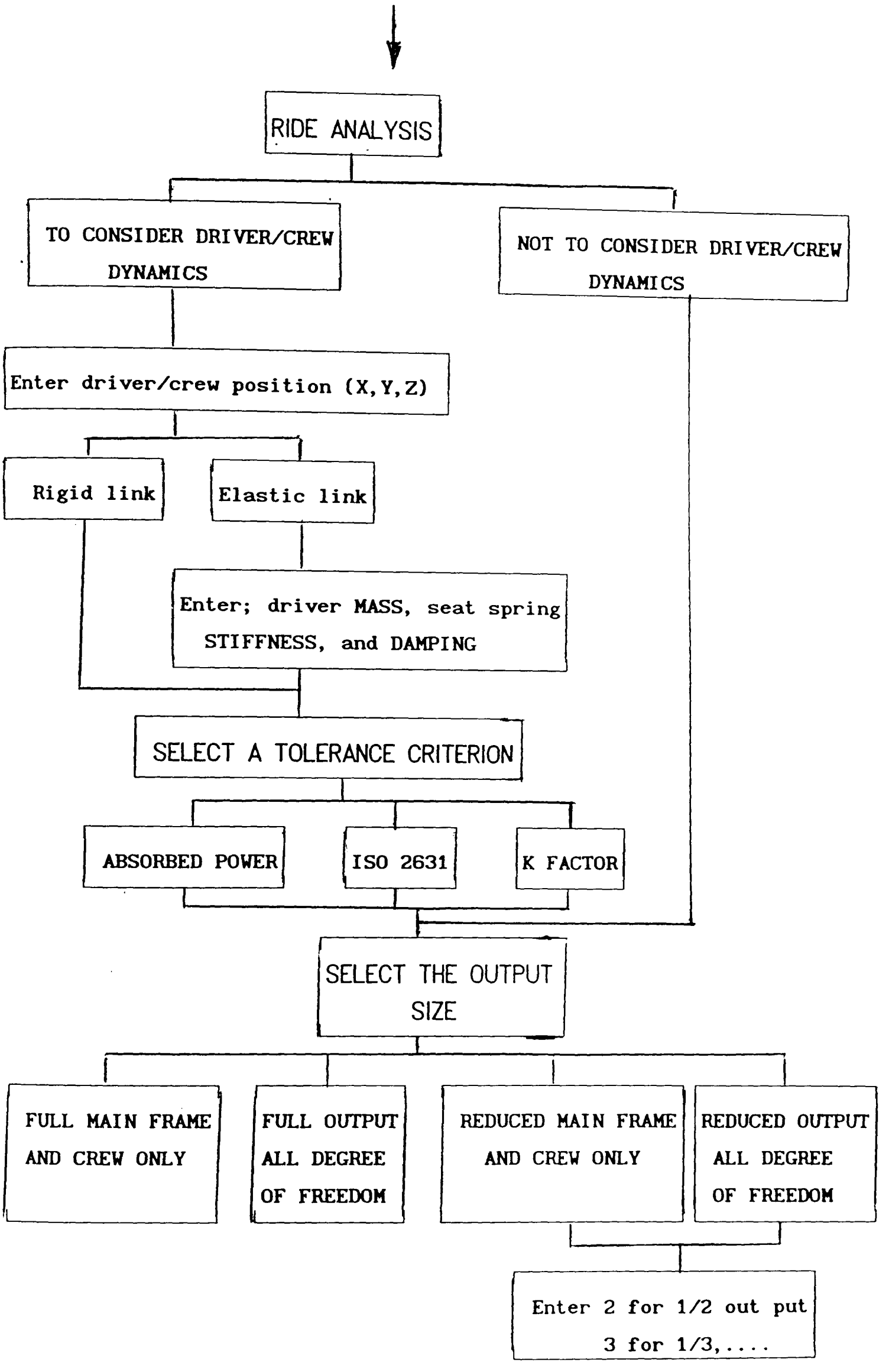
RIDE ANALYSIS
TO CONSIDER DRIVER/CREW DYNAMICS
NOT TO CONSIDER DRIVER/CREW DYNAMICS
Enter driver/crew position (X,Y,Z)
Rigid link
Elastic link
Enter; driver MASS, seat spring STIFFNESS, and DAMPING
SELECT A TOLERANCE CRITERION
ABSORBED POWER
ISO 2631
K FACTOR
SELECT THE OUTPUT SIZE
FULL MAIN FRAME AND CREW ONLY
FULL OUTPUT ALL DEGREE OF FREEDOM
REDUCED MAIN FRAME AND CREW ONLY
REDUCED OUTPUT ALL DEGREE OF FREEDOM
Enter 2 for 1/2 out put
3 for 1/3, ...

Fig (E.3) Two D Tracked Vehicle Non-Linear Input Data File.

VEHICLE DATA

The main frame data

N M_s I_{xx} Y_o Z_o

5, 3750., 7550, 0.0, 0.0

Element type No.

4,4,4,4,4

The track data

t T_w

0.057, 0.6

K_{TT}

0.0, 420000., 420000., 420000., 0.0

K_f L_f A_f

20000., 0.3, 30

Suspension assembly No. 1

Y Y_c Z Z_T

1.407,1.331,-0.193,-0.243

K C m K_T C_T

10599.71921,17840.9,40.0,1000000.,2000.

D_T b L_2 L_o λ

0.58,0.4,-0.296,-0.382,1.6

Suspension assembly No. 2

0.782,0.0,-0.193,-0.243
10599.71921,0.0,40.0,1000000.,2000.
0.58,0.4,0.0,-0.382,0.0

Suspension assembly No. 3

0.154,0.0,-0.193,-0.243
10599.71921,0.0,40.0,1000000.,2000.
0.58,0.4,0.0,-0.382,0.0

Suspension assembly No. 4

-0.467,0.0,-0.193,-0.243
10599.71921,0.0,40.0,1000000.,2000.
0.58,0.4,0.0,-0.382,0.0

Suspension assembly No. 5

-1.095,-1.6,-0.193,-0.243
10599.71921,17840.9,40.0,1000000.,2000.
0.58,0.4,-0.296,-0.382,1.5

TERRAIN DATA

Number of data point

39

Y_3 , Z_3

0.,0. ,.1,.00667 ,.2,.01333 ,.3,.02 ,.4,.02667,
.5,.03333 ,.6,.04 ,.7,.04667 ,.8,.05333 ,.9,.06 ,
1.0,.06667 ,1.1,.07333 ,1.2,.08 ,1.3,.08667 ,1.4,.09333,
1.5,.1 ,1.6,.1 ,1.7,.1 ,1.8,.1 ,1.9,.1 ,
2.0,.1 ,2.1,.1 ,2.2,.1 ,2.25,.1 ,2.35,.09333,
2.45,.08667,2.55,.08 ,2.65,.07333 ,2.75,.06667 ,2.85,.06 ,
2.95,.05333,3.05,.04667 ,3.15,.04 ,3.25,.03333 ,3.35,.02667,
3.45,.02 ,3.55,.01333 ,3.65,.00667 ,3.75,0.0

BUMP STOPS DATA

(Bump stop spring stiffness , Static to bump stop stroke)

1000000.0,0.28 , 1000000.0,0.28 , 1000000.0,0.28
1000000.0,0.28 , 1000000.0,0.28

MAIN SPRINGS CHARACTERISTICS

Number of data points

14

(Deflection , Force)

-0.6,-6359.8 ,-0.5,-5299.9 ,-0.4,4239.9 ,-0.3,-3179.9 ,-0.2,-2119.9 ,-(
1059.97 ,-0.001,-10.5997 ,0.001,10.5997 ,0.1,1059.97 ,0.2,2119.9 ,0.3,
0.4,4239.9 ,0.5,5299.9 ,0.6,6359.8

MAIN DAMPERS CHARACTERISTICS

Number of data points

19

(Velocity , Force)

```
-7.0, 10000.   ,   -6.5,8600.   ,   -6.,7550.   ,   -5.,5900.   ,
-4.0,4600.     ,   -3.0,3600.   ,   -2.,2800.   ,   -1.,2200.   ,
-0.33,1800.    ,    0.0,0.0     ,   0.3,1330.   ,    1.,1800.   ,
 2.0 ,1900.    ,    3.0,2400.   ,    4.,3200.   ,    5.,4200.   ,
 6.0 ,5800.    ,    6.5,7000.   ,    7.,9600.
```

Suspension reassemble data

to update the matrices

```
1.407,1.331,-0.193,-0.243
10599.71921,17840.9,40.0,1000000.,2000.
0.58,0.4,-0.296,-0.382,1.6
0.782,0.0,-0.193,-0.243
10599.71921,0.0,40.0,1000000.,2000.
0.58,0.4,0.0,-0.382,0.0
0.154,0.0,-0.193,-0.243
10599.71921,0.0,40.0,1000000.,2000.
0.58,0.4,0.0,-0.382,0.0
-0.467,0.0,-0.193,-0.243
10599.71921,0.0,40.0,1000000.,2000.
0.58,0.4,0.0,-0.382,0.0
-1.095,-1.6,-0.193,-0.243
10599.71921,17840.9,40.0,1000000.,2000.
0.58,0.4,-0.296,-0.382,1.5
```

Fig (E.4) Actual Input Data File.

```
5,3750,7550,0.0,0.0
4,4,4,4,4
0.057,0.6
0.0,4200000.,4200000.,4200000.,0.0
20000.,0.3,30
1.407,1.331,-0.193,-0.243
10599.71921,17840.9,40.0,1000000.,2000.
0.58,0.4,-0.296,-0.382,1.6
0.782,0.0,-0.193,-0.243
10599.71921,0.0,40.0,1000000.,2000.
0.58,0.4,0.0,-0.382,0.0
0.154,0.0,-0.193,-0.243
10599.71921,0.0,40.0,1000000.,2000.
0.58,0.4,0.0,-0.382,0.0
-0.467,0.0,-0.193,-0.243
10599.71921,0.0,40.0,1000000.,2000.
0.58,0.4,0.0,-0.382,0.0
-1.095,-1.6,-0.193,-0.243
10599.71921,17840.9,40.0,1000000.,2000.
0.58,0.4,-0.296,-0.382,1.5
39
0.,0.       ,.1,.00667      ,.2,.01333      ,.3,.02       ,.4,.02667,
.5,.03333   ,.6,.04         ,.7,.04667      ,.8,.05333    ,.9,.06    ,
1.0,.06667  ,1.1,.07333     ,1.2,.08        ,1.3,.08667   ,1.4,.09333,
1.5,.1      ,1.6,.1         ,1.7,.1         ,1.8,.1       ,1.9,.1    ,
2.0,.1      ,2.1,.1         ,2.2,.1         ,2.25,.1      ,2.35,.09333,
2.45,.08667,2.55,.08        ,2.65,.07333    ,2.75,.06667 ,2.85,.06   ,
2.95,.05333,3.05,.04667     ,3.15,.04       ,3.25,.03333 ,3.35,.02667,
3.45,.02    ,3.55,.01333    ,3.65,.00667    ,3.75,0.0
1000000.0,0.28      ,       1000000.0,0.28      ,       1000000.0,0.28    ,
1000000.0,0.28      ,       1000000.0,0.28
14
-0.6,-6359.8 ,-0.5,-5299.9 ,-0.4,4239.9 ,-0.3,-3179.9 ,-0.2,-2119.9
,-0.1,1059.97,-0.001,-10.5997,0.001,10.5997,0.1,1059.97 ,0.2,2119.9
,0.3,3179.9 ,0.4,4239.9 ,0.5,5299.9 ,0.6,6359.8
19
-7.0, 10000.    ,    -6.5,8600.    ,    -6.,7550.     ,    -5.,5900.     ,
-4.0,4600.      ,    -3.0,3600.    ,    -2.,2800.     ,    -1.,2200.     ,
-0.33,1800.     ,     0.0,0.0      ,    0.3,1330.     ,     1.,1800.     ,
 2.0 ,1900.     ,     3.0,2400.    ,     4.,3200.     ,     5.,4200.     ,
 6.0 ,5800.     ,     6.5,7000.    ,     7.,9600.
1.407,1.331,-0.193,-0.243
10599.71921,17840.9,40.0,1000000.,2000.
0.58,0.4,-0.296,-0.382,1.6
0.782,0.0,-0.193,-0.243
10599.71921,0.0,40.0,1000000.,2000.
0.58,0.4,0.0,-0.382,0.0
0.154,0.0,-0.193,-0.243
10599.71921,0.0,40.0,1000000.,2000.
0.58,0.4,0.0,-0.382,0.0
-0.467,0.0,-0.193,-0.243
10599.71921,0.0,40.0,1000000.,2000.
0.58,0.4,0.0,-0.382,0.0
-1.095,-1.6,-0.193,-0.243
10599.71921,17840.9,40.0,1000000.,2000.
0.58,0.4,-0.296,-0.382,1.5
```

Fig (E.5) The Package output Listing Results.

WILSON METHOD SOLUTION

(1)Vehicle Velocity= 4.1667 m/s

(2)Time Range= 0.0000 Sec : 2.0000 Sec

* Tank with Rotary-Vane damper

* The Track were used

RESULTS

MAXIMUM ACCELERATION = 6.804 ms-2
MINIMUM ACCELERATION =-7.994 ms-2

* DOF NO	* Max.Acc. ms-2	* Min.Acc. ms-2	* R.M.S.acc. ms-2
* 1	* 1.399	*-.9132	* .5953
* 2	* 0.8301	*-1.256	* .4975
* 3	* 3.690	*-3.236	* 1.570
* 4	* 4.405	*-4.207	* 2.279
* 5	* 2.793	*-5.071	* 1.967
* 6	* 6.804	*-7.994	* 4.616
* 7	* 5.950	*-3.901	* 2.372

#The acceleration unit for DOF NO 2 is (rad.s-2)

Driver/Member Dynamics

Driver/Member position (X,Y,Z) = (0.00 , 0.00 , 0.00) M

Maximum driver/member acceleration= 1.399 M.S-2
Minimum driver/member acceleration= -0.9132 M.S-2
Average absorbed power = 0.4745 Watt

The Driver Response

Elapsed time(Sec.)	Displacement(m)	Velocity(m/s)	Acceleration(m.s
0.1000	0.7948E-03	0.2384E-01	0.4769
0.2000	0.5021E-02	0.5525E-01	0.1513
0.3000	0.1225E-01	0.9895E-01	0.7226
0.4000	0.2488E-01	0.1446	0.1911
0.5000	0.3981E-01	0.1491	-0.1025
0.6000	0.5380E-01	0.1269	-0.3414

0.7000	0.6554E-01	0.1155	0.1140
0.8000	0.7629E-01	0.8578E-01	-0.7085
0.9000	0.8098E-01	0.4695E-02	-0.9132
1.0000	0.7713E-01	-0.7928E-01	-0.7662
1.1000	0.6560E-01	-0.1492	-0.6320
1.2000	0.4763E-01	-0.2091	-0.5670
1.3000	0.2479E-01	-0.2385	-0.2032E-01
1.4000	0.2081E-02	-0.2032	0.7256
1.5000	-0.1466E-01	-0.1320	0.6996
1.6000	-0.2319E-01	-0.2703E-01	1.399
1.7000	-0.2035E-01	0.6925E-01	0.5260
1.8000	-0.1167E-01	0.9561E-01	0.1254E-02
1.9000	-0.2488E-02	0.8426E-01	-0.2282
2.0000	0.4448E-02	0.5097E-01	-0.4376

Elapsed time(s)	Displacement(m)	Velocity(m/s)	Acceleration(m.s-2
********** Degree of freedom No. 1			
0.1000	0.7948E-03	0.2384E-01	0.4769
0.2000	0.5021E-02	0.5525E-01	0.1513
0.3000	0.1225E-01	0.9895E-01	0.7226
0.4000	0.2488E-01	0.1446	0.1911
0.5000	0.3981E-01	0.1491	-0.1025
0.6000	0.5380E-01	0.1269	-0.3414
0.7000	0.6554E-01	0.1155	0.1140
0.8000	0.7629E-01	0.8578E-01	-0.7085
0.9000	0.8098E-01	0.4695E-02	-0.9132
1.0000	0.7713E-01	-0.7928E-01	-0.7662
1.1000	0.6560E-01	-0.1492	-0.6320
1.2000	0.4763E-01	-0.2091	-0.5670
1.3000	0.2479E-01	-0.2385	-0.2032E-01
1.4000	0.2081E-02	-0.2032	0.7256
1.5000	-0.1466E-01	-0.1320	0.6996
1.6000	-0.2319E-01	-0.2703E-01	1.399
1.7000	-0.2035E-01	0.6925E-01	0.5260
1.8000	-0.1167E-01	0.9561E-01	0.1254E-02
1.9000	-0.2488E-02	0.8426E-01	-0.2282
2.0000	0.4448E-02	0.5097E-01	-0.4376
********** Degree of freedom No. 2			
0.1000	0.6697E-03	0.2009E-01	0.4018
0.2000	0.3928E-02	0.3747E-01	-0.5417E-01
0.3000	0.8269E-02	0.5798E-01	0.4644
0.4000	0.1538E-01	0.7422E-01	-0.1398
0.5000	0.2208E-01	0.5944E-01	-0.1558
0.6000	0.2706E-01	0.3848E-01	-0.2633
0.7000	0.2794E-01	-0.3745E-01	-1.256
0.8000	0.1920E-01	-0.1246	-0.4875
0.9000	0.4646E-02	-0.1630	-0.2811
1.0000	-0.1191E-01	-0.1565	0.4125
1.1000	-0.2479E-01	-0.9433E-01	0.8301
1.2000	-0.3038E-01	-0.2053E-01	0.6459
1.3000	-0.2918E-01	0.4473E-01	0.6591
1.4000	-0.2206E-01	0.9126E-01	0.2716
1.5000	-0.1204E-01	0.1045	-0.6955E-02

1.6000	-0.3059E-02	0.6085E-01	-0.8660
1.7000	-0.1078E-03	0.1016E-01	-0.1478
1.8000	0.3276E-03	0.1418E-03	-0.5245E-01
1.9000	0.1193E-03	-0.3912E-02	-0.2864E-01
2.0000	-0.2739E-03	-0.2538E-02	0.5613E-01

********** Degree of freedom No. 3

0.1000	0.4552E-02	0.1365	2.731
0.2000	0.2330E-01	0.1529	-2.405
0.3000	0.3672E-01	0.2171	3.690
0.4000	0.6534E-01	0.2398	-3.236
0.5000	0.7827E-01	0.7001E-01	-0.1608
0.6000	0.8364E-01	0.2908E-01	-0.6577
0.7000	0.8173E-01	-0.8259E-01	-1.576
0.8000	0.6718E-01	-0.1923	-0.6192
0.9000	0.4534E-01	-0.2398	-0.3291
1.0000	0.2329E-01	-0.1653	1.817
1.1000	0.1357E-01	-0.5181E-01	0.4534
1.2000	0.7974E-02	-0.8697E-01	-1.156
1.3000	-0.2183E-02	-0.7295E-01	1.437
1.4000	-0.3670E-02	0.2944E-01	0.6110
1.5000	-0.2850E-03	0.1211E-01	-0.9575
1.6000	-0.1613E-02	-0.1618E-01	0.3916
1.7000	-0.1615E-02	0.1272E-01	0.1864
1.8000	-0.2257E-03	0.6931E-02	-0.3021
1.9000	-0.2439E-03	0.6975E-03	0.1774
2.0000	0.2315E-03	0.3996E-02	-0.1114

********** Degree of freedom No. 4

0.1000	0.2815E-02	0.8444E-01	1.689
0.2000	0.1463E-01	0.1010	-1.358
0.3000	0.2696E-01	0.2358	4.053
0.4000	0.5733E-01	0.2368	-4.033
0.5000	0.7013E-01	0.1120	1.537
0.6000	0.8325E-01	0.9294E-01	-1.918
0.7000	0.8517E-01	-0.3250E-01	-0.5905
0.8000	0.7647E-01	-0.1663	-2.086
0.9000	0.5419E-01	-0.2316	0.7798
1.0000	0.3273E-01	-0.2195	-0.5365
1.1000	0.1487E-01	-0.6982E-01	3.530
1.2000	0.1265E-01	-0.1037	-4.207
1.3000	-0.4401E-02	-0.9374E-01	4.405
1.4000	-0.1753E-02	0.4666E-01	-1.597
1.5000	-0.1481E-02	-0.5297E-02	0.5582
1.6000	-0.1116E-02	-0.6365E-02	-0.5795
1.7000	-0.2263E-02	0.7317E-02	0.8532
1.8000	-0.4742E-04	0.9168E-02	-0.8161
1.9000	-0.7903E-03	0.1844E-03	0.6365
2.0000	0.4819E-03	0.5973E-02	-0.5207

********** Degree of freedom No. 5

0.1000	0.1859E-02	0.5577E-01	1.115
0.2000	0.9827E-02	0.7175E-01	-0.7957
0.3000	0.1867E-01	0.1617	2.595
0.4000	0.4165E-01	0.2360	-1.109
0.5000	0.5979E-01	0.1278	-1.057
0.6000	0.7271E-01	0.1848	2.198
0.7000	0.9006E-01	0.4112E-01	-5.071
0.8000	0.8067E-01	-0.1104	2.041
0.9000	0.7035E-01	-0.1909	-3.652
1.0000	0.4374E-01	-0.2339	2.793
1.1000	0.2850E-01	-0.1289	-0.6921
1.2000	0.1297E-01	-0.1735	-0.1999

1.3000	-0.2120E-02	-0.9591E-01	1.751
1.4000	-0.4131E-02	0.4394E-01	1.046
1.5000	0.6594E-03	0.3550E-02	-1.853
1.6000	-0.2828E-02.	-0.1905E-01	1.401
1.7000	-0.1148E-02	0.1844E-01	-0.6514
1.8000	-0.1018E-02	-0.4126E-03	0.2743
1.9000	-0.3240E-03	0.7932E-02	-0.1074
2.0000	0.6810E-04	0.1267E-02	-0.2594E-01

********** Degree of freedom No. 6

0.1000	0.1434E-02	0.4303E-01	0.8606
0.2000	0.7687E-02	0.5850E-01	-0.5513
0.3000	0.1496E-01	0.1288	1.958
0.4000	0.3314E-01	0.1900	-0.7345
0.5000	0.4806E-01	0.1042	-0.9810
0.6000	0.6230E-01	0.2680	4.258
0.7000	0.8998E-01	0.8123E-01	-7.994
0.8000	0.8044E-01	-0.4874E-01	5.394
0.9000	0.8111E-01	-0.1522	-7.463
1.0000	0.5126E-01	-0.2180	6.148
1.1000	0.4168E-01	-0.1591	-4.970
1.2000	0.1567E-01	-0.2135	3.882
1.3000	0.2797E-02	-0.1533	-2.678
1.4000	-0.1012E-01	0.5298E-01	6.804
1.5000	0.5577E-02	0.2480E-01	-7.368
1.6000	-0.6596E-02	-0.4637E-01	5.945
1.7000	0.1632E-02	0.4231E-01	-4.171
1.8000	-0.3162E-02	-0.1989E-01	2.927
1.9000	0.1161E-02	0.2310E-01	-2.067
2.0000	-0.1067E-02	-0.9652E-02	1.412

********** Degree of freedom No. 7

0.1000	-0.3223E-03	-0.9669E-02	-0.1934
0.2000	-0.1344E-02	-0.1636E-02	0.3540
0.3000	-0.7635E-03	0.2976E-02	-0.2618
0.4000	-0.8669E-03	0.4034E-02	0.2829
0.5000	0.3412E-03	0.1403E-01	-0.8307E-01
0.6000	0.1464E-02	0.9778E-02	-0.1902E-02
0.7000	0.1235E-01	0.3072	5.950
0.8000	0.5640E-01	0.4096	-3.901
0.9000	0.8446E-01	0.2178	0.6604E-01
1.0000	0.1038	0.1411	-1.601
1.1000	0.1083	-0.6756E-01	-2.571
1.2000	0.9100E-01	-0.2547	-1.171
1.3000	0.6078E-01	-0.3389	-0.5139
1.4000	0.2716E-01	-0.3051	1.190
1.5000	0.2161E-03	-0.2576	-0.2408
1.6000	-0.1647E-01	0.2663E-01	5.925
1.7000	-0.1313E-03	0.1406	-3.645
1.8000	0.1836E-02	-0.3997E-01	0.3342E-01
1.9000	-0.7421E-03	0.9216E-03	0.7844
2.0000	0.1070E-02	0.1330E-01	-0.5368